



The University of
Nottingham

UNITED KINGDOM • CHINA • MALAYSIA

The role of HER family signalling in breast cancer

Anchala Ishani Kuruppu

B.Sc., B.Sc. (Hons), M.Sc.

Thesis submitted to the University of Nottingham, United Kingdom

for the degree of Doctor of Philosophy

February 2016

“This thesis is dedicated to the memory of my precious loving mother”

Abstract

The HER family of receptors plays a major role in a variety of cancers including breast cancer. Several researchers have shown that HER family overexpression in breast cancer is a significant prognostic factor, especially for survival and relapse. Therefore, many therapeutics are being developed to test the impact of HER family blockade in breast cancer. Although numerous therapies have been developed, many have not been very successful in the clinic. This is often a consequence of cancer cells developing new mechanisms to activate HER family signalling indirectly through cross talk with compensatory pathways. Thus, it is vital to consider the biology of the HER signalling network to a greater extent, which includes RAS/MAPK, PI3K/AKT, mTOR, JAK/STAT, ER and AhR pathways and, also identify breast cancer patient populations that will benefit from specific targeted therapies that target these pathways.

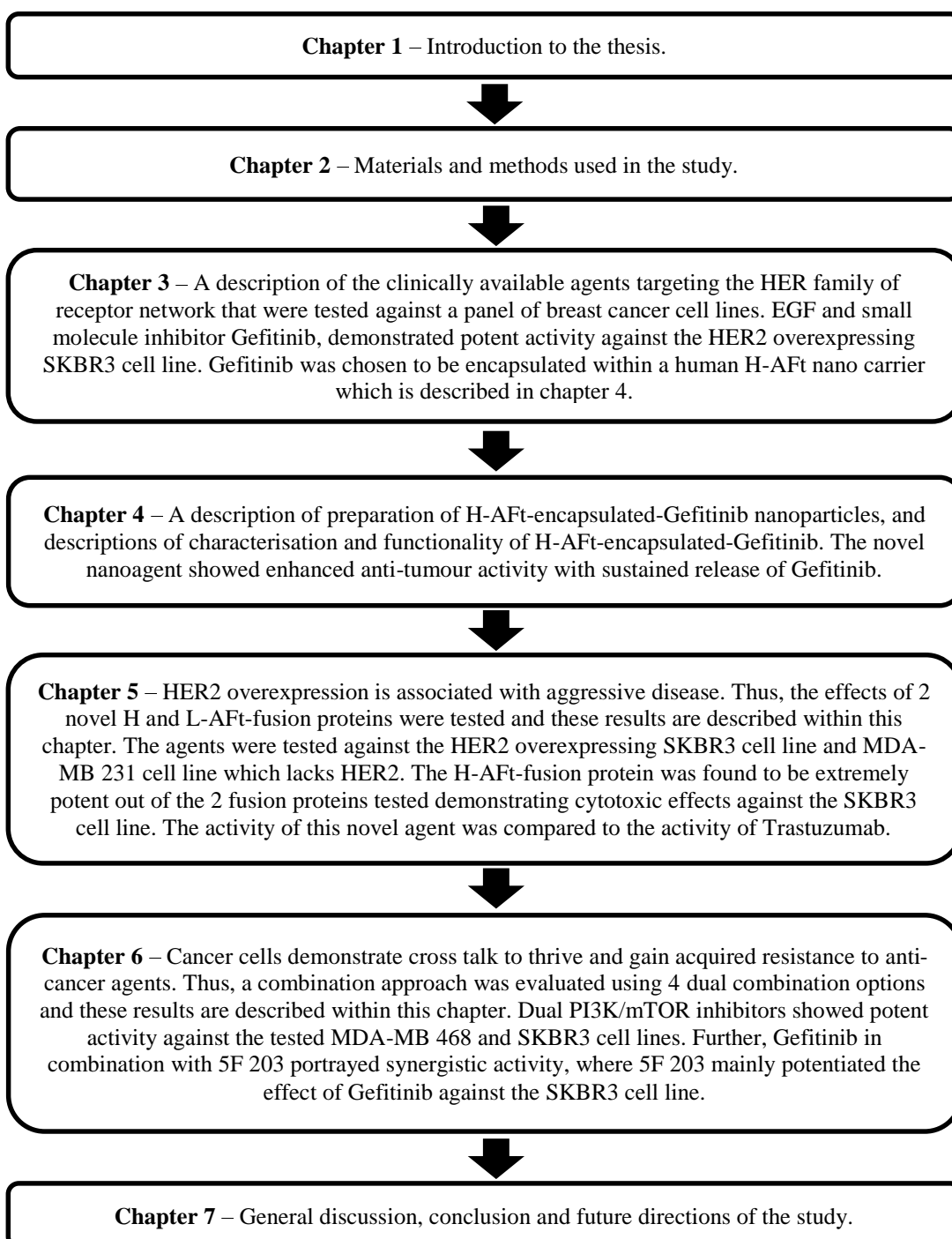
In the current study, 6 breast cancer cell lines (MCF7, T47D and ZR-75-1, SKBR3, MDA-MB 468 and MDA-MB 231) representing distinct molecular subtypes of breast cancer have been used to investigate anti-cancer effects of a variety of agents. These agents include clinical as well as currently experimental and entirely novel pharmacological agents alone or in combination. Among the clinical agents studied, it was found that EGF and Gefitinib were significantly potent against the HER2 overexpressing SKBR3 cell line, out of the panel of cell lines studied. EGF and Gefitinib showed a slightly different spectrum of activity from each other against the SKBR3 cell line. However, more research is needed to determine whether EGF could be used as a therapy for HER2 overexpressing breast cancer. Even though Gefitinib is currently used as a treatment in the clinic, the therapeutic window of this agent is drastically narrowed by its poor bioavailability, acquired resistance and systemic toxicity. Thus, in the current study, encapsulation of Gefitinib within the cavity of human heavy chain (H) apoferritin (AFt), provided a route for sustained release of Gefitinib from the H-AFt cavity, which demonstrated enhanced anti-tumour activity, at a longer duration against the SKBR3 cell line compared to Gefitinib alone.

Overexpression of HER2 is considered to confer a more aggressive phenotype in breast cancer. Many patients have shown resistance to existing clinical agents such as Trastuzumab, demonstrating the need for novel therapies. Hence, 2 novel HER2 targeting human H and light chain (L)-AFt-fusion proteins were tested, and it was found that the nanoagent - H-AFt-fusion protein was very potent against the SKBR3 cell line compared to the L-AFt-fusion protein. This novel H-AFt-fusion protein abolished SKBR3 colony formation completely, caused a G1 arrest and a reduction in the orchestration of S and G2/M cell cycle events and also induced a large SKBR3 apoptotic population demonstrating its potent cytotoxic effects. Furthermore, this agent down-regulated the HER2 protein remarkably which resulted in significant down-regulation of the RAS/MAPK, PI3K/AKT and JAK/STAT signal transduction pathways in SKBR3 cells.

Previous research has shown that a combination of pharmacological agents are more effective against cancer than individual agents due to up-regulation of compensatory signalling pathways which cancer cells use to thrive and acquire resistance to agents. Thus, several agents were tested in combination. Out of the agents tested it was found that 3 dual PI3K/mTOR inhibitors were potent against the triple negative breast cancer cell line - MDA-MB 468 and the HER2 overexpressing SKBR3 cell line. Further,

Gefitinib in combination with an experimental AhR ligand - 5F 203, showed synergistic growth inhibition against the SKBR3 cell line by inducing CYP1A1, thereby resulting in a large apoptotic population. It was observed that the effect of Gefitinib was mainly potentiated by the effect of 5F 203 within the agent combination. There is a momentous unmet medical need for the development of effective therapies that can stabilise or slow the progression of breast cancer, therefore, these results may contribute to existing knowledge or enhance further understanding of the HER signalling network and therapies targeting this network. It may also guide potential treatment options which might lead to significant improvements in breast cancer therapy in the clinic thereby personalising therapy for patients with breast cancer.

Below is a flowchart which provides a short description of each chapter in the thesis.



Acknowledgements

At the very outset, I wish to convey my deep gratitude and appreciation to my primary supervisor, Dr. Tracey D. Bradshaw for her constant support and guidance throughout my research. At the same time, I am extremely grateful to Dr. Bradshaw for providing me with an opportunity to study for a PhD at the University of Nottingham. This opportunity has helped me to broaden my horizon from her excellent intellectual insight and passion for science, which I am indeed indebted. A great part of success of this research was due to her bountiful understanding, patience and kindness. I am truly privileged to work under her supervision and she will be blessed abundantly for all the support, advice and encouragement given to me throughout my studies.

I would like to extend my appreciation to faculty for the future - FFTF/Schlumberger foundation for providing me with a fellowship to carry out my research. I am truly grateful to the FFTF board of directors and the staff. They were extremely helpful in making my research a reality. I wholeheartedly appreciate all the help given to me throughout the study, and thank all of them for their contribution in this regard.

A special word of thanks goes to my second supervisor Dr. Keith Spriggs for his continuous support and guidance during my PhD, which is truly appreciated. Further, I sincerely thank Dr. Claire Seedhouse for her critical evaluation on my research work.

I would like to thank Prof. Neil R. Thomas and Dr. Lei Zhang for providing me with innovative pharmacological agents, resources and assistance for my laboratory work. I would also like to thank Dr. Michael Stocks for providing me with novel pharmacological agents for my research work. I wish to mention and thank all who provided me with technical support at some point during the research, especially - Dr. Hilary Collins, Dr. Lyudmila Turyanska, Dr. Lodewijk Dekker, Dr. David Onion, Dr. Michel Fay, Tim Self, Dr. Charlie Matthews, Dr. Abdullahi Abbas, Dr. Jessica Chu, Dr. Tiangong Lu, Dr. Melchior Cini, Dr. Paddy Tighe and Dr. Ola Negm. Their co-operation has been extremely useful and to each one goes a massive thank you.

My thanks extends to my colleagues in the laboratory to both past and present for their assistance and for making my work experience enjoyable. I wish to particularly thank - Dr. Sivanewary Genapathy, Dr. Vijay Raja, Dr. Yidong Liu, Badraddin Kareem, Khalid Elfsei, Mohammed Qazzaz, Mohammed Al-Hayali and Francesca Citossi.

A heartfelt thank you to my flat mate, Ashira for all the time spent together and also for all the assistance and encouragement given to me during the course of the study period. Further, I would also like to acknowledge, all my friends who were supportive, and my friends who made my stay in the United Kingdom enjoyable and memorable. In this regard a special thank you goes out to Allen, Lorraine, Lesley, Amila, Amal, Roni, Najah, Erina, Samanthika, Hasula, Dinali, Gaya, Hemal and Harshini.

I wish to pay a glowing tribute to my father and my late mother for all their efforts in bringing me up and helping me at all stages of life. I wish to record a very special thank you to my father who made my expectations and desire to study for a PhD a reality. I am ever so grateful to him for his continuous guidance and also for motivating me to do the best. Finally, I would like to thank my close family members and close friends in Sri Lanka, and also many others for their assistance during the study period.

Anchala I. Kuruppu, Nottingham, 2016.

Abbreviations

1° antibody – primary antibody

2° antibody – secondary antibody

4E-BP1 - eukaryotic translation initiation factor-binding protein 1

AFt - apoferritin

AhR - aryl hydrocarbon receptor

AIB1 - amplified in breast cancer 1

AKT - AKT8 virus oncogene cellular homolog

AR - amphiregulin

ARD - adjusted relative densities

ARNT - aryl hydrocarbon receptor nuclear translocator

ATP - adenosine triphosphate

Bcl-2 - B-cell lymphoma 2

BRCA1 - breast cancer gene 1

BRCA2- breast cancer gene 2

BSA - bovine serum albumin

cDNA - complementary DNA

CDK - cyclin-dependent kinase

CI - combination index

CO₂ - carbon dioxide

CYP - cytochrome p450

DAPI - 4',6-diamidino-2-phenylindole dihydrochloride

DDSBs - DNA double strand breaks

ddH₂O – doubled distilled water

dH₂O - distilled water

DMSO - dimethyl sulfoxide

DNA - deoxyribonucleic acid

dNTP - deoxynucleotide solution mix

DTT – dithiothreitol

ECL - enhanced chemiluminescence

EDTA - ethylenediaminetetraacetic acid

EE – encapsulation efficiency

EGF - epidermal growth factor
EGFR - epidermal growth factor receptor
eIF4E - eukaryotic translation initiation factor 4E
eIF4G - eukaryotic translation initiation factor 4 gamma
EMT - epithelial mesenchymal transition
EPR – enhanced permeability and retention
ER – oestrogen receptor
ERK - extracellular signal regulated kinases
FACS – fluorescence activated cell sorter
FBS - foetal bovine serum
FDA - food and drug administration
FITC - fluorescein isothiocyanate
G0 – quiescent state
G1 – gap 1
G2 – gap 2
GI - growth inhibition
GRB2 - Growth factor receptor-bound protein 2
GSK - glycogen synthase kinase
H – heavy chain
h – hours
H₂O - water
H₂O₂ - hydrogen peroxide
HB-EGF - heparin-binding EGF
HCl - hydrochloric acid
HER – human epidermal growth factor receptor
HGF - hepatocyte growth factor
HIF - hypoxia inducible factor
HRP - horseradish peroxidase
Hsp90 - heat shock protein 90
IC - inhibitory concentration
IMS - industrial methylated spirit
JAK - janus kinase
JNK - jun terminal kinases
L – light chain
M – mitotic

MALDI - matrix assisted laser desorption ionisation
MAPK - mitogen activated protein kinase
MAPKK - mitogen activated protein kinase kinase
MAPKKK - mitogen activated protein kinase kinase kinase
MEK – MAPK/ERK kinase
MEKK – MAPK/ERK kinase kinase
MeOH – methanol
min – minutes
MKK – MAP kinase kinase
MMP - matrix metalloproteinases
MNK1 – MAP kinase interacting kinase 1
MNK2 - MAP kinase interacting kinase 2
mRNA - messenger RNA
mTOR - mammalian target of rapamycin
mTORC1 – mTOR complex 1
mTORC2 - mTOR complex 2
MTT - 3-(4,5-dimethyl-2-thiazolyl)-2,5-diphenyltetrazolium bromide
MW – molecular weight
NP40 - nonidet-P40
NPs – nanoparticles
NRG – neuregulins
OD – optical density
p70S6K1 - phosphorylation of 70-kDa ribosomal protein S6 kinase 1
p300 - A histone acetyltransferase
PAGE - polyacrylamide gel electrophoresis
PARP – poly (ADP-ribose) polymerase
PBS - phosphate buffered saline
PbS – lead sulphide
PBT - triton x-100 in phosphate buffered saline
PC – product code
PCR - polymerase chain reaction
PDK1 - phosphoinositide dependent kinase 1
PE – plating efficiency
PI - propidium iodide
PI3K - phosphoinositide 3 kinase

PIK3CA - phosphatidylinositol-4,5-bisphosphate 3-kinase, catalytic subunit alpha
PIP - 3'-phosphatidylinositol phosphate
PR – progesterone receptor
PS – phosphatidylserine
PTEN - phosphatase and tensin homolog
QPCR - quantitative polymerase chain reaction
Rb – retinoblastoma
RLU – relative light units
ROS - reactive oxygen species
RPMA - reverse phase protein microarray
RNA - ribonucleic acid
S - synthesis
SAPK - stress activated protein kinase
SD – standard deviation
SDS - sodium dodecyl sulfate
sec - seconds
Ser – serine
SERM - selective oestrogen receptor modulator
SF – survival fraction
SOS - son of sevenless
SRC - steroid receptor coactivator
STAT - signal transducer and activator of transcription
T0 – time zero
TCDD - 2,3,7,8-tetrachlorodibenzo-p-dioxin
T-DM1- Ado-Trastuzumab-Emtansine
TEM - transmission electron microscopy
TEMED - N, N, N', N'-tetramethylethylenediamine
TfR1 - transferrin receptor 1
TGF- α - transforming growth factor-alpha
Thr - threonine
TKI - tyrosine kinase inhibitor
TNBC - triple negative breast cancers
TNM - tumour node metastasis
TSC1/2 - tuberous sclerosis complex 1 and 2
Tyr – tyrosine

UV – ultraviolet

VEGF - vascular endothelial growth factor

XRE - xenobiotic responsive elements

Table of Contents

Chapter 1 – Introduction.....28

1.1 Breast cancer – A global burden 28

1.2 Molecular subtypes of breast cancer 34

1.3 Breast cancer cell lines used..... 39

 1.3.1 MCF7 cell line 41

 1.3.2 T47D cell line..... 41

 1.3.3 ZR-75-1 cell line 42

 1.3.4 SKBR3 cell line 42

 1.3.5 MDA-MB 468 cell line 42

 1.3.6 MDA-MB 231 cell line 43

1.4 Hallmarks of cancer..... 44

 1.4.1 Self-sufficiency in growth signals..... 45

 1.4.2 Insensitivity to growth inhibitory signals..... 45

 1.4.3 Evading apoptosis 48

 1.4.4 Limitless replication potential..... 49

 1.4.5 Sustained angiogenesis..... 49

 1.4.6 Tissue invasion and metastasis 50

 1.4.7 Emerging hallmarks and enabling characteristics..... 51

1.5 HER family, the importance of HER receptors in the development of the mammary gland and in the induction of breast cancer.....	52
1.5.1 EGFR	55
1.5.2 HER2.....	55
1.5.3 HER3.....	57
1.5.4 HER4.....	58
1.6 Signalling pathways	59
1.6.1 RAS/MAPK pathway.....	60
1.6.2 PI3K/AKT pathway	63
1.6.3 mTOR pathway	66
1.6.4 JAK/STAT pathway.....	69
1.6.5 ER pathway	71
1.6.6 AhR pathway.....	73
1.7 HER mediated signalling as a target for cancer therapy	76
1.7.1 Clinically available targeted pharmacological agents.....	76
1.7.2 Clinical trials of targeted pharmacological agents.....	79
1.8 The importance of nanomedicine for cancer therapy.....	82
1.9 Agents tested in the current study	86
1.9.1 EGF	88
1.9.2 Gefitinib	89
1.9.3 Erlotinib	90

1.9.4	Raloxifene	91
1.9.5	Aft (H and L chains) and affibody molecules	92
1.9.6	H or L-Aft-fusion protein.....	96
1.9.7	H-Aft-encapsulated-Gefitinib.....	96
1.9.8	Trastuzumab.....	97
1.9.9	Sirolimus	97
1.9.10	CGP57380.....	98
1.9.11	5F 203	99
1.9.12	Gedatolisib (MS-73)	99
1.9.13	MS-74.....	100
1.9.14	MS-76.....	101
1.10	Overall aim and objectives of the study	101
Chapter 2 - Materials and Methods.....		104
2.1	General cell culture	104
2.1.1	Materials.....	104
2.1.2	Cell lines	104
2.1.3	Reviving frozen cells.....	105
2.1.4	Freezing and storing cells.....	106
2.1.5	Passaging of cells	106
2.2	Growth curve experiment.....	107

2.3 The 3-(4,5-dimethyl-2-thiazolyl)-2,5-diphenyltetrazolium bromide (MTT) assay	109
2.4 Clonogenic assay	113
2.5 Flow cytometry.....	114
2.5.1 Cell cycle assay	114
2.5.2 Annexin V- Fluorescein isothiocyanate (FITC)/PI apoptosis assay ..	116
2.5.3 γ -H2AX assay.....	118
2.6 Cellular uptake study by flow cytometry	120
2.7 Confocal microscopy.....	121
2.7.1 Materials.....	121
2.7.2 Method for fixed cell imaging.....	121
2.7.3 Method for live cell imaging.....	122
2.8 Evaluation of protein expression	122
2.8.1 Preparation of protein lysates.....	123
2.8.2 Determining protein concentration	124
2.8.3 Sodium dodecyl sulfate (SDS) - polyacrylamide gel electrophoresis (PAGE) (SDS-PAGE).....	125
2.8.4 Western blotting.....	127
2.8.5 Immunological detection.....	131
2.9 Coomassie dye protein staining experiment.....	132
2.10 Transmission electron microscopy (TEM).....	133

2.11 Reactive oxygen species (ROS)	134
2.12 Quantitative polymerase chain reaction (PCR) - (QPCR) (Real time PCR)	135
2.12.1 RNA purification.....	136
2.12.2 Reverse transcription (Preparation of cDNA).....	137
2.12.3 Amplification of cDNA by real time PCR (QPCR).....	138
2.13 Reverse phase protein microarray (RPMA)	139
2.14 Preparation and measuring encapsulation efficiency (EE) of H-AFt- encapsulated-Gefitinib NPs	141
2.14.1 Preparation of H-AFt-encapsulated-Gefitinib NPs	141
2.14.2 Determining encapsulation efficiency.....	142
2.15 Mass spectrometry (Matrix Assisted Laser Desorption Ionisation- MALDI).....	143
2.16 Confirmation of encapsulation of Gefitinib in H-AFt by flow cytometry ...	144
2.17 Release of Gefitinib from H-AFt cavity	144
2.18 Statistical analyses	145
Chapter 3 - Retooling existing agents - EGF, Gefitinib, Erlotinib and Raloxifene.....	146
3.1 Introduction	146
3.2 Results and Discussion	147
3.2.1 HER family protein expression and ER protein expression in the panel of breast cancer cell lines	147

3.2.2	Cellular growth assay	149
3.2.3	<i>In vitro</i> growth inhibitory effects of EGF, Gefitinib, Erlotinib and Raloxifene	158
3.2.4	Effects of EGF and Gefitinib on SKBR3 colony formation	167
3.2.5	Effects of EGF and Gefitinib on SKBR3 cell cycle.....	168
3.2.6	Effects of EGF and Gefitinib on SKBR3 cellular apoptosis.....	173
3.2.7	Effects of EGF and Gefitinib on EGFR, HER2, RAS/MAPK, PI3K/AKT, JAK/STAT signalling pathways, PARP and cyclin D1 in SKBR3 cells by Western blotting.....	179
3.3	Conclusion.....	189
Chapter 4 - Encapsulation of Gefitinib in H-AFt.....		191
4.1	Introduction	191
4.2	Results and Discussion.....	193
4.2.1	Characterisation of H-AFt-encapsulated-Gefitinib	193
4.2.2	<i>In vitro</i> growth inhibitory effects of H-AFt-encapsulated-Gefitinib..	199
4.2.3	Effects of H-AFt-encapsulated-Gefitinib on SKBR3 colony formation	209
4.2.4	Release of Gefitinib from H-AFt	211
4.2.5	Cellular uptake of H-AFt-encapsulated-Gefitinib by confocal microscopy	215
4.2.6	Cellular uptake of H-AFt-encapsulated-Gefitinib by flow cytometry	217

4.3 Conclusion.....	218
Chapter 5 - Anti-proliferative effects of novel HER2 targeting heavy (H) and light (L) chain AFt-fusion proteins.....	
219	
5.1 Introduction	219
5.2 Results and Discussion	220
5.2.1 <i>In vitro</i> growth inhibitory effects of H and L-AFt-fusion proteins, H and L-AFt only, targeting protein and Trastuzumab	220
5.2.2 Effects of H and L-AFt-fusion proteins, targeting protein and Trastuzumab on SKBR3 and MDA-MB 231 colony formation	225
5.2.3 Confocal microscopy imaging of SKBR3 cells treated with H-AFt-fusion protein	228
5.2.4 Effects of H and L-AFt-fusion proteins and Trastuzumab on SKBR3 and MDA-MB 231 cell cycle.....	229
5.2.5 Effects of H and L-AFt fusion proteins, targeting protein and Trastuzumab on SKBR3 and MDA-MB 231 cellular apoptosis.....	237
5.2.6 Effects of H-AFt-fusion protein, targeting protein and Trastuzumab on HER2/P-HER2, RAS/MAPK, PI3K/AKT and JAK/STAT signalling pathways and PARP in SKBR3 and MDA-MB 231 cells by Western blotting.....	243
5.2.7 Effects of H-AFt-fusion protein, targeting protein and Trastuzumab on EGFR/P-EGFR, HER2/P-HER2, HER3/P-HER3, RAS/MAPK, PI3K/AKT and JAK/STAT signalling pathways and PARP in SKBR3 and MDA-MB 231 cells by reverse phase protein microarray (RPMA)	258
5.3 Conclusion.....	261

Table of contents

9.1.3	Densitometry analysis for Western blotting experiments in chapter 6	373
9.2	Appendix II	376
9.2.1	Combinations of H-AFt alone and H-AFt-fusion protein	376
9.3	Appendix III	377
9.3.1	Effects of Sirolimus and CGP57380 alone and in combination in Mia PaCa-2 cells	377
9.4	Appendix IV	379
9.4.1	The effect of dual PI3K/mTOR inhibitor – MS-73 on the PI3K/AKT pathway	379
9.5	Appendix V	380
9.5.1	Publications	380

List of Tables

Table 1.1: Molecular characteristics of breast cancer subtypes	38
Table 1.2: Cell lines representing each of the breast cancer subtypes, HER receptor statuses, hormone receptor statuses and common genetic mutations associated with each cell line.....	40
Table 1.3 Agents tested summarising their molecular target and activity	87
Table 2.1: Agents tested during the study period.....	110
Table 2.2: List of 1° and 2° antibodies.....	129
Table 3.1: Mean $GI_{50} \pm SD$ values of (a) EGF, (b) Gefitinib, (c) Erlotinib, (d) Raloxifene and (e) DMSO (vehicle control).....	160
Table 4.1: Mean $GI_{50} \pm SD$ values of Gefitinib, H-AFt, and H-AFt-encapsulated-Gefitinib..	205
Table 5.1: Mean $GI_{50} \pm SD$ values of H and L-AFt-fusion proteins, Trastuzumab, targeting protein, H and L-AFt only	220
Table 6.1: Mean $GI_{50} \pm SD$ values of Sirolimus and CGP57380.....	265
Table 6.2: Mean $GI_{50} \pm SD$ values of MS agents.....	272
Table 6.3: Mean $GI_{50} \pm SD$ values of 5F 203	297
Table 9.1: Mean $GI_{50} \pm SD$ values of different combinations of H-AFt and H-AFt-fusion proteins.....	376
Table 9.2: Mean $GI_{50} \pm SD$ values of Sirolimus and CGP57380 of Mia PaCa-2 cells	377

List of Figures

Figure 1.1: The 6 hallmark capabilities of cancer.....	44
Figure 1.2: The mammalian cell cycle	47
Figure 1.3: HER family receptors and their ligands	53
Figure 1.4: Cross talk of signalling pathways - RAS/MAPK, PI3K/AKT, mTOR, JAK/STAT, ER and AhR signalling pathways	60
Figure 1.5: The RAS/MAPK pathway.....	63
Figure 1.6: The PI3K/AKT pathway.....	66
Figure 1.7: The mTOR pathway.....	68
Figure 1.8: The JAK/STAT pathway.....	70
Figure 1.9: The ER pathway.	72
Figure 1.10: AhR pathway	75
Figure 1.11: EGF.....	88
Figure 1.12: Chemical structure of Gefitinib	89
Figure 1.13: Chemical structure of Erlotinib	90
Figure 1.14: Chemical structure of Raloxifene	91
Figure 1.15: Protein structure of human H-AFt with the exterior surface view and interior cavity	92
Figure 1.16: H or L-AFt-fusion protein	96
Figure 1.17: Chemical structure of Sirolimus.....	97
Figure 1.18: Chemical structure of CGP57380.....	98

Figure 1.19: Chemical structure of 5F 203	99
Figure 1.20: Chemical structure of MS-73	99
Figure 1.21: Chemical structure of MS-74	100
Figure 1.22: Chemical structure of MS-76	101
Figure 3.1: Western blot analysis of HER family and ER in the breast cancer cell line panel.....	147
Figure 3.2: Densitometry plots of protein expression levels of (a) EGFR (b) HER2 (c) HER3 (d) HER4 and (e) ER in the breast cancer cell line panel	148
Figure 3.3: Cellular growth curves for all 6 cell lines.....	152
Figure 3.4: Growth inhibitory curves for EGF and Gefitinib against SKBR3 cells.....	166
Figure 3.5: Effects of EGF and Gefitinib on SKBR3 colony formation.....	167
Figure 3.6: Cell cycle analysis following treatment of SKBR3 cells with EGF and Gefitinib	170
Figure 3.7: Representative cell cycle histograms of SKBR3 cells treated with EGF and Gefitinib	171
Figure 3.8: Apoptotic analysis of SKBR3 cells following exposure to EGF and Gefitinib	175
Figure 3.9: Representative apoptotic quadrant plots of SKBR3 cells treated with EGF and Gefitinib.....	176
Figure 3.10: Western blot analysis of EGFR and HER2 following exposure of SKBR3 cells to EGF and Gefitinib.....	180

Figure 3.11: Adjusted relative density (ARD) levels of EGFR, P-EGFR, HER2 and P-HER2 for EGF and Gefitinib..	181
Figure 3.12: Western blot analysis of RAS/MAPK pathway following exposure of SKBR3 cells to EGF and Gefitinib.....	184
Figure 3.13: Western blot analysis of PI3K/AKT pathway following exposure of SKBR3 cells to EGF and Gefitinib.....	187
Figure 3.14: Western blot analysis of P-STAT5, PARP and Cyclin D1 following exposure of SKBR3 cells to EGF and Gefitinib	188
Figure 4.1: Characterisation of H-AFt-encapsulated-Gefitinib	199
Figure 4.2: Growth inhibitory curves for Gefitinib and H-AFt-encapsulated-Gefitinib after 72 h exposure	206
Figure 4.3: Growth inhibitory curves for Gefitinib and H-AFt-encapsulated-Gefitinib after 120 h exposure	207
Figure 4.4: GI ₅₀ values for Gefitinib alone and H-AFt-encapsulated-Gefitinib at each time point tested in the SKBR3 cell line.....	208
Figure 4.5: Growth inhibitory curves after 72 h exposure at pH 7.0	209
Figure 4.6: Effects of Gefitinib and H-AFt-encapsulated-Gefitinib on colony formation.....	210
Figure 4.7: Detection of Gefitinib release from the H-AFt cavity.....	214
Figure 4.8: Confocal microscopy images of SKBR3 and MDA-MB 231 cells following exposure to Gefitinib and H-AFt-encapsulated-Gefitinib	216

Figure 4.9: Mean fluorescence uptake by SKBR3 and MDA-MB 231 cells using flow cytometry.....217

Figure 5.1: Growth inhibitory curves of H and L-AFt-fusion proteins, Trastuzumab, targeting protein, H and L-AFt only.222

Figure 5.2: Effects of H and L-AFt-fusion proteins, targeting protein and Trastuzumab on colony formation226

Figure 5.3: Confocal microscopy images of SKBR3 cells following exposure to H-AFt-fusion protein.....229

Figure 5.4: Effects of H-AFt-fusion protein, L-AFt-fusion protein and Trastuzumab on SKBR3 and MDA-MB 231 cell cycle233

Figure 5.5: Representative cell cycle histograms of cells treated with HER2 targeting agents.....235

Figure 5.6: Effects of H-AFt-fusion protein, L-AFt-fusion protein and Trastuzumab on SKBR3 and MDA-MB 231 cellular apoptosis.....238

Figure 5.7: Representative apoptotic quadrant plots of cells treated with HER2 targeting agents240

Figure 5.8: Western blot analysis of HER2 and P-HER2 following exposure of SKBR3 and MDA-MB 231 cells to H-AFt-fusion protein, Trastuzumab and targeting protein244

Figure 5.9: ARD levels for HER2 and P-HER2 of HER2 targeting agents.....245

Figure 5.10: Western blot analysis of RAS/MAPK pathway following exposure of SKBR3 and MDA-MB 231 cells to H-AFt-fusion protein, Trastuzumab and targeting protein.....249

Figure 5.11: Western blot analysis of PI3K/AKT pathway following exposure of SKBR3 and MDA-MB 231 cells to H-AFt-fusion protein, Trastuzumab and targeting protein.....253

Figure 5.12: Western blot analysis of JAK/STAT pathway and PARP following exposure of SKBR3 and MDA-MB 231 cells to H-AFt-fusion protein, Trastuzumab and targeting protein.256

Figure 5.13: RPMA analysis for HER2 and P-HER2 following exposure of SKBR3 and MDA-MB 231 cells to H-AFt-fusion protein, Trastuzumab and targeting protein261

Figure 6.1: Growth inhibitory curves of MS-73, MS-74 and MS-76.275

Figure 6.2: Effects of MS-73, MS-74 and MS-76 on colony formation.....277

Figure 6.3: Cell cycle analysis following treatment of cells with MS-73, MS-74 and MS-76.....282

Figure 6.4: Representative cell cycle histograms at the highest concentration (1500 nM) tested of MS-73, MS-74 and MS-76283

Figure 6.5: Apoptosis analysis of cells following exposure to MS-73, MS-74 and MS-76.....287

Figure 6.6: Representative apoptotic quadrant plots at the highest concentration (1500 nM) tested of MS-73, MS-74 and MS-76.288

Figure 6.7: Western blot analysis of PI3K/AKT and mTOR pathways following exposure of cells to MS-73, MS-74 and MS-76290

Figure 6.8: *In vitro* growth inhibitory effects of 5F 203 and Gefitinib (a) alone and (b) in combination against the SKBR3 cell line.305

Figure 6.9: Effects of 5F 203 and Gefitinib in combination on SKBR3 colony formation.....306

Figure 6.10: Apoptosis analysis of SKBR3 cells following exposure to 5F 203 and Gefitinib alone and in combination.....310

Figure 6.11: mRNA expression levels of *CYP1A1* and *EGFR* after exposure to 5F 203 and Gefitinib alone and in combination for 24 h in SKBR3 cells.313

Figure 6.12: Induction of ROS following exposure to 5F 203 and Gefitinib alone and in combination for 24 h in SKBR3 cells315

Figure 6.13: γ -H2AX analysis of SKBR3 cells following exposure to 5F 203 and Gefitinib alone and in combination.....318

Figure 6.14: Western blot analysis of the effects of 5F 203 and Gefitinib alone and in combination for 24 h in SKBR3 cells322

Figure 9.1: ARD levels of the RAS/MAPK pathway for results in chapter 3367

Figure 9.2: ARD levels of the PI3K/AKT pathway for results in chapter 3.....368

Figure 9.3: ARD levels of the JAK/STAT pathway and Cyclin D1 for results in chapter 3.....368

Figure 9.4: ARD levels of the RAS/MAPK pathway for results in chapter 5370

Figure 9.5: ARD levels of the PI3K/AKT pathway for results in chapter 5.....371

Figure 9.6: ARD levels of the JAK/STAT pathway and PARP for results in chapter 5372

Figure 9.7: ARD levels of the PI3K/AKT and mTOR pathways for results in chapter 6.....373

Figure 9.8: ARD levels of EGFR, HER2, CYP1A1, RAS/MAPK and c-MET pathways for results in chapter 6.....375

Figure 9.9: *In vitro* growth inhibitory effect of (a) Sirolimus and CGP57380 alone and in (b) combination against the Mia PaCa-2 cell line.....378

Figure 9.10: Western blot analysis of PI3K/AKT pathway with use of MS-73 (10 μ M)379

1 Chapter 1 – Introduction

1.1 Breast cancer – A global burden

Breast cancer is the most frequent cause of cancer deaths among women worldwide [1]. However, the incidence varies considerably between women in different populations and in diverse geographic regions around the world [2]. For instance, it has been shown that the incidence of breast cancer development in Asia is relatively low compared to all other continents [3] [4]. However, in the past 20 years the incidence in Asia has been rising very rapidly with an incidence rate of 29.1 per 100,000 shown in 2012 [4] [5]. This dramatic increase renders that in the near future, a large majority of breast cancer patients worldwide will be from Asian populations [6].

In Europe, development of new breast cancer cases have remained high with an incidence of 71.1 per 100,000 in 2012 [4] [5] [7]. Breast cancer incidence in the United Kingdom is portrayed to be rising with 52,399 cases (32.3%) and 11,716 deaths reported in 2012 [5] [8]. For women in the United Kingdom, the life time risk of being diagnosed with breast cancer is 1 in 8 [8]. The factors that contribute to the international variation in incidence rates mostly stem from variations in reproductive and hormonal factors, diet and the availability of early detection services [9]. For instance, one of the reasons for a low incidence rate in Asia could be due to the diet. For example, soy intake has shown to have a protective effect on breast cancer risk in women of Asian ethnicity [6]. In contrast, a reason for the high breast cancer incidence

observed in many Western countries from the late 1990s could be because of increased screening intensities [9].

Age is one of the strongest risk factors for breast cancer and it has been shown that the incidence of this disease rises with age [2] [10]. In Asia, the incidence of this disease peaks among premenopausal women in their forties, whereas in the West, breast cancer peaks among postmenopausal women in their sixties [2] [3]. Development of breast cancer at an earlier age could be due to mutations in the breast cancer susceptibility genes carried by individual Asian populations. In addition it could be due to adapting to a modernised lifestyle, having denser breasts and due to vitamin D deficiencies [2] [8]. On the other hand, in the West, postmenopausal women tend to be more obese. Obese women tend to have high levels of circulating oestrogens due to their greater peripheral conversion of androgens to oestrogens by aromatase in adipose tissues which may contribute to breast cancer [11].

Compelling evidence suggests that reproductive factors such as age at menarche (before age of 12), age at menopause (after the age of 55), age at first live birth (after the age of 35), a reduced duration of breast feeding and low parity are strong risk factors for breast cancer development [3] [10]. Further, the use of exogenous hormones such as hormone replacement therapy and oral contraceptives have also been shown to have an association with an increase in risk of the disease [10]. A number of lifestyle factors have also been linked to breast cancer which include the use of tobacco, alcohol consumption, consumption of a high fat diet, obesity and a

sedentary life style [10]. It has been outlined that the risk of breast cancer is increased 2-to 3-fold in women with a first degree relative with breast cancer [12]. Nevertheless, it has been shown that only about 10% of women are at increased risk due to inherited mutated forms of breast cancer susceptibility genes such as breast cancer gene 1 (*BRCA1*) and breast cancer gene 2 (*BRCA2*) and the remaining cases develop sporadic breast cancer [12]. Maintaining a healthy life style is the best available strategy to reduce the risk of developing breast cancer [9]. Early detection of the disease has shown to increase treatment options and reduce mortality [13].

Breast cancer is derived from the epithelial cells found in the terminal duct lobular unit of the breast [14]. These epithelial cancer cells that disseminate outside the basement membrane of the ducts and lobules into the adjacent surrounding tissues become invasive carcinomas [14]. Invasive carcinomas of the breast are divided into 2 major histopathological classifications - ductal and lobular carcinomas where they both arise from the terminal duct lobular unit of the breast [14]. Invasive ductal carcinoma comprises the majority of all breast cancers with a frequency of 50 - 80% and invasive lobular carcinomas present with a frequency of 5 - 15% around the world [15]. There are some morphologically distinct special types of breast cancers that represent minor groups which comprise around 5 - 10% of breast cancers including mixed ductal and lobular, cribriform, mucinous, medullary and papillary carcinomas [15].

Invasive breast cancer is diagnosed by several investigation methods such as by a clinical and radiological examination that involve a mammography and a whole breast ultrasound [14]. If there is any evidence of suspected disease it may be further confirmed by a pathological examination which most often involves a fine needle aspiration or a core needle biopsy [16]. With certain cases a surgical biopsy may be needed such as an excisional or an incisional biopsy to establish exact diagnosis [16]. After diagnosis, breast tumours are classified into different stages which may have prognostic implications. This is known as the tumour node metastasis (TNM) system [14]. The TNM system includes the size of the tumour, the involvement of regional lymph nodes and the number of metastatic tumours present [14]. Metastatic tumours of the breast commonly spreads to the lung, liver, bone, adrenal glands and brain [15].

Currently, breast tumours are also classified according to the degree of differentiation of the tumour tissue compared to the appearance of normal breast tissue, which is graded from 1 - 3 where grade 1 represents a well differentiated tumour while grade 3 represents a poorly differentiated tumour with higher risk of recurrence and death [17]. The most frequently used histological grading system of breast cancer is the Nottingham grading system. The Nottingham grading system has been combined with the breast cancer tumour staging system to develop the Nottingham prognostic index. The Nottingham prognostic index is widely used to determine prognostic information for patients with breast cancer in the United Kingdom [17]. Ki67 which is a nuclear protein is also evaluated most often to determine cellular proliferation [18]. In addition, classifications according to biomarkers such as hormone receptors by immunohistochemistry and growth factor receptors such as human epidermal growth

factor receptor 2 (HER2) either by immunohistochemistry or fluorescence in situ hybridisation exist to guide therapeutic options [14]. Thus, breast cancer is currently classified by many different parameters in the clinic. However, with advances in molecular biology it is evident that breast cancer is no longer one disease but a heterogeneous disease and there are different types of breast cancers, which behave differently. While these classification systems have incorporated differences in types of breast tumours, some tumours may not demonstrate correlation between these parameters used with the predicted clinical outcome and the effective therapeutic options to be used [14].

The main treatment options available for breast cancer are surgery, radiotherapy, chemotherapy and targeted therapy [14] [19]. Most patients with breast cancer may have local treatment to control the disease and also systemic treatment to combat any micrometastatic disease. Local treatment may comprise of surgery and radiotherapy [14]. There are 2 types of breast cancer surgery. Surgery can be excision of the tumour with adjacent normal breast tissues (wide local excision) which is also known as breast conservation surgery or removal of the whole breast which is known as mastectomy [14] [20].

Radiotherapy which uses x-rays to damage deoxyribonucleic acid (DNA) in tumour cells is commonly given to patients after surgery which will reduce local recurrence [14]. Chemotherapy which is also known as adjuvant therapy is the treatment given after surgery that will help eradicate breast metastatic disease. In some cases,

chemotherapy may be given before surgery which may be used to shrink a large tumour prior to surgery which is then known as neo-adjuvant therapy. However, older women who are more than 70 years of age are offered a customised treatment option which takes into account age dependent variances such as physical capability, stage of the tumour, personal preferences and also predicted life expectancy to reduce treatment related morbidity and mortality compared to younger women. Most often, majority of patients of this group may benefit from surgical treatment, however, frail elderly patients may not benefit from surgical treatment with respect to overall survival. These patients are rarely given standard chemotherapy as well. However, if nodal disease is identified, radiotherapy might be given as a better option with adjusted protocols which will provide local control of the disease, or endocrine therapy if the tumour is oestrogen receptor (ER)+ [20].

Standard chemotherapy has shown a wide range of acute and long term side effects that substantially affects the patient's quality of life [15]. Targeted therapies are a special type of chemotherapy that will be active on an underlying molecular target critical in breast cancer pathogenesis, offering a reduced effect on normal cells in the body thereby reducing the level of toxicity [19]. These molecular targets will assist in tailoring the treatment strategies to individual patient's tumour [15]. Some of the molecular targets are growth factor receptors, components of intracellular signalling pathways and hormonal receptors [19]. However, the selection of patients for targeted therapy remains a challenge and molecular characterisation of breast cancer sub populations may guide better selection of patients and reduce resistance to therapy [21].

1.2 Molecular subtypes of breast cancer

Molecular techniques have certainly transformed the understanding of the basic biology of breast cancer and provided a foundation for personalised prognostic and predictive testing. The traditional staging of breast cancer that involves the TNM system does predict the outcome but it is evident that all breast tumours presenting the same stage will not consist of the identical underlying biology or clinical behaviour. Further, histopathological assessments can be used to determine prognostic information, but once again, there is certainly more biological diversity among breast tumours than the histopathological classification scheme. For instance around 50 - 80% of breast tumours are classified histopathologically as invasive ductal carcinoma demonstrating that a large proportion of the breast tumours are histopathologically identical [15]. Thus, it is evident that these existing histological classifications do not fully capture the varied clinical behaviour of this heterogeneous disease [22]. Furthermore, additional factors such as hormonal (oestrogen, progesterone) receptor status and HER2 status also influence prognosis and the probability of response to therapy [23]. It should also be noted that there might be substantial intra- and inter-laboratory variations in immunohistochemistry and fluorescence in situ hybridisation techniques used and also in the interpretations of the results to determine the hormone receptor and HER2 statuses [23].

Currently, all these clinical variables including hormone receptor genes and HER2 related genes which are the major drivers of breast cancer biology can be combined by high throughput microarray based gene expression profiling methods [18] [22]. These methods provide a platform to evaluate a large amount of genes in a single

experiment [18]. Seminal studies evaluating these genetic profiles have classified at least 6 molecular subtypes in breast cancer [24]. The ultimate goal of identifying breast cancer subtypes is to contribute to a personalised model of breast cancer management, where therapeutic agents can be tailored to individual patients [25]. These subtypes are: luminal A, luminal B, HER2, normal-like, basal and recently identified claudin low [24] [25]. Luminal A and luminal B are amenable to hormone therapy [24]. Luminal A tumours portray high expression of ER. They also have lower proliferation rates and tend to be of low histological grade as such they tend to have the best prognosis [18] [22]. Most often older women demonstrate tumours with ER+ and lower histological grade and fall into this subgroup [20]. Luminal B tumours show lower expression of ER, they are more often of higher histological grade and have higher proliferation rates. As such patients with these tumours will have a worse prognosis when compared to patients having luminal A tumours [18] [22].

The HER2 subtype demonstrates *HER2* gene amplification and receptor overexpression. This subtype is amenable to therapies that target the HER2 receptor and often demonstrate aggressive clinical behaviour. Many patients have showed resistance after initiating treatment against HER2+ disease, thus, novel therapies are necessary to improve survival [18] [24]. The normal-like subtype, as the name suggests demonstrates similar expression patterns to normal breast adipose tissue [18]. The significance of this subtype is yet to be determined, and some researchers argue that it may represent a mere contamination of samples with normal breast tissue [18] [22] [24]. Thus, this subtype was not explored further in the current study. The basal subtype is positive for epidermal growth factor receptor (EGFR) expression and also

for expression of basal cytokeratins 5/6 and cytokeratins 14/17 [18] [26]. This group is negative for the expression of ER, progesterone receptor (PR) and HER2 related genes. Thus, this group is associated with triple negative breast cancers (TNBC) [26]. Further, basal breast cancers demonstrate high histological grade and high Ki67 [18]. Interestingly, a large proportion of *BRCA1* associated breast cancers appear to have a basal molecular profile, suggesting a common pathway of carcinogenesis in patients with this molecular profile. In contrast a basal molecular profile might not necessarily incorporate *BRCA* mutations [22]. Further it has been shown that a higher frequency of younger premenopausal women will fall into the TNBC category [26].

The claudin low subtype which is the latest molecular subtype identified, demonstrates the lack of expression of claudin proteins (claudin-3 and claudin-4), which are important in cell to cell adhesion [24]. Around 25 - 39% of TNBCs fall into the claudin low subtype [26]. Due to inconsistent expression of cytokeratins and a significantly lower expression of Ki67 this subtype differs from the basal subtype [24]. Both basal and claudin low subtypes are not amenable to hormone therapy nor to therapy targeting the HER2 receptor. These 2 subtypes are biologically more aggressive and often have poor prognosis [24]. As such, it is especially important that novel therapeutic targets are developed for women with these tumours.

Molecular testing in breast cancer is still evolving [22]. However, in order to understand the underlying biology of breast cancer, molecular gene expression profiling, has contributed immensely. Further, it has enabled characterisation of vital

genes and pathways that are deregulated in each subtype thereby identifying novel targets for therapeutic interventions and selection of patient populations that can be targeted with the potential for personalised treatment which otherwise is a challenge in breast cancer [18] [21]. Molecular characteristics of the breast cancer subtypes are summarised in the below table (Table 1.1).

Subtype	Immunoprofile	Common histological grades and histological types	Other characteristics	Prognosis
Luminal A	ER+, PR+/-, HER2-	Grade 1/2, invasive ductal carcinoma, lobular, cribriform, mucinous	Ki67 low, responsive to hormone therapy, often responsive to chemotherapy	Good
Luminal B	ER+, PR+/-, HER2+/-	Grade 2/3, invasive ductal carcinoma, papillary	Ki67 high, usually responsive to hormone therapy, variable to chemotherapy, might be responsive to therapies that target HER2	Intermediate
HER2	ER-, PR-, HER2+	Grade 2/3, invasive ductal carcinoma, papillary	Ki67 high, responsive to therapies that target HER2, responsive to chemotherapy	Poor
Basal	ER-, PR-, HER2-	Grade 3, invasive ductal carcinoma, medullary	Ki67 high, EGFR+, BRCA mutations shown, often responsive to chemotherapy	Poor
Claudin low	ER-, PR-, HER2-	Grade 3, invasive ductal carcinoma, medullary	Ki67 lower than Basal subtype, intermediate response to chemotherapy	Poor

Table 1.1: Molecular characteristics of breast cancer subtypes [18] [22] [24] .

1.3 Breast cancer cell lines used

Cell lines are powerful experimental tools and in many instances in the past, the information derived from these cell lines has translated into numerous clinical improvements. Despite their crucial role in improving clinical outcomes, their ability to accurately reflect phenotypes of tumours remains controversial. However, many studies have shown that these cell lines actually mirror many of the characteristics of the breast cancer subtypes from which they have been derived [24].

During the study period, finding cell lines that most accurately resemble the genomic alterations of the molecular subtypes of breast cancer was challenging as breast cancer is extremely heterogeneous. Further, having access only to a limited number of cell lines for each molecular subtype, restricted the choice of cell lines to be used within the current study. Thus, 1 breast cancer cell line or 2 breast cancer cell lines in the case of the luminal A subtype, were chosen that represents each molecular subtype of breast cancer after careful consideration. Further the cell lines chosen were cell lines which were most frequently used within preclinical settings. All pharmacological agents tested within the current study were initially screened against the panel of breast cancer cell lines chosen. This helped to determine which cell line responded to a particular agent tested which led to further investigations with the selected cell line/s. A detailed phenotypic characterisation of each cell line used is demonstrated in the below table (Table 1.2) and a brief overview of each cell line is described in sections 1.3.1 to 1.3.7.

Subtype	Cell line	EGFR	HER2	HER3	HER4	ER	PR	TP53	PTEN	PIK3CA
Luminal A	MCF7	Very low expression	Very low expression/negative	Moderate expression	Moderate expression	Positive	Positive	Wildtype	Wildtype	Mutant
	T47D	Moderate expression	Moderate expression	Moderate expression	Very low expression/negative	Positive	Positive	Mutant	Wildtype	Mutant
Luminal B	ZR-75-1	Moderate expression	Very low expression/negative	Negative	Negative	Positive	Negative	Wildtype	Mutant	Wildtype
HER2	SKBR3	Moderate expression	Over expression	Moderate expression	Negative	Negative	Negative	Mutant	Wildtype	Wildtype
Basal	MDA-MB 468	Over expression	Negative	Low expression	Negative	Negative	Negative	Mutant	Mutant	Wildtype
Claudin low	MDA-MB 231	Over expression	Negative	Moderate expression	Negative	Negative	Negative	Mutant	Wildtype	Wildtype

Table 1.2: Cell lines representing each of the breast cancer subtypes, HER receptor statuses, hormone receptor statuses and common genetic mutations associated with each cell line [24] [27] [28] [29].

1.3.1 MCF7 cell line

The MCF7 breast cancer cell line was derived from a pleural effusion taken from a 69 year old female patient with metastatic invasive ductal carcinoma [27] [28]. MCF7 cells as shown in table 1.2 belong to the luminal A subtype. These cells form tightly cohesive structures demonstrating robust cell to cell adhesions [24]. As these cells are ER+ and PR+ they are extensively used in studies aimed at analysing the mechanisms by which hormones and endocrine therapy affect cell proliferation and protein synthesis [27] [28]. Further, no overexpression of the HER family receptors are observed in this cell line [29].

1.3.2 T47D cell line

The T47D cell line was isolated from a 54 year old female patient's pleural effusion having invasive ductal carcinoma [27]. This cell line is also categorised under Luminal A subtype and displays epithelial morphology and demonstrates tightly cohesive structures like the MCF7 cell line [24]. Further, it has been shown that these cells demonstrate enhanced ER levels than MCF7 cells [30]. Furthermore, T47D cells express all 4 members of the HER receptor family, but none of the receptors are found to be overexpressed as shown in the above table (Table 1.2). However, when compared to the MCF7 cell line, once again this cell line expresses more EGFR levels and HER2 levels [29].

1.3.3 ZR-75-1 cell line

The ZR-75-1 cell line is derived from a 63 year old female's ascites fluid with invasive ductal carcinoma [27]. This cell line has been reported to be categorised under luminal B subtype, however some researchers have categorised this cell line under luminal A subtype which is controversial [24] [31]. ZR-75-1 cells exhibit an epithelial morphology and they grow as fused colonies [32].

1.3.4 SKBR3 cell line

The SKBR3 cell line was isolated from a pleural effusion from an adenocarcinoma of the breast of a 43 year old female patient [27]. These cells are epithelial and found to form loosely cohesive grape like structures [24]. Previous studies have shown that SKBR3 cells show low levels of EGFR compared to the amount of HER2 levels they express as these cells overexpress HER2 [31]. SKBR3 cancer cell are found to express between 1,000,000 and 2,000,000 HER2 receptors per cell compared to normal cells that express ~ 20,000 HER2 receptors [33].

1.3.5 MDA-MB 468 cell line

This cell line was first isolated from the pleural effusion of a metastatic breast adenocarcinoma from a 51 year old female [27]. These cells possess an epithelial morphology and form a loosely cohesive grape like structure. They are also consistent with a more invasive phenotype [24]. This cell line is reported to be TNBC that is -ER-, PR- and HER2- [27]. MDA-MB 468 cells overexpress EGFR, expressing

between 1,300,000 and 2,000,000 EGF binding sites per cell compared to normal cells that express ~ between 10,000 and 100,000 receptors per cell [34] [35] [36]. Although these cells overexpress EGFR they do not express detectable levels of HER2 [31].

1.3.6 MDA-MB 231 cell line

MDA-MB 231 cells were obtained from a 51 year old female. These cells were isolated from a pleural effusion of a metastatic breast adenocarcinoma. MDA-MB 231 cells appear phenotypically as a stellate structure and they are also TNBC [24] [27]. This cell line represents the claudin low breast cancer subtype which demonstrates highly invasive characteristics with poor prognosis [24] [27]. These cells overexpress EGFR but the levels are not as high as in MDA-MB 468 cells. MDA-MB 231 cells express ~ 130,000 EGF binding sites per cell and HER2 receptors are undetectable in these cells [31] [35].

Evidence demonstrates that carcinogenesis is a multistep process [37]. This process involves the activation or modification of expression in growth promoting oncogenes or the loss of activation of growth regulatory tumour suppressor genes or a combination of these pathogenic events [37]. These cancer gene mutations might occur in the germline leading to hereditary predispositions to breast cancer or in single somatic cells leading sporadic breast cancer. Ultimately these mutations enhance cell growth which drives normal cells to a neoplastic state by acquiring many biological capabilities during this multistep process [37] [38].

1.4 Hallmarks of cancer

Hanahan and Weinberg described the essence of several biological capabilities acquired during the multistep process of development of carcinogenesis [37] [39]. These capabilities which are called the ‘hallmarks of cancer’ are a set of unique characteristics of cancer cells that enable them to become tumourigenic and ultimately malignant. These hallmark capabilities include self-sufficiency in growth signals, insensitivity to growth inhibitory signals, evasion of programmed cell death, limitless replicative potential, sustained angiogenesis and tissue invasion and metastasis (Figure 1.1) [37] [39].

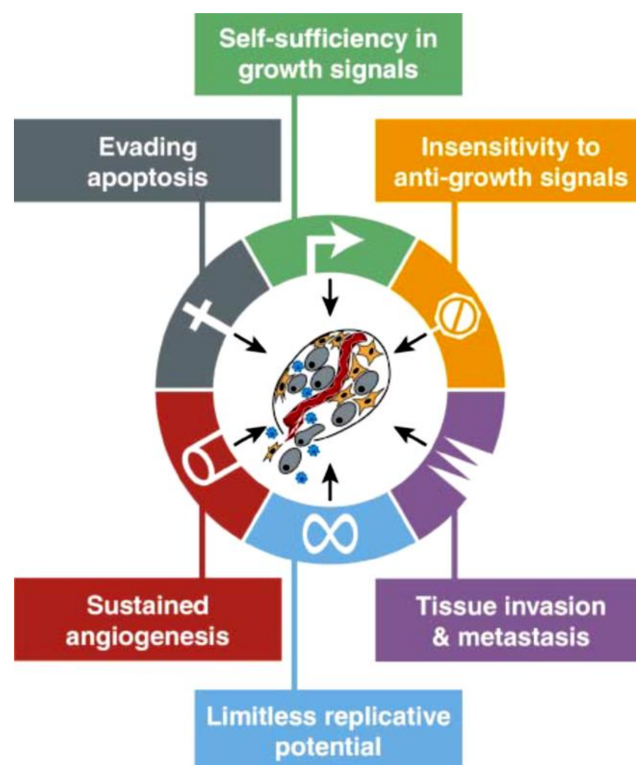


Figure 1.1: The 6 hallmark capabilities of cancer. Figure adapted from [37].

1.4.1 Self-sufficiency in growth signals

Proliferation of normal cells occur only when supplied with appropriate mitogenic growth factors/growth signals [37]. These growth signals are transmitted via transmembrane receptors that bind to specific classes of signalling molecules which enable normal cells to proliferate; usually such signal transduction is strictly regulated [37]. These normal cells are unable to proliferate in the absence of mitogenic growth stimulatory signals. In contrast, tumour cells, invariably show a greatly reduced dependence on exogenous mitogenic growth factors/growth signals. Tumour cells are able to generate many of their own mitogenic growth stimulatory signals, which results in reduced dependence on stimulation from their normal tissue microenvironment [37] [39]. Further in cancer, growth factor receptors are often overexpressed and this overexpression of receptors enables cells to be hyperresponsive to growth factor signalling, leading to sustained proliferation. Furthermore, receptors may demonstrate ligand independent signalling via structural modifications of receptors [37] [39].

1.4.2 Insensitivity to growth inhibitory signals

Numerous anti-proliferative signals operate to maintain cellular quiescence and tissue homeostasis within normal cells [37]. These signals are growth inhibitors, inhibitors embedded in the extracellular matrix and on the surfaces of surrounding cells [37]. These inhibitors act on the cell cycle (Figure 1.2) by forcing cells out of the active proliferation into the quiescent (G0) state which usually involves terminal differentiation of the cell [37]. In contrast, cancer cells are able to escape these anti-

proliferative signals by mutations and hence inactivation of tumour suppressor genes [39]. A few main examples of such mutated tumour suppressor genes are retinoblastoma (*Rb*) and *TP53* genes [39]. It has been shown that the Rb protein plays a major role in the G1 checkpoint where it blocks S phase entry and cell growth by promoting cell cycle exit [40]. However, cancer cells with mutations in the *Rb* gene may not control entry into the cell cycle permitting continuous cell proliferation [40] [41]. *TP53* determines whether the cell cycle should progress, halt or whether the cell should undergo apoptosis [40] [41]. Around 50% of human cancers demonstrate mutations in the *TP53* gene and if the cancer cells possess mutated *TP53* then cells may demonstrate aberrant cell cycle progression [37] [39] [40]. Further, this becomes important in the face of DNA damage as the *TP53* protein evokes cell cycle arrest in response to DNA damage to allow DNA repair. However, when *TP53* is mutated, DNA repair is inhibited which results in propagation of genetic errors that will lead to cancer [18].

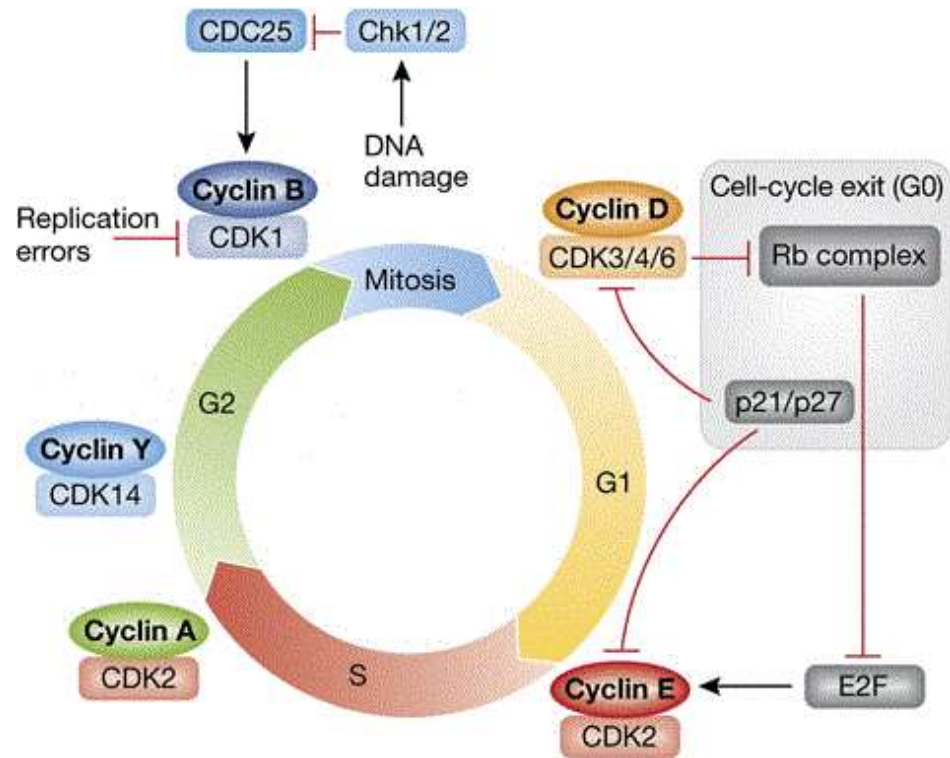


Figure 1.2: The mammalian cell cycle. Figure adapted from [42]. G0 phase - The phase where the cell has left the cell cycle and in a resting phase. Gap 1 (G1) phase - Cells increase in size preparing for DNA synthesis in G1. The G1 checkpoint ensures that all conditions are favourable for cell division to proceed in the synthesis (S) phase. S phase - DNA synthesis occurs in the S phase. Gap 2 (G2) phase - The cells will continue to grow and at the end of the G2 phase the G2 checkpoint ensures whether the cell can proceed into the mitosis phase and divide. Mitosis (M) phase- Cell growth stops and the M checkpoint ensures that the cell is ready to complete cell division. Cyclins and cyclin-dependent kinase (CDKs) complexes are shown to regulate the progression through the cell cycle. For instance, cyclin D1 is required for progression through G1 phase. Cyclin D1 is a regulatory subunit of CDK4 and CDK6. Thus, cyclin D1 dimerises with CDK4 and CDK6 to regulate the G1/S phase transition and entry into the S phase. Following anti-proliferative signals or DNA damage, p21^{cip1} and p27^{kip1} which are cyclin-dependent kinase inhibitors are shown to bind to cyclin-CDK complexes to induce cell cycle arrest [40].

1.4.3 Evading apoptosis

Apoptosis is a form of programmed cell death by which cells undergo death in the event of DNA damage [37]. Cancer cells in contrast can bypass this mechanism by acquiring resistance to apoptosis. During the course of tumorigenesis or as a result of anti-cancer therapy, apoptosis is triggered in response to various physiological stresses in cancer cells [37]. Based on the source of stress signals received apoptosis can be triggered via the extrinsic apoptotic pathway where signals are received extracellularly or the intrinsic apoptotic pathway where the signals are received intracellularly [39]. Regardless of the initial source of the signals the apoptotic pathways culminate by caspase activation which proceeds to initiate a cascade of proteolysis involving effector caspases responsible for the execution phase of apoptosis, in which the cell is gradually broken down and then consumed, both by its nearby cells and by phagocytic cells. It has been shown that the apoptotic process is regulated by counterbalancing pro and anti-apoptotic members of the B-cell lymphoma 2 (Bcl-2) family [39]. In cancer, expression of anti-apoptotic regulators are increased by down-regulating pro-apoptotic factors and also by short circuiting the apoptotic pathways which allows cancer cells to evade apoptotic mechanisms. Further, TP53 also plays a role in evoking apoptosis in response to damage of DNA. However, in cancer, the loss of *TP53* tumour suppressor function eliminates critical DNA damage sensors from the apoptosis inducing circuitry, leading to tumour progression [37]. Additionally hyper-expression of oncogenes such as *RAS* or loss of expression of tumour suppressor genes such as phosphatase and tensin homolog (*PTEN*), up-regulates the phosphatidylinositol-3-OH kinase (PI3K)/AKT8 virus oncogene cellular homolog (AKT) pathway which is likely to be involved in mitigating apoptosis in cancer cells [37]. The multiplicity of

apoptosis evading mechanisms demonstrates the selective pressure overriding apoptosis during the multistage carcinogenesis [37] [39].

1.4.4 Limitless replication potential

Passing through successive cell growth and division cycles are limited for normal cells. This limitation has been associated with senescence [37] [39]. Senescence is an irreversible entry into a nonproliferative state where the cells are still viable that ultimately involves cell death. In contrast, cancer cells require unlimited replicative potential in order to generate macroscopic tumours. In cell culture, cancerous cells are immortalised, a characteristic that most established cell lines retain with the ability to proliferate in culture without evidence of either senescence or apoptosis [39]. Unlimited proliferation in cells has been shown to be associated with telomerase activity [39]. In normal cells the length of telomeric DNA is shortened during each cell cycle leading to senescence and ultimately cell death. However, 85 - 90% of cancers portray up-regulation of telomerase, the specialised DNA polymerase that maintains telomeric DNA which leads to limitless replication [37] [39].

1.4.5 Sustained angiogenesis

Cancerous cells require a high amount of nutrients and oxygen as well as an ability to evacuate metabolic wastes and CO₂ [39]. This is because of the enhanced levels of proliferation and continuous replication potential, cancer cells demonstrate that leads to increased angiogenesis. Angiogenesis is the development of new blood vessels from

existing blood vessels. During tumour development and progression, an 'angiogenic switch' is triggered and remains switched on, which drives continual development of new blood vessels which will assist in sustaining and expanding neoplastic growth [39]. Many tumours show increased expression of vascular endothelial growth factor (VEGF) as a result of hypoxia and oncogene signalling which in turn stimulates angiogenesis [39]. Further, an angiogenesis inhibitor thrombospondin-1 has been found to be regulated by TP53. Loss of *TP53* causes reduction of thrombospondin-1 levels and ultimately allows increased angiogenesis in cancer cells [37].

1.4.6 Tissue invasion and metastasis

Cancer cells are able to escape from the primary tumour by invading surrounding tissues and travelling to distant sites where they may succeed in developing new colonies [37] [39]. These newly formed colonies are able to form metastases which has shown to be the cause for > 90% of human cancer deaths [39]. Metastasis is the last step in multistep primary tumour progression [39]. The loss of E-cadherin which is a cell to cell adhesion molecule in carcinoma cells is associated with invasion and metastasis. Down-regulation or inactivation of E-cadherin by mutations is shown to be strongly associated with invasion and metastasis in cancer [37] [39]. Cancer cells in the course of invasion and metastasis is able to activate epithelial mesenchymal transition (EMT). This is a process by which transformed epithelial cells lose their cell polarity and cell to cell adhesion, and gain migratory and invasive properties thereby become mesenchymal stem cells. These cells are recruited to distant sites via the cardiovascular and lymphatic system and reverted back to form epithelial tissues. Metastasis can be categorised into 2 major phases - cancer cells being disseminated

from the primary tumour to distant tissues and the adaptation of these cancer cells from micrometastases into macroscopic tumours. However, in some patients including in breast cancer patients these micrometastases which have disseminated stay dormant for long periods of time and never progress to macroscopic metastatic tumours. This is because of suppressor factors released by the primary tumour. For instance, it has been shown that in patients with breast cancer, brain metastasis can stay dormant for a long period and appear years after diagnosis of the primary tumour [39].

1.4.7 Emerging hallmarks and enabling characteristics

After Hanahan and Weinberg's seminal article in 2000 with the 6 notable hallmarks of cancer, 2 additional emerging hallmarks were introduced in 2011 [39]. These are reprogramming energy metabolism and evading immune destruction. Further, 2 additional enabling characteristics were also introduced, which are genome instability and mutation and tumour promoting inflammation [39].

Cancer cells are able to reprogramme energy metabolism by modifying cellular metabolism to support cancer cell proliferation. Cancer cells can reprogramme to select glycolysis as the metabolic program over mitochondrial oxidative phosphorylation, even in the presence of oxygen. Glycolysis has been shown to be associated with mutant tumour suppressor genes such as *TP53* and activated oncogenes such as *RAS* where alterations in cancerous cells have been selected primarily to thrive and proliferate [39].

The immune system protects the host from various pathogens [43]. When the host develops cancer, a major challenge for the immune system is to identify and eradicate cancerous cells [39] [43]. Thus, the second emerging hallmark describes how cancer cells evade immunological destruction by T and B lymphocytes, macrophages and natural killer cells. Although the immune system operates as a significant barrier to tumour formation and progression, immune evasion in cancer still remains to be firmly established [39].

Additionally, the 2 enabling characteristics of neoplasia have been shown to facilitate the key and emerging hallmarks. Genomic instability is inherent to a variety of human cancer cells and any mutations in DNA and in the DNA repair mechanisms, become advantageous for tumour progression [39]. Further, inflammation is a biological response by the immune system as a result to harmful pathogens. However, in cancer, inflammation can instead lead to the inadvertent contribution of multiple hallmark capabilities by supplying growth factors and proliferative signals which will allow tumour cells to survive and thrive [39].

1.5 HER family, the importance of HER receptors in the development of the mammary gland and in the induction of breast cancer

The human epidermal growth factor receptor (HER) family comprises 4 structurally related tyrosine kinase receptors namely EGFR (HER1/ErbB1), HER2 (ErbB2), HER3 (ErbB3) and HER4 (ErbB4) [44] [45]. In common all members have an extracellular ligand binding domain, a single hydrophobic transmembrane domain and

an intracellular protein tyrosine kinase domain [44] [46]. Around 11 ligands bind to HER receptors [44]. These ligands are categorised into 2 classes, ligands which predominantly bind to EGFR and ligands that bind to HER3 and/or HER4 [44] [47]. Epidermal growth factor (EGF) is shown to exclusively bind to EGFR and other ligands such as neuregulins (NRG) bind to HER3 and HER4 [47] [48]. HER2 is ligandless, no known ligand binds to HER2 indicating that it is a co-receptor [44]. Ligand binding to HER receptors induces formation of homodimerisation and/or heterodimerisation with other HER receptors [46]. Activation of HER receptors results in activation of the intrinsic kinase domain and subsequent phosphorylation on specific tyrosine residues within the cytoplasmic tail. These phosphorylated residues serve as docking sites for number of signalling molecules, which in turn activates intracellular pathways [44] [46] [48] [49] [50] (Figure 1.3).

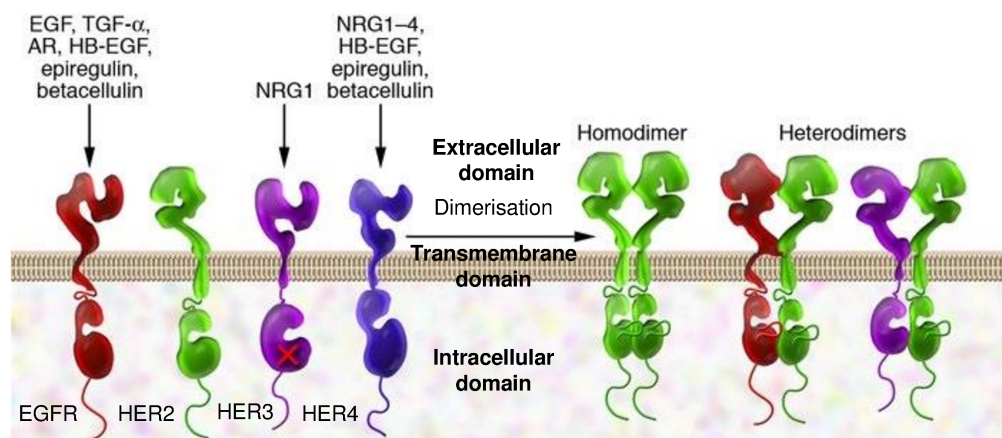


Figure 1.3: HER family receptors and their ligands. Figure adapted from [50]. Note that the kinase domain of HER3 is catalytically inactive and that no known ligand is bound to HER2. HER2 has been found to be the preferred dimerisation partner for other HER receptors.

It has been found that HER receptors play a role in mammary gland development during menarche, pregnancy and also in postnatal mammary development [49]. EGFR has shown to promote ductal growth in the mammary gland development whereas HER2 and HER4 play a major part in lobuloalveolar differentiation and lactation during pregnancy [51]. HER3 is also expressed and active during pregnancy. In contrast HER4 is down-regulated and inactivated which is shown to be important during the latter stages of pregnancy and to sustain lactation. Further, HER3/HER4 heterodimers have also demonstrated a role in proliferation and differentiation both in pregnancy and after childbirth [51]. Overall, HER family members possess a variety of functions at multiple stages in the development of the mammary gland. Thus, it is likely that both expression and activity of the HER receptors in the endogenous mammary epithelium, sets the stage for the selection of precancerous cells in which HER receptor activity is overexpressed [52].

As outlined in section 1.4, overexpression of growth factor receptors is a hallmark of oncogenesis [37]. This overexpression of receptors enables cells to be hyperresponsive to growth factor signalling leading to sustained proliferation [37] [39]. Many types of human cancers including breast cancer have shown overexpression of HER receptors, which is correlated to deregulation of HER signalling [49] [51]. Thus, the role of HER receptors in cancer has been studied extensively in the recent past [52]. Especially, EGFR and HER2 has shown to have important roles in the development of breast cancer [52].

1.5.1 EGFR

EGFR is a 170 kDa plasma membrane glycoprotein which is encoded by the *EGFR* gene on chromosome 7 and there are several homologous ligands that can bind specifically to EGFR [36]. These ligands include EGF, transforming growth factor-alpha (TGF- α) and amphiregulin (AR) that binds specifically to EGFR while heparin-binding EGF (HB-EGF), epiregulin and betacellulin binds to EGFR and HER4 demonstrating dual specificity [46] [53]. EGFR, most widely expressed in epithelial and mesenchymal cells, plays an important role in growth and differentiation including in the mammary gland as outlined above [52]. It has been shown that around 14 - 91% of human breast cancers express EGFR [53]. The role of EGFR in breast cancer biology has been a subject of intense study and controversy, thus, more studies are warranted to understand the function of EGFR [48]. For instance, EGFR expression has been associated with poor prognosis along with high histological grade and lymph node involvement, and controversies exist between EGFR expression and survival in breast cancer [36] [48]. Further, EGFR overexpression is commonly expressed in TNBC (basal and claudin low subtypes) [36] [51]. Breast cancer patients harbouring TNBCs fail to respond to endocrine therapy [51]. Hence, EGFR is a vital target for anti-cancer therapy for this category of patients.

1.5.2 HER2

The second member of the HER family which is HER2 is a 185 kDa transmembrane protein encoded on chromosome 17 [36]. A mutation (G to A polymorphism) at amino acid codon 655 of the *HER2* gene alters the structure of the receptor transmembrane

domain leading to active HER2 homodimers which ultimately results in continuous uncontrolled growth [36] [48] [54]. This genetic mutation is associated with the risk of breast cancer [36]. Gene amplification or overexpression of the HER2 receptor is found approximately in 9 - 39% of breast cancers [44] [53]. Further, HER2 overexpression is shown to be correlated with an aggressive phenotype of breast cancer with increased rates of recurrence and poorer survival especially in patients with node+ breast cancer [36] [48] [51]. Furthermore, *HER2* gene amplification and protein overexpression have most often been associated with a high cellular proliferation rate, negative receptors for oestrogen and progesterone and also *TP53* mutation, which is linked to metastatic occurrences of breast cancer [51]. As outlined before HER2 is a unique member of the HER family because no known ligand is bound to HER2 with high affinity [36] [49]. Nevertheless, HER2 is able to act as a co-receptor with high affinity for other HER receptors of the family and is the preferred heterodimeric partner [49]. It has been portrayed that homo and heterodimerisation leads to the activation of the HER signalling network and heterodimers are more potent and mitogenic [49]. Heterodimerisation is shown to provide additional phosphotyrosine residues for the recruitment of binding partners which is responsible for strong and prolonged activation of downstream signalling pathways [46] [49]. Moreover, co-expression of HER2 with EGFR and also HER2 with HER3 has been shown to depict an aggressive phenotype compared with the expression of a single HER protein in many carcinomas including breast cancer [49] [53]. Thus, HER2 needs to be considered as an ideal therapeutic target [55]. Monoclonal antibodies directed against HER2 and small molecule tyrosine kinase inhibitors (TKIs) that compete with the ATP pocket in the tyrosine kinase domain of the receptor are used currently in the clinic as HER2 inhibitors against breast cancer

[55]. Nevertheless, many patients with HER2+ metastatic breast cancer demonstrate acquired resistance to these HER2 inhibitors and this remains a major challenge to successful treatment. In this regard additional studies are indeed necessary to determine novel therapeutics and also to retool existing clinical agents which will expand the treatment options available [55]. Furthermore, concurrent blockade of several HER receptors such as EGFR, HER2 and HER3 might result in more significant anti-cancer effects compared with treatment with agents that block a single receptor [53].

1.5.3 HER3

The *HER3* gene, located on chromosome 12 encodes a 180 kDa glycoprotein [48] [56]. HER3 overexpression is found to be associated with poor prognosis in breast cancer and around 22 - 90% of breast cancers overexpress HER3 [53] [57]. HER3 overexpression is often co-expressed with overexpression of EGFR and HER2 [48] [57]. NRG1 binds to HER3 with high affinity [56]. HER3 signalling relies on the formation of heterodimers with other HER family members because HER3 receptor has no intrinsic kinase activity [57]. Even though it is kinase defective, HER3 can be phosphorylated by other receptors such as HER2 [52]. HER2/HER3 has been shown to be the most potent mitogenic heterodimer compared to EGFR/HER2 in HER2+ breast cancer [49] [57]. Thus, many studies have shown that HER3 plays a role in HER2 mediated breast carcinogenesis, as HER3 is commonly co-expressed with HER2 in breast cancer [56] [57]. In this regard, it has been revealed that the efficacy of anti-HER2 therapeutics is related to HER3 inhibition in breast cancer and reactivation of HER3 is reported to contribute significantly to acquired resistance to

these anti-cancer therapies [52] [57]. Furthermore among all HER receptors, when HER3 is phosphorylated it has been shown to have the highest affinity for PI3K and results in a strong activation of the PI3K/AKT signalling pathway promoting cell survival [48] [52] [56] [57]. Thus, HER3 is likely to become increasingly a centre of attention for breast cancer therapeutics.

1.5.4 HER4

HER4 is a 180 kDa transmembrane glycoprotein which is encoded by chromosome 2 [36] [56]. The encoded protein can be activated by both NRGs and ligands of the EGF family including HB-EGF, epiregulin and betacellulin. In contrast to the other HER receptors, overexpression of HER4 has been associated with well differentiated tumours [53] [58]. Thus, HER4 expression is shown to be a favourable prognostic factor with increased survival [36] [51] [58]. Around 58 - 82% of breast cancers overexpress HER4 [53] [58]. Further, HER4 expression has been correlated with ER+ status [58]. Although HER4 has been most often associated with better survival, a few reports have shown no association with survival while some with poor survival in breast cancer [48] [58]. This may be due to co-expression of 2 or more members of the HER family which is shown to be associated with an adverse effect on breast cancer prognosis [58]. Thus, these details may suggest that the combined profile expression patterns of the HER receptor family members may provide more precise information on the breast tumour behaviour than studying the expression of each receptor individually [58].

1.6 Signalling pathways

Fundamentally all HER receptors are in an inactive form and dimerise in response to ligand binding [49]. This dimerisation process which results after ligand binding activates tyrosine kinase mediated phosphorylation [49] [59]. This in turn produces a cascade of metabolic events constituting a complex downstream signalling network. This leads to specific effects of cellular functions such as growth, proliferation, differentiation, migration and survival [59]. However, when receptor function is dysregulated downstream processes may be disrupted, leading to cellular transformation and ultimately malignancy [49]. The RAS activated mitogen activated protein kinase (MAPK) and PI3K/AKT signalling pathways are the 2 most researched components of the HER signalling network [44] [49] [59]. The HER receptors also stimulate the activity of mammalian target of rapamycin (mTOR) pathway via the PI3K/AKT pathway and also the janus kinase (JAK)/signal transducer and activator of transcription (STAT) pathway [47]. Further, oestrogen of the ER pathway has been shown to cross talk with the HER family receptors, providing a mechanism for resistance to hormonal therapy in breast cancer [60]. Furthermore, cross talk between aryl hydrocarbon receptor (AhR) and EGFR pathway has been shown [61]. Thus, targeting downstream signalling events of the above mentioned pathways with anti-cancer therapy will be an effective strategy against breast cancer [47]. A generalised diagram including RAS/MAPK, PI3K/AKT, mTOR, JAK/STAT, ER and AhR pathways demonstrating cross talk between the signalling pathway is shown in the below figure (Figure 1.4). Further, a detailed figure for each signalling pathway is also shown in each section with its description in sections 1.6.1 to 1.6.6.

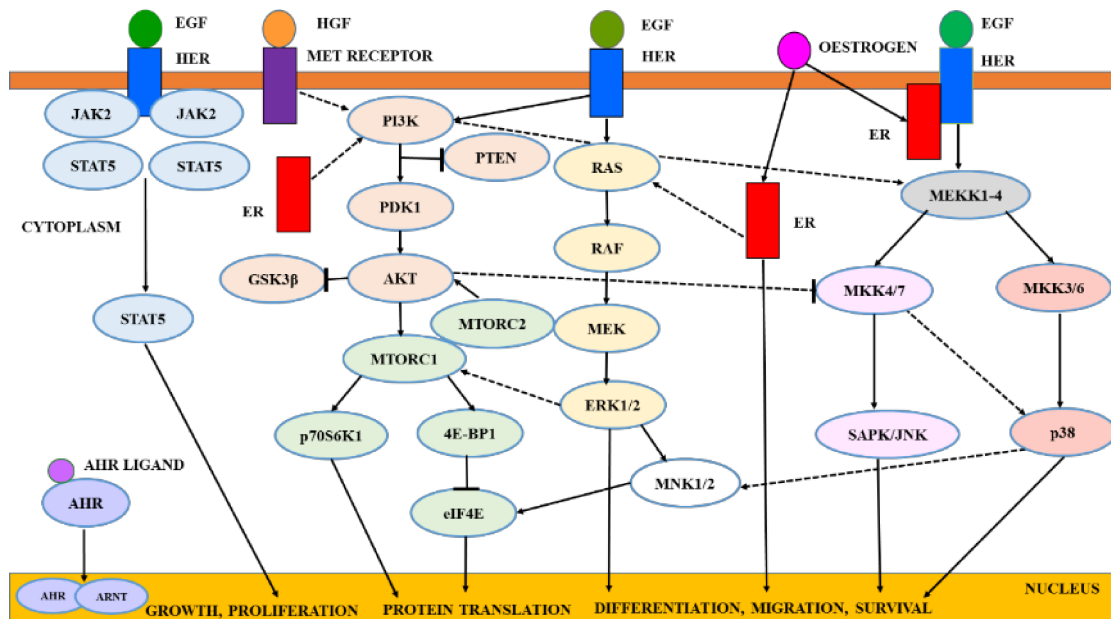


Figure 1.4: Cross talk of signalling pathways - RAS/MAPK, PI3K/AKT, mTOR, JAK/STAT, ER and AhR signalling pathways.

1.6.1 RAS/MAPK pathway

RAS/MAPK pathway regulates fundamental cellular processes such as growth, proliferation, differentiation, migration and apoptosis [62]. In mammalian cells, 3 major MAPK pathways exist. The first includes extracellular signal regulated kinases (ERK). A second cascade involves the activation of stress activated protein kinase/c-Jun terminal kinases (SAPK/JNK) and a third involves p38 MAPK isoforms (α , β , γ , δ) [62] [63].

RAS/MAPK pathway which comprises ERKs is a superfamily of protein serine threonine kinases that are activated by many numbers of stimuli including EGF [47] [63]. When EGF is bound to the receptor, it is phosphorylated on tyrosine residues within the cytoplasmic tail. Growth factor receptor-bound protein 2 (GRB2) and SHC

which are adaptor proteins then bind to the phosphotyrosine residues of the activated receptor. Subsequently, GRB2 then bind to son of sevenless (SOS) which is a guanyl nucleotide-release protein [63]. When the GRB2-SOS complex docks to the phosphorylated receptor, SOS becomes activated. Activated SOS causes the small G protein RAS to release GDP and exchange it for GTP. When RAS has GTP bound to it, it becomes active [47]. RAS is a sub family of H-RAS, N-RAS and K-RAS [62]. It has been revealed that the oncogenic mutations of these human *RAS* genes are uncommon in breast cancer with a low frequency of < 2% of *RAS* mutations [64]. Activation of RAS leads to the activation of the mitogen activated protein kinase kinase kinases (MAPKKK) (RAF). RAF is a sub family of A-RAF, B-RAF and RAF-1 [62]. RAF-1 is also known as C-RAF [62]. C-RAF is mainly found to activate mitogen activated protein kinase kinases (MAPKK)/MAPK/ERK kinase (MEK1/2) [62]. Activated MEK1/2 then phosphorylates and activates MAPK, also known as ERK1/2 respectively [47] [63]. This pathway subsequently results in the enhanced transcription of the anti-apoptotic survival factors such as Bcl-2 family members thereby promoting cell survival in cancer [47] [63].

The SAPK/JNK pathway plays a critical role in physiological processes such as cellular proliferation, differentiation, apoptosis and survival in response to many types of stresses including UV irradiation, growth factors, toxins and cytokines [65] [66]. JNKs are part of a 3 kinase signalling pathway. Activation of JNK are mediated by MAPKKK, MAPKK and MAPK though sequential protein phosphorylation [66]. MAPKKK, typically known as MEKK1 – MEKK4 phosphorylates and activates MKK4 and MKK7. Upon activation MKK4 and MKK7 activate JNKs (JNK1 - 3)

where tyrosine and threonine residues are sequentially phosphorylated in living cells [65]. Activated SAPK/JNK translocates to the nucleus and regulates a diverse set of responses such as induction of apoptosis and enhancing cell survival according to the stimuli, the strength and duration of JNK activation. SAPK/JNK dysregulation has been implicated in cancer. Although the role of SAPK/JNK has been known the underlying mechanism in which this role is established remains controversial [65] [66].

The p38 pathway is also activated by environmental stress responses similar to the SAPK/JNK pathway [62]. MAPKKKs- MEKK1 - MEKK4 are shown to phosphorylate downstream MKK3 and MKK6 which ultimately phosphorylates the p38 isoforms (α , β , γ and δ) [67]. Further, it has been shown that MKK4, the upstream kinase of SAPK/JNK, assists in the activation of p38 α and p38 δ in specific cell types [62] [67]. In fact, overexpression of MAPKKKs results in the co-activation of both p38 and JNK pathways [67]. The downstream signalling of p38 is quite divergent and coordinates cellular processes such as apoptosis, cell cycle progression, growth and differentiation according to specific cell types [62]. Thus, it is evident that all 3 MAPK pathways (ERK, SAPK/JNK and p38) are regulated by cross cascade interactions and loss of control ultimately promotes tumourigenesis (Figure 1.5).

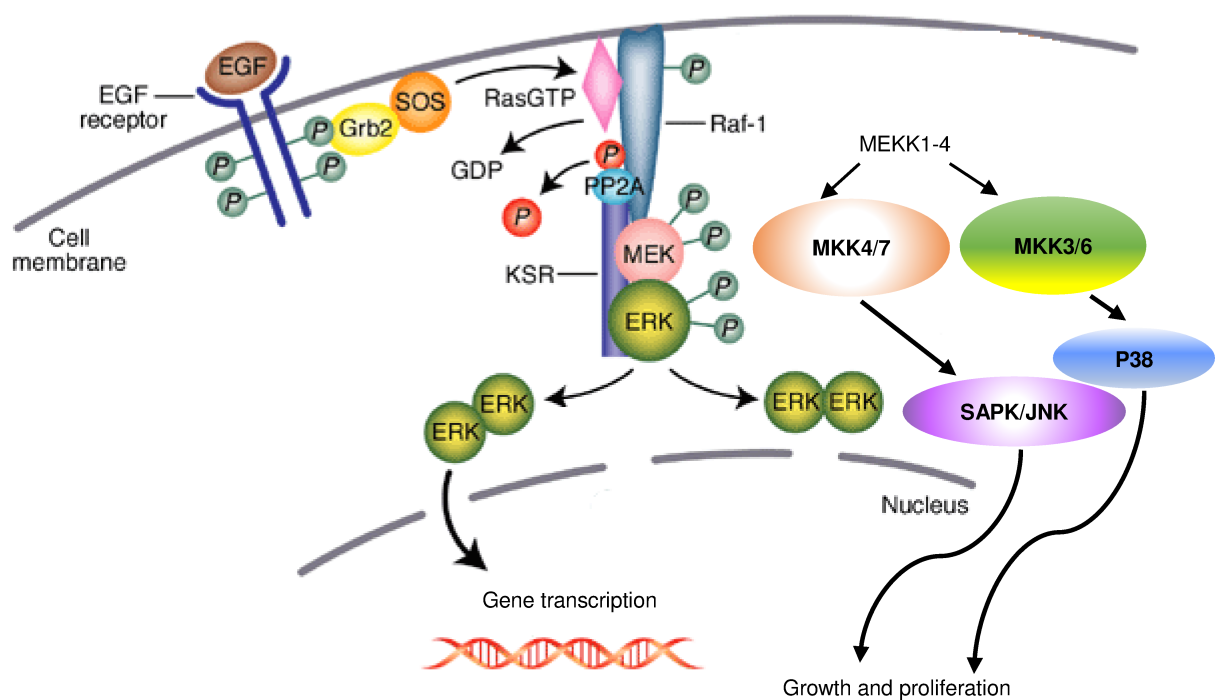


Figure 1.5: The RAS/MAPK pathway. The binding of the ligand to the receptor activates receptor dimerisation and autophosphorylation which is shown by P on tyrosine residues. These residues function as docking sites for many signalling molecules which ultimately activates RAS that starts the cascade of signals. Figure adapted from [68].

1.6.2 PI3K/AKT pathway

PI3K/AKT pathway activation starts with EGF binding to its receptor [47]. This pathway is also involved in cellular functions such as cell growth, proliferation, differentiation, migration and survival. Upon ligand binding, receptor dimerisation takes place. PI3K is then recruited to the plasma membrane mediated by binding of its SH2 domain to tyrosine phosphorylated proteins [47] [69]. PI3K is a heterodimeric protein with a 85 kDa regulatory subunit and a 110 kDa catalytic subunit which has 4

different isoforms (p110 α , p110 β , p110 γ , and p110 δ) [70] [71]. The *PIK3CA* gene, which encodes the p110 α isoform shows a high level (18 - 32.5%) of mutations in breast cancer [72] [73]. Activation of PI3K catalyses the transfer of a phosphate group from ATP to phosphatidylinositol generating a 3'-phosphatidylinositol phosphate (PIP) 2 [47]. PI3K then phosphorylates PIP2 to produce PIP3 [69]. PIP3 is a second messenger that promotes the translocation of AKT to the cell membrane. PTEN dephosphorylates and reduces PIP3 to PIP2, thereby reversing the action of PI3K [69]. Interestingly, around 30% of breast cancer tumours show *PTEN* mutations with low or loss of *PTEN* activity that increases EGF mediated AKT activation and cell survival [47] [74]. Membrane translocated AKT is phosphorylated and activated by phosphoinositide dependent kinase 1 (PDK1) [69]. PDK1 is found to phosphorylate AKT on threonine at position 308 (Thr308). This in turn phosphorylates and inactivates the tumour suppressor complex comprising the tuberous sclerosis complex 1/2 (TSC1 and TSC2), resulting in the activation of mTORC1 by Rheb-GTP [69]. Full activation of AKT occurs only following an additional phosphorylation, on serine at position 473 (Ser473) which is mediated by the downstream, mTOR complex 2 (mTORC2) of the mTOR pathway [69]. Activated AKT then translocates to the cytoplasm and the nucleus after dissociating from the membrane where it phosphorylates multiple proteins involved in cell proliferation and survival [69]. Some of these proteins are members of the Bcl-2 family, glycogen synthase kinase (GSK)-3 β and MKK4 [47]. GSK-3 β is a downstream target for AKT phosphorylation. It has been shown that phosphorylation of AKT inactivates GSK-3 β kinase activity by blocking transcription and regulation of metabolism. This inactivation of GSK-3 β , in turn protects cells from apoptosis. However, the exact mechanism is yet to be determined [47]. Interestingly, it has been demonstrated that AKT phosphorylation

inhibits MKK4 activity of the SAPK/JNK pathway portraying cross talk between pathways [47]. This inhibition prevents activation of JNK which is found to mediate apoptosis in certain cells [47].

Much evidence reveals the importance of the PI3K/AKT pathway in determining sensitivity and resistance of tumour cells with overexpressed HER receptors such as HER2 or tumours with mutated *PTEN* to targeted inhibitors [71]. The PI3K/AKT pathway is disrupted in many types of cancers including breast cancer. It has been found that breast cancers that overexpresses the HER2 receptor maintain high PI3K activity and that HER2 achieves high PI3K activity via HER3 [71]. Further, breast cancer tumours that overexpress HER2 is shown to up-regulate another receptor, c-MET in varying degrees. c-MET and its ligand hepatocyte growth factor (HGF) is shown to be up-regulated in breast tumours resulting in activation of PI3K/AKT pathway [71] [75]. In addition PI3K is also shown to cross talk between the RAS/MAPK pathway since PI3K is found to activate RAS and vice versa leading to increased cell survival in cancer [47] [72] (Figure 1.6).

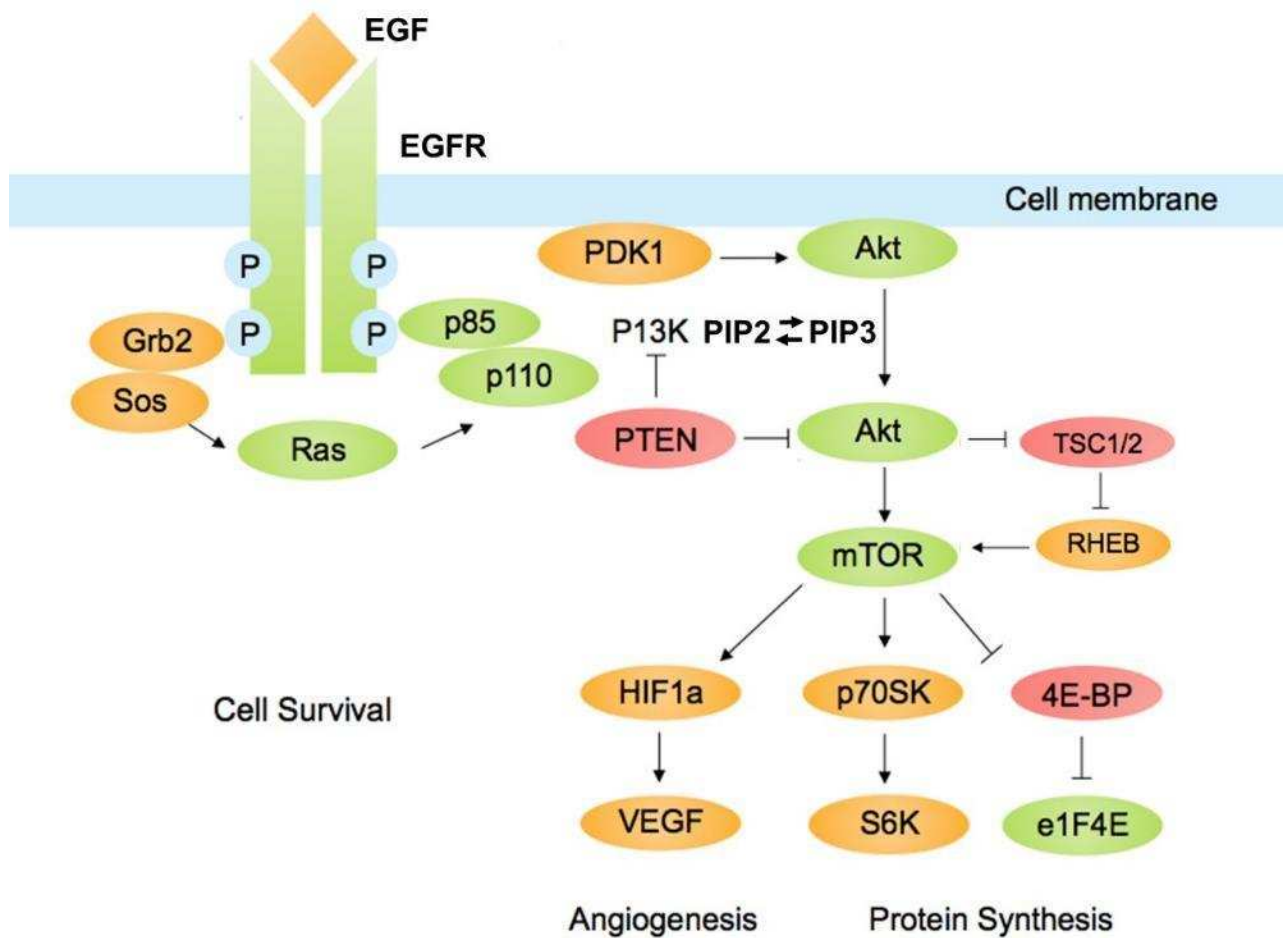


Figure 1.6: The PI3K/AKT pathway. Upon growth factor binding, the receptor activates PI3K which converts PIP2 to PIP3. AKT is then activated following recruitment to the cell surface by PIP3 and acts downstream of PI3K which controls cellular processes such as cell survival. mTOR is one of the key proteins within the signalling cascade which acts both upstream and downstream of AKT. Figure adapted from [76].

1.6.3 mTOR pathway

mTOR is a central regulator of cell growth proliferation and survival. mTOR resides in 2 distinct multi protein complexes, mTOR complex 1 (mTORC1) and mTORC2 [74] [77]. mTORC1 plays a major role in controlling protein synthesis. When PDK1

in the PI3K/AKT pathway activates AKT, this in turn inactivates TSC1/2 leading to activation of mTORC1 by Rheb-GTP [77] [78]. As PTEN negatively regulates the PI3K/AKT pathway, the loss of *PTEN* activity increases AKT activity, which thereby increases mTORC1 signalling [78]. As a result, eukaryotic initiation factor 4E (eIF4E) binding protein 1 (4E-BP1) and phosphorylation of 70-kDa ribosomal S6 kinase 1 (p70S6K1) are phosphorylated by mTORC1 which in turn promotes protein synthesis [74] [77]. The phosphorylation of 4E-BP1 prevents its binding to eIF4E, enabling eIF4E to interact with the scaffold protein eIF4G permitting assembly of the eIF4F complex which will promote cap dependent translation [78]. The second important target of mTOR is p70S6K1. Activation of p70S6K1 results in increased messenger RNA (mRNA) translation including translation of mRNAs that encode for ribosomal proteins, elongation factors and insulin growth factors [79]. mTORC2 which was more recently discovered, promotes cellular survival by phosphorylating AKT serine at position 473 (Ser473) which is required for maximal activation of AKT of the PI3K/AKT pathway as outlined before [77]. A further layer of complexity is added on to this pathway by the negative feedback loop from the mTOR-p70S6K1 pathway to the upstream insulin receptor substrate pathway. Activation of mTORC1 and p70S6K1 controls the insulin receptor substrate pathway through direct phosphorylation on specific residues which prevent its recruitment and binding to receptor tyrosine kinases resulting in a negative feedback regulation in PI3K/AKT and RAS/MAPK pathways. Thus, in human cancer direct inhibition of mTORC1 by anti-cancer agents relieves this negative feedback loop by paradoxically activating AKT. Further, inhibition of mTORC1 may also lead to the activation of ERK1/2 of the RAS/MAPK pathway [78]. Interestingly, eIF4E is also shown to be a target of the RAS/MAPK pathway. It is shown that ERK1/2 and p38 phosphorylates MAP kinase

interacting kinase 1 (MNK1) and MAP kinase interacting kinase 2 (MNK2) in response to multiple extracellular stimuli. Subsequently, MNK1 and MNK2 phosphorylate serine 209 of eIF4E within the eIF4F complex [78] [80]. Thus, MNKs play an important role in controlling cap dependent translation [80]. The existence of these negative feedback loops and cross talk between signalling pathways add complexity and promote cell survival in cancer [69] [77] (Figure 1.7).

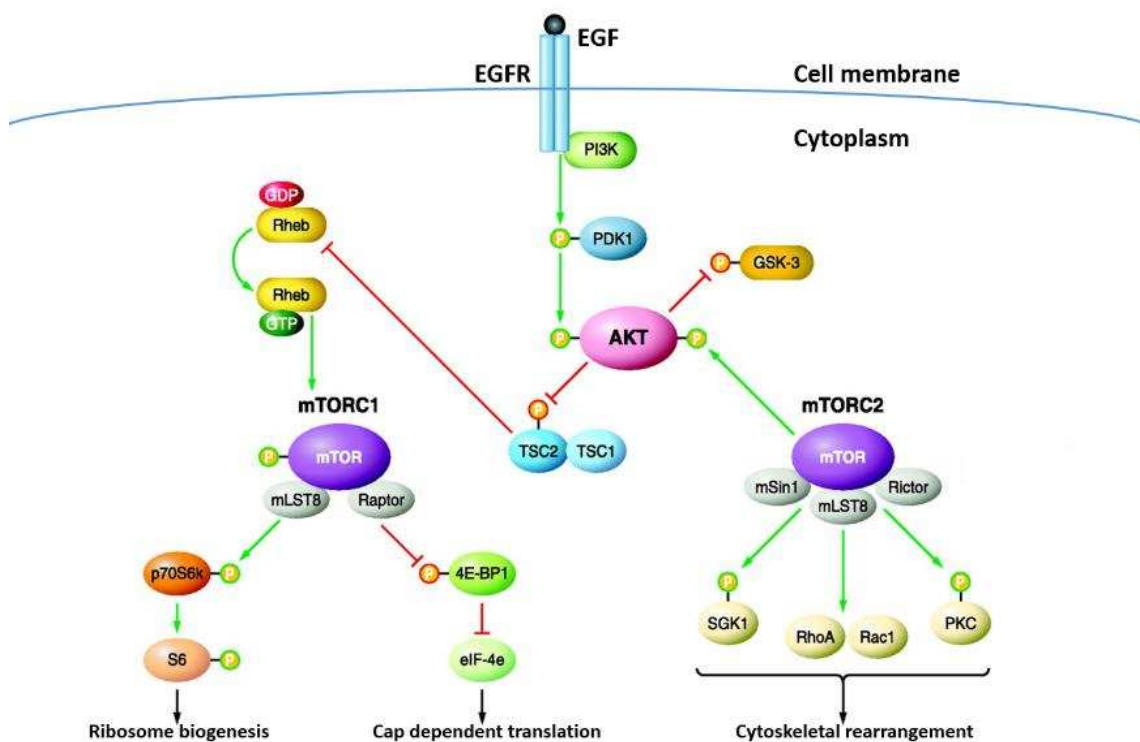


Figure 1.7: The mTOR pathway. mTOR forms complexes with mTORC1 (Raptor) or mTORC2 (Rictor). Activation of the PI3K/AKT pathway leads to mTORC1 activation. AKT is pivotal in mTOR signalling, since it is both an upstream activator of mTORC1 and downstream effector of mTORC2. Figure adapted from [81].

1.6.4 JAK/STAT pathway

EGF also initiates the JAK/STAT pathway which has been implicated in cancer [47]. JAK activation triggers cell proliferation, differentiation, migration and apoptosis [82]. STATs comprise a family of 7 structurally and functionally related proteins - STAT1 - 4, 5A, 5B and 6 and JAKs represent a family of 4 non receptor tyrosine kinases - JAK1 - 3 and tyrosine kinase 2 [47]. Upon ligand binding conformational changes are produced in receptors that alters the alignment of receptor associated JAKs, which allows phosphorylation of particular tyrosine residues that converts inactive JAKs into catalytically active tyrosine kinases [82]. Subsequently, active JAKs phosphorylate tyrosine residues in the cytoplasmic region of the receptor creating binding sites that recruit STATs [82]. STATs are latent proteins that reside in the cytoplasm until activated. STATs can homodimerise or heterodimerise with other types of STAT molecules [82]. Upon dimerisation, STAT proteins are translocated to the nucleus where they activate gene transcription that promotes cellular proliferation, differentiation and survival [82] [83]. Generally cancer cells demonstrate persistent activation of STATs which can contribute to malignancy [84]. Interestingly, in normal cells, STAT5 (both STAT5A and STAT5B) promotes terminal differentiation of mammary epithelial cells necessary for lactation [84]. Further, prolactin a hormone which stimulates lactation during pregnancy induces STAT5 activity through JAK2. However, JAK2/STAT5 has shown controversial activity in breast cancer. Restoring prolactin receptor expression in TNBC cell lines, has been shown to decrease the invasive capacity of the tumours. In contrast, blocking JAK2/STAT5 activity in luminal breast cancer cell lines increases invasiveness, suggesting that prolactin activation of STAT5 restricts the metastatic potential of TNBC [84]. Taken together

this implies that STAT5 activity may show a suppressive role or an invasive role depending on the subtype of breast cancer [84]. Furthermore, it has been shown that hyper-activation of the JAK2/STAT5 interaction in cancer may actually drive resistance to PI3K/AKT/mTOR inhibitors. Thus, dual inhibition of PI3K/AKT/mTOR and JAK2/STAT5 may have an added benefit to circumvent anti-cancer drug resistance [84] (Figure 1.8).

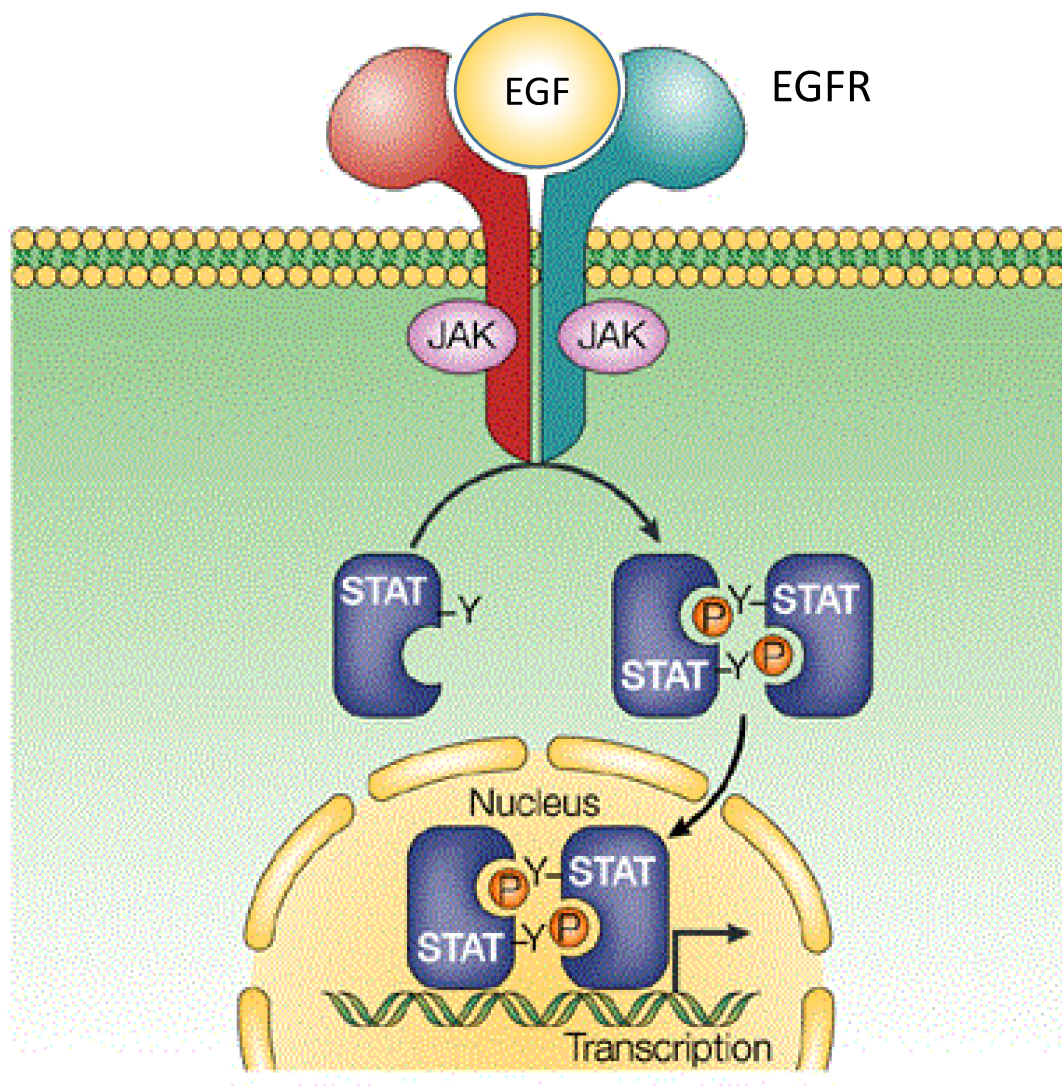


Figure 1.8: The JAK/STAT pathway. The binding of ligands to the receptors activate JAKs, enhancing their kinase activity, which in turn recruits STATs to the receptors where they are phosphorylated by JAKs. Activated STATs form homo or heterodimers and accumulate in the nucleus where they promote cellular processes. Figure adapted from [85].

1.6.5 ER pathway

Oestrogen plays a major role in the mammary gland by initiating growth, development, reproduction, and maintenance. Oestrogen also plays a role in breast cancer development and progression [86]. Binding of oestrogen to ER, induces receptor phosphorylation, modifies its conformation and triggers receptor dimerisation [60]. Subsequently, the ligand activated ER translocates to the nucleus and stimulates gene transcription [86]. These transcriptional effects of the ER are modulated by interactions with coregulatory proteins that function as either coactivators or corepressors [60]. The transcriptional outcome of ER is controlled by dynamic chromatin modifications of the histone tails, and ligand bound ER facilitates these modifications *via* recruitment of coregulatory proteins [86]. For instance, coactivators such as steroid receptor coactivator 1 (Src)1 and amplified in breast cancer (AIB1/Src3) have been demonstrated to possess histone acetyltransferase activity which is favoured by the altered conformation of ER that increases gene expression. In contrast, corepressors are associated with histone deacetylases [60] [86]. Interestingly, each coregulatory protein does not perform an overlapping function *in vivo*. However, in cancer, expression of coregulatory proteins is distinct from normal tissue and their functions are altered resulting in tumour progression [86]. For instance, coactivators such as Srcs exhibit elevated expression in breast cancer and they are known to play a role in the development of breast cancer [87] [88]. Furthermore, ER has shown to function as a coactivator protein itself by binding to other transcription factors and recruiting acetyltransferase activity [87]. ER localised outside the nucleus, on the cell membrane and within the cytoplasm is involved in activating receptor tyrosine kinases, such as EGFR, HER2 and also PI3K/AKT and RAS/MAPK

pathways demonstrating cross talk between signalling pathways. This process involves activation of Srcs and matrix metalloproteinases (MMP) which helps to activate the HER networking cascades. This provides another mechanism for the growth promoting effects of oestrogen, which in turn may contribute to hormonal therapy resistance in breast cancer [60] [87] [89] (Figure 1.9).

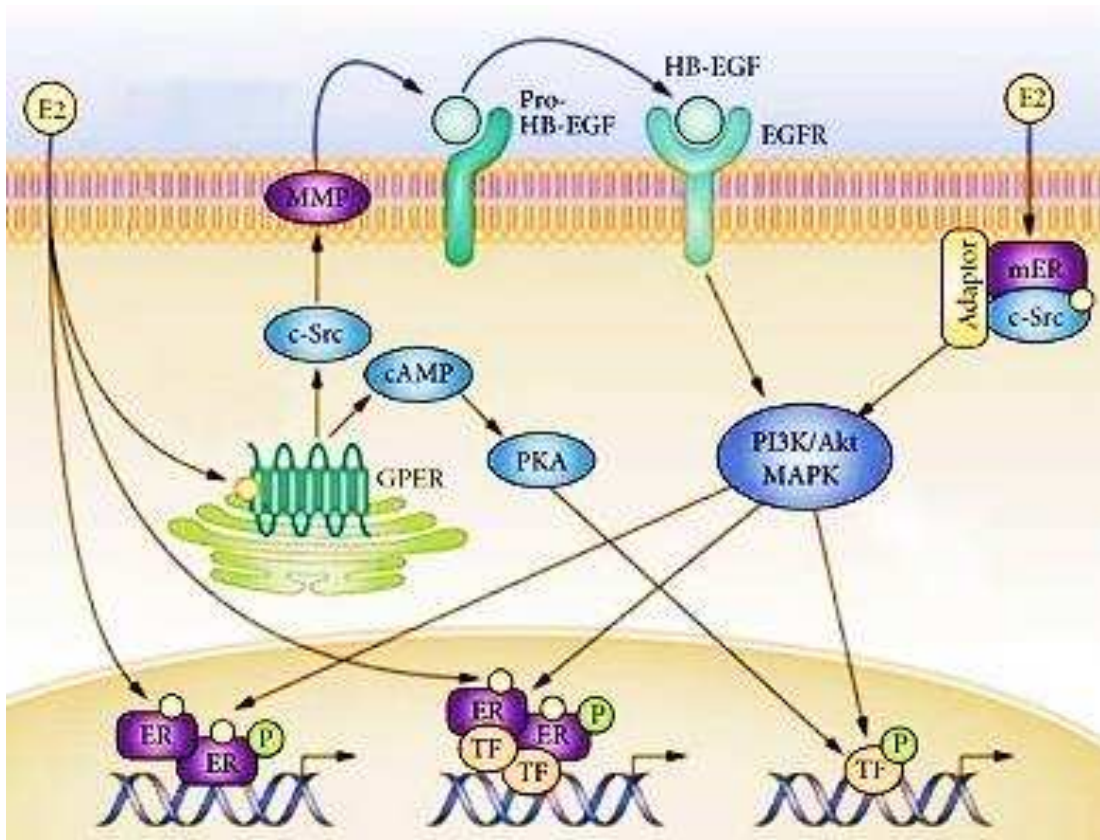


Figure 1.9: The ER pathway. Oestrogen which is shown as E2 in the diagram phosphorylates (which is shown by P) nuclear ER and dimerises the receptor, that promotes gene transcription. Membrane bound ER and cytosolic ER are also activated by oestrogen which in turn interacts with signalling molecules such as Src that mediates signalling via RAS/MAPK and PI3K/AKT cascades. Figure adapted from [90].

1.6.6 AhR pathway

AhR is highly expressed in the breast [91]. It is a ligand activated transcription factor that induces expression of genes encoding drug metabolising enzymes, such as cytochrome p450 (CYP) - CYP1A1, CYP1A2 and CYP1B1 [92]. AhR is shown to have a physiological function by detoxification of environmental pollutants [93]. AhR was first discovered as the receptor that binds to 2,3,7,8-tetrachlorodibenzo-p-dioxin (TCDD) with high affinity; which is described as a tumour promoter [91] [92]. It has been shown that when TCDD is bound to AhR; it is capable of sustaining hyperactivation, resulting in a number of toxicological outcomes such as liver and skin carcinogenesis in rodents [91]. AhR is constitutively present in the cytosol as an inactive complex together with a 90 kDa heat shock protein 90 (Hsp90) and a chaperone protein, p23. Hsp90 serves as a chaperone for AhR, preventing nuclear translocation in the absence of a ligand and also by preventing premature dimerisation with DNA binding partners while keeping AhR in a configuration that favours ligand binding [92] [94]. The hydrophobic ligands that bind to AhR, enter the cell by diffusion. Ligand binding triggers a conformational change in AhR that increases the affinity of AhR for DNA, and slowing the rate of ligand dissociation. This event releases AhR from the cytosolic complex and promotes nuclear translocation. Following translocation into the nucleus, AhR heterodimerises with the aryl hydrocarbon receptor nuclear translocator (ARNT), which is also known as hypoxia inducible factor 1 β (HIF)-1 β [92] [94]. Transcription is activated following binding of this heterodimer to xenobiotic responsive elements (XRE) or to the core binding motif of dioxin responsive elements within the promoter regions of genes in the AhR battery [92]. This then activates AhR controlled genes that encode phase I and phase II drug

metabolism enzymes such as CYP1A1. These CYP enzymes favour AhR agonists and activation of this signalling pathway appears as a defence system aimed at the elimination of the inducer and its metabolites [92] [94]. Many signalling pathways are implicated to cross talk with the AhR pathway thus, AhR has shown to influence cellular functions including cell proliferation, vascularisation and hypoxia [61] [92]. Some of these signalling pathways include ER, EGFR, RAS/MAPK [94] [95]. Research has demonstrated that AhR ligands such as TCDD are able to activate EGFR and in contrast it has been depicted that EGFR ligands are able to block AhR signalling in an autocrine/paracrine manner [61] [96]. Further, depending on the cell type investigated, TCDD has been shown to activate the RAS/MAPK pathways by activating ERK1/2, SAPK/JNK and p38 [97]. On the other hand, MAPKs are also known to regulate AhR demonstrating mutual cross talk between AhR and RAS/MAPK pathways [97]. Thus, it seems that AhR signalling impinges upon number of signalling molecular pathways and the exact molecular mechanisms by which AhR ligands exert their effects still remain ambiguous as further investigations are warranted to determine the cross talk between AhR and other signalling pathways [92] [94] [97] (Figure 1.10).

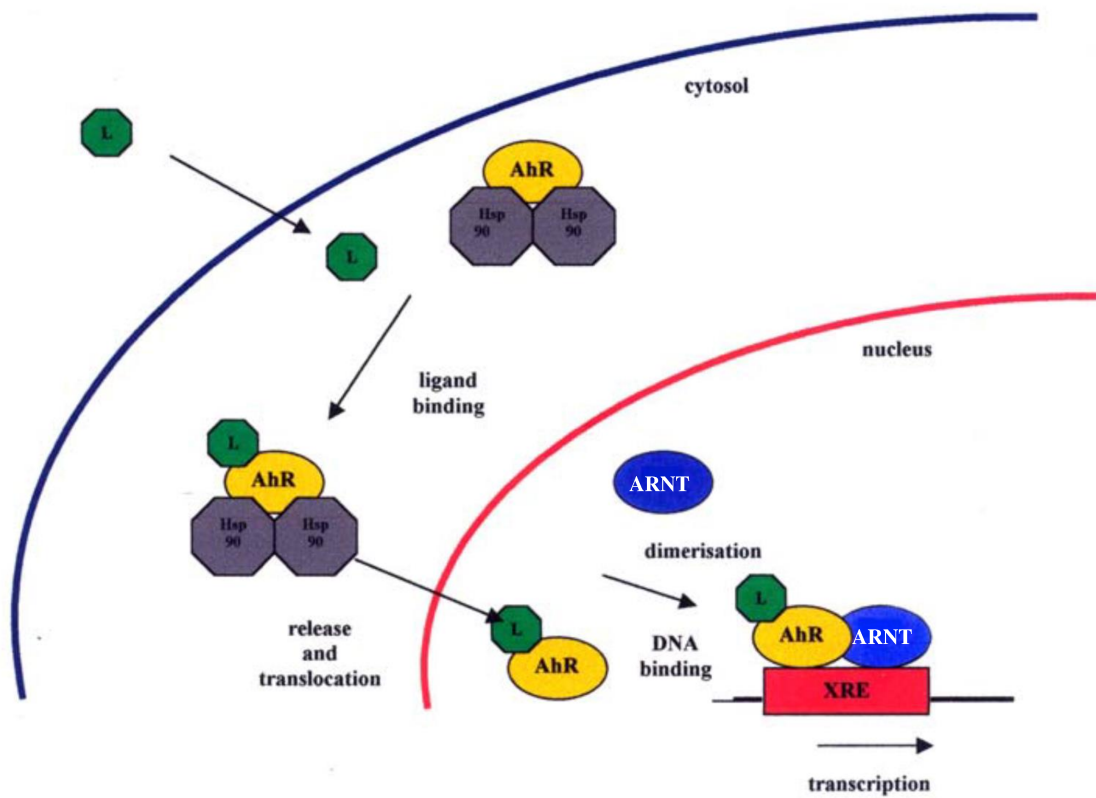


Figure 1.10: AhR pathway. Ligand binding triggers conformational changes in the AhR/Hsp90 complex which promotes AhR nuclear translocation leading to AhR heterodimerisation with ARNT. This results in changes in the chromatin structure allowing transcription of AhR controlled genes. Figure adapted from [92].

1.7 HER mediated signalling as a target for cancer therapy

The importance of the HER family, especially EGFR, HER2 and the HER mediated signalling pathways has been discussed. Targeting these pathways by anti-cancer therapy to increase survival responses in breast cancer is important [47]. Targeted anti-cancer therapy, aims at specific genes or proteins which contribute to cellular growth, proliferation and survival in cancer as outlined before. Further, targeted therapy is potent and interestingly less toxic to normal cells which is tailored to an individual patient's tumour specifications. There are many targeted therapies available currently for mostly all breast cancer molecular subtypes, exploiting the different drivers of breast carcinogenesis within these individual tumours [19]. Some of these agents have shown remarkable activity in the clinic. However, there are yet some challenges involved with targeted therapy such as matching the precise molecular subtype of breast cancer with the targeted agents and also acquired and primary resistance to these therapies. It is demonstrated that acquired resistance is common and ultimately develops in most patients with advanced disease, which could be due to cross talk and up-regulation of compensatory signalling pathways associated with the HER family network [19].

1.7.1 Clinically available targeted pharmacological agents

TKIs and monoclonal antibodies are 2 frequently used clinically available approaches to target the HER family [45]. As described before EGFR is highly overexpressed in breast cancer. Gefitinib and Erlotinib are reversible small molecule inhibitors of the intracellular tyrosine kinase domain of EGFR which is mainly used for advanced non–

small-cell lung cancer [98] [99]. Interestingly, Gefitinib is shown to inhibit other HER receptors such as HER2 as well. Although initially used for advanced non–small-cell lung cancer, Gefitinib is shown to inhibit the growth of a range of human cancers such as breast, colon, ovarian and gastric cancers both *in vitro* and *in vivo* [100]. It has been shown that *in vitro*, Gefitinib inhibits EGFR kinase activity potently with very low concentrations. Further, it has been shown that Gefitinib inhibits the growth of human cancer cells *in vitro* and *in vivo* by inhibiting molecular signalling pathways thereby inducing cell cycle arrest and/or apoptosis [100]. Erlotinib is also shown to be active in a similar tumour subset to Gefitinib with a related mechanism of action [98]. Although, Gefitinib is a highly promising molecular targeted anti-cancer agent, the results from monotherapy clinical studies of advanced breast cancer patients have been relatively unsuccessful. This may reflect inadequate patient selection that will better predict those patients likely to respond favourably to these EGFR inhibitors [21]. Moreover, EGFR overexpression and response to EGFR inhibitor therapy may not appear straight forward due to the complexity of the HER signalling network as outlined [100]. Most often c-MET amplification has been reported in many patients, which contribute to resistance of Gefitinib [101]. Furthermore, toxicities such as diarrhoea, nausea and skin rashes correlated with the EGFR inhibitors limit the use of these agents [98] [102].

HER2 overexpression is also associated with aggressive disease and decreased survival in breast cancer as mentioned before [53]. Thus, taking into consideration the role that HER2 plays in this disease, a number of therapeutic approaches have been developed. Trastuzumab, was the first humanised anti-HER2 monoclonal agent that

was approved for therapeutic use for breast cancer patients with HER2+ tumours. As HER2 activates multiple cellular signalling pathways such as RAS/MAPK and PI3K/AKT, Trastuzumab is able to bind to HER2 and reduce the signalling of these pathways promoting cell cycle arrest and apoptosis [103]. Despite the advances that have been brought by Trastuzumab, many patients with HER2+ metastatic breast cancer who initially responded to Trastuzumab ultimately develop resistance [55]. This has been shown as mainly due to increased signalling via the PI3K/AKT pathways or loss of function of the *PTEN* gene which is the negative regulator of AKT that results in resistance to this agent [55].

Thus, resistance to anti-HER2 therapies have shown to arise as a result of aberrant activation of signalling pathways downstream of the HER2 receptor such as PI3K/AKT and also due to activation of compensatory pathways such as c-MET in order to rescue cancer cells from the inhibitory effects of blocking just one target or one pathway [55]. In this regard, identification of specific patient populations according to molecular subtypes of breast cancer who are likely to benefit from targeted therapy might be a crucial step towards making targeted therapy effective in the clinic. For those patients in which HER signalling represents a dominant driving force in cancer progression, it is unlikely that these patient populations will achieve durable disease control by just monotherapy [21]. This is especially relevant with reference to the HER receptor family members that are known to be mostly interdependent and are found to interact with each other in signal transduction, although in certain cases monotherapy has shown efficacy [19] [21]. Thus, the use of a combination approach that will combine existing molecular targeted agents that may

act on 2 or more signalling pathways and also on compensatory pathways might improve outcomes. Further, this will improve the effects of the agents relative to using as single agents.

Further, it is important that continued research takes place in order to optimise targeted agents that are already in the clinic. One approach would be reducing toxicities in order to improve the quality of life of patients receiving these agents. Nanotechnology based drug delivery systems can be used to reduce such toxicities [104] [105]. In addition, fuelling the design of novel targeted therapies taking into consideration the interactions of the HER family signalling is very crucial. This is because development of new targeted agents is yet a slow process with particularly high failure rates [106]. Most of these novel agents fail during clinical trials. These clinical trials help to identify the effectiveness and the safety of novel agents in humans [107]. Number of clinical trials have been conducted with TKIs and monoclonal antibodies either alone or in combination. Section 1.7.2 summarises the findings of a few major clinical trials carried out in the recent past with anti-HER agents.

1.7.2 Clinical trials of targeted pharmacological agents

In the beginning, TKIs such as Gefitinib and Erlotinib were indicated for second and third line treatment for patients with advanced non–small-cell lung cancer after failure of at least one initial platinum treatment [108]. As stated before, however, Gefitinib as a monotherapy has showed only low activity and the response rates have not shown significant improvement in patients with breast cancer [21] [109]. Nevertheless, many

reports have shown that combining Gefitinib with other anti-cancer agents enhanced the effect of Gefitinib in patients with breast cancer [109]. Further, monoclonal antibodies such as Trastuzumab has shown successful improvements in patients with metastatic HER2+ breast cancer which helped it to gain food and drug administration (FDA) approval in 1998. Many clinical trials to date have studied its role in adjuvant, neoadjuvant and in a metastatic setting. In 1998, Trastuzumab was first approved as a first line therapy to be administered in combination with Paclitaxel and also to be administered as a single agent for patients who have failed one or more chemotherapy regimens before [109]. Pivotal clinical trials have shown that when this agent was combined with other anti-cancer agents the results were more impressive than it was used as a single agent in both early stage and metastatic breast cancer [110].

There have been number of clinical trials lately, which have showed the efficacy of novel targeted agents alone and in combination for HER2+ breast cancer. Ado-Trastuzumab-Emtansine (T-DM1) is a novel therapy for HER2+ cancer. This is an antibody drug conjugate where Trastuzumab is linked with a potent microtubule inhibitor named Emtansine. When T-DM1 alone was compared with Trastuzumab and Docetaxel as a first line treatment in patients with metastatic breast cancer in a phase II clinical trial, it was found that T-DM1 demonstrated a favourable safety profile with a significant 5 month improvement in progression free survival compared to Trastuzumab and Docetaxel. These results were validated in the MARIANNE trial which ended in 2014 [110]. This trial evaluated 3 HER2 targeted regimens in previously untreated metastatic and locally advanced HER2+ breast cancer patients. The targeted agents included T-DM1, Trastuzumab and Pertuzumab. Pertuzumab is a

novel humanised monoclonal antibody that inhibits the dimerisation of both HER2 and HER3. The trial looked at the efficacy of T-DM1 with or without Pertuzumab which was compared to Trastuzumab with a taxane. The results showed similar progression free survival among the 3 arms [110]. The CLEOPATRA trial looked at first line treatment of Pertuzumab, Trastuzumab and a taxane (Docetaxel) which was compared with a placebo, Trastuzumab and Docetaxel in HER2+ metastatic breast cancer patients. They found that, Pertuzumab, Trastuzumab and Docetaxel improved overall survival providing an increase of survival of 15.7 months [111].

The results of these clinical trials validate that the successful development of novel agents such as T-DM1 and Pertuzumab, and also the effects of Trastuzumab, have helped to improve the disease biology by treating the underlying molecular driver. These new HER2+ targeted therapies such as Pertuzumab and T-DM1 are now being used in the clinic and have earned regulatory approval based on the data of clinical trials. However, it should be noted that, while the results associated with breast cancer has been dramatically improved with the use of these targeted agents, resistance to these approaches such as cross talk still remain as an unmet clinical need. Thus, it is very important to understand the mechanisms of resistance which leads to improving existing therapeutic agents and developing novel therapeutic agents.

Therefore, a number of clinical, currently experimental and novel pharmacological agents were tested as single agents and in combination against the chosen panel of breast cancer cell lines. All agents tested are described in section 1.9. Nanotechnology

was also incorporated to increase effectiveness and reduce toxicities of existing clinical agents and also to develop novel agents targeting HER2+ breast cancer, thereby enhancing the element of personalised medicine.

1.8 The importance of nanomedicine for cancer therapy

Nanotechnology is positively impacting healthcare and the application of nanotechnology to healthcare is known as nanomedicine [105]. Nanomedicine is the design and development of tools for treatment, diagnosis and imaging. The recent success in nanomedicine applications has heightened the awareness in this area, which has accelerated the pace of discovery of more complex nanoscale systems. Nanomedicine uses nanoscale particles typically in the range of 1 – 1000 nm [104]. Due to this nanoscopic size, nanoparticles (NPs) become ideal vehicles for drug delivery [112]. The main goals of drug delivery systems are specific drug targeting and delivery, reducing toxicity of the free drug to non-target organs while maintaining the therapeutic effects, ease of crossing biological membranes such as the blood brain barrier and overcoming inherent or acquired drug resistance [105]. The successful clinical translation of a therapeutic drug delivery system warrants optimisation of a few important variables such as variation in the composition of the carrier system, drug encapsulation efficiency, particle size, surface hydrophilicity, density of possible ligands for targeting [113].

Nanomedicine can reach a tumour by passive targeting or by active targeting. Passive targeting is based on the size of the NP and also the leaky neovasculature of the

tumour. Thus, NPs demonstrate enriched biodistribution via leaky vasculature surrounding the tumours by the enhanced permeability and retention (EPR) effect. By this effect tumours are able to retain more NPs than other tissues. The lymphatic drainage system is also impaired in tumours, further entrapping NPs. Moreover, with the longer blood circulation time achieved by nanomedicine, the accumulation of NPs through the EPR effect increases within the tumour. In active targeting, targeting ligands are attached at the surface of the NPs for binding to certain receptors expressed at the target site while eliminating off target adverse effects in normal tissues. These ligands for instance are antibodies, affibody molecules, nucleic acid aptamers or carbohydrates. The binding affinity of these ligands influences the penetration to the diseased site which might be triggered by receptor mediated endocytosis [112].

A further advantage of drug delivery systems is that the encapsulated drug is released in a controlled manner ensuring that optimal concentrations are maintained for a desired duration at the tumour site. NPs may commonly release the encapsulated drug by diffusion or alternately drug release can be triggered by the environment or other external events such as variations in pH, temperature, or the presence of an analyte such as glucose. Thus, controlled release by NPs may increase the efficacy of the drug and enhance the facility to use highly toxic and poorly soluble drugs [113].

There are various nanomedicine vehicles researched and some of them for example are liposomes, dendrimers, polymers and proteins [105]. Out of most of these vehicles, protein based drug carriers are shown to be superior due to being naturally self-

assembled subunits, being biocompatible and biodegradable which is associated with low toxicity. Protein cages which is a sub group of protein based carriers have emerged to overcome some of the drawbacks of other carriers such as polymer based drug delivery systems due to their uniform nanometer size. This size allows loading of relatively even amounts of delivery drug, and avoidance of random macromolecular aggregation of NPs. The interior and exterior of protein cages can also be easily modified chemically and genetically, without affecting the whole architecture for encapsulating drugs or for attaching targeting ligands [107]. Some of the commonly used proteins cages are ferritin/apoferritin (AFt), viral capsids and small heat shock proteins [114]. Human AFt was chosen as a targeted NP in the current study because human AFt is extracted from bodily tissues and it links nanomedicine with personalised medicine perfectly. The results associated with AFt NPs are described in chapters 4 and 5.

At present a variety of therapeutic nanodrugs have been exploited by number of researchers. However, there are only a few approved agents in clinical practice. Some of these drugs are used to treat breast cancer. Doxil a Doxorubicin encapsulated liposome is the first nanodrug to gain FDA approval to treat acquired immune deficiency syndrome-associated Kaposi's sarcoma. As of 2003, this agent is used for metastatic breast cancer. Doxil liposomes entail a single lipid bilayer membrane composed of hydrogenated soy phosphatidylcholine and cholesterol with an internal compartment encapsulated with Doxorubicin. The vesicle has a size of 80 - 90 nm. Around 15,000 Doxorubicin molecules are encapsulated within the internal compartment as Doxorubicin is a small molecule. In order to accumulate at the tumour

site via the vascularity of the tumours, Doxil vesicles depend on a passive targeting mechanism along with the EPR effect. Further, it has been shown that the long circulation which is around 2 to 3 days enhances the distribution throughout the tumour site compared to Doxorubicin which has a half-life of around 5 min *in vivo*. Many studies have also shown that the efficacy of Doxil is a lot higher than the free drug. Regardless of its longer circulation time compared to the free drug, Doxil has shown less severe side effects than Doxorubicin. In particular, Doxil has demonstrated a drastic decrease in the cardiotoxicity for which cardiotoxicity is the dose limiting side effect of the free drug. Phase I and II clinical trials with Doxil has demonstrated that the cardiotoxicity in solid tumour patients was negligible attributed to minimal distribution of Doxil in the heart [107].

Abraxane which is a Paclitaxel encapsulated albumin is given to patients with advanced breast cancer. Albumin has shown to be an ideal vehicle for nanomedicine as it is a natural carrier due to biocompatibility. Paclitaxel has been broadly used as a chemotherapeutic agent for many types of cancers, however, the original formulation has showed a number of adverse reactions in patients, such as acute hypersensitivity. Thus, a nonpolar carrier had been used due to Paclitaxel's hydrophobic nature to make it clinically viable. In this case, albumin has worked as an ideal carrier as it is a natural carrier of hydrophobic molecules such as hormones and vitamins with favourable noncovalent binding interactions in the human body. The nanoconjugates of Paclitaxel and albumin are synthesised by mixing the agent with human serum albumin in an aqueous solvent by passing the solution through a high pressure jet, resulting in nanoparticles in the size of around 130 nm. Upon injection into biological systems,

the NPs dissolve swiftly into 10 nm complexes consisting of albumin molecules that is bound to Paclitaxel. This agent uses passive targeting to reach its target. Abraxane has demonstrated not only to decrease toxicity of the free drug but also to increase the efficacy of the drug in patients with advanced breast cancer. This increased efficacy has been suggested to be because of enhanced uptake and an increased transport into cancer cells [107]. These successful nanodrug examples verify that nanomedicine could improve the properties of cancer therapeutics effectively.

In the recent, past number of NP platforms have been screened and studied by many researchers. However, one of the largest challenges that these NP formulations faces at present is meeting all the safety guidelines required for gaining clinical acceptance, such as those required by the FDA and other regulatory bodies. Thus, the use of biocompatible natural carriers such as AFt may have an added advantage [107].

1.9 Agents tested in the current study

Number of clinically available agents, currently experimental agents and entirely novel pharmacological agents were tested in the current study. Below table (Table 1.3) will summarise whether each agent tested is currently in clinical use, an experimental agent or whether it is a totally novel agent. Further, the molecular target of the agent and a brief description of the agent's activity is also shown. Furthermore, an enhanced description is also given for some of the agents used in the study between sections 1.9.1 and 1.9.14.

Agent	Novel, experimental or in clinical use	Molecular target of the agent	Brief description of the agent's activity
EGF	Experimental	EGFR	Binds to EGFR and activates the HER family network.
Gefitinib	Clinical	EGFR	Binds to EGFR and inhibits the activation of the HER family network.
Erlotinib	Clinical	EGFR	Binds to EGFR and inhibits the activation of the HER family network.
Raloxifene	Clinical	ER	Binds to ER and prevents the transcription activation of genes that contain the estrogen response element in the mammary tissue.
Heavy (H) or Light (L) chain-AFt-fusion protein	Novel	HER2	Binds with high affinity to the HER2 receptor and inhibits the activation of the HER family network.
H-AFt-encapsulated-Gefitinib	Novel	EGFR	Released Gefitinib from the H-AFt cavity will bind to EGFR and inhibit the activation of the HER family network.
Trastuzumab	Clinical	HER2	Binds to the HER2 receptor and inhibits the activation of the HER family network.
Sirolimus	Clinical	mTOR	Binds to cytosolic FK-binding protein 12. The Sirolimus- FK-binding protein 12 complex inhibits mTOR.
CGP57380	Clinical	MNK1 and MNK2	Binds to MNK1 and MNK2 of the RAS/MAPK pathway and inhibits the activity of MNK1 and MNK2.
5F 203	Experimental	AhR	Binds to AhR as an AhR agonist which is followed by induction of CYP1A1 that converts 5F 203 to a nitrenium ion that is potent in certain cancer cells.
Gedatolisib (MS-73)	Experimental	PI3K and mTOR	Binds to PI3K and mTOR by competing with the ATP binding sites of these molecules and inhibits the activity of PI3K/AKT and mTOR pathways.
MS-74	Novel	PI3K and mTOR	Binds to PI3K and mTOR by competing with the ATP binding sites of these molecules and inhibits the activity of PI3K/AKT and mTOR pathways.
MS-76	Novel	PI3K and mTOR	Binds to PI3K and mTOR by competing with the ATP binding sites of these molecules which in turn inhibits the activity of PI3K/AKT and mTOR pathways.

Table 1.3 Agents tested summarising their molecular target and activity [70] [78] [92] [108] [115] [116] [117].

1.9.1 EGF

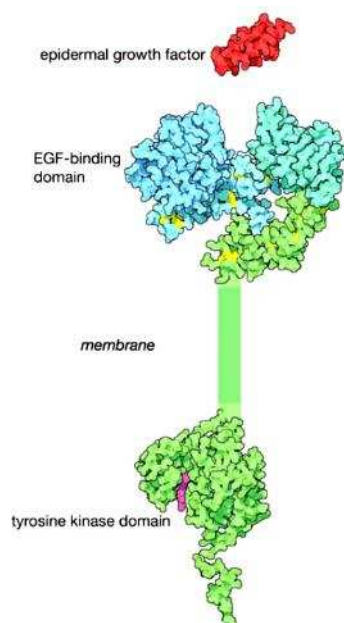


Figure 1.11: EGF (shown in red) binds to the extracellular domain of its receptor which is EGFR (shown in blue). Figure adapted from [118].

EGF belongs to an extensive class of growth factors [119]. It is a 6,045 Da protein with 53 amino acids that has distinct biological properties [119]. It has been shown that levels of EGF is higher in females compared to males. It is further enhanced by pregnancy and exogenous hormones in females which are conditions that drastically alter mammary gland growth [120]. EGF specifically binds to EGFR and activates an extensive network of signalling pathways as mentioned before, thus, EGF may regulate growth of mammary epithelium [47] [120]. The effect of EGF was investigated against the panel of breast cancer cell lines in the current study. Recombinant, human EGF expressed in *E. coli* was used. This is demonstrated to be identical to human EGF except for an additional N-terminal methionine [121].

1.9.2 Gefitinib

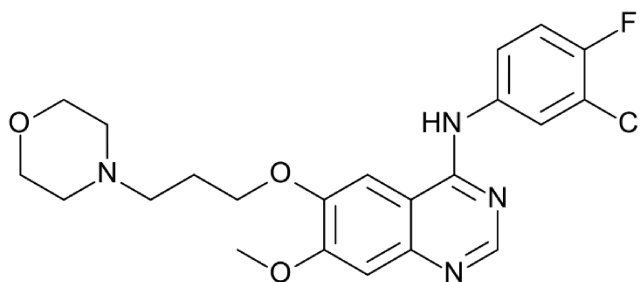


Figure 1.12: Chemical structure of Gefitinib. Figure adapted from [122].

Gefitinib, which is a small molecule also known as Iressa or ZD1839 (AstraZeneca Pharmaceuticals) is an orally active non-peptide anilinoquinazoline compound that inhibits the tyrosine kinase activity of EGFR [123]. Gefitinib was first approved for clinical use in patients with non-small-cell lung cancer in May 2003 as a third line therapy. In June 2005, FDA withdrew approval for this agent due to lack of evidence of extended life and back in July 2015 the agent gained approval from the FDA to be used in non-small-cell lung cancer as a first line therapy [124]. The molecular weight (MW) of Gefitinib is found to be 446.9 Da. Gefitinib competes with the binding of ATP to the tyrosine kinase domain of EGFR. As a consequence, Gefitinib inhibits receptor autophosphorylation thereby inhibiting signal transduction [125].

1.9.3 Erlotinib

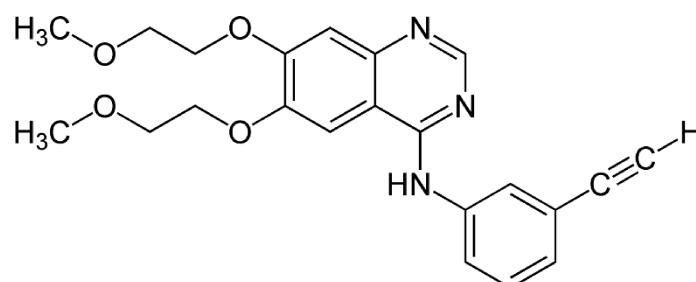


Figure 1.13: Chemical structure of Erlotinib. Figure adapted from [122].

Erlotinib is a small molecule which is also known as Tarceva (OSI Pharmaceuticals). It is an orally active non-peptide anilinoquinazoline compound that inhibits the tyrosine kinase activity of EGFR similar to Gefitinib. The MW of Erlotinib is 429.9 Da [99] [108]. Erlotinib received full approval from the FDA in November 2004 for treatment in patients with metastatic or locally advanced non-small-cell lung cancer after failure of prior chemotherapy and in 2013 this agent received approval as a first line therapy for patients with metastatic non-small-cell lung cancer [126].

1.9.4 Raloxifene

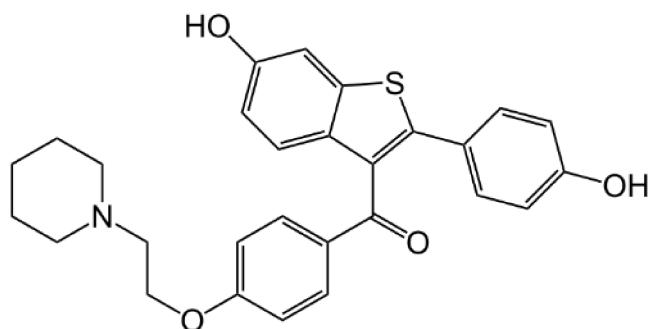


Figure 1.14: Chemical structure of Raloxifene. Figure adapted from [122].

Raloxifene also known as Evista (Eli Lilly and company) is a second generation selective oestrogen receptor modulator (SERM). It has a MW of 473.5 Da [122]. It is currently used for the reduction of the risk of development of invasive breast cancer in postmenopausal women with osteoporosis and in postmenopausal women at high risk for invasive breast cancer [115] [122]. Raloxifene is shown to act as an ER antagonist by competing with oestrogen for binding to ER and also by causing conformational changes that block interactions of ER with coactivators in the breast and uterus [122] [127]. In contrast, Raloxifene is shown to act as an oestrogen agonist in the bone [122]. Raloxifene received FDA approval in September 2007 [128].

1.9.5 AFt (H and L chains) and affibody molecules

AFt (H and L chains)

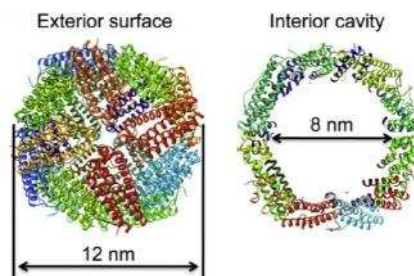


Figure 1.15: Protein structure of human H-AFt with the exterior surface view and interior cavity. Figure adapted from [114].

In biological systems the protein cage ferritin is used to store iron, preventing accumulation of toxic levels in humans through to invertebrates, plants and microorganisms [129]. When the iron atoms are removed from ferritin, AFt is formed. AFt protein cages are composed of 24 subunits, which assemble into hollow cages consisting of an outer diameter of 12 nm and an inner diameter of 8 nm [114] [129]. The interior of AFt can accommodate up to a maximum of 4,500 iron atoms. The mammalian protein subunits are of 2 types, heavy (H) and light (L) chains of 21,000 Da and 19,000 Da respectively. The 2 classes of subunits share nearly identical homology. However, the subunits are expressed in different ratios depending upon the tissue type examined [129]. H and L subunits are shown to play different roles [130]. H chain is known to catalyse iron oxidation (Fe^{2+} to Fe^{3+}) and also facilitates accumulation of iron [130]. The L subunit lacks ferroxidase activity but facilitates iron nucleation [114]. The AFt cage can disassemble into subunits at low pH (pH = 2.0) allowing release of cargo and it is able to reassemble at higher pH (pH > 5.0). Thus, AFt can be used as an ideal NP for drug encapsulation due to its size, hollow cage and sequestration by viable cells. In addition to its ability to encapsulate anti-cancer agents,

AfT is able to bind to a variety of cell types due to the presence of transferrin receptors on the cell surface namely transferrin receptor 1 (TfR1). AfT internalisation within cells is carried out by clathrin-mediated endocytosis during the acidification of endosomes and lysosomes which gradually releases the cargo. The AfT protein cage can also be genetically modified. For instance, this modification may show high affinity towards a particular tumour cell. Further AfT can also be fused with other peptides in order to produce chimeras. Furthermore, due to its unique cavity structure, AfT can be used in further applications such as encapsulation of drugs which makes it an ideal drug delivery system, in diagnostics and in imaging which makes it suitable for therapeutic applications [131]. AfT's high stability, biodegradability, biocompatibility, and its unique structure, makes AfT a successful platform for drug delivery systems. Moreover, since it can withstand number of environmental influences, AfT may eliminate the early release of its cargo that may protect tissues against the adverse effects of numerous pharmacological agents. Also, the size uniformity of the protein cage offers simplicity and reproducibility for the encapsulation of cargo [131].

Affibody molecules (Targeting protein)

Affibody molecules are a new class of relatively small molecules ~ 7,000 Da. They are high affinity proteins, structurally based on a 58 amino acid scaffold derived from the Z domain of *Staphylococcus aureus* protein A, produced by combinatorial protein engineering [132]. In the development of next generation therapeutics, these high affinity proteins have become vital tools. Their capability to bind to a given molecular structure with high affinity, selectivity and robustness are seen to be important key

features. Further, affibody proteins are isolated by non-immunoglobulin scaffolds using synthetic combinatorial libraries and *in vitro* selection systems in contrast to monoclonal antibodies which are generated by immunisation of laboratory animals combined with hybridoma technology. These affibody molecules are currently utilised in a variety of applications. For instance, affibody molecules are currently used in imaging. Imaging improves diagnosis and in cancer, it will show a global view of the metastatic tumours in the body compared to a biopsy which is restricted to a local lesion. High specificity and affinity will be ideal characteristics of an imaging agent for its target. Further, rapid biodistribution and tissue penetration which will lead to high local concentrations at the particular tumour site together with rapid clearance of unbound tracer will help in high contrast tumour imaging between the injection and examination. Recent investigations have shown that affibody molecules are among the most promising tracers for HER2 specific molecular imaging compared to antibodies or antibody fragments with the above mentioned characteristics [133]. Sorensen et al, 2014, has carried out a first in humans imaging study with affibody molecules. It was carried out to evaluate the distribution, safety, efficacy and uptake in tumour metastases and also to compare the background uptake in normal organs of the affibody molecules. Additionally, this investigation determined the HER2+ status in metastatic breast cancer tumours. These affibody molecules have been selected from a library of several billion unique variants providing high affinity binders to a variety of targets such as HER2. Interestingly, this research group found that the mean effective dose given to humans were safe to use and well tolerated without any adverse side effects. The highest normal tissue uptake was in the kidneys, which has been followed by the liver and spleen. Further, they have found that 1 breast cancer patient out of the 7 patients used in the trial demonstrated a HER2- metastatic tumour who

initially had a HER2+ primary tumour. These results validate that affibody molecules are safe to be used in humans and that it is a promising tool to be used in the clinic [134].

Another interesting application of affibody molecules are providing affinity mediated recognition cellular targets. This recognition enhances the specificity. It has been shown previously that uptake and cytotoxicity was increased significantly in HER2 targeted particles carrying the anti-cancer agent Paclitaxel as compared to the non-targeted particles *in vitro* studies. However, when compared to imaging applications, when affibody molecules are used for targeted therapy to direct a payload to a specific disease site, one property which is necessary to optimise is extending its half-life. This is because sufficient drug exposure in a controlled manner is important to obtain a desired therapeutic effect. There are a few technologies available to increase its half-life such as fusion of small proteins. Thus, fusion of affibody molecules to proteins can transform these molecules from optimal imaging tracers to potent candidates for targeted therapy. Furthermore, affibody molecules have also been used in biotechnology applications where it has been used for bioseparation of antibodies in immunoprecipitation and other bead based assays. These descriptions illustrate that affibody molecules which are vital tools have favourable properties which can be used in a multitude of applications [133]. Thus, affibody molecules were used as a successful targeting protein to target HER2+ breast cancer cells in the current study. The affibody molecule/the targeting protein used in the current study has a MW of ~ 10,279 Da.

1.9.6 H or L-AFt-fusion protein

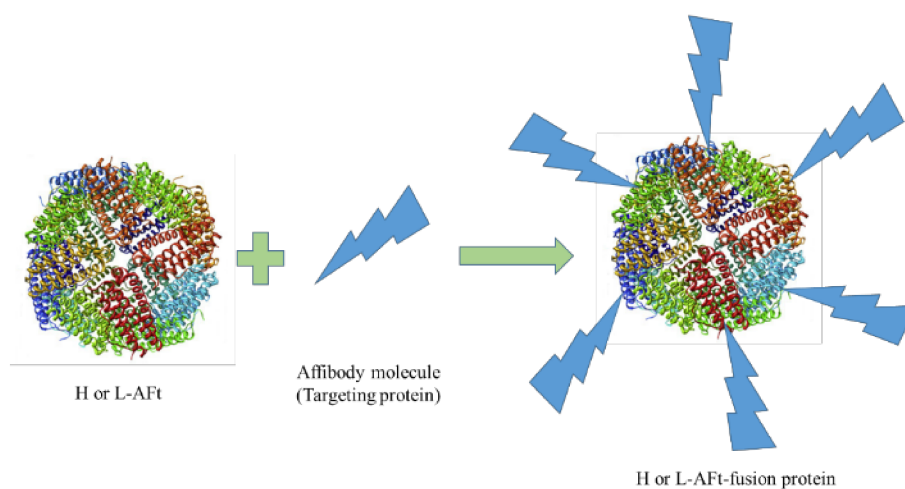


Figure 1.16: H or L-AFt-fusion protein.

Novel agents termed H or L-AFt-fusion proteins were developed by using affibody molecules (targeting protein) fused to H or L chain AFt. In fact, each AFt subunit has been fused to a affibody molecule/targeting protein. The affibody molecules were used for targeting HER2 overexpression in breast cancer. The H-AFt-fusion protein has a MW of ~ 30,756 Da and the L-AFt-fusion protein has a MW of ~ 29,222 Da.

1.9.7 H-AFt-encapsulated-Gefitinib

A novel agent was developed where Gefitinib was encapsulated within the H-AFt NP cage by diffusion.

as an anti-fungal agent. Subsequent studies revealed its immunosuppressive and anti-tumour properties [117] [122]. Sirolimus has a MW of 914.1 Da. Due to its anti-tumour properties Sirolimus has become of significant interest as an anti-cancer agent. Sirolimus inhibits mTOR by binding to one of the intracellular binding proteins, FK-binding protein 12 [117].

1.9.10 CGP57380

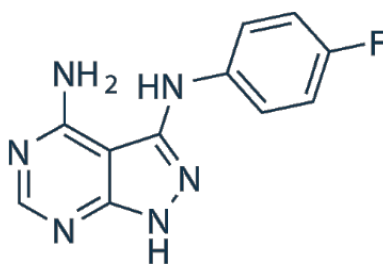


Figure 1.18: Chemical structure of CGP57380. Figure adapted from [122].

CGP57380 which is a MNK inhibitor (Novartis pharmaceuticals) is found to inhibit both MNK1 and MNK2 activity [80]. It has a MW of 244.2 Da [122].

1.9.11 5F 203

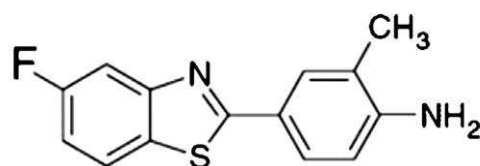


Figure 1.19: Chemical structure of 5F 203. Figure adapted from [137].

2-(4-Amino-3-methylphenyl)-5-fluorobenzothiazole (5F 203) is an experimental anti-tumour agent. 5F 203 was originally synthesised as part of a programme which developed a series of novel anti-cancer benzothiazoles. It is a high affinity AhR ligand, sequestered and metabolised by sensitive cancer cells only [92] [94] [138]. It is shown to induce CYP1A1 in sensitive cancer cell lines *in vitro* and also *in vivo* [94]. The MW of 5F 203 is 258.3 Da [139].

1.9.12 Gedatolisib (MS-73)

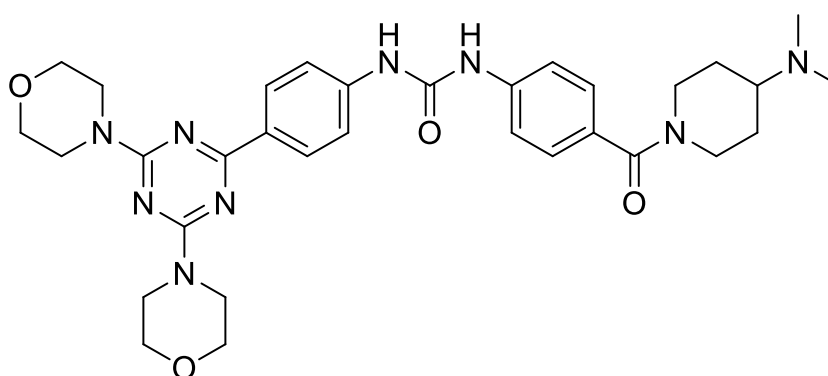


Figure 1.20: Chemical structure of MS-73.

Gedatolisib, is also known as PKI-587 and PF-05212384 (Pfizer) [140]. In the current study Gedatolisib is named as MS-73. This agent is a highly potent dual PI3K/mTOR

inhibitor and is shown to be a pan PI3K inhibitor displaying potency against PI3K isoforms (p110 α , p110 β , p110 γ , and p110 δ). This agent has currently entered phase I clinical trials for patients with malignant solid tumours who were unresponsive to previous therapy [70]. The MW of MS-73 is 615.7 Da. In order to investigate the structure-activity relationship of MS-73, 2 novel analogues have been developed - MS-74 and MS-76. Further, the analogues had been designed to increase solubility because MS-73 is found to be poorly soluble.

1.9.13 MS-74

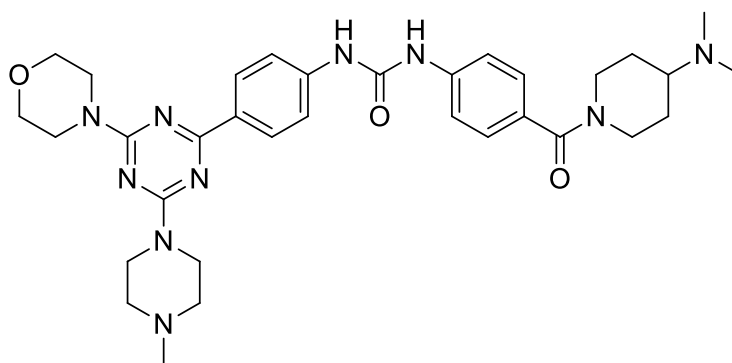


Figure 1.21: Chemical structure of MS-74.

MS-74 is a novel agent. It is an analogue of MS-73 and the MW of MS-74 is 628.7 Da.

1.9.14 MS-76

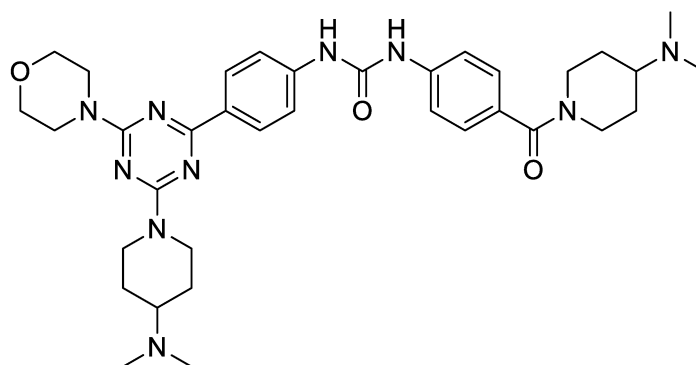


Figure 1.22: Chemical structure of MS-76.

MS-76 is a novel agent. It is an analogue of MS-73 and the MW of MS-76 is 656.8 Da.

1.10 Overall aim and objectives of the study

Overall aim

The overall aim of this study was to investigate the activity of pharmacological agents that are clinically available, agents which are yet in an experimental stage and also that are novel and which targets the HER receptor family and the signal transduction network associated with the HER family. These signal transduction pathways are most commonly involved in the regulatory mechanisms of several cellular processes, including growth, proliferation, differentiation and apoptosis. According to research, RAS/MAPK and PI3K/AKT pathways are some of the most researched signalling components of the HER signalling cascade [51]. These 2 pathways are triggered downstream of the HER dimers. EGFR and HER2 are especially found to be overexpressed and associated with aggressive disease followed by poor survival in

breast cancer [51] [53]. Thus, the agents listed under section 1.9 were tested against the panel of breast cancer cell lines described, representing the molecular subtypes of breast cancer. This analysis may help to understand the HER signalling network further and identify patient populations that would ideally benefit from these therapies as single agents or in combination and ultimately guide treatment strategies tailored to individual patients thereby enhancing personalising therapy.

Objectives

1. The first objective was to test clinically available pharmacological agents targeting the HER family, especially EGFR and HER2 and retool these existing agents by identifying specific breast cancer patient populations who will ideally benefit from these therapies using the panel of breast cancer cell lines. In the pursuit of developing new therapies for breast cancer, it is crucial to characterise existing agents as well, which in turn would expand the variety of therapies beneficial for breast cancer patients [141]. The results associated with this objective are discussed in chapter 3.
2. Nanomedicine has the potential to revolutionise cancer therapy. Many of the existing anti-cancer agents are shown to incorporate poor bioavailability and toxicities which degrades the quality of life of patients receiving these agents. Therefore in this context, human H-AFt NPs were incorporated as a carrier to encapsulate existing clinical agents. The results associated with this objective are discussed in chapter 4.

3. There is an enormous need for the development and evaluation of novel therapies for breast cancer. Novel agents associated with nanomedicine are revolutionising the treatment of cancer. Thus, 2 novel agents targeting the HER2 receptor in breast cancer were investigated and compared to existing pharmacological agents. The results associated with this objective are discussed in chapter 5.

4. Targeting a distinct HER receptor or a molecule within a signalling pathway by a single agent may most often contribute to activation of alternative and compensatory signalling pathways, multiple feedback loops and cross talk within the complex signalling network thereby acquiring resistance to therapy [142]. These complexities mandate to study agents in combination which may combat drug resistance and enhance the effect of pharmacological agents in breast cancer [143]. Thus, agents alone and in combination were evaluated for synergistic effects. The results associated with this objective are discussed in chapter 6.

2 Chapter 2 - Materials and Methods

2.1 General cell culture

Cell culture is the process where cells are grown under controlled conditions outside of their natural surroundings. It is an important tool to study a range of cellular functions and behaviour in response to external stimuli [144]. A variety of cell culture experiments were used throughout the current study and these experiments are described in this chapter.

2.1.1 Materials

T25 cm² tissue culture flasks (Corning (0.2 µm vented cap), Product Code (PC) - 3056), cryopreservation vials (Thermo Scientific, PC - 10440613), RPMI-1640 medium stored at 4 °C (Sigma-Aldrich, PC - R8758), heat inactivated foetal bovine serum (FBS) stored at -20 °C (Sigma-Aldrich, PC - F9665), freezing medium stored at 4 °C (95% FBS and 5% DMSO), 6 human epithelial breast cancer cell lines (discussed in section 2.1.2), trypsin-EDTA stored at -20 °C (Sigma-Aldrich, PC - T4174), phosphate buffered saline (PBS) stored at room temperature (Sigma-Aldrich, PC - P4417; 1 tablet was dissolved in 200 ml of dH₂O).

2.1.2 Cell lines

The cell lines used in this study had been purchased from the European Collection of Cell Cultures (supplied via Sigma-Aldrich); 6 human epithelial breast cancer cell lines

were used. For each cell line a new batch of cells were taken out of liquid nitrogen storage (-196 °C) and passaged $\leq 3 - 4$ months before being discarded and a new batch of cells thawed for culture to minimise genotypic and phenotypic drift during continuous culture. As a part of quality control, cells were tested regularly for mycoplasma infection which is one of the most common contaminants present in cell culture laboratories. The MycoAlert mycoplasma detection kit (Lonza, PC - LT07-118) was used for this purpose. The breast cancer cell lines used in this study were - MCF7, T47D, ZR-75-1, SKBR3, MDA-MB 468 and MDA-MB 231.

2.1.3 Reviving frozen cells

Each cell line used was preserved in liquid nitrogen. A database with cell bank information was checked to retrieve the specific location of stored cell vials within the liquid nitrogen storage. Afterwards, the vials were taken out of liquid nitrogen storage and they were thawed rapidly at 37 °C. Subsequently these vials were carefully sterilised by wiping the vials with 70% industrial methylated spirit (IMS) in dH₂O. All procedures from this point onwards were carried out under strict aseptic conditions. The cells were re-suspended in vented T25 cm² culture flasks with 7 ml of RPMI-1640 medium with 10% FBS (pre-warmed complete growth medium). All culture flasks were labelled with the name of the cell line, initials of user, date and passage number. Cells were allowed to attach overnight incubated at 37 °C in an atmosphere of 5% CO₂. Cells were then examined under the microscope for cell adhesion, viability and accurate morphology. Thereafter, medium was replaced to remove DMSO and any unattached cells, and incubated further. When cells were ~ 80% confluent they were passaged twice to resume normal growth before experiments were initiated.

2.1.4 Freezing and storing cells

For long term maintenance cell lines were cryopreserved. In order to carry out this procedure, medium was aspirated and cells washed with sterile PBS (pre-warmed) to remove dead cells and serum. PBS was then aspirated and viable cells were detached using a minimum amount of 1x trypsin-EDTA. Hence, 500 µl of trypsin-EDTA was added to the flasks and the flasks were gently agitated to ensure complete coverage of the trypsin-EDTA solution over the cells. The flasks were then incubated at room temperature and after ~ 2 min, trypsin-EDTA was aspirated. Afterwards, these flasks were incubated at 37 °C to allow cells to detach for a further 1 - 2 min and then re-suspended in 1 ml of sterile freezing medium. The cell suspension was transferred to sterile cryogenic vials labelled with the name of the cell line, initials of user, date and passage number. Cryogenic vials were frozen overnight at -20 °C in a well-insulated box then at -80 °C for 1 - 2 days before being transferred to liquid nitrogen for long term storage.

2.1.5 Passaging of cells

All cell culture techniques were carried out in a class II biological safety cabinet which was decontaminated with 70% IMS before use. All cell lines were routinely passaged in T25 cm² culture flasks using RPMI-1640 medium supplemented with 10% FBS. Logarithmic growth was maintained by passaging T47D, ZR-75-1, SKBR3 and MDA-MB 468 cell lines once a week and other cell lines twice per week. Passaging was carried out when cells were ~ 80% confluent. Subsequently, complete growth medium was aspirated and 1 ml of 1x trypsin-EDTA solution was added. SKBR3 and MDA-

MB 468 cell lines were rinsed briefly with PBS prior to adding 1x trypsin-EDTA as these cells were not easily detached by 1x trypsin-EDTA if traces of serum remained.

After adding 1x trypsin-EDTA the flasks were gently agitated to ensure complete coverage of cells with 1x trypsin-EDTA solution. The flasks with trypsin were re-incubated at 37 °C for ~ 5 min to facilitate cell detachment. When the majority of cells had detached, the cell suspension was re-suspended in 5 ml medium to neutralise the trypsin-EDTA solution. Subsequently 0.5 - 1 ml of the cell suspension was transferred to a new T25 cm² culture flask with 7 ml fresh complete growth medium and flasks were labelled as mentioned above. The cells were then incubated at 37 °C in an atmosphere of 5% CO₂. All cell lines were discarded when the passage number reached ~ 20 in order to minimise phenotypic drift. New batches of cells were then taken from the liquid nitrogen and re-suspended as before.

2.2 Growth curve experiment

Growth curves were constructed by plotting the escalation of cell numbers versus incubation time and used to determine growth characteristics for each cell line [145].

2.2.1 Method

All cell lines were plated in triplicate in RPMI-1640 medium supplemented with 2% or 10% FBS using 6 well plates (Corning, PC - 3506). The seeding densities used for

the cell lines were as follows - MCF7, T47D, ZR-75-1, MDA-MB 231 - 2×10^4 , SKBR3, MDA-MB 468 - 5×10^4 .

The initial seeding cell densities for SKBR3 and MDA-MB 468 cells had to be increased as their growth was much slower, especially at low cell densities. As described in section 2.1.5, cells were harvested by trypsinisation. Subsequently clumped cells were dispersed using a syringe equipped with a 23-gauge needle to obtain a near single cell suspension. Cells were counted using a haemocytometer and seeded at the desired densities in 3 ml culture medium. The cells were incubated overnight at 37 °C to allow cell attachment and commencement of mitosis. Afterwards, cell counting was performed daily until cell growth reached a plateau phase and cells died. Medium was replaced every 4 days in all plates in order to maintain nutrient availability. Prior to cell counting, medium in each well was aspirated and cells were harvested with 200 µl of 1x trypsin-EDTA. Following dispersal of cells, 800 µl of medium was added into each well to make the total volume to 1 ml. Once again the cell suspension was passed gently through a syringe equipped with a 23-gauge needle, in order to obtain a single cell suspension. The resulting cell suspension was transferred to labelled bijou tubes for all 6 cell lines to facilitate cell counting. Cells were counted using a hemocytometer. When preparing the haemocytometer for counting the counting chambers and the cover-slip were carefully cleaned with 70% IMS. A coverslip was placed over the counting surface prior to introducing the cell suspension. Cell suspension (~ 20 µl) was introduced into both sides of the counting chamber using a pipette. The area under the cover-slip was filled by capillary action. Cell counts for each bijou tube were repeated if the difference in counts in both sides

of the counting chambers were $\geq \pm 10\%$. All growth curve experiments were done in triplicate and repeated thrice. Cell doubling times were measured by graphical interpolation.

2.3 The 3-(4,5-dimethyl-2-thiazolyl)-2,5-diphenyltetrazolium bromide (MTT) assay

The 3-(4,5-dimethyl-2-thiazolyl)-2,5-diphenyltetrazolium bromide (MTT) assay can be used to measure *in vitro* growth inhibitory or cytotoxic effects of drugs on cell lines. It was introduced by Mosmann in 1983. In this assay, mitochondrial dehydrogenases of viable cells convert tetrazolium salt MTT into formazan crystals, which can be solubilised and measured [146].

2.3.1 Materials

MTT stored at 4 °C (Sigma-Aldrich, PC - M2128-1 g) (2 mg/ml MTT solution was prepared using sterile PBS) and DMSO stored at room temperature (Sigma-Aldrich, PC - D5879-1 l).

2.3.2 Pharmacological agents tested with the concentration ranges

Several clinical, currently experimental and entirely novel pharmacological agents were tested throughout the course of the study period. All agents tested are listed in

Table 2.1 with the concentration ranges that were used. Some of the concentrations ranges were guided by previous literature.

Agent tested	Obtained from	Final concentration range
1. EGF	Calbiochem	0.01 nM – 10 nM
2. Gefitinib	Cayman chemical	0.01 μ M - 25 μ M
3. Erlotinib	Cayman chemical	0.01 μ M - 25 μ M
4. Raloxifene	Cayman chemical	0.005 μ M – 25 μ M
5. H-AFt-encapsulated-Gefitinib	Novel testing agent synthesised by author with the assistance of Dr. Lei Zhang	0.05 μ M – 25 μ M
6. H-AFt and L-AFt	Kindly provided by Prof. Neil Thomas	0.004 μ M – 20 μ M
7. H-AFt-fusion protein and L-AFt-fusion protein	Novel testing agents synthesised by Dr. Lei Zhang and kindly provided for testing	0.003 μ M – 2 μ M
8. Targeting protein	Kindly provided by Prof. Neil Thomas	0.01 μ M – 5 μ M
9. Trastuzumab	Roche	0.0006 μ M – 0.3 μ M
10. Sirolimus	Cayman chemical	0.1 nM - 1 μ M
11. CGP57380	Cayman chemical	0.01 μ M – 100 μ M
12. 5F 203	Experimental testing agent kindly provided by Dr. Tracey D. Bradshaw	1 nM – 10 μ M
13. MS-73, MS-74 and MS-76	Experimental and novel testing agents kindly provided by Dr. Michael Stocks	0.5 nM – 10 μ M
14. DMSO	Sigma-Aldrich	0.01% - 1%

Table 2.1: Agents tested during the study period. DMSO was used as a solvent to dissolve agents 2, 3, 4, 10, 11, 12 and 13. Thus, effects of DMSO alone were also tested. All test agents except DMSO were stored at -20 °C.

2.3.3 Method

Cells from flasks that were ~ 80% confluent were harvested by trypsinisation. Subsequently, the cell suspension was gently passed through a syringe equipped with a 23-gauge needle to obtain a near single cell suspension. Cells were counted using a hemocytometer and decanted with RPMI-1640 medium supplemented with 2% FBS (used for MTT experiments described in chapter 3) or 10% FBS, according to the required seeding density (seeding density for 24 h drug exposure - 5×10^3 , 72 h drug exposure - 2.5×10^3 and 120 h drug exposure - 2.5×10^3 cells per well). Thereafter 180 μ l or 160 μ l (used for combination MTT experiments where 2 agents were tested together, described in chapter 6) of cell suspension was added into each well of 96 well microtiter plates (Nunclon) (VWR, PC - 734-2097). The 2 peripheral lanes of the plate were filled with 300 μ l of medium only, to minimise evaporation from experimental wells. Cells were allowed 24 h to adhere before treatment. In addition a time zero (T0) plate was also set up to determine the absorbance of cells (optical density (OD)) at the time of test agent treatment.

In each plate one column contained cells that were untreated (control). The other columns containing cells were exposed to increasing concentrations of the pharmacological agents listed in table 2.1. The agent concentrations were prepared to 10 x the final concentrations required prior to each experiment by serial dilutions using FBS-free RPMI-1640 medium. Then 20 μ l of the agents were added into each well to make up a final volume of 200 μ l. FBS-free medium only (20 μ l) was added to the control wells. In each experiment ~ 8 wells received the same agent concentration. MTT assays were also performed at pH 7.0 (used for MTT experiments described in

chapter 4). Standard RPMI-1640 medium supplemented with 10% FBS is at pH 7.5. Concentrated 1 M HCl (Fisher Scientific, PC - 10487830) was introduced into RPMI medium drop-wise to obtain the desired pH level of 7.0.

Cells were then incubated at 37 °C in an atmosphere of 5% CO₂ for the required exposure period (24 h, 72 h or 120 h). After the required time or at the time of drug addition for the T0 plate, 50 µl MTT was added to cells and incubated for a further 2.5 h. Medium was then carefully aspirated and insoluble formazan produced by the metabolism of MTT by mitochondrial dehydrogenases was solubilised by the addition of 150 µl DMSO per well. Subsequently, all plates were shaken for 5 min using a plate shaker (Amersham) to ensure complete formazan solubilisation. The coloured formazan product was then quantified by measuring OD using a microtiter plate reader (PerkinElmer precisely - Envision 2104 mulilabel reader) at 550 nm. The OD values were obtained by Wallac Envision manager software (version 1.12) and the values obtained were directly related to viable cell numbers. Graphs with OD values against drug concentrations were plotted and the concentration required to achieve 50% growth inhibition (GI₅₀) values were determined for each agent as below - $[(\text{OD of control} - \text{OD of T0})/2] + \text{OD of T0} = \text{OD at GI}_{50}$ and thereafter the GI₅₀ values were calculated by interpolation. This served as an index of growth inhibition by the tested agents and the GI₅₀ values obtained from the MTT experiments were used in successive experiments.

2.4 Clonogenic assay

The clonogenic assay is a cell survival assay which tests the ability of single cells to survive challenge with a test agent and retain proliferative capacity to form progeny colonies, which is indicative of the ability to repopulate a tumour [147].

2.4.1 Materials

0.05% Methylene blue in a 1:1 solution of dH₂O:MeOH stored at 4 °C.

2.4.2 Method

Initially cells were seeded at 250, 500 or 1000 cells per well in 2 ml complete medium to determine the optimal seeding density for each cell line used in this experiment. Afterwards, 250 cells per well was chosen as the optimal seeding density and cells were seeded into 6 well plates and allowed to attach overnight. After 24 h, pharmacological agents (1x and 2x GI₅₀ concentrations obtained from the MTT experiments) were introduced to wells. Following 24 h exposure, medium containing agents were removed from the plates (plates containing cells that were continuously exposed to test agents remained in the incubator). Cells were washed twice in 1 ml PBS (pre-warmed) and 3 ml of fresh complete growth medium was introduced into wells. Plates were placed at 37 °C, 5% CO₂ and colonies were allowed to form until \geq 50 cells per colony were visible in control wells. The time period to form colonies (\geq 50 cells per colony) varied with each cell line used (~ 10 - 14 days). At that point medium was removed from wells and colonies were washed twice with 1 ml ice cold

PBS. Colonies were then fixed with 100% MeOH (Sigma-Aldrich, PC – 32213 - 2.5 l) for 10 min and stained using 1 ml 0.05% methylene blue in a 1:1 solution of dH₂O:MeOH for a further 10 - 15 min. Colonies were then rinsed with H₂O, air dried, photographed and counted. The plating efficiency (PE) and survival fraction (SF) were calculated as below:

$$\text{PE} = \text{Number of colonies formed} / \text{Number of cells seeded} \times 100\%$$

$$\text{SF} = \text{PE of treated sample} / \text{PE of control} \times 100\%$$

2.5 Flow cytometry

Flow cytometry is used to determine the characteristics of a cell as it passes through a laser. Cells are fluorescently labelled and excited by the laser to emit light at varying wavelengths. The fluorescence can be measured to determine cell size, granularity and fluorescence intensity [148] [149].

2.5.1 Cell cycle assay

Cell cycle analysis is quantified by the DNA content of cells. Thus, it reveals the distribution of the percentage of cells in the 3 main phases of the cell cycle G1 vs S vs G2/M. In order to analyse the DNA content, cells are stained with a fluorescent dye that binds to DNA such as propidium iodide (PI). Thus, the emitted fluorescence is proportional to DNA content present in the cells [149].

2.5.1.1 Materials

Hypotonic fluorochrome solution stored at 4 °C (50 µg/ml PI (Sigma-Aldrich, PC – 81845 - 25 mg), 0.1 mg/ml ribonuclease A stored at -20 °C (Sigma-Aldrich, PC - R4642), 0.1% v/v Triton X-100 (Sigma-Aldrich, PC - X100 - 5 ml), 0.1% w/v sodium citrate (Sigma-Aldrich, PC – 1613859 - 1 g) in PBS).

2.5.1.2 Method

Cell cycle analysis was carried out using the method based on Nicoletti et al, 1991. Cells were trypsinised and seeded in 6 well plates at a density of 3×10^5 (24 h), 2×10^5 (48 h), and 1×10^5 (72 h) cells per well in 2 ml complete growth medium according to treatment exposure time. Cells were allowed to attach for 24 h prior to treatment. Cells were treated with pharmacological agents at desired concentrations. Following the required exposure period, medium within the wells with any floating cells was decanted to a labelled fluorescence activated cell sorter (FACS) tube and kept on ice. Subsequently, cells were harvested by adding 200 µl 1x trypsin-EDTA and pooled together with addition of 800 µl of medium. Cells were then centrifuged at 1,200 rpm for 5 min, at 4 °C. Supernatant was discarded and the pellets were broken down by gently flicking the tube. Next, 1 ml chilled PBS was added and the FACS tubes were vortexed. Thereafter the cells were centrifuged as before. The supernatant was discarded and the pellet was broken down by gently flicking the FACS tube and the cells were re-suspended in 500 µl cold hypotonic fluorochrome solution and stored overnight at 4 °C protected from light. Cells were vortexed and passed gently through a 23-gauge needle immediately prior to analysis to obtain a single cell suspension. The

samples were analysed on a Beckman Coulter Epics-XL MCL flow cytometer and 10,000 - 20,000 events were recorded for each sample. The results obtained were analysed using EXPO32 software.

2.5.2 Annexin V- Fluorescein isothiocyanate (FITC)/PI apoptosis assay

The annexin V-FITC/PI assay is used to measure the percentage of cells that are actively undergoing apoptosis. Phosphatidylserine (PS), a phospholipid which is confined to the inner leaflet of the plasma membrane translocates to the outer leaflet of the plasma membrane during apoptosis thereby exposing PS to the external environment. Annexin V bound to FITC can bind specifically in the presence of calcium, to PS. Annexin V-FITC can be used with dyes such as PI to determine the different stages of apoptosis such as early and late apoptotic populations and necrotic populations. Viable cells possess intact membranes and will exclude PI [150].

2.5.2.1 Materials

Annexin V-FITC apoptosis detection kit stored at 4 °C (BD Pharmingen, PC - 556547). The kit contained -FITC annexin V, PI staining solution, 10 x annexin V binding buffer (diluted 1 part 10 x annexin V binding buffer to 9 parts dH₂O).

2.5.2.2 Method

Cells were trypsinised and seeded in 6 well plates at densities of 3×10^5 (24 h), 2×10^5 (48 h) and 1×10^5 (72 h) cells per well in 2 ml complete growth medium according to treatment exposure times. Cells were allowed to attach for 24 h. Following treatment with pharmacological agents at particular concentrations, cells were trypsinised with 200 μ l of 1x trypsin-EDTA and once detached pooled together with any floating cells in a total of 1 ml complete growth medium. Subsequently the cells were decanted to labelled FACS tubes and kept on ice. Cells were then centrifuged at 1,200 rpm for 5 min at 4 °C. Thereafter, the supernatant was discarded and the pellet disrupted by gently flicking the tube. Cold PBS (1 ml) was added and the cells were centrifuged as before. The supernatant was discarded and the pellet disrupted by gentle flicking the tube, this step was repeated once more. Afterwards, 100 μ l of 1x annexin binding buffer and 5 μ l annexin V-FITC was added to each tube. The tube was briefly vortexed and incubated at room temperature for 15 min in the dark. Next, 400 μ l 1x annexin binding buffer and 5 μ l of PI solution were added to each tube which was vortexed and incubated for 10 min at room temperature in the dark prior to analysis on the flow cytometer. Samples were analysed within 1 h of completion of the above protocol. The samples were analysed by Beckman Coulter Epics-XL MCL flow cytometer and 10,000 - 20,000 events were recorded for each sample. The results obtained were analysed using EXPO32 software.

During analysis by flow cytometry, 4 populations were identified in the quadrant plots. The lower left quadrant contained the viable cell population (A3- annexin V-/PI-), the upper left quadrant contained the necrotic population (A1- annexin V-/PI+), the upper

right quadrant contained the late apoptotic population or dead cells (A2- annexin V+/PI+) and the lower right quadrant contained the early apoptotic population (A4- annexin V+/PI-) [21]. Early and late apoptotic populations were summed to determine the total apoptotic population of cells.

2.5.3 γ -H2AX assay

γ -H2AX expression is an indicator of DNA double strand breaks (DDSBs). When DDSBs occur histone H2AX becomes rapidly phosphorylated at Ser139 forming γ -H2AX visible as nuclear foci. Previous research has shown that dephosphorylation of γ -H2AX and dispersal of γ -H2AX foci in irradiated cells correlates with the repair of DNA DDSBs [151] [152]. Thus, analysis of γ -H2AX can be used to determine DDSBs in a cell population after certain agent treatment.

2.5.3.1 Materials

Formaldehyde (1% formaldehyde in PBS) stored at 4 °C (1 ml 16% MeOH-free formaldehyde (Life technologies, Pierce, PC - 28906) in 15 ml ddH₂O), 0.4% Triton X-100 in PBS stored at 4 °C (40 μ l Triton X-100 in 20 ml PBS), 1% FBS in PBS, anti-phospho-histone H2A.X (Ser139) mouse monoclonal primary antibody (1° antibody) (Merck Millipore, PC - 05-636), goat anti-mouse secondary antibody (2° antibody) (Alexa fluorophore 488 conjugate (Life technologies, PC - A-10684)).

2.5.3.2 Method

Cells were trypsinised and seeded in 10 cm tissue culture treated petri dishes (Corning, PC - 430167) at a seeding density of 1×10^6 (24 h exposure) and 5×10^5 (72 h exposure) in 10 ml complete growth medium. After 24 h, cells were treated with 1x GI_{50} concentrations of agents. Following the required exposure period, medium was decanted with any floating cells into labelled 15 ml falcon tubes. Afterwards, cells in the petri dishes were washed with 1 ml PBS and aspirated. Cells were trypsinised with 500 μ l of 1x trypsin-EDTA and transferred to falcon tubes. Cells were then centrifuged at 1,250 rpm for 10 min, at room temperature. Subsequently, supernatant was aspirated and the pellet disrupted by gentle flicking the tube. This was followed by adding 1 ml of PBS and the cells were centrifuged at 1,250 rpm for 10 min at room temperature, PBS was aspirated and the pellet was disrupted as before. Thereafter, cells were fixed by adding 500 μ l 1% formaldehyde in PBS, which was followed by pipetting the cell suspension up and down several times to ensure a single cell suspension. Samples were then incubated for 5 min at room temperature, and the tubes were gently flicked occasionally. Thereafter, 500 μ l of 0.4% Triton X-100 in PBS were added and the tubes were flicked gently as before to permeabilise the cells. After around 5 min, the tubes were centrifuged at 1,250 rpm for 10 min at room temperature; supernatant was aspirated and the pellet was spun down. FBS (1 ml 1% in PBS) was added and mixed gently. Samples were incubated for 30 min at room temperature; centrifuged and the supernatant was aspirated as before. Subsequently, 200 μ l 1^o antibody (1:5000 diluted in 1% FBS in PBS) was added and the solution was pipetted up and down several times followed by a 1.5 h incubation period at room temperature. Subsequently, 1 ml 1% FBS in PBS was added, centrifuged and aspirated as mentioned before and 2^o

antibody (200 μ l of 1:1750 diluted in PBS containing 1% FBS) was added with gentle mixing. The solution was incubated for 1 h in the dark at room temperature before addition of 1 ml 1% FBS in PBS. The solution was centrifuged, aspirated and finally 300 μ l of PBS was added. Samples were analysed on a Beckman Coulter Epics-XL MCL flow cytometer and 10,000 events were recorded for each sample. The results obtained were analysed using EXPO32 software.

2.6 Cellular uptake study by flow cytometry

Flow cytometry was used to quantify the cellular uptake of pharmacological agents – Gefitinib which is fluorescent under UV (excitation 345 and emission 385 nm) and H-AFt-encapsulated-Gefitinib which is also fluorescent under UV [153].

2.6.1 Method

Cells were seeded in 6 well plates at a density of 2.5×10^5 in 2 ml complete growth medium and allowed to attach for 24 h. Subsequently, cells were treated with Gefitinib or H-AFt-encapsulated-Gefitinib (5 μ l) and exposed for an additional 24 h. Cells were washed with PBS and harvested by scraping the cells. Cells were collected into FACS tubes in a total of 1 ml PBS. Using a Beckman Coulter Astrios EQ flow cytometer, samples were analysed and 20,000 events were recorded. The emitted fluorescence from these pharmacological agents were collected using a 405/30 band pass filter. The results were analysed by Beckman Coulter Summit software (version 6.2.3.1561).

2.7 Confocal microscopy

Confocal microscopy is an optical imaging method. It is able to enhance the visual optical resolution of a sample by using a pinhole placed on the focus planes of the microscope where fluorescent light travels through, whilst the light coming from out of focus planes is eliminated by the pinhole [154]. Prior to imaging, samples were labelled with a fluorescent dye or autofluorescence of the samples were used for imaging.

2.7.1 Materials

Paraformaldehyde (4%) (Sigma-Aldrich, PC - P6148 - 500 g) in PBS, PBT buffer (0.2% Triton X-100 in PBS), PBS, 4',6-Diamidino-2-phenylindole dihydrochloride (DAPI) (Life technologies, PC - 62248 - 1 ml).

2.7.2 Method for fixed cell imaging

SKBR3 cells (1×10^4) were seeded into μ -slide 8 well slides (Ibidi, PC - 80826) in 300 μ l medium and allowed to attach overnight. Cells were then treated with 20 μ l H-AFt-fusion protein (16 μ M) labelled with Alexa 488 fluorophore via thiol maleimide conjugation using the manufacturer's instructions (Life technologies, PC - A-10254) for 2 h, 6 h, 12 h and 24 h. After the desired exposure time, cells were washed twice with PBS. Paraformaldehyde solution (300 μ l) was added to samples which were incubated for 20 min. Cells were washed 2 x with PBS and incubated with 300 μ l of PBT buffer (0.2% Triton X-100 in PBS) for 20 min and followed by washing 3 x with

PBS and 1 x with dH₂O. Cells were incubated with DAPI (0.5 µg in 1 ml PBS) for 2 min and visualised using a fluorescence confocal microscope (Zeiss LSM 510 Meta). The images were analysed by Zeiss LSM image browser software (version 4.2.0.121). This experiment was carried out in collaboration with Dr. Lei Zhang and the author extends her appreciation.

2.7.3 Method for live cell imaging

SKBR3 and MDA-MB 231 cells (1×10^4) were seeded into µ-slide 8 well slides in 300 µl medium and allowed to attach overnight. Cells were then treated with Gefitinib alone or H-AFt-encapsulated-Gefitinib (5 µM). As Gefitinib is fluorescent in cells, live imaging of cells was carried out after 24 h exposure of cells to agents using a fluorescence confocal microscope (Zeiss LSM 510) equipped with a UV laser of 351 nm excitation and LP385 emission filter. Images were analysed by Zeiss LSM image browser software (version 4.2.0.121).

2.8 Evaluation of protein expression

Western blotting was carried out to determine protein expression which involved number of steps such as preparation of protein lysates, determining protein concentration, sodium dodecyl sulfate-polyacrylamide gel electrophoresis (SDS-PAGE), Western blotting and immunological detection. Further, a coomassie dye protein staining experiment was carried out to visualise protein bands and to determine MWs of proteins resolved by SDA-PAGE which is discussed in section 2.9.

2.8.1 Preparation of protein lysates**2.8.1.1 Materials**

Nonidet-P40 (NP40) lysis buffer (10 ml) stored at 4 °C – (NP40 (Fluka, PC - 74385) (100 µl), 1 M NaCl (1.5 ml), 1 M Tris pH 8.0 (500 µl), dH₂O (7.9 ml), 1 tablet each of protease inhibitors (Roche (complete ultra-tablets), PC - 05892791001) and phosphatase inhibitors (Roche (PhosSTOP), PC - 04906845001).

2.8.1.2 Method

All cell lines were harvested by trypsinisation and the cells were seeded in 10 cm petri dishes in 10 ml of complete growth medium at a seeding density of 1×10^6 . The petri dishes were incubated for 24 h at 37 °C allowing cells to attach. After 24 h, cells were treated with the required pharmacological agent and incubated for a further 24 h. After the exposure period, cells were lysed with NP40 lysis buffer. During this procedure, the petri dishes with cells were kept on ice. Medium was aspirated and cells were washed 2 x with PBS. Lysis buffer (300 µl) was added to each petri dish. Cells were harvested by scraping using a cold plastic cell scraper and transferred to labelled microcentrifuge tubes. These tubes were kept on ice. Subsequently, the dishes were washed with an additional 200 µl of lysis buffer to disperse any remaining adherent cells and added to the labelled microcentrifuge tubes. The tubes were centrifuged at 1,500 rpm at 4 °C for 5 min. The microcentrifuge tubes were incubated on ice for 30 min with occasional flicking. After 30 min the tubes were centrifuged at 13,000 rpm for a further 10 min at 4°C to pellet insoluble material. The soluble supernatant was

transferred to new labelled microcentrifuge tubes and the protein cell lysates were stored at -20 °C.

2.8.2 Determining protein concentration

The Bradford assay introduced by Marion M. Bradford in 1976 is a colorimetric assay used to determine the protein concentration. It involves the binding of coomassie brilliant blue G-250 to a particular protein which causes a shift in the absorption maximum of the dye from 465 to 595 nm, and this increase in absorption at 595 nm is measured [155].

2.8.2.1 Materials

Bradford reagent (Sigma-Aldrich, PC - B6916) and bovine serum albumin (BSA) (Sigma-Aldrich, PC – 05470 - 1 g).

2.8.2.2 Method

Protein standard solutions of BSA using NP40 lysis buffer were prepared as follows - 0.25, 0.5, 1, 1.5 and 2 mg/ml. Protein lysates were thawed on ice and centrifuged at 13,000 rpm for 5 min at 4 °C to remove any insoluble proteins and cell debris before protein analysis. Prepared protein lysates and BSA standards (5 µl) were pipetted and added in triplicate into a 96 well microtiter plate. The protein lysates were then diluted 10 x with the NP40 lysis buffer. Subsequently, 250 µl of the Bradford reagent was

added into all wells and the plate was shaken for 2 min using the plate shaker to ensure all reagents were mixed well. Afterwards the plate was incubated for 15 - 45 min at room temperature and the OD was measured at 595 nm using a microtiter plate reader (PerkinElmer precisely - Envision 2104 multilabel reader). The OD values were obtained by Wallac Envision manager software (version 1.12) and the average OD readings were calculated for both protein lysates and for BSA standards. A standard curve was plotted for the BSA standards with their average OD values versus their concentrations in mg/ml. The standard curve was then used to determine the protein concentrations in the volumes of the protein lysates used for the assay according to the principle of Beer-Lambert law. Subsequently, protein content for each cell lysate containing 50/75 µg protein were calculated.

2.8.3 Sodium dodecyl sulfate (SDS) - polyacrylamide gel electrophoresis (PAGE) (SDS-PAGE)

This method is used to separate proteins by electrophoresis according to MWs of proteins. A polyacrylamide gel is used as a support medium with SDS to denature the proteins. Thus, this technique is called sodium dodecyl sulfate polyacrylamide gel electrophoresis (SDS-PAGE) [156] [157].

2.8.3.1 Materials

Molecular marker (Thermo Scientific, PageRuler plus prestained protein ladder, PC - 26619).

4 x loading buffer in a total volume of 10 ml - 4 ml glycerol (Sigma-Aldrich, PC - G5516 - 100 ml), 2.4 ml Tris 1M (pH 6.8), 0.8 g SDS, 4 mg bromophenol blue, 0.5 ml β -mercaptoethanol (Sigma-Aldrich, PC-M6250 - 10 ml) and 3.1 ml dH₂O.

1.5 M Tris (pH 8.8) - 90.8 g Tris (Sigma-Aldrich, PC - T6066 - 1 kg) was dissolved in 500 ml of dH₂O and adjusted to the desired pH concentration with HCl.

1 M Tris (pH 6.8) - 60.57 g of Tris was dissolved in 500 ml of dH₂O and adjusted to the desired pH concentration with HCl.

10% SDS (Sigma-Aldrich, PC - L3771 - 25 g) - 1 g SDS dissolved in 10 ml of dH₂O.

10% APS (Sigma-Aldrich, PC - A3678 - 100 g) - 1 g of APS dissolved in 10 ml of dH₂O.

10% resolving gel in a total volume of 10 ml - 4.0 ml dH₂O, 3.3 ml 30% acrylamide/bis acrylamide stock solution (Sigma-Aldrich, PC - A2917 - 100 ml), 2.5 ml 1.5 M Tris (pH 8.8) (prepared as above), 100 μ l 10% SDS (prepared as above), 100 μ l 10% APS (prepared as above) and 4 μ l N, N, N', N'-tetramethylethylenediamine (TEMED) (Sigma-Aldrich, PC - T9281 - 25 ml).

4% stacking gel in a total volume of 4 ml - 2.7 ml dH₂O, 670 μ l 30% acrylamide/bis acrylamide stock solution, 500 μ l 1.0 M Tris (pH 6.8) (prepared as above), 40 μ l 10% SDS, 40 μ l 10% APS and 4 μ l TEMED.

1 x running buffer- 3.03 g Tris, 14.4 g glycine and 1 g SDS were dissolved in 1 l dH₂O.

2.8.3.2 Method

The first step in SDS-PAGE was to prepare the gels. A 10% resolving gel and a 4% stacking gel were cast in a gel cassette (Life technologies, PC - NC2015) immediately prior to running the gel. Initially, the resolving gel was allowed to polymerise at room temperature for 30 min after removing any air bubbles formed within the gel by drops of isopropanol (Sigma-Aldrich, PC - 563935-1 l). Once the resolving gel had set, the isopropanol was removed by H₂O and the 4% stacking gel was prepared and poured on top of the resolving gel. A 10 well electrophoresis gel comb was placed immediately within the stacking gel solution and gels were allowed to set for 30 min at room temperature. Subsequently, protein lysates were thawed on ice and centrifuged and samples containing 50/75 µg of protein were prepared for SDS-PAGE analysis by denaturation with heat. The protein lysates were mixed with 4 x loading buffer and heated for 5 min at 95 °C. The samples were then centrifuged (5,000 rpm, 1 min) and sonicated for 30 sec before being loaded into sample wells of the stacking gel. Sonication was done to shear DNA and reduce sample viscosity. Molecular markers (10 µl) were also loaded into one of the peripheral lanes of the gel. The proteins were separated by SDS-PAGE in 1 x running buffer at 100 V for 2.5 h.

2.8.4 Western blotting

With the use of specific antibodies Western blotting allows identification of proteins that have been separated from one another according to their size by SDS-PAGE.

2.8.4.1 Materials

Nitrocellulose membrane (0.45 μm) (Bio-Rad, PC - 162-0115), blotting paper/chromatography paper (Whatman, PC - 3030 672).

1x transfer buffer - 3.03 g Tris, 14.4 g glycine, 0.375 g SDS, 200 ml MeOH were dissolved in 800 ml dH_2O .

1 x TBS-T - 8 g NaCl and 2.42 g Tris were dissolved in 1 l dH_2O and added conc. HCl was added to adjust to pH 7.6, tween (0.5 ml) (Fisher Scientific, PC - 10485733) was also added and mixed.

10% non-fat milk - 5.0 g non-fat dried milk in 50 ml TBS-T.

All antibodies used in Western blotting are listed in table 2.2

Antibodies
EGFR (PC - 4267)
P-EGFR (Tyr1068) (PC - 3777)
HER2 (PC - 4290)
P-HER2 (Tyr 1221/1222) (PC - 2243)
HER3 (PC - 4754)
P-HER3 (Tyr1222) (PC - 4784)
HER4 (PC - 4795)
P-HER4 (Tyr1284) (PC - 4757)
ER (Sigma-Aldrich, PC - E0521)
SAPK/JNK (PC - 9258)
P-SAPK/JNK (Thr183/Tyr185) (PC - 9251)
p38 (PC - 9212)
P-p38 (Thr180/Tyr182) (PC - 4511)
ERK1/2 (p44/42) (PC - 4695)
P-ERK1/2 (P-p44/42) (PC - 4370)

CRAF (PC - 9422)
P-CRAF (Ser259) (PC - 9421)
AKT (PC - 4691)
P-AKT (Ser473) (PC - 4060)
P-AKT (Thr308) (PC - 2965)
PTEN (PC - 9188)
P-PTEN (Ser380) (PC - 9551)
GSK-3 β (PC - 12456)
P-GSK-3 β (Ser9) (PC - 5558)
P-PDK1 (Ser241) (PC - 3438)
P-JAK2 (Tyr1007/1008) (PC - 3776)
P-STAT5 (Tyr694) (PC - 9351)
Cyclin D1 (PC - 2922)
4E-BP1 (PC - 9644)
P-4E-BP1 (Ser65) (PC - 9451)
eIF4E (PC - 2067)
P-eIF4E (Ser209) (PC - 9741)
c-MET (PC - 8198)
CYP1A1 (Sigma-Aldrich, PC - SAB1410273)
GAPDH (PC - 5174)
β -actin (PC - 3700)
Anti-rabbit immunoglobulins, horseradish peroxidase (HRP) - 2 $^{\circ}$ (PC - 7074)
Anti-rabbit immunoglobulins, HRP - 2 $^{\circ}$ (Dako, PC - P044801-2)

Table 2.2: List of 1 $^{\circ}$ and 2 $^{\circ}$ antibodies. All antibodies were purchased from Cell signalling technologies except ER and CYP1A1 which were purchased from Sigma-Aldrich. All 1 $^{\circ}$ antibodies were of rabbit origin except β -actin which was mouse origin. One of the anti-rabbit goat immunoglobulins HRP 2 $^{\circ}$ antibodies was purchased from Dako. All 1 $^{\circ}$ antibodies were diluted 1:1000, except for CYP1A1, where a dilution of 1:500 was used and 2 $^{\circ}$ antibodies were diluted 1:2000 for Western blotting. All 1 $^{\circ}$ antibodies including the 2 $^{\circ}$ antibody from Cell signalling - PC - 7074 were stored at -20 $^{\circ}$ C and the 2 $^{\circ}$ antibody from Dako, PC - P044801-2 was stored at 4 $^{\circ}$ C.

2.8.4.2 Method

Following gel electrophoresis, the separated proteins were transferred to a nitrocellulose membrane by semi dry transfer for further analysis. The gel was equilibrated in transfer buffer for ~ 2 - 4 min. During equilibration the nitrocellulose membrane and chromatography paper were cut to the dimensions of the gel and the membrane was then placed in 50 ml 1 x transfer buffer for 2 min. At the same time chromatography papers were also soaked in 50 ml 1 x transfer buffer for 2 min. Subsequently, the transfer apparatus (Invitrogen) was assembled from gel to membrane as a 'transfer sandwich'. All trapped air bubbles were removed and protein transfer was conducted at 25 V for 1.5 h.

To block nonspecific protein binding, the membrane was blocked in 10% non-fat milk for 1 h at room temperature with gentle agitation. Subsequently, the membrane was washed 3 x 5 min with TBS-T and then incubated with the appropriate 1° antibody (Table 2.2) in 5% non-fat milk with TBS-T overnight at 4 °C with gentle agitation. The membrane was then washed again 3 x 10 min in TBS-T to take away excess unbound 1° antibody after which the membrane was incubated with a goat anti-rabbit HRP-conjugated 2° antibody (Table 2.2) in 5% non-fat milk with TBS-T for a further 1 h at room temperature with gentle agitation. This was followed by washing the membrane for 3 x 10 min in TBS-T to remove excess unbound 2° antibody.

2.8.5 Immunological detection

In order to identify specific proteins blotted to membranes immunological detection systems are used.

2.8.5.1 Materials

Enhanced chemiluminescence (ECL) Western blotting detection reagent (GE Healthcare Life Sciences, Amersham ECL, PC - RPN2209), hyperfilm (GE Healthcare Life Sciences, Amersham Hyperfilm ECL, PC - 28-9068-39), developer (Sigma-Aldrich, Kodak autoradiography GBX developer, PC - P7042 - 1 gal), fixer (Sigma-Aldrich, Kodak autoradiography GBX fixer, PC - P7167 - 1 gal).

2.8.5.2 Method

Following the final washing step, the membrane was incubated with ECL substrate mixture (Reagent A and B were mixed to a ratio of 1:1) for 1 min at room temperature. The membrane was removed from the substrate and excess substrate was drained. The membrane was sandwiched between cellulose acetate sheets and taped inside a film cassette removing any air bubbles and exposed to the hyperfilm in the dark for variable exposure periods depending on the strength of the signals. The film was developed using appropriate developing solution and fixative. Subsequently, the film was washed, air dried and then scanned using a densitometer (GS-800, Bio-Rad) in grayscale using the quality one software version 4.6.5. Densitometry of the blots was conducted using ImageJ software (version 1.48). Mean area densities and the relative

densities were calculated, and adjusted according to the loading control used. The adjusted relative densities (ARD) were used throughout the results chapters to show densitometry analysis.

2.9 Coomassie dye protein staining experiment

Coomassie brilliant blue staining is one of the widely used techniques for visualisation of proteins separated by SDS-PAGE. It requires staining the complete gel followed by destaining of the gel to allow visualisation of protein bands, because the dye is retained better by the proteins than the gel [158].

2.9.1 Materials

12% resolving gel in a total volume of 10 ml - 3.3 ml dH₂O, 4.0 ml 30% acrylamide/bis acrylamide stock solution, 2.5 ml 1.5 M Tris (pH 8.8), 100 µl 10% SDS, 100 µl 10% APS and 4 µl TEMED.

Coomassie blue staining solution - 0.5% coomassie blue in 10% acetic acid in dH₂O.

Destaining solution - 50% MeOH and 10% acetic acid in dH₂O.

2.9.2 Method

A 12% resolving gel and a 4% stacking gel were prepared. H-AFt alone and H-AFt encapsulated Gefitinib (10 µl of each) were loaded for SDS-PAGE analysis following

denaturing by heat. Molecular markers (5 μ l) were loaded into the peripheral lanes of the gel. The samples were separated by SDS-PAGE at 100 V for 2.5 h. Afterwards the gel was stained overnight with 0.5% coomassie blue staining solution. Subsequently the gel was destained using destaining solution, which was replaced several times until protein bands were visible. The bands were visualised using a transilluminator (BioDoc-it imaging system) and protein band sizes were compared against the molecular marker.

2.10 Transmission electron microscopy (TEM)

Transmission electron microscopy (TEM) enables observation of objects which cannot be observed optically. Instead of using optical light for imaging, TEM uses electrons with energies in the typical range of 100 - 200 keV thus, images can be observed at higher resolution [159].

2.10.1 Materials

Amorphous holey carbon grids (Agar scientific, PC - AGS147) and 20 mM Tris (pH 8.0) - 2.43 g Tris was dissolved in 1 l dH₂O and added conc. HCl to adjust to pH 8.0.

2.10.2 Method

Size and morphology of the NPs were examined by TEM (JEOL 2100F), operating at 200 keV. H-AFt-encapsulated-Gefitinib (3 μ l) in 20 mM Tris buffer (pH 8.0) was

placed on a carbon grid and allowed to dry at room temperature. Micrographs were taken with a field of view in nm scale.

2.11 Reactive oxygen species (ROS)

Reactive oxygen species (ROS) are reactive molecules and free radicals derived from molecular oxygen. It has been shown that cancer cells generate a greater concentration of endogenous ROS levels than normal cells due to high level of metabolic activity requiring energy. Enhanced ROS production in cancer cells can result in cell death. Thus, some pharmacological agents are able to induce elevated ROS levels in tumours causing cell death [160]. The method below was used to measure cellular ROS levels after agent treatment.

2.11.1 Materials

ROS-Glo H₂O₂ assay kit (Promega, PC - G8820) stored at -20 °C. The kit contained 40 µl H₂O₂ substrate (10 mM), 100 µl signal enhancer solution, 100 µl D-cysteine (100 X), 2 ml H₂O₂ substrate dilution buffer, luciferin detection reagent and 10 ml reconstitution buffer.

2.11.2 Method

Cell were trypsinised and seeded in 96 white well opaque walled plates (Corning, PC - 3917) in a volume of 64 µl per well with a density of 5×10^3 cells. Cells were

incubated in 37 °C, 5% CO₂ for 24 h. Subsequently, cells were treated with the pharmacological agent alone or in combination at a maximum volume of 80 µl per well for a further 24 h. H₂O₂ substrate dilution buffer was thawed on ice and prepared to a final concentration of 125 µM with chilled H₂O₂ substrate dilution buffer. The solution was mixed by vortexing to optimise mixing. The solution was freshly prepared prior to each use. H₂O₂ substrate solution (20 µl) was added to each well to a maximum volume of 100 µl and mixed in a shaker for 2 min during the final 6 h of treatment and cells were incubated for further 6 h.

The thawed reconstitution buffer was mixed with lyophilised luciferin detection reagent to produce reconstituted luciferin detection reagent. Immediately prior to use, 10 µl each of D-cysteine and signal enhancer solution was added per 1 ml of luciferin detection reagent to produce the ROS-Glo detection solution. After the required incubation period, 100 µl of ROS-Glo detection solution was added to each well and the plates were incubated for 20 min at room temperature. The relative luminescence was recorded by a luminometer (Promega GloMax, 96 Microplate Luminometer). It was noted that RPMI-1640 without pharmacological agents produced ROS via spontaneous oxidation of components within the medium. According to the manufacturer varying signals may be seen for the agents if tested in different media.

2.12 Quantitative polymerase chain reaction (PCR) - (QPCR) (Real time PCR)

QPCR incorporating SYBR green technology was used to measure gene expression following exposure of the cell lines to different agents [161]. This experiment

incorporated ribonucleic acid (RNA) purification, reverse transcription and amplification of the complementary DNA (cDNA) by real time PCR using primers specific for the genes of interest. The real time signal is a measure of the fluorescence generated when the SYBR green dye intercalates into the minor groove of double stranded DNA following each PCR cycle.

2.12.1 RNA purification

2.12.1.1 Materials

TRI reagent (Sigma-Aldrich, PC - T9424), chloroform (Sigma-Aldrich, PC - C2432 - 25 ml), 2-propanol (Sigma-Aldrich, PC - I9516 - 25 ml), 75% ethanol (Sigma-Aldrich, PC - E7023 - 500 ml) (75 ml of ethanol was mixed with 25 ml of dH₂O to make 75% ethanol).

2.12.1.2 Method

Cells were seeded at a density of 2×10^6 in 10 cm petri dishes and incubated for 24 h. Following treatment and the required exposure period, cells were then trypsinised and pelleted into microcentrifuge tubes. TRI reagent (1 ml) was added into each tube and the cell pellets were passed through a pipette several times to form homogenous cell lysates which were allowed to stand for 5 min at room temperature. Chloroform (200 μ l) was added and the samples were shaken vigorously for 15 sec and left at room temperature for 15 min. The resulting mixture was centrifuged at 12,000 rpm for 15 min at 4 °C. Centrifugation separated the mixture into 3 phases and the colourless

upper aqueous phase which contained RNA was transferred to fresh tubes. Afterwards, 0.5 ml of 2-propanol was added with mixing. Then the samples were allowed to stand for 10 min at room temperature and centrifuged at 12,000 rpm for 10 min at 4 °C. RNA was precipitated and a pellet was formed. The supernatant was removed and the RNA pellet was washed with 1 ml 75% ethanol. The samples were vortexed and then centrifuged at 7,500 rpm for 5 min at 4 °C. The RNA pellet was air-dried for 10 min and 20 µl of ddH₂O was added to the pellet. RNA concentration was measured by a nanodrop (Thermo Scientific, NanoDrop, 1000) and stored at -80 °C.

2.12.2 Reverse transcription (Preparation of cDNA)

2.12.2.1 Materials

SuperScript III reverse transcriptase kit stored at -20 °C (Life technologies, PC - 18080-093). The kit contained SuperScript III RT (200 U/µl) 10 µl, 5 x first-strand buffer 1000 µl and 0.1 M dithiothreitol (DTT) 500 µl, Oligo (dT)₂₀ primer (Life technologies, PC- 18418-020), deoxynucleotide solution (dNTP) mix (10 mM each) (Life technologies, PC - R0192) and RNaseOUT recombinant RNase inhibitor (Life technologies, PC – 10777-019).

2.12.2.2 Method

Oligo (dT)₂₀ (1 µl), 5 µg RNA, 1 µl dNTP mix and 13 µl ddH₂O was added into a microcentrifuge tube and mixed. The mixture was heated up to 65 °C for 5 min and incubated on ice for 1 min. First-strand buffer (4 µl; 5 x), 1 µl 0.1 M DTT, 1 µl

RNaseOUT, 1 µl SuperScript III RT was added and mixed by pipetting. This mixture was incubated for 60 min at 50 °C and the reaction was inactivated by heating at 70 °C for 15 min. cDNA was stored at -20 °C.

2.12.3 Amplification of cDNA by real time PCR (QPCR)

2.12.3.1 Materials

Brilliant II SYBR green QPCR master mix stored at -20 °C (Agilent technologies, PC - 600828).

Below mentioned primers were designed from ‘Universal Probe Library Assay Design Center’ of the Roche website and they were ordered from Sigma-Aldrich.

EGFR- Forward (5’-3’)- TTCCTCCCAGTGCCTGAA

Reverse (5’-3’)- GGGTTCAGAGGCTGATTGTG

CYP1A1- Forward (5’-3’)- AGTGGCAGATCAACCATGAC

Reverse (5’-3’)- TTGTCGATAGCACCATCAGG

GAPDH- Forward (5’-3’)- AGGTGAAGGTCGGAGTCAAC

Reverse (5’-3’)- GATGACAAGCTTCCCGTTCT

2.12.3.2 Method

cDNA (1 µl) was added to the master mix (10 µl of brilliant II SYBR green QPCR master mix, 0.05 µl each of forward and reverse primers, 8.9 µl of dH₂O). The samples were then introduced into 96 well plates and analysed in a QPCR machine (Agilent technologies, Mx3005P qPCR System) for 2.5 h. Negative dH₂O blanks were included in every analysis. Denaturation (10 min; 95 °C) activated taq polymerase, which was followed by 40 PCR cycles, in accordance with the following protocol - denaturation at 95 °C (30 sec), annealing at 58 °C for all 3 primer pairs and elongation at 72 °C (1 min). At the end of the PCR, a melting curve analysis was performed by gradually increasing the temperature to 95 °C for 1 min, annealing at 58 °C for 30 sec and denaturation at 95 °C for 30 min. After PCR was completed the SYBR green fluorescent signal was transformed into a relative number of copies of target molecules. Signals were normalised to the expression of the house keeping gene *GAPDH* and the relative expression of each gene of interest was calculated.

2.13 Reverse phase protein microarray (RPMA)

Reverse phase protein microarray is a technology which is used for profiling the protein functional state of cellular signalling pathways [162].

2.13.1 Materials

Nitrocellulose-coated glass slides (Grace-Bio-labs, PC - 305116), blocking solution - 0.2% I-block (Applied biosystems, PC - T2015) and 0.1% tween in PBS, antibody diluent (Dako, PC - S080981-2).

2.13.2 Method

Cells were seeded at a density of 1×10^6 in 10 cm petri dishes and incubated for 24 h. Following treatment and the required exposure period, cell lysates were collected by adding NP40 lysis buffer with phosphatase and protease inhibitors. Lysates were solubilised in 4 x SDS sample buffer at a ratio of 1:3 respectively and heated for 5 min at 100 °C. Samples (10 µl) were loaded onto a 384 well plate (Life technologies, PC - AB-1055). Samples were robotically spotted in duplicates onto nitrocellulose-coated glass slides using a microarraying robot (MicroGrid 610, Digilab). Slides were incubated overnight in blocking solution at 4 °C with constant shaking. After washing 3 x 5 min each in 1 x TBS-T, the slides were incubated with the 1° antibodies (Table 2.2, except HER4, ER, CYP1A1, 4E-BP1, eIF4E and c-MET antibodies). Subsequently, antibodies were diluted in antibody diluent (1:1000). In addition, β -actin (diluted 1:1000 in the same diluent) was used as a protein loading control. Slides were incubated overnight at 4 °C while shaking.

Following washing, as described above, the slides were incubated with diluted infrared Licor 2° antibodies (1:5000 in 1 x TBS-T) - 800 CW (green) anti-rabbit antibody for detection of rabbit 1° antibodies and 700 CW (red) anti-mouse antibody for detection of β -actin, for 30 min at room temperature in the dark while shaking. Then slides were

washed and dried by centrifugation at 500 rpm for 5 min and scanned with a Licor Odyssey scanner (LI-COR, Biosciences) at 21 μm resolution at 800 nm (green) and 700 nm (red). The resulting TIFF images were processed with Axon Genepix Pro-6 microarray image analysis software (Molecular Devices Inc.) to obtain fluorescence data for each spot and to generate standardised Genepix results files. Protein signals were finally determined with background subtraction and normalised to the internal housekeeping proteins using RPPanalyser, an open source software within the R statistical language on the CRAN platform [163] [164]. This experiment was conducted in collaboration with Dr. Lei Zhang, Dr. Ola Negm and Dr. Paddy Tighe, and the author extends her appreciation.

2.14 Preparation and measuring encapsulation efficiency (EE) of H-AFt-encapsulated-Gefitinib NPs

2.14.1 Preparation of H-AFt-encapsulated-Gefitinib NPs

2.14.1.1 Materials

20 mM Tris (pH 8.0), dialysis membrane (Spectra/Por, PC – 132650).

2.14.1.2 Method

As Gefitinib is fluorescent under UV, its fluorescence was checked under a UV transilluminator (UVP BioDoc-It imaging system) and compared to H-AFt which does not fluoresce. Gefitinib (1 mg) was dissolved in DMSO (1 ml) to make a homogenous solution. Subsequently, an aqueous solution of Gefitinib was freshly prepared by

dissolving the Gefitinib solution in 1ml of PBS (pH 7.2) (1:1 solution of DMSO:PBS) to make a final concentration of 1 mM. H-AFt at a concentration of 160 μ M was added to this solution where the concentration of Gefitinib was ~ 40-fold in excess of H-AFt. The resulting solution was stirred overnight at 4 °C so that Gefitinib would be diffused into H-AFt. Afterwards, this solution was exhaustively dialysed for 48 h at 4 °C in 20 mM Tris (pH 8.0) using a dialysis membrane (MW cut off 8,000 Da) to remove all molecules < 8,000 Da MW, and therefore to remove un-encapsulated Gefitinib. The solution was centrifuged at high speed (13,000 rpm, 12 min, 4 °C) to remove any impurities and the supernatant was transferred to a new tube and stored at -20 °C. The fluorescence of the resulting solution was visualised under UV. The protein concentration of the encapsulated agent was determined by Bradford assay. In order to avoid degradation of the prepared test agent, a fresh agent was prepared every 3 months.

2.14.2 Determining encapsulation efficiency

2.14.2.1 Method

Encapsulated Gefitinib was quantified by UV spectrometry after weighing and freeze-drying the encapsulated NPs for 8 h and dissolving in DMSO. Afterwards, the absorbance of Gefitinib was read at 250 nm by Perkin Elmer precisely Lambda 25 UV/VIS spectrometer. Results were analysed using Perkin Elmer UV WinLab software (version 6.0.4.0738). A standard curve for Gefitinib was assembled using 6 serial dilutions in the range of 0.5 - 250 μ M; subsequently, the amount of Gefitinib encapsulated within H-AFt was determined according to the Beer-Lambert law which

showed that absorbance was proportional to concentration. Finally, the encapsulation efficiency (EE) was calculated by using the formula below:

$$EE = \frac{\text{Molar concentration of the drug in the NPs}}{\text{Molar concentration of the drug encapsulated initially}} \times 100\%$$

2.15 Mass spectrometry (Matrix Assisted Laser Desorption Ionisation- MALDI)

In order to confirm the purity and the MWs of H-AFt and Gefitinib within the novel test agent - H-AFt-encapsulated-Gefitinib, matrix assisted laser desorption ionisation (MALDI) mass spectrometry was used.

2.15.1 Materials

Sinapic acid solution diluted in acetyl nitrite (Sigma-Aldrich, PC – 85429 - 1 g).

2.15.2 Method

H-AFt-encapsulated-Gefitinib and Gefitinib alone (10 µl) were mixed separately with 20 µl saturated sinapic acid solution. The resulting solution (0.5 µl) was loaded onto a MALDI target sample plate. The plate was left to air dry for 5 min. The plate was then loaded to the MALDI mass spectrometer for analysis (Bruker Ultraflex III). The results were analysed using the flexControl (Ultraflex) software (version 3.0).

2.16 Confirmation of encapsulation of Gefitinib in H-AFt by flow cytometry**2.16.1 Method**

As Gefitinib is fluorescent under UV illumination, NPs were analysed using an Astrios EQ flow cytometer (Beckman Coulter) equipped with blue (488 nm) and UV (355 nm) lasers to detect scatter and Gefitinib fluorescence respectively in order to confirm encapsulation of Gefitinib in H-AFt. Freshly prepared H-AFt-encapsulated-Gefitinib or H-AFt alone (1 ml) was mixed with 1 ml PBS and analysed using an Astrios EQ flow cytometer. Emitted fluorescent light from Gefitinib was collected using a 405/30 band pass filter. Freshly prepared H-AFt-encapsulated-Gefitinib was compared to H-AFt alone. Results were analysed by Beckman Coulter Summit software (version 6.2.3.1561).

2.17 Release of Gefitinib from H-AFt cavity**2.17.1 Method**

Dialysis bags (MW cut off 8,000 Da) containing H-AFt-encapsulated-Gefitinib diluted in 20 mM Tris buffer to make a final concentration of 100 μ M were placed in separate beakers containing 20 mM Tris buffer at varying pH levels (2, 4 and 7.5) at 37 °C, 5% CO₂. A dialysis bag with Gefitinib alone diluted in 20 mM Tris buffer (100 μ M) was also placed in a beaker containing 20 mM Tris buffer, pH 7.5 at 37 °C, 5% CO₂. Release of Gefitinib into the buffer was monitored after 2, 6, 12 and 24 h. Buffer within the beaker was refreshed at each time interval. Subsequently, released Gefitinib was quantified by UV spectrophotometry (Perkin Elmer precisely Lambda 25 UV/VIS Spectrometer), the results were analysed using the Perkin Elmer UV WinLab software

(version 6.0.4.0738) at 250 nm. The obtained values were used to calculate the cumulative mean of the released drug. The residual buffer within the dialysis bags after 24 h containing NPs was studied using the Astrios EQ flow cytometer (Beckman Coulter) equipped with blue and UV lasers. Fluorescence emitted by Gefitinib was detected with a 405/30 band pass filter. The results were analysed by Beckman Coulter Summit software (version 6.2.3.1561).

2.18 Statistical analyses

All experiments were repeated ≥ 3 times. Representative figures are shown. Results were analysed using GraphPad Prism, version 6.0 and presented as means \pm standard deviation (SD). All the results were subjected to one-way or two-way ANOVA. Tukey's or Dunnett's multiple comparison tests were applied to assess significance. Significant differences were defined as * ($P < 0.05$), ** ($P < 0.01$), *** ($P < 0.001$), **** ($P < 0.0001$).

3 Chapter 3 - Retooling existing agents - EGF, Gefitinib, Erlotinib and Raloxifene

3.1 Introduction

EGFR is overexpressed in breast cancer, and thus, has emerged as a potential target for therapy [53]. EGFR and ER expression are generally inversely correlated [165]. Cross talk may modulate HER family and ER activity in breast cancer. Promising new targeted therapies such as TKIs, targeting the HER family of receptors and anti-oestrogen therapy targeting ER, have been introduced to the clinic [89]. However, most of the TKIs have failed to elicit a significant response in breast cancer and only half of all ER+ tumours are responsive at first presentation to anti-oestrogen therapy. In the metastatic setting, initially responsive tumours to these therapies eventually become resistant to these treatment options, leading to tumour progression and ultimately death [87] [89]. As breast cancer is heterogeneous, HER and ER pathway activity may vary between patients, thus, leading to different patient responses [89]. Therefore, it is imperative to better understand the molecular pathogenesis as an essential part of pre-treatment and diagnostic procedures, and every effort should be made to personalise the treatment strategy to the individual patient. Therefore, existing pharmacological agents such as EGF, Gefitinib, Erlotinib and Raloxifene have been tested on a panel of breast cancer cell lines to verify the type of breast cancer against which they are most effective, and these findings are discussed in this chapter.

3.2 Results and Discussion

3.2.1 HER family protein expression and ER protein expression in the panel of breast cancer cell lines

Initially protein expression levels of the HER family were analysed by Western blots in the breast cancer cell line panel. Subsequently ER expression in each cell line was also analysed (Figure 3.1).

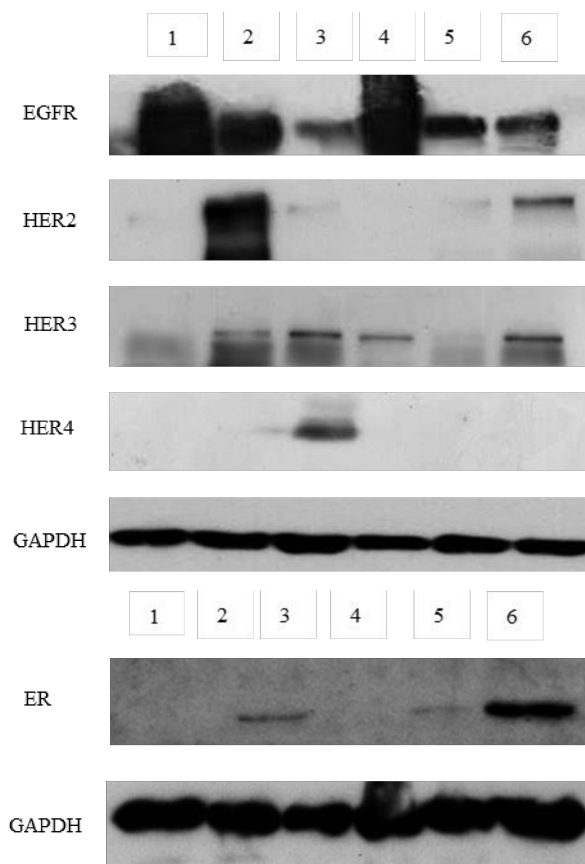


Figure 3.1: Western blot analysis of HER family and ER in the breast cancer cell line panel. EGFR (170 kDa), HER2 (185 kDa), HER3 (180 kDa), HER4 (180 kDa), ER (67 kDa) and GAPDH (37 kDa). GAPDH was probed as a loading control. (1) MDA-MB 468, (2) SKBR3, (3) MCF7, (4) MDA-MB 231, (5) ZR-75-1 and (6) T47D. Whole cell protein lysates (50 μ g for HER family protein detection and 75 μ g for ER detection) were subjected to 8% (HER3) and 10% SDS polyacrylamide gel electrophoresis.

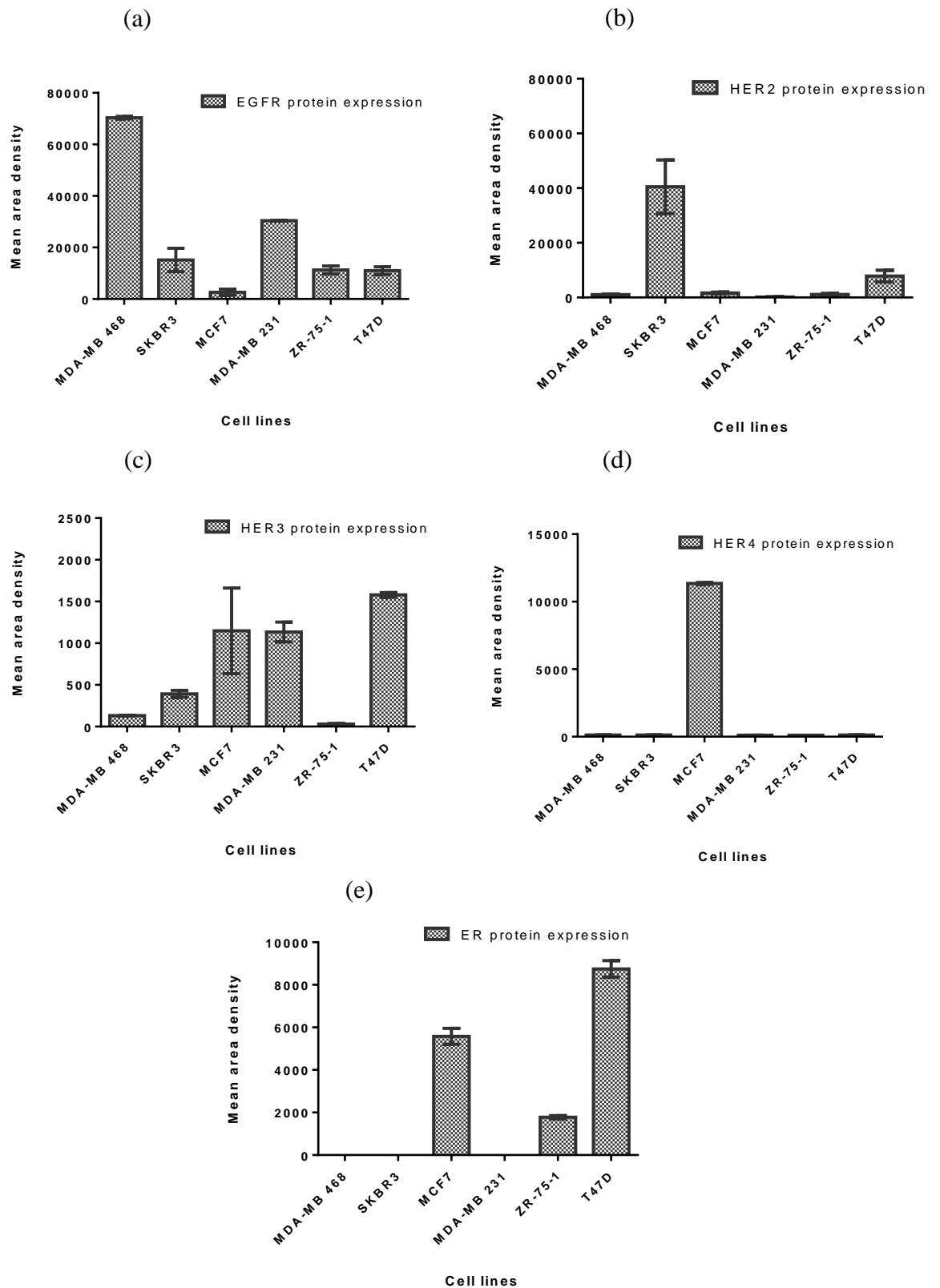


Figure 3.2: Densitometry plots of protein expression levels of (a) EGFR (b) HER2 (c) HER3 (d) HER4 and (e) ER in the breast cancer cell line panel. Mean and SD of trials ≥ 3 .

It was observed that MDA-MB 468 cell line expressed EGFR to the greatest extent, corroborating previous observations of EGFR overexpression on this cell line [34]. MDA-MB 231 also overexpressed EGFR. SKBR3, ZR-75-1 and T47D cell lines expressed moderate levels of EGFR. MCF7 expressed the least amount of EGFR. SKBR3 cell line overexpressed HER2 and the T47D cell line expressed moderate levels of HER2. Among the breast cancer cell lines, T47D expressed large levels of HER3 while MCF7 and MDA-MB 231 cell lines expressed moderate levels of HER3. SKBR3 expressed low levels of HER3 while MDA-MB 468 and ZR-75-1 barely expressed HER3. MCF7 cell line was the only cell line that expressed HER4 (Figure 3.1) and (Figure 3.2 (a-d)).

T47D expressed ER most abundantly among the 6 breast cancer cell lines, corroborating previous studies [166]. The MCF7 cell line expressed moderate levels of ER while ZR-75-1 expressed low levels of ER. MDA-MB 468, SKBR3 and MDA-MB 231 cell lines did not express ER, as expected (Figure 3.1) and (Figure 3.2 (e)). These results corroborated previous literature as mentioned in chapter 1, section 1.3, with respect to HER family and ER protein expression confirming that these breast cancer cell lines have retained their established molecular phenotypes in the panel of cell lines used [27] [31] [166] [167].

3.2.2 Cellular growth assay

It has been shown that various steroid hormones, peptide hormones and growth factors are involved in the growth and regulation of breast cancer cells [168]. Thus, propagation of these cancerous cells *in vitro* requires specific culture conditions and

culture media. Various culture media have been developed in many laboratories to support the growth of breast cancer cells of different lineages. In general, the culture medium used has to provide all essential nutrients for cell metabolism, growth and proliferation. Commonly culture media are supplemented with animal serum, and most commonly with FBS to promote cell growth and proliferation. It has been demonstrated that animal serum is an extremely complex mixture of low and high weight biomolecules with diverse growth promoting and growth inhibiting activities [169] [170].

The main function of serum in culture media is to provide hormonal and growth stimulating factors that initiate cell growth and proliferation. However, in the tissue culture environment, the presence of hormones and growth factors in the serum at times complicates the demonstration of specific effects on growth of cells [168]. FBS is found to be of better quality than serum from adult animals because of its low gamma globulin content while a high content of antibodies from adult animal serum may inhibit growth and proliferation [169].

In the current study, the effect of FBS on the proliferation of breast cancer cell types was studied. Previous studies have portrayed that growth of ER⁺ breast cancer cells is stimulated by both oestrogens and growth factors which enhance the production and secretion of a number of proteins, while cells which are ER⁻ are only stimulated by growth factors [171]. Further, following long term oestrogen deprivation, breast cancer cell lines have shown an adaptive process with an increase in ER expression and high sensitivity to low levels of oestrogen. Furthermore, cancer cells have been

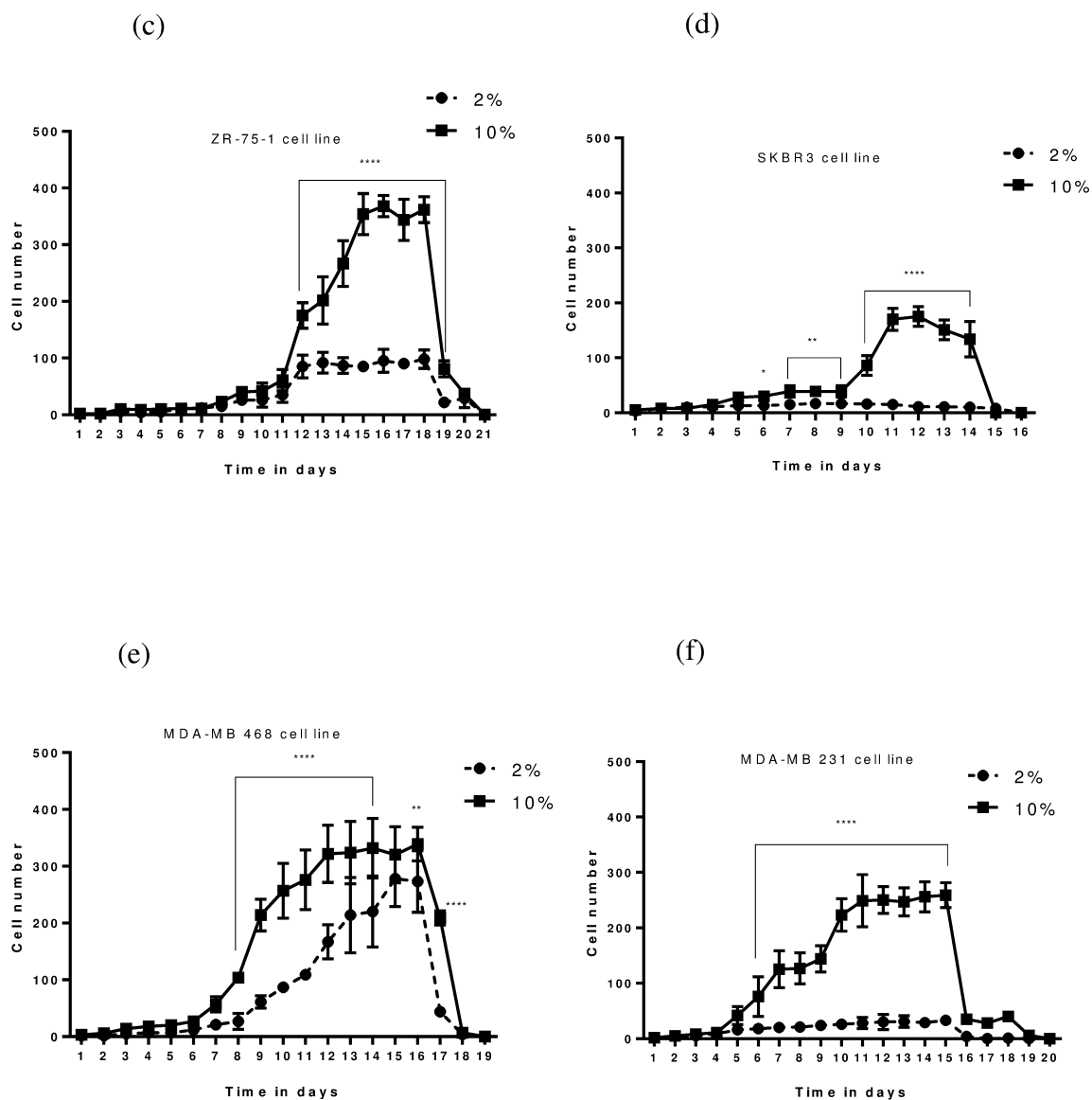


Figure 3.3: Cellular growth curves for all 6 cell lines. (a) MCF7, (b) T47D, (c) ZR-75-1, (d) SKBR3, (e) MDA-MB 468 and (f) MDA-MB 231. Each point represents the number of cells against time. Mean and SD of trials ≥ 3 , ($n = 3$ per trial). * indicates significant difference between growth in medium supplemented with 2% and 10% FBS. * ($P < 0.05$), ** ($P < 0.01$), *** ($P < 0.001$), **** ($P < 0.0001$).

A typical growth curve will immediately show a lag phase lasting up to 48 h. Subsequently, the cells enter into an exponential growth phase termed as the log phase, in which the cell population doubles repeatedly. During the log phase the effects of pharmacological agents or chemical agents that stimulate or inhibit cell growth can be studied. After the log phase, when the cell population becomes very dense, cells enter into a stationary phase and the growth rate ceases. Finally the cells enter into a decline phase where cells die and the cell population declines [145].

The MCF7 cell line showed a high growth rate in 2% FBS compared to all other cell lines. The growth curves for both FBS levels were not statistically different from each other, apart from days 5 and 9 in log phase and days 14 - 17 in stationary phase (Figure 3.3 (a)) ($P < 0.01$). The cells showed a high exponential growth from days 8 - 14 in both growth curves. The population doubling time was 36 h for MCF7 cells that were in medium supplemented with 10% FBS. The population doubling time for cells in medium supplemented with 2% FBS was also ~ 36 h. The cell number reduced rapidly \geq day 17 in medium supplemented in 2% FBS when compared to 10% FBS.

MCF7 cells are ER⁺ and express very low levels of EGFR [28] [173]. Oestrogens are well known to stimulate an array of biosynthetic processes in hormone responsive target cells. Studies have shown that MCF7 cells are able to convert oestrone sulfate which is a non-oestrogenic compound included in culture medium to oestrone and that these cells are able to stimulate growth even at low serum levels such as 0.05% FBS [174]. Further, it has been reported that these cells are able to produce growth factors such as EGF and TGF α to stimulate growth, confirming the hallmark 'self-sufficiency

in growth signals' [37] [175]. Another study has shown that phenol red the commonly used pH indicator in tissue culture medium has some structural resemblance to certain nonsteroidal oestrogens and that phenol red possesses oestrogenic properties. It stimulates cell proliferation in a dose dependent manner in oestrogen responsive cells. Thus, MCF7 cells grown in phenol red-containing medium may be oestrogen stimulated [176]. Further as outlined in chapter 1, it is reported that oestrogens are able to activate the RAS/MAPK pathway showing cross talk between ER and RAS/MAPK which plays a role in cell growth and differentiation thus, increasing cell growth in this cell line even in low serum levels [177]. In contrast a study done by Clark et al, 2002, has shown that MCF7 cells show low levels of AKT phosphorylation due to wild type *PTEN* expression in medium supplemented with 10% FBS and in serum deprived medium implying that these cells do not hyperactivate the PI3K/AKT pathway. Thus, it can be suggested that oestrogen stimulation may play a key role in the growth of this cell line and that these cells are secreting their own growth factors that stimulate growth even in serum depleted medium.

T47D cells grew rapidly in medium supplemented with 10% FBS from day 10 onwards when compared to cells in medium supplemented with 2% FBS ($P < 0.0001$) (Figure 3.3 (b)). The doubling time for cells in medium supplemented with 10% FBS was 48 h. These results suggest that T47D cell proliferation heavily depends on the level of serum compared to MCF7 cells although, both cell lines are ER+ and categorised under the luminal A subtype.

Further, it implies that T47D cells are unable to secrete autocrine growth factors to stimulate growth unlike MCF7 cells although T47D expressed a higher level of ER. Indeed, it has been shown previously that MCF7 cells are able to produce more growth factors compared to T47D and ZR-75-1 cells [30]. On the other hand, T47D cells expressed higher levels of EGFR, HER2 and HER3 than MCF7 cells, suggesting that these cells may depend on exogenous growth factors for stimulation. Hence, in 2% FBS which had low levels of growth factors these cells demonstrated low growth.

ZR-75-1 cells also demonstrated hindered growth in medium supplemented with 2% FBS with a short log phase whereas cells in medium supplemented with 10% FBS showed rapid growth during the log phase. There was a significant difference in the cell numbers between cells cultured in medium with 2% and 10% FBS during the 12th day and 19th day ($P < 0.0001$) (Figure 3.3 (c)). The cell doubling time in medium supplemented with 10% was ~ 48 h. This cell line is also ER⁺ and showed similar growth characteristics to the T47D cell line.

SKBR3 cells did not show a high growth rate in medium supplemented 10% FBS and these cells had the shortest incubation period compared to the other cell lines as all cells detached and died at ~ day 16. Further, cells in medium with 2% FBS showed retarded growth and entered a quiescent state from day 3 which has been shown previously [178]. High cell numbers were observed in the log and stationary phases between days 10 - 14 in medium supplemented with 10% FBS compared to cells that were in medium with 2% FBS ($P < 0.0001$) (Figure 3.3 (d)). This cell line showed a doubling time of 24 h for cells in medium supplemented with 10% FBS. As these cells

are ER- and PR- their growth is not stimulated by hormones. Therefore, growth factors, receptors and activated signal transduction cascades may play a major role in SKBR3 cell proliferation [179]. It has been reported that serum starvation decreased AKT (Ser473) phosphorylation in SKBR3 cells, suggesting that this cell line depends on serum derived growth factors for AKT (Ser473) phosphorylation in the PI3K/AKT pathway when compared to other breast cancer cell lines which have also been serum starved. In contrast, these cells have shown AKT (Thr308) phosphorylation in response to serum starvation and that Thr308 phosphorylation may be associated with HER2 overexpression in this cell line [180]. However, for AKT to achieve full activation, phosphorylation is needed at both Ser473 and Thr308, upon growth factor and receptor binding [181]. Therefore, this may underpin the retarded growth in medium supplemented with 2% FBS.

MDA-MB 468 cells showed excellent growth in medium supplemented with 2% FBS (Figure 3.3 (e)). However, there was a significant difference in the cell numbers between days 8 - 14 ($P < 0.0001$) and days 16 - 17 ($P < 0.01$) with a population doubling time of 24 h for cells that were in medium supplemented with 10% FBS and a population doubling time of ~ 48 h for cells that were in depleted medium. This cell line is PTEN deficient, thus, Clark et al, 2002, has demonstrated that even under serum starvation MDA-MB 468 cells have showed phosphorylation at both Ser473 and Thr308 residues of AKT [180] [182]. Further, the mTOR pathway is also highly activated in these cells which demonstrates the reason for somewhat large cell numbers in medium supplemented with 2% FBS [182].

The MDA-MB 231 cell line showed significantly reduced growth in medium supplemented with 2% FBS when compared to growth in medium supplemented with 10% FBS during days 6 - 15 ($P < 0.0001$) (Figure 3.3 (f)). The doubling time for cells that were in medium with 10% FBS was 36 h. Clark et al, 2002, demonstrated that MDA-MB 231 cells showed low levels of phosphorylated AKT in medium supplemented with 10% FBS and serum deprived medium suggesting that these cells show reduced AKT activity [180]. In contrast, MDA-MB 231 cells harbour a mutant form of the *RAS* gene (*K-RAS*) [72]. Thus, the RAS/MAPK pathway is constitutively activated in these cells, which could be a reason for high cell numbers in medium supplemented with 10% FBS. Furthermore, Leong et al, 2010, reported that MDA-MB 231 cell proliferation was inhibited when cells were subjected to prolonged serum starvation and that they entered an inactive state [183]. Interestingly, the same authors have shown that in serum starvation, MDA-MB 231 cells showed a loss of phosphorylated ERK although these cells exhibit a mutated form of *RAS* which may indicate another reason for hindered growth in medium supplemented with 2% FBS [183].

3.2.3 *In vitro* growth inhibitory effects of EGF, Gefitinib, Erlotinib and Raloxifene

Using MTT viability assays the anti-proliferative effects of EGF, Gefitinib, Erlotinib and Raloxifene were investigated in all 6 breast cancer cell lines in the presence of medium supplemented with 2% FBS and 10% FBS. GI₅₀ values were determined for all agents; results are summarised in the tables below.

(a)	EGF Mean GI ₅₀ ± SD (72 h MTT assays)	
Cell line	Medium supplemented with 2% FBS	Medium supplemented with 10% FBS
MCF7	>10 nM	>10 nM
T47D	>10 nM	>10 nM
ZR-75-1	>10 nM	>10 nM
SKBR3	9.89 nM ± 2.97	0.50 nM ± 0.38
MDA-MB 468	6.78 nM ± 3.40	7.78 nM ± 3.15
MDA-MB 231	>10 nM	>10 nM

(b)	Gefitinib Mean GI ₅₀ ± SD (72 h MTT assays)	
Cell line	Medium supplemented with 2% FBS	Medium supplemented with 10% FBS
MCF7	15.83 µM ± 10.34	>25 µM
T47D	1.26 µM ± 0.88	4.12 µM ± 1.53
ZR-75-1	1.77 µM ± 1.14	4.84 µM ± 2.07
SKBR3	0.25 µM ± 0.15	0.94 µM ± 0.85
MDA-MB 468	0.24 µM ± 0.15	2.01 µM ± 1.21
MDA-MB 231	16.68 µM ± 1.40	21.80 µM ± 0.74

(c)	Erlotinib Mean GI₅₀ ± SD (72 h MTT assays)	
Cell line	Medium supplemented with 2% FBS	Medium supplemented with 10% FBS
MCF7	>25 µM	>25 µM
T47D	10.47 µM ± 4.29	12.96 µM ± 2.07
ZR-75-1	10.95 µM ± 0.69	14.72 µM ± 4.11
SKBR3	12.23 µM ± 1.36	17.34 µM ± 1.75
MDA-MB 468	2.48 µM ± 2.20	13.90 µM ± 1.15
MDA-MB 231	>25 µM	>25 µM

(d)	Raloxifene Mean GI₅₀ ± SD (72 h MTT assays)	
Cell line	Medium supplemented with 2% FBS	Medium supplemented with 10% FBS
MCF7	7.06 µM ± 0.22	18.88 µM ± 1.96
T47D	6.59 µM ± 3.12	16.76 µM ± 1.42
ZR-75-1	5.94 µM ± 0.83	15.75 µM ± 1.60
SKBR3	13.64 µM ± 1.07	19.22 µM ± 0.71
MDA-MB 468	6.95 µM ± 1.67	15.00 µM ± 0.87
MDA-MB 231	7.37 µM ± 2.28	16.81 µM ± 0.90

(e)	DMSO Mean GI ₅₀ ± SD (72 h MTT assay)
Cell line	Medium supplemented with 10% FBS
MCF7	>1%
T47D	0.82% ± 0.11
ZR-75-1	0.85% ± 0.03
SKBR3	>1%
MDA-MB 468	>1%
MDA-MB 231	>1%

Table 3.1: Mean GI₅₀ ± SD values of (a) EGF, (b) Gefitinib, (c) Erlotinib, (d) Raloxifene and (e) DMSO (vehicle control). Pharmacological agents' activity was tested in cells grown in medium supplemented with 2% and 10% FBS. DMSO was used as the solvent for some pharmacological agents. The effect of DMSO was tested in medium supplemented with 10% FBS. Cells were seeded in 96 well plates at a density of 2.5×10^3 cells/well. After allowing time to adhere (24 h), cells were exposed to agents (72 h; n = 8). Mean and SD of trials ≥ 3 .

EGF is an important regulator of cell growth. It has been reported that EGF acts as a mitogen in some human breast cancer cell lines, suggesting that it may be an additional hormonal factor regulating growth of breast cancer in certain patients with this disease [120]. In contrast, EGF mediated apoptosis has also been reported in some tumour cell lines [34] [184]. However, the results of studies investigating the effect of EGF still remain controversial as conflicting results have been reported. Therefore, the effect of EGF was investigated on growth of all 6 breast cancer cell lines in medium supplemented with 10% and 2% FBS. It has been reported that > 1,000 proteins are

present in serum, thus EGF could be also present [170]. Hence, by using serum depleted medium the effect of EGF could be more readily observed.

Out of the 6 cell lines, the HER2 overexpressing SKBR3 cell line appeared to be most sensitive to growth inhibitory properties of EGF showing a low GI_{50} value in medium supplemented with 10% FBS ($GI_{50} = 0.50$ nM) (Table 3.1 (a)). It has been found that there is an inverse relationship between the amount of EGFR and EGF induced mitogenesis. Thus, low expression of EGFR is associated with growth stimulation by EGF, while high EGFR expression is correlated with growth inhibition by EGF [34] [185]. In this study, MCF7, T47D and ZR-75-1 cell lines express low levels of EGFR, and are ER⁺ (Figure 3.1) and (Figure 3.2) and were not inhibited by EGF in neither medium supplemented with 2% nor 10% FBS. Fitzpatrick et al, 1984, revealed that EGF (10 nM) was able to stimulate cell proliferation in MCF7 and T47D cells and that it works as a mitogen [186]. In contrast to these results, the HER2 overexpressing SKBR3 cell line was inhibited by EGF in 10% FBS as outlined above. Previous studies have portrayed that cells which express high levels of both EGFR and HER2 invariably undergo apoptosis rather than proliferation in response to EGF [178]. It has been suggested that ligand dependent apoptosis in cells that express high levels of EGFR and HER2 such as SKBR3 cells is a natural mechanism that protects cells from excessive proliferation in response to high amounts of EGF activated signalling [178]. However, in serum depleted medium, SKBR3 cells showed a GI_{50} value of 9.89 nM. The growth of this cell line was compromised heavily as shown in section 3.2.2, in 2% FBS. As a consequence, EGF could be creating conflicting signals in 2% FBS since EGF is known to act as a mitogen and also an inhibitor. Although MDA-MB

468 and MDA-MB 231 cell lines express high levels of EGFR, this agent was not potent in these cells in both 2% and 10% FBS. It could be because both these cell lines express high levels of EGFR only. Further, MDA-MB 468 cells possess deficient PTEN and MDA-MB 231 cells harbour mutant *K-RAS* leading to constitutive activation of the PI3K/AKT and RAS/MAPK pathways [62] [180] [187].

In medium supplemented with 2% FBS, increased Gefitinib potency was observed compared to medium supplemented with 10% FBS in all 6 breast cancer cell lines (Table 3.1 (b)). However, this could be due to growth of some cell lines being much reduced in serum depleted medium. Further, it has been shown that serum has an inhibitory effect and pharmacological agents are shown to bind to specific proteins of serum which partially prevents uptake of the agents by cells; thus reducing potency [188]. On the other hand, among all the cell lines tested in medium supplemented with 10% FBS; SKBR3 cells showed the highest sensitivity to Gefitinib ($GI_{50} = 0.94 \mu\text{M}$). Amidst the cell lines expressing high levels of EGFR; the MDA-MB 468 cell line demonstrated a GI_{50} value of $2.01 \mu\text{M}$ and the MDA-MB 231 cell line did not show sensitivity ($GI_{50} = 21.80 \mu\text{M}$) in medium supplemented with 10% FBS. Of the ER+ cell lines both T47D and ZR-75-1 cell lines showed moderate sensitivity while the MCF7 cell line was unresponsive to Gefitinib.

Previous research has demonstrated that efficacy of Gefitinib is not directly related to EGFR expression levels. In fact, high EGFR expression levels have not been shown sensitivity to Gefitinib due to molecular defects in downstream signalling pathways [189]. HER2 expression appeared to be important for the sensitivity of this agent.

Indeed, prior work has demonstrated that Gefitinib is extremely effective in inhibiting tumours that express high HER2; hence high sensitivity was observed in the HER2 overexpressing SKBR3 cell line [189]. HER2 remains the preferred dimerisation partner of other HER receptors. Although both homo- and heterodimerisation activates the EGFR network, heterodimers are found to be more potently mitogenic and HER2 heterodimers generate the strongest biological activity compared to other heterodimers [49] [189]. However, Gefitinib does not directly inactivate HER2 thus, the presence of EGFR is necessary for inactivation of HER2 signalling which explains the sensitivity of SKBR3 cells to Gefitinib [189] [190].

Similar to Gefitinib the effect of Erlotinib was investigated by MTT assays using the 6 breast cancer cell lines. All cell lines tested were resistant to this agent when compared to the results of Gefitinib (Table 3.1 (c)). Gefitinib and Erlotinib are structurally related, but distinct and possess different affinities towards EGFR [99]. Further, Guix et al, 2005, reported that treatment with Erlotinib before surgery in 14 patients diagnosed with breast cancer resulted in significant down-regulation in the RAS/MAPK pathway with reduced cell proliferation. However, they did not see cell apoptosis and down-regulation of the PI3K/AKT pathway [191]. In fact, Normanno et al, 2006, indicated that anti-EGFR agents are effective only in tumours that demonstrate down-regulation of both RAS/MAPK and PI3K/AKT pathways, which may explain a reason for resistance towards this agent in this study [192].

Research has shown cross talk between ER and EGFR pathways; thus membrane bound ER is able to activate EGFR, HER2, PI3K and Src. The Src family of protein

tyrosine kinases, plays a major role in regulating signal transduction by a diverse set of cell surface receptors including steroid receptors [88]. Further, ERK1/2 of the RAS/MAPK pathway also activate ER and the ER coactivator AIB1 (Src3) [60] [87]. Osborne et al, 2005 has shown that growth of the MCF7 xenografts in athymic mice is stimulated by oestrogen and inhibited by oestrogen deprivation either alone or in the presence of Tamoxifen. Tamoxifen is a pioneering SERM and used as an anti-cancer targeted therapy for ER+ breast cancers. This agent is also used to prevent development of breast cancer in high risk women [115]. However, the anti-cancer effects of Tamoxifen is temporary because resistance emerges after several months of treatment in some patients [87] [89]. Indeed, in the presence of excessive levels of ER, AIB1 and HER2, Tamoxifen has shown to behave as an oestrogen agonist and stimulate tumour growth. These results imply that other SERMs might be more effective than Tamoxifen [87]. Raloxifene is a second generation SERM similar to Tamoxifen. Raloxifene has also been shown to possess mixed agonist and antagonist activity similar to Tamoxifen [193]. Nevertheless, Raloxifene is primarily used to treat postmenopausal osteoporosis and it is also used to reduce the risk of developing breast cancer in postmenopausal women but with fewer side effects compared to Tamoxifen [115]. Hormone replacement therapy has shown to reduce menopausal symptoms and protect postmenopausal women from osteoporosis. However, as outlined in chapter 1 hormone replacement therapy is associated with an increased risk of breast cancer. This effect restricts the clinical use of hormone replacement therapy for long periods for the prevention of osteoporosis. Raloxifene has shown to act as an oestrogen agonist in the skeleton and it counteracts the effects of oestrogen in the breast and uterus [193]. The effect of Raloxifene was tested against the panel of breast cancer cell lines in this study to determine the effect of this agent on breast cancer, although it is not used as

a therapy currently for breast cancer. It was found that none of the cell lines tested were sensitive towards Raloxifene in both medium supplemented with 2% or 10% FBS (Table 3.1 (d)). However, this agent portrayed a dose dependent growth inhibitory effect at higher concentrations in the MTT assays with all tested breast cancer cell lines. Interestingly, Raloxifene was found to function as an AhR ligand [141]. Thus, its action as an AhR ligand was evaluated. These results are described in chapter 6.

DMSO was used as a solvent to dissolve many pharmacological agents in this study. It is a chemical that dissolves both polar and nonpolar compounds and it is found to be miscible with a wide range of organic solvents and with H₂O [194]. DMSO was tested in all 6 breast cancer cell lines to determine whether it contributed to the inhibition seen with the pharmacological agents. It was tested at a concentration range of 0.01% - 1%. MCF7, SKBR3, MDA-MB 468 and MDA-MB 231 cell lines were not influenced by DMSO vehicle control. However, a marginal effect was observed with T47D and ZR-75-1 cell lines between 0.5% and 1% concentrations of DMSO (Table 3.1 (e)). Nevertheless, the final concentration of DMSO vehicle used within the agents never exceeded 0.05% which is a negligible concentration to impact cell viability.

Out of the 4 pharmacological agents tested, EGF and Gefitinib were found to be potent in the HER2 overexpressing SKBR3 cell line. Thus, these 2 agents were selected for further investigations against this cell line. Although Gefitinib demonstrated a potent effect in SKBR3 cells in medium supplemented with 2% FBS, this cell line showed hindered growth with 2% FBS. Hence, only medium supplemented with 10% was used for further studies. Further, it has been shown that 10% FBS, would provide a more

natural context and the results found may be more physiologically relevant [184]. Below are representative MTT dose response curves of EGF and Gefitinib against the SKBR3 cell line in medium supplemented with 2% and 10% FBS (Figure 3.4). As it is seen in the graphs treatment with EGF and Gefitinib for 72 h resulted in dose dependent growth inhibition. An extremely significant growth inhibition was observed at higher concentrations ($P < 0.0001$).

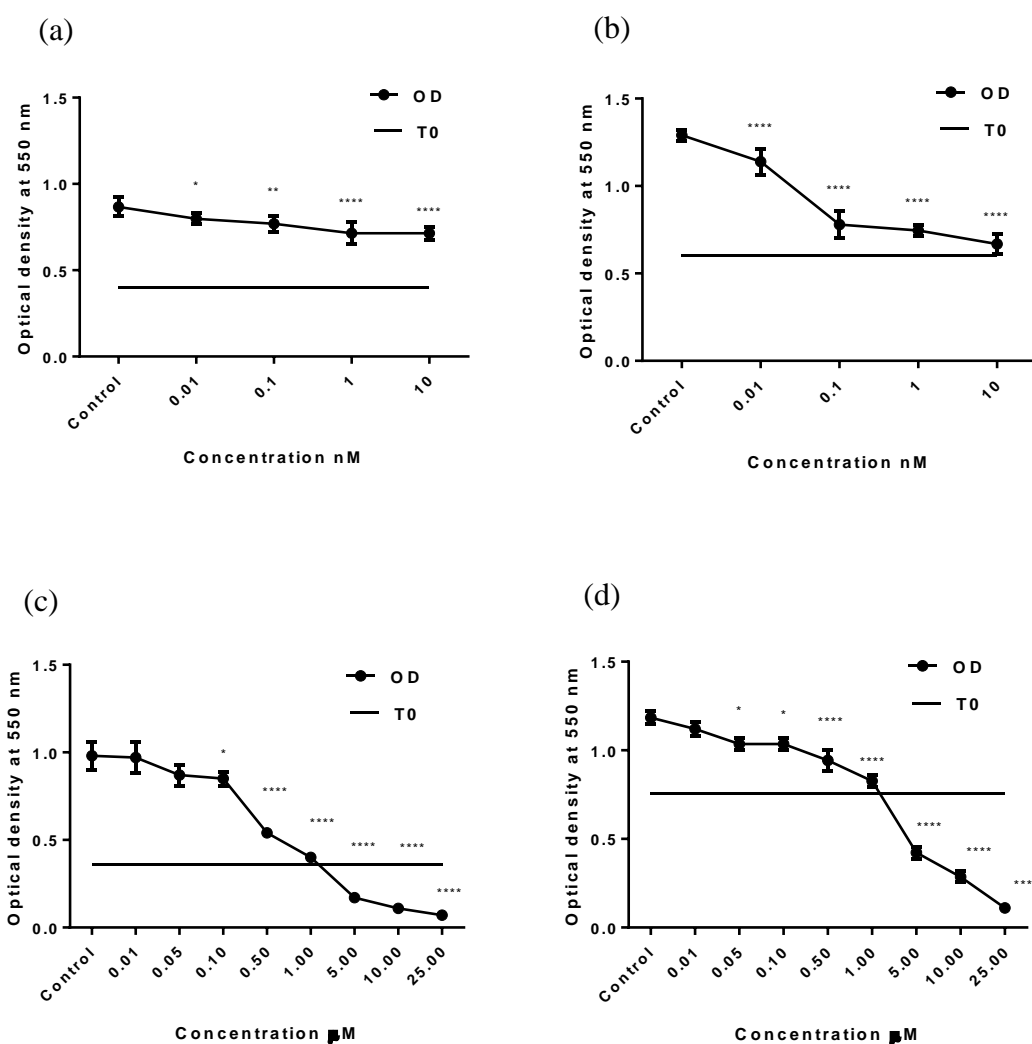


Figure 3.4: Growth inhibitory curves for EGF and Gefitinib against SKBR3 cells. (a) EGF in medium supplemented with 2% FBS, (b) EGF in medium supplemented with 10% FBS, (c) Gefitinib in medium supplemented with 2% FBS and (d) Gefitinib in medium supplemented with 10% FBS. Mean and SD of representative experiments are shown ($n = 8$ per trial); trials ≥ 3 . * indicates significant difference compared to control, * ($P < 0.05$), ** ($P < 0.01$), *** ($P < 0.001$), **** ($P < 0.0001$).

3.2.4 Effects of EGF and Gefitinib on SKBR3 colony formation

Clonogenic assays were performed to determine whether single SKBR3 cells were able to survive a brief exposure (24 h) to EGF and Gefitinib (1x and 2x GI_{50} concentrations) and subsequently form progeny colonies, indicative of capacity for tumour repopulation. The exceptionally low number of cells in the clonogenic assay means cells are isolated. Thus, the survival and proliferative capacity of individual cells can be easily determined by a clonogenic assay [147].

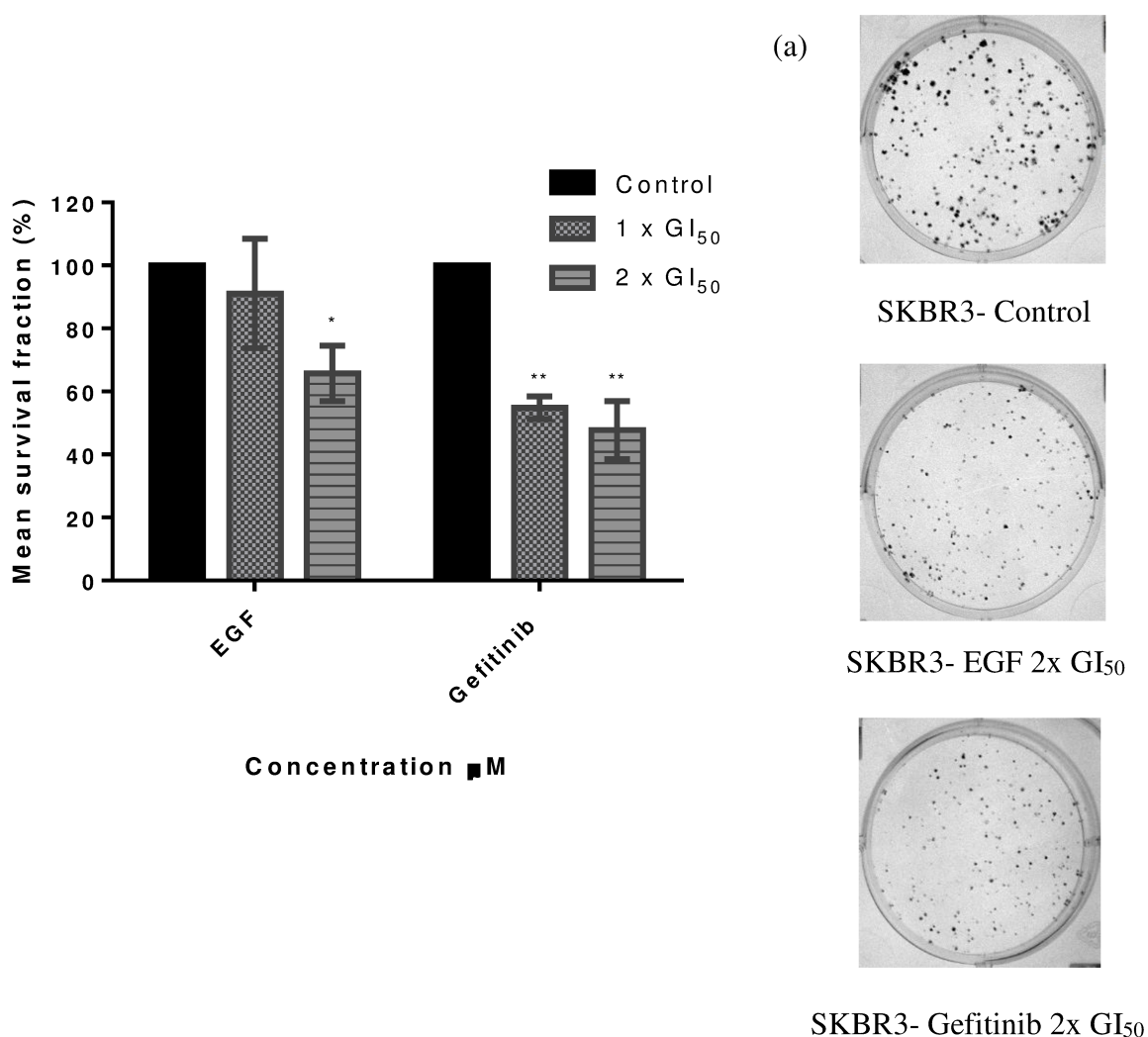


Figure 3.5: Effects of EGF and Gefitinib on SKBR3 colony formation. (a) Representative images of colony formation after exposure to agents. Mean SF as % plating efficiency of control represented as the mean \pm SD of trials ≥ 3 , ($n = 3$ per trial). * indicates significant difference compared to control, * ($P < 0.05$), ** ($P < 0.01$), *** ($P < 0.001$), **** ($P < 0.0001$) in colony formation.

The mean SFs obtained indicated that both EGF (2x GI₅₀) SF = 65.78%; P < 0.05) and Gefitinib (2x GI₅₀) SF = 47.71%; P < 0.01) affected survival and proliferative capacity of SKBR3 cells significantly by reducing the number of colonies and also the size of the colonies formed compared to SKBR3 control within 14 days. These results corroborate with the results of the MTT assays and these results suggest that both agents exert a cytostatic as well as a moderate cytotoxic effect at the concentrations tested - 1x and 2x GI₅₀.

3.2.5 Effects of EGF and Gefitinib on SKBR3 cell cycle

To determine the effect of EGF and Gefitinib on SKBR3 cell cycle progression, flow cytometry analysis was performed on cells treated with 2x GI₅₀ concentrations of EGF and Gefitinib for 24, 48 and 72 h. As shown in figure 3.6, significant G1 arrests were caused by EGF (67.39%) (P < 0.01) and Gefitinib (80.67%) (P < 0.0001) compared to control (62.26%) after 24 h. This was followed by a corresponding decreased S phase (6.69%) which was extremely significant (P < 0.0001) and a significantly decreased G2/M phase (12.18%) (P < 0.05) in cells treated with Gefitinib compared to control cells (S phase - 15.25% and G2/M phase - 16.83%) in 24 h. In contrast, EGF caused a non-significant increased S phase (17.96%) compared to control cells whereas the G2/M phase (15.68%) was similar to control at 24 h.

After 48 h, EGF maintained accumulated G1 events (67.20%) (P < 0.001) compared to control (62.72%). Unlike 24 h, after 48 h EGF treatment demonstrated decreased S (15.69%) and G2/M phases (16.81%); although they were not significant, compared to control. Gefitinib evoked an extremely significant G1 peak (72.45%) (P < 0.0001),

declined S phase (9.70%) and a reduced G2/M phase (13.70%); $P < 0.0001$ compared to control (S phase – 17.01% and G2/M phase - 19.06%).

After 72 h, EGF induced an increased G1 peak which was extremely significant (72.49%) ($P < 0.0001$) and this was followed by significantly reduced S (12.69%) ($P < 0.001$) and G2/M phases (12.14%) ($P < 0.01$) compared to control cells (G1 phase – 67.29%, S phase – 16.11% and G2/M phase – 15.10%). Gefitinib also elicited a significant G1 peak (73.46%) ($P < 0.0001$), reduced S (12.06%) ($P < 0.0001$) and G2/M phases (12.15%) ($P < 0.05$). Nevertheless, it was observed that the number of events had decreased for the G1 phase and correspondingly the number of events had somewhat increased for S and G2/M phases with time in Gefitinib treated cells. On the other hand, EGF showed a reversed response with time. It was also observed that there were no significant pre-G1 events observed at all 3 time points for both agents tested.

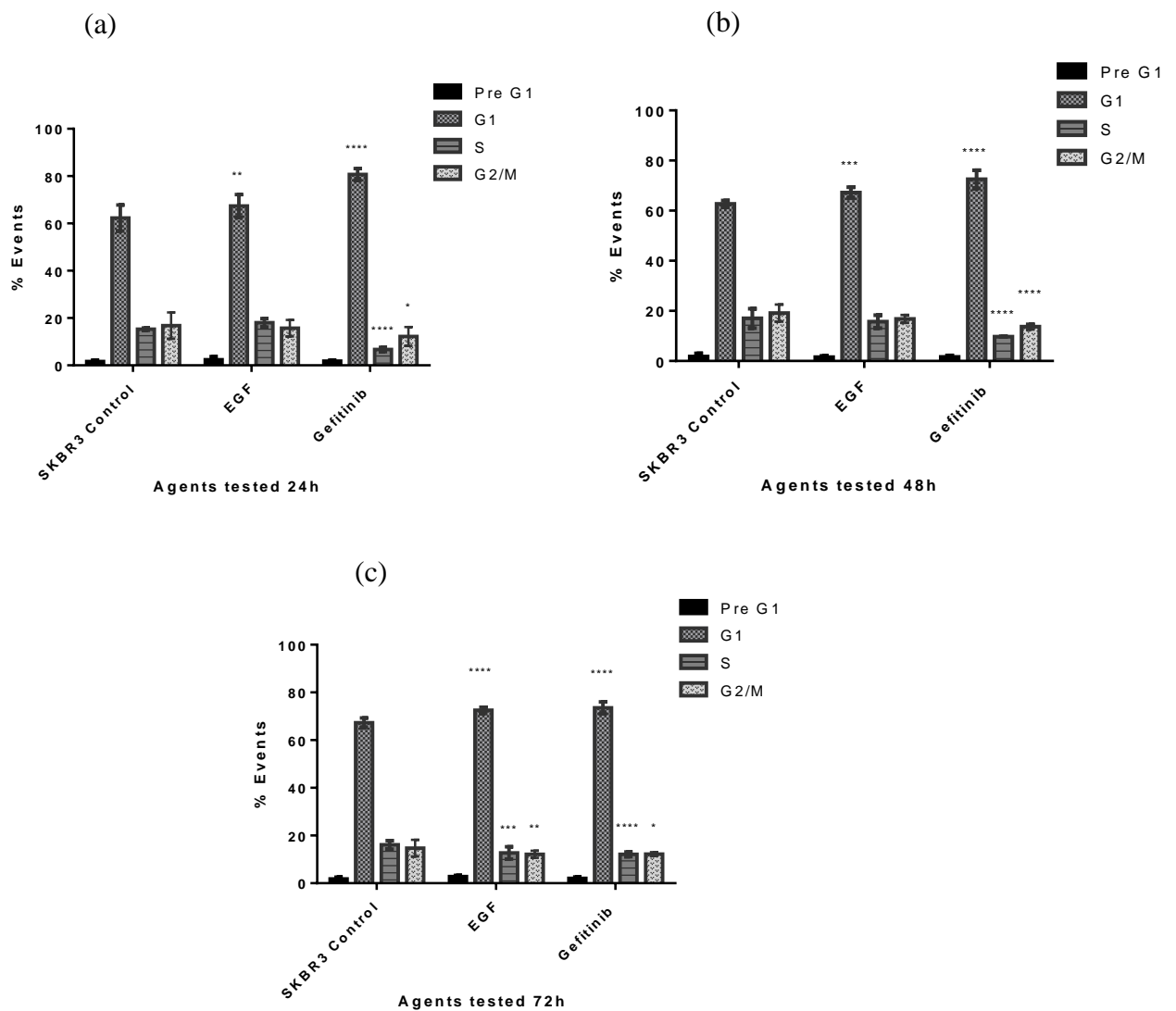


Figure 3.6: Cell cycle analysis following treatment of SKBR3 cells with EGF and Gefitinib. Cells were treated with 2x GI₅₀ concentrations of these agents for 3 time points (a) 24, (b) 48 and (c) 72 h. Mean and SD of trials ≥ 3 , (n = 2 per trial). * indicates significant difference compared to control, * (P < 0.05), ** (P < 0.01), *** (P < 0.001), **** (P < 0.0001).

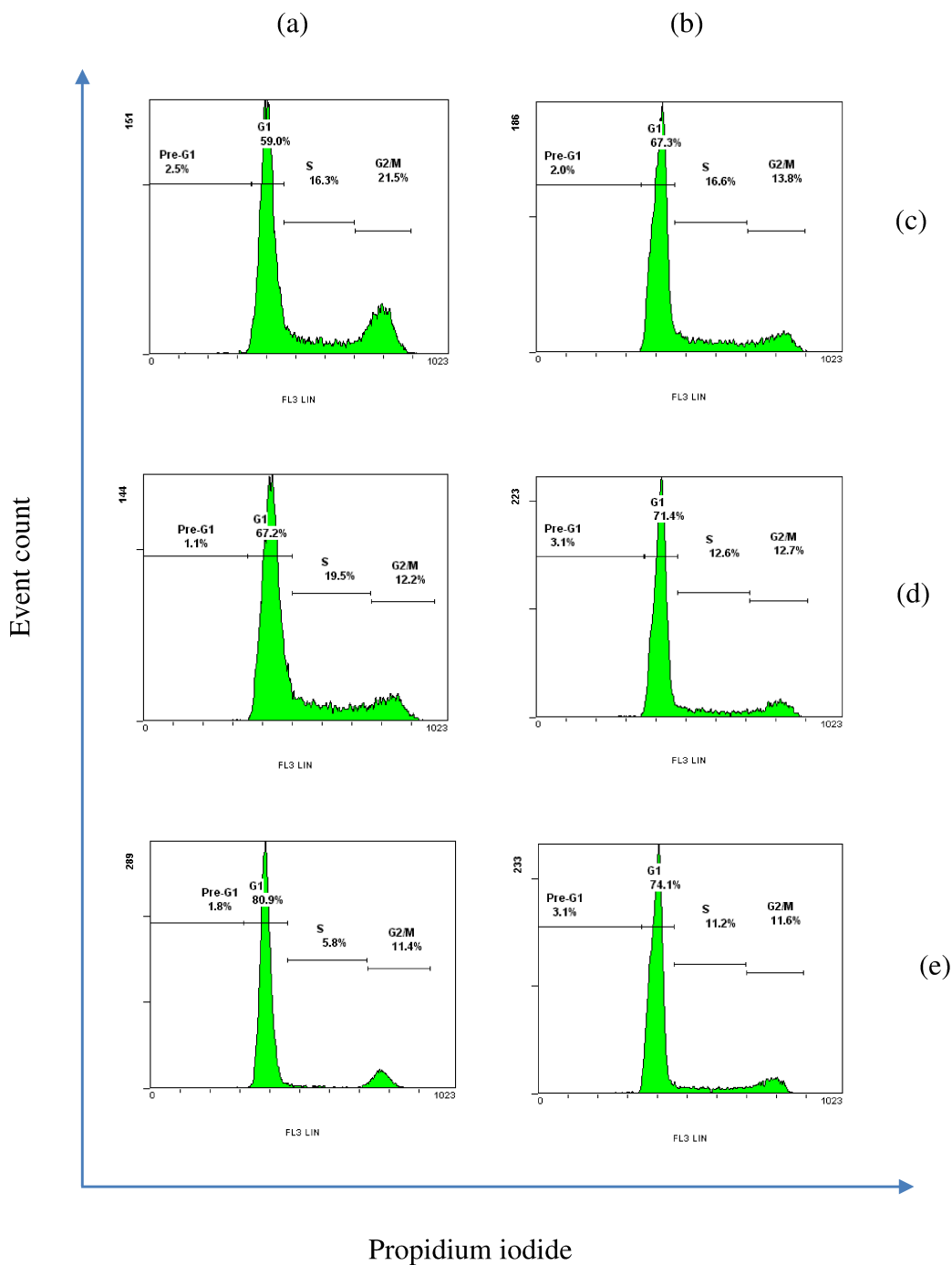


Figure 3.7: Representative cell cycle histograms of SKBR3 cells treated with EGF and Gefitinib. Cells were treated with 2x GI_{50} concentrations of these agents, (a) 24 h, (b) 72 h, (c) Control, (d) EGF and (e) Gefitinib. These are representative histograms, 15,000 events were analysed in each experiment.

An accumulation of a pre-G1 peak in the cell cycle, is suggestive of apoptosis. A previous report has shown that Gefitinib did not cause a pre-G1 peak in SKBR3 cells supporting the results of the current study. The same report has shown that Gefitinib caused a G1 accumulation in SKBR3 cells [195]. Further, 2 additional research groups have also reported that Gefitinib caused significant G1 accumulations with the same cell line [196] [197]. Cyclin D1 is required for the progression of the G1 to S phase and is shown to be an important target for proliferative signals in the G1 phase [198]. In addition, reduction in cyclin D1 synthesis in cells has been shown to be followed by a decrease in CDK activity. CDKs are a family of serine and threonine kinases that play a key role in controlling cell cycle progression as mentioned in chapter 1 [198] [199]. In actual fact, in the current study it was observed by Western blots that both EGF and Gefitinib (1x and 2x GI₅₀ concentrations) abolished cyclin D1 protein levels completely in SKBR3 cells that were treated for 24 h compared to untreated cells (Figure 3.14) confirming the results of the cell cycle analysis. Researchers have shown that cell cycle progression is regulated through cycle regulatory proteins, such as cyclins, CDKs and CDK inhibitors [195]. However, cancer cells are insensitive to these regulatory proteins and are able to proliferate continuously as mentioned by the ‘insensitivity to antigrowth signals’ hallmark [37]. These researchers mentioned above have shown that the G1 accumulation induced by Gefitinib is due to reduction in cyclin D1 and CDK2, CDK4 and CDK6 protein levels. Further, they have shown that Gefitinib induces high levels of p27^{kip1} and phosphorylated Rb levels which is associated with the G1 arrest; thereby explaining the effect of Gefitinib in the cell cycle [195] [200] [201].

Garcia et al, 2006 investigated the effect of EGF in MCF7 cells in serum deprived medium. They revealed an arrest in the G1 phase and a reduction in the S phase of the cell cycle that was associated with a loss of EGFR expression in the absence of other growth factors over a period of 6 days. However, these researchers observed increased cyclin D1 levels and they also observed an increase in p21^{cip1} protein levels which is associated with inhibition of the cell cycle. An increase in p21^{cip1} protein expression has found to inhibit cell cycle progression through the interaction with cyclin D1. They have also shown that p21^{cip1} levels could inhibit cyclin D1 levels with time and that EGFR activation *via* EGF in the absence of other growth factors causes G1 arrest and a reduction in MCF7 S phase cells [202]. It could be suggested that a similar effect is taking place in SKBR3 cells exposed to EGF. However, SKBR3 cells express high levels of HER2 and moderate levels of EGFR compared to MCF7 cells (Figure 3.1) and (Figure 3.2). In the presence of a large amount of EGF, excessive ligand binding would result in homo- and heterodimerisation of EGFR and HER2 receptors. In fact, heterodimerisation is preferred in cells that express both EGFR and HER2 [203]. These heterodimers remain longer on the cell surface compared with EGFR homodimers and thus exaggerate signalling [203]. This results in loss of nutrients with time, which in turn reduces cellular proliferation. At 72 h, the number of cells in the S phase and G2/M phase reduced significantly in this experiment, possibly due to a similar effect.

3.2.6 Effects of EGF and Gefitinib on SKBR3 cellular apoptosis

One of the major hallmarks of human cancers is acquired resistance to apoptosis as mentioned in chapter 1. Evasion of apoptosis contributes to tumour development,

invasion and also resistance to treatment [37]. Although there was no significant pre-G1 phases suggestive of apoptosis observed in the cell cycle analysis, the clonogenic assay results demonstrated a moderate cytotoxic effect, thus it was investigated whether the agents induced cell death in SKBR3 cells using an apoptotic assay.

Apoptosis and necrosis are 2 major cell death pathways. Characteristics of apoptosis include cell shrinkage, cell fragmentations, nuclear fragmentations and membrane blebbing [204] [205]. Necrosis is initiated by cellular accidents such as physical damage and energetic failure. Necrosis, or primary necrosis is characterised by loss of plasma membrane integrity, cell swelling and cell lysis [204] [205]. Further, secondary necrosis takes place when late stage apoptotic cells are not being recognised by phagocytes [206]. Furthermore, necroptosis is a programmed form of necrotic death and shares key processes with apoptosis [207]. However, there are many other mechanisms of cell death such as autophagy and paraptosis as well [208].

SKBR3 cells were treated with 2x GI₅₀ concentrations of these 2 agents for 24, 48 and 72 h. To quantify apoptotic or necrotic populations; fluorescein isothiocyanate (FITC)-labelled annexin V was used. Early and late apoptotic populations were summed to determine the total apoptotic population in cells following treatment.

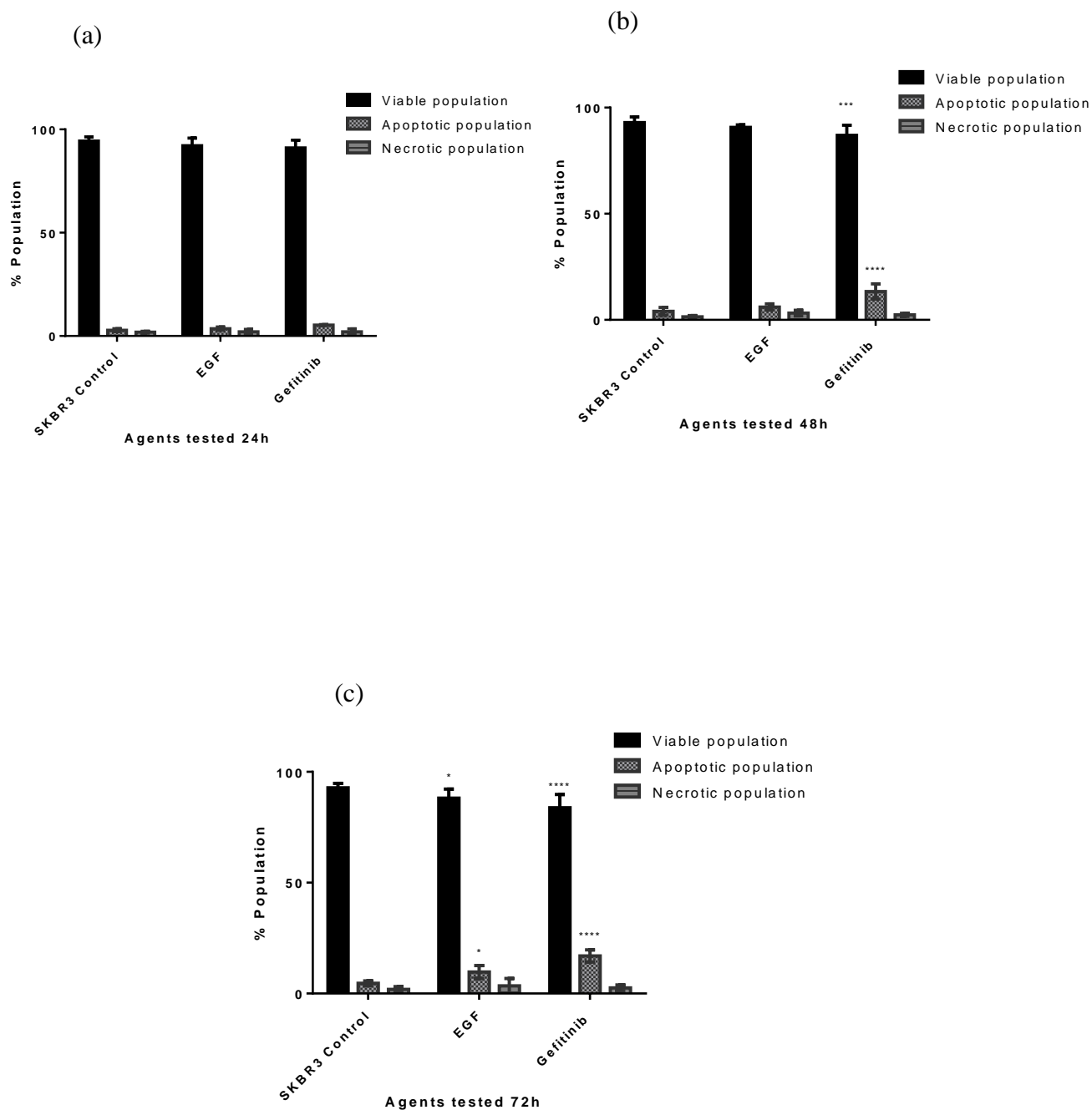


Figure 3.8: Apoptotic analysis of SKBR3 cells following exposure to EGF and Gefitinib. Cells were treated with 2 x GI_{50} concentrations of these agents for 3 time points 24, 48 and 72 h. Mean and SD of trials ≥ 3 , ($n = 2$ per trial). * indicates significant difference compared to control, * ($P < 0.05$), ** ($P < 0.01$), *** ($P < 0.001$), **** ($P < 0.0001$).

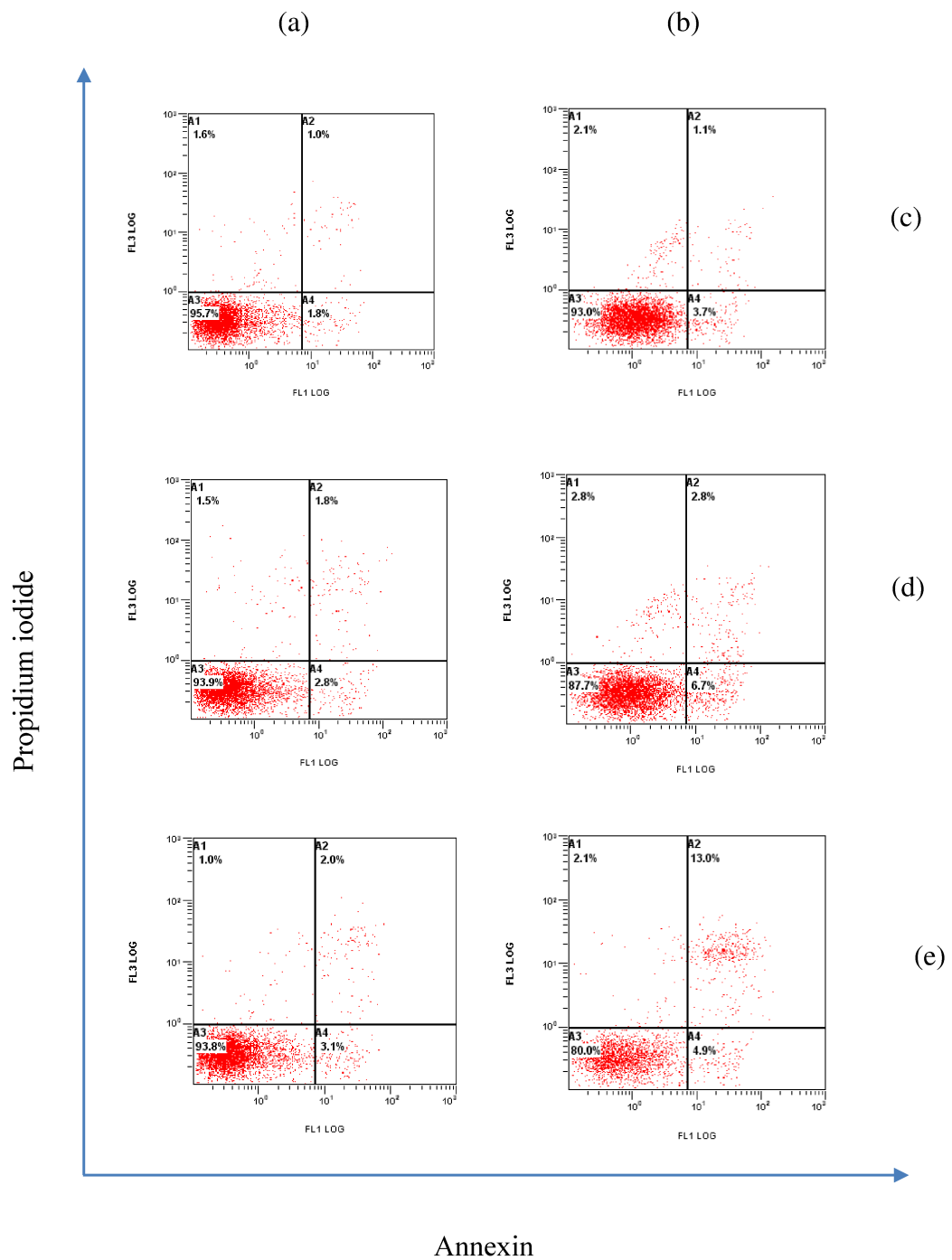


Figure 3.9: Representative apoptotic quadrant plots of SKBR3 cells treated with EGF and Gefitinib. Cells were treated with 2x GI₅₀ concentrations of these agents, (a) 24 h, (b) 72 h, (c) Control, (d) EGF and (e) Gefitinib. These are representative quadrant plots analysed by flow cytometry, 10,000 events were recorded for each experiment.

There was no significant apoptosis or necrosis observed after 24 h exposure to either EGF or Gefitinib in SKBR3 cells. However, after 48 h, Gefitinib caused a small but significant total apoptotic population (13.38%) ($P < 0.0001$) relative to control (4.05%), in contrast EGF did not demonstrate apoptosis after 48 h. After 72 h both EGF (9.70%) ($P < 0.05$) and Gefitinib (16.98%) ($P < 0.0001$) induced apoptosis compared to control (4.62%). Even after 72 h, no significant necrotic population was observed for both agents (Figure 3.8). It was observed that Gefitinib evoked a ~ 4-fold increase in the total apoptotic population at 72 h. The increase in apoptotic population was time dependent, nevertheless there was no significant difference between the early and late apoptotic populations in cells exposed to Gefitinib. On the other hand, it was observed that EGF evoked an increased early apoptotic population relative to the late apoptotic population which was significant at 72 h ($P < 0.01$).

From the results obtained, it was evident that EGF evoked an apoptotic population in SKBR3 cells only after 72 h, whereas Gefitinib caused a significant apoptotic effect in SKBR3 cells after 48 h. However, the apoptotic population observed was low for both EGF and Gefitinib. In fact, EGF has been shown to cause progressive cell death only with prolonged treatment (~ 144 h) in A431 epidermoid cancer cells that express high EGFR and HER2, which supports the current study results [184].

The small apoptotic populations indicates that these agents exert a cytostatic effect together with a moderate cytotoxic effect. Prior research has shown that Gefitinib acts as more of a cytostatic agent in sensitive cells but is able to induce a low or moderate level of apoptosis as well. This low or intermediate level ability to mediate apoptotic

signals have shown to be underlying the low regression rate observed in tumour xenografts treated with Gefitinib. Further, this type of response has shown to be associated with disease stability in contrast to standard chemotherapy which aims to kill tumour cells and achieve a partial response or a high regression rate [189]. Thus, the results of the present study corroborate with previous literature, and also with the results of the clonogenic assay within this chapter.

Further, SKBR3 cells possess mutant *TP53*, and are able to inhibit apoptotic responses necessary for tumour suppression [207] [209]. However, Tikhomirov and Carpenter, 2004, reported that SKBR3 cells with high levels of EGFR and HER2 do not depend on TP53 accumulation in response to EGF induced apoptosis [178]. Furthermore, it has been also shown that Gefitinib mediated anti-proliferative action does not require functional TP53 since TP53 and its downstream molecule p21^{cip1} were not regulated by this agent, demonstrating that this agent is effective in a range of tumour types [201]. Many researchers have reported that Gefitinib induces apoptosis by a variety of mechanisms including down-regulation of anti-apoptotic proteins and up-regulation of pro-apoptotic proteins of the Bcl-2 family. These proteins are found to be mediated by the TP53 protein [210]. As SKBR3 expresses mutant *TP53*, it was thought that Bcl-2 family of proteins may not play a major role in SKBR3 cell death with EGF and Gefitinib treatment. Thus, it was evident that these effects were cell type- and dose-dependent [184] [192] [201] [211] [212]. It has been shown that caspases initiate the execution phase of apoptosis where many substrates such as poly (ADP-ribose) polymerases (PARP) are cleaved [210]. Thus, PARP activity was investigated in the present study as a small level of apoptosis was observed by agent treatment. However,

no PARP cleavage was observed in these cells following both EGF and Gefitinib treatment after 24 h (Figure 3.14). Indeed no apoptosis was observed at 24 h in the apoptotic analysis assay in treated SKBR3 cells corroborating the findings of PARP. Gefitinib has also been shown to inhibit major cell survival and growth signalling pathways such as RAS/MAPK and PI3K/AKT pathways, as a consequence of inactivation of EGFR and HER2. In addition, EGF induced HER2 down-regulation has been reported. These effects were investigated subsequently in detail and the results are shown in section 3.2.7 where it was observed that both EGF and Gefitinib down-regulated EGFR and HER2 activated RAS/MAPK and PI3K/AKT pathways.

3.2.7 Effects of EGF and Gefitinib on EGFR, HER2, RAS/MAPK, PI3K/AKT, JAK/STAT signalling pathways, PARP and cyclin D1 in SKBR3 cells by Western blotting

SKBR3 cells were treated with 1x and 2x GI_{50} concentrations of EGF and Gefitinib for 24 h and the protein expression levels of EGFR, P-EGFR (Tyr1068), HER2 and P-HER2 (Tyr1221/1222) were evaluated. It was observed that EGF increased the total EGFR protein expression levels at 24 h, however, the results were not significant. Gefitinib did not alter total EGFR protein levels significantly. In contrast, EGF down-regulated P-EGFR levels extremely significantly at 1x and 2x GI_{50} concentrations ($P < 0.0001$) - P-EGFR (Tyr1068) ARD - 1x GI_{50} EGF - 1.45% and 2x GI_{50} - 1.20%. Gefitinib also down-regulated P-EGFR levels, but the levels were not as low as EGF-1x GI_{50} - ARD - 43.17% and 2x GI_{50} - ARD - 41.00% compared to SKBR3 control ($P < 0.0001$).

Further, it was observed that EGF increased total HER2 expression levels at 2x GI₅₀ although results were not significant compared to control. However, Gefitinib did not significantly alter total HER2 protein expression levels in SKBR3 cells. Interestingly, EGF did not alter P-HER2 (Tyr1221/1222) expression levels significantly while only 2x GI₅₀ Gefitinib reduced P-HER2 (Tyr1221/1222) significantly (ARD – 66.94%) compared to SKBR3 control (P < 0.05) (Figure 3.10) and (Figure 3.11 (a) - (d)).

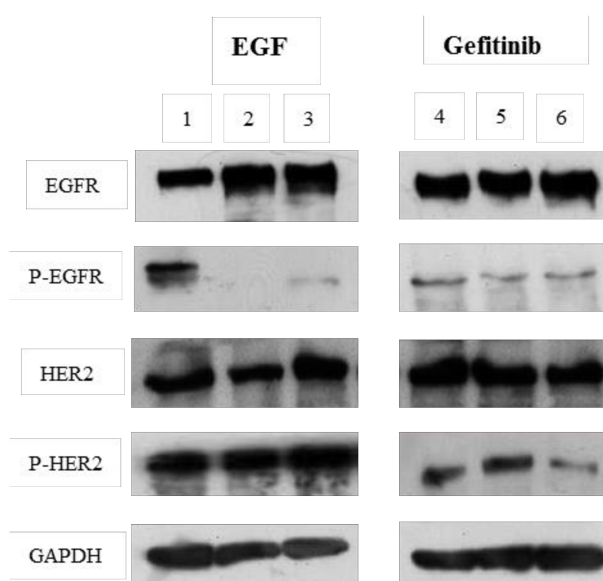


Figure 3.10: Western blot analysis of EGFR and HER2 following exposure of SKBR3 cells to EGF and Gefitinib. EGFR, P-EGFR (175 kDa), HER2, P-HER2 (185 kDa) and GAPDH (37 kDa). GAPDH was probed as a loading control and adjusted relative densities (ARD) were calculated. (1) SKBR3 control, (2) 1x GI₅₀ EGF, (3) 2x GI₅₀ EGF, (4) SKBR3 control, (5) 1x GI₅₀ Gefitinib, (6) 2x GI₅₀ Gefitinib. Representative blots are shown; experiments were conducted ≥ 3 times. SKBR3 whole cell protein lysates (50 μ g) were subjected to 10% SDS-polyacrylamide gel electrophoresis.

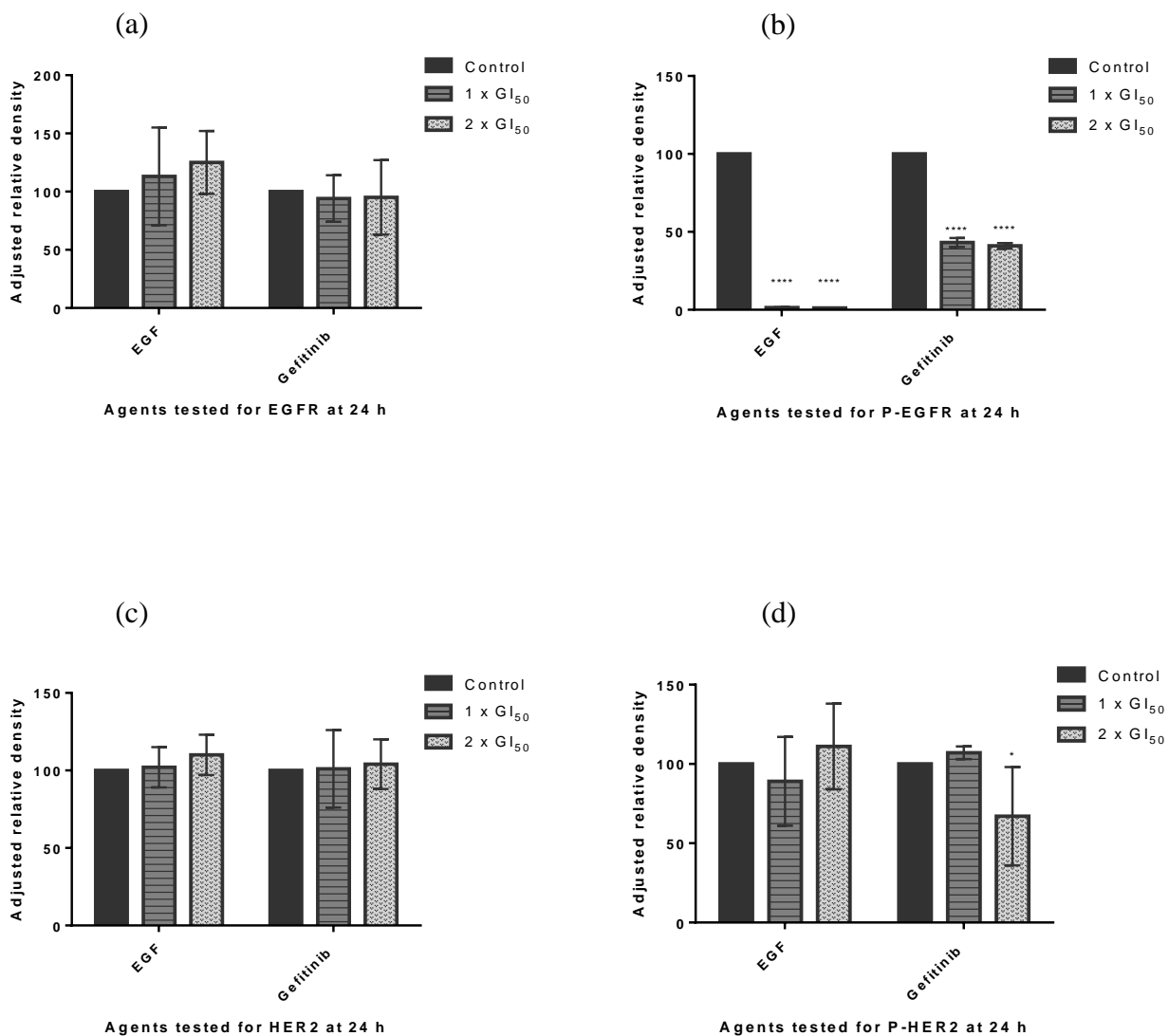


Figure 3.11: Adjusted relative density (ARD) levels of EGFR, P-EGFR, HER2 and P-HER2 for EGF and Gefitinib. (a) EGFR, (b) P-EGFR, (c) HER2 and (d) P-HER2 levels in SKBR3 cells. Cells were treated with EGF and Gefitinib for 24 h. Mean and SD of trials ≥ 3 . * indicates significant difference compared to control, * (P < 0.05), ** (P < 0.01), *** (P < 0.001), **** (P < 0.0001).

In the current study, the activity of EGF was investigated and it was found that EGF abolished EGFR phosphorylation (Tyr1068) at 24 h in SKBR3 cells suggesting that EGF would block downstream EGFR signalling in these cells. In contrast EGF caused enhanced up-regulation of basal levels of EGFR at 24 h. These results may infer that, when EGF is bound to EGFR and when it is being phosphorylated the phosphorylated form gets degraded with time. Subsequently, when phosphorylation of EGFR ceases, basal levels of EGFR may be enhanced to maintain receptor stabilisation after 24 h [213].

EGF did not down-regulate P-HER2 (Tyr1221/1222) thus continued signalling through activated HER2 could persist in SKBR3 cells. In fact, the mechanism by which EGF inhibits SKBR3 proliferation is complex and controversial. Prior research has reported that EGF was able to reduce both EGFR and HER2 levels in a human mammary epithelial cell line due to accelerated degradation, as such it may be that the effect of EGF is cell type specific [214].

As expected Gefitinib reduced both phosphorylated EGFR and HER2 in SKBR3 cells indicating that Gefitinib blocks EGFR and HER2 downstream events. In fact, mounting evidence suggests that Gefitinib blocks both the RAS/MAPK and PI3K/AKT pathways which are strictly regulated by either EGFR or HER2 in cancers [189] [213]. Thus, these pathways were explored with Gefitinib treated SKBR3 cells and also EGF treated cells.

It was observed that EGF lowered P-CRAF (Ser259) levels significantly at 2x GI₅₀ (ARD – 60.58%) compared to control (P < 0.0001) and similarly reduced P-ERK 1/2 levels at both 1x GI₅₀ (ARD – 55.92%) and 2x GI₅₀ concentrations (ARD – 48.55%) significantly (P < 0.0001). Further, EGF elicited an increase in the P-SAPK/JNK levels at 2x GI₅₀ (ARD – 135.09%) (P < 0.05). EGF did not alter any other protein expression levels investigated of this pathway nor total protein expression levels.

It was noticed that Gefitinib treated SKBR3 cells expressed significantly lower levels of P-CRAF (Ser259) (1x GI₅₀ - 51.42% and 2x GI₅₀ ARD - 42.18%) (P < 0.0001), compared to control. Interestingly, Gefitinib diminished P-ERK1/2 levels, that is downstream of CRAF in SKBR3 cells showing that this agent inhibits the RAS/MAPK pathway effectively in these cells (1x GI₅₀ concentration - ARD - 7.68% and 2x GI₅₀ concentration - ARD - 6.25%) (P < 0.0001). Further, Gefitinib induced increased phosphorylation in p38 (Thr180/Tyr182) significantly (1x GI₅₀ concentration - ARD - 133% and 2x GI₅₀ concentration - ARD - 123%) (P < 0.0001). In contrast, the same agent decreased P-SAPK/JNK (Thr183/Tyr185) protein expression levels significantly at both concentrations tested (1x GI₅₀ concentration - ARD – 60.40% (P < 0.01) and 2x GI₅₀ concentration - ARD – 45.30% (P < 0.001)). Gefitinib did not perturb total expression levels of the proteins investigated in this pathway (Figure 3.12). Densitometry analysis with the ARD values for the significant results are shown in appendix I under section 9.1.1.1.

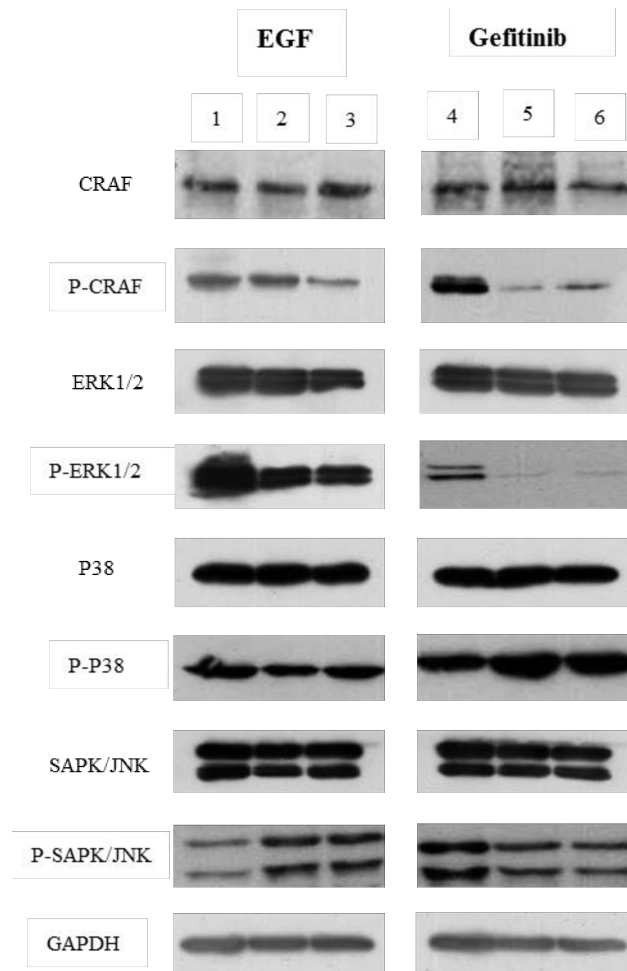


Figure 3.12: Western blot analysis of RAS/MAPK pathway following exposure of SKBR3 cells to EGF and Gefitinib. CRAF, P-CRAF (74kDa), ERK 1/2, P-ERK 1/2 (44 and 42 kDa), p38, P-p38 (43 kDa), SAPK/JNK, P-SAPK/JNK (46 and 54 kDa) and GAPDH (37 kDa). GAPDH was probed as a loading control and adjusted relative densities (ARD) were calculated. (1) SKBR3 control, (2) 1x GI₅₀ EGF, (3) 2 x GI₅₀ EGF, (4) SKBR3 control, (5) 1 x GI₅₀ Gefitinib, (6) 2 x GI₅₀ Gefitinib. Representative blots are shown; experiments were conducted ≥ 3 times. SKBR3 whole cell protein lysates (50 μ g) were subjected to 10% SDS-polyacrylamide gel electrophoresis.

Previously it has been reported that EGF down-regulated P-ERK1/2 in A431 cells. ERK1/2, of the RAS/MAPK pathway acts as a crucial protein that phosphorylates many cytoplasmic proteins which in turn leads to cell growth and proliferation [49]. Thus, inhibiting P-CRAF which is upstream of ERK1/2 and also inhibiting P-ERK1/2

would eventually inhibit SKBR3 cell growth and proliferation. Previous research has shown that EGF could induce phosphorylation of p38 where EGF mediates apoptosis [178] [184]. However, in the current study this was not observed. On the contrary activation of P-SAPK/JNK by EGF was noticed in SKBR3 cells which has not been reported before. SAPK/JNK controls a spectrum of cellular processes including cell proliferation, differentiation and apoptosis as outlined in chapter 1 [65]. Further, SAPK/JNK activation has shown to trigger the mitochondria-dependent apoptotic pathway in response to many types of cell stress suggesting one of the mechanisms by which EGF inhibits cellular proliferation and apoptosis in SKBR3 cells [65]. However, further work is needed to verify the actual function of P-SAPK/JNK in EGF treated SKBR3 cells.

The findings of Gefitinib are mostly consistent with previous reports where it has been shown that this agent is able to abolish P-ERK1/2 in SKBR3 cells at concentrations used in this study [189]. Further, Gefitinib evoked an increase in P-p38. p38 has been implicated in a variety of cellular responses such as cell cycle, cell death, cell differentiation and senescence according to cell type, indicating that Gefitinib may induce apoptosis through this pathway [67] [184] [215]. Intriguingly, this agent reduced the levels of P-SAPK/JNK. It has been also shown that SAPK/JNK activation depends on the nature of the stimulus or the activity of other pathways [65] [216].

PI3K/AKT pathway activity was also reduced after SKBR3 cells were exposed to EGF and Gefitinib. It was observed that P-AKT (Ser473) activity was significantly down-regulated by both 1x GI₅₀ (ARD – 46.55%) (P < 0.01) and 2x GI₅₀ EGF (ARD –

65.04%) ($P < 0.05$). It was noted that there was increased phosphorylation in cells exposed to 2x GI₅₀ concentrations compared to 1x GI₅₀. However the results were not significant. EGF also reduced P-AKT (Thr308) levels significantly - at 1x GI₅₀ (ARD – 53.97%) and 2x GI₅₀ (ARD – 52.88%); $P < 0.01$.

Similarly, Gefitinib treated SKBR3 cells demonstrated reduced levels of P-AKT (Ser473) - 1x GI₅₀ (ARD – 48.28%) and 2x GI₅₀ (ARD – 25.24%); $P < 0.01$ and P-AKT (Thr308) - 1x GI₅₀ (ARD – 66.62%); $P < 0.05$ and 2x GI₅₀ (ARD – 58.31%); $P < 0.01$ compared to control. Neither EGF nor Gefitinib altered total AKT levels. Further, no other protein expression levels tested in this pathway were significantly affected by these 2 agents (Figure 3.13). Densitometry analysis with the ARD values for the significant results are shown in appendix I under section 9.1.1.2.

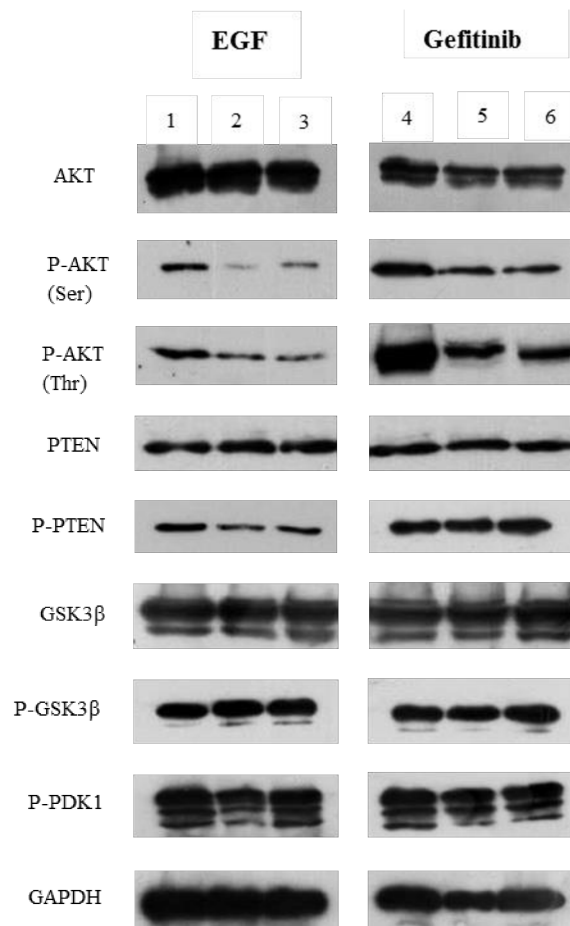


Figure 3.13: Western blot analysis of PI3K/AKT pathway following exposure of SKBR3 cells to EGF and Gefitinib. AKT, P-AKT (Ser473), P-AKT (Thr308) (60 kDa), PTEN, P-PTEN (54 kDa), GSK3 β , P-GSK3 β (46 kDa), P-PDK1 (58-68 kDa) and GAPDH (37 kDa). GAPDH was probed as a loading control and adjusted relative densities (ARD) were calculated. (1) SKBR3 control, (2) 1x GI₅₀ EGF, (3) 2x GI₅₀ EGF, (4) SKBR3 control, (5) 1x GI₅₀ Gefitinib, (6) 2x GI₅₀ Gefitinib. Representative blots are shown; experiments were conducted ≥ 3 times. SKBR3 whole cell protein lysates (50 μ g) were subjected to 10% SDS-polyacrylamide gel electrophoresis.

The results of the PI3K/AKT pathway show that the SKBR3 cell line is sensitive to the effects of EGF and Gefitinib and that the anti-apoptotic effect of AKT in SKBR3 cells has been reduced by these agents efficiently, corroborating previous research [189].

As discussed in section 3.2.5, SKBR3 cells treated with EGF and Gefitinib completely diminished cyclin D1 activity ($P < 0.0001$). Further, neither agent caused PARP cleavage after 24 h. Gefitinib (2x GI_{50}) caused significantly depleted P-STAT5 (ARD – 26.88%) ($P < 0.0001$) whereas EGF did not alter P-STAT5 protein expression levels (Figure 3.14). Densitometry analysis with the ARD values for the significant results are shown in appendix I under section 9.1.1.3.

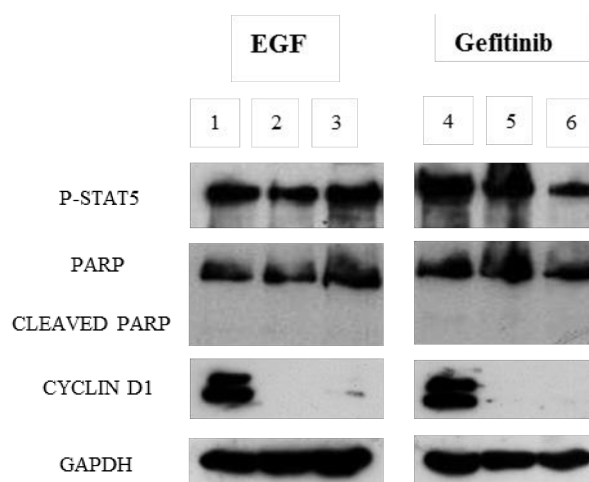


Figure 3.14: Western blot analysis of P-STAT5, PARP and Cyclin D1 following exposure of SKBR3 cells to EGF and Gefitinib. P-STAT5 (90 kDa), PARP (116 kDa), CLEAVED PARP (89 kDa), Cyclin D1 (36 kDa) and GAPDH (37 kDa). GAPDH was probed as a loading control and adjusted relative densities (ARD) were calculated. (1) SKBR3 control, (2) 1x GI_{50} EGF, (3) 2x GI_{50} EGF, (4) SKBR3 control, (5) 1x GI_{50} Gefitinib, (6) 2x GI_{50} Gefitinib. Representative blots are shown; experiments were conducted ≥ 3 times. SKBR3 whole cell protein lysates (50 μ g) were subjected to 10% SDS-polyacrylamide gel electrophoresis.

Cyclin D1 results confirm the results obtained in the cell cycle experiment where a prominent G1 arrest was observed in cells treated with EGF and Gefitinib. Further, there was no significant apoptosis measured by the annexin v assay in SKBR3 cells exposed to EGF and Gefitinib at 24 h, verifying the results obtained for full length PARP. This again suggests that these 2 agents act more like cytostatic agents at 1x and

2x GI₅₀ concentrations verifying the results of MTT, clonogenic, cell cycle and apoptosis assays. However, at increasing concentrations and longer exposure periods, these agents may act as cytotoxic agents [213].

Constitutive activation of the JAK/STAT pathway is found in many cancers and activation of this pathway stimulates many cellular processes such as proliferation, differentiation and survival [83]. These results suggest that Gefitinib treated SKBR3 cells which demonstrated depleted P-STAT5 levels would inhibit this pathway. P-STAT5 is also found to regulate cyclin D1 [217]. In fact, Xiong et al, 2009 has shown that STAT5 was involved in the blocking of cell cycle progression at the G1 phase endorsing further the results of the cell cycle analysis obtained for the SKBR3 cells treated with Gefitinib [218].

3.3 Conclusion

A number of growth factors have been shown to play a role in growth and proliferation of breast cancer cells [170]. FBS which is used in culture media is shown to contain many growth factors. Thus, the effect of serum (2% and 10% FBS) on the growth of the breast cancer cell line panel was investigated [170]. This experiment helped to determine how each cell line used behaved in culture, prior to initiating experiments. It was found that MCF7 (ER+) and MDA-MB 468 (ER-) cell lines showed significant growth in serum depleted (2% FBS) medium which is indicative of a probable role of exogenous growth factor-independent survival. Correspondingly, these data show that there is no correlation with ER status and survival in serum depleted medium.

EGF and Gefitinib showed potent growth inhibitory effects in the HER2 overexpressing SKBR3 cell line. From the clonogenic assay it was found that both agents showed a cytostatic and also a moderate cytotoxic effect in SKBR3 cells. Further, both EGF and Gefitinib elicited a remarkable G1 arrest at all 3 time points in the cell cycle analysis and it was found that both agents abolished cyclin D1 levels which is important for the progression of G1 to S phase in the cell cycle. The agents also showed a small amount of apoptosis but a significant percentage of apoptosis was found only after 48 h of treatment for Gefitinib and 72 h of treatment for EGF. The apoptotic effect of EGF could be associated with up-regulation of P-SAPK/JNK pathway. EGF abolished P-EGFR whereas Gefitinib reduced P-EGFR levels. Only Gefitinib was found to lower P-HER2 levels. In addition, it was found that both RAS/MAPK and PI3K/AKT pathways are involved in the growth inhibition of EGF. Various mechanisms have been proposed for EGF activity in the literature, however, results within this chapter verify that these mechanisms are cell type specific. Gefitinib inhibition was associated with simultaneous down-regulation of RAS/MAPK, PI3K/AKT and the JAK/STAT pathways in this study, suggesting that breast cancer cells overexpressing activated EGFR/HER2 have high intrinsic sensitivity to EGF and Gefitinib *via* inhibition of simultaneous receptor signalling pathways. Nevertheless, it was also observed that both EGF and Gefitinib showed a slightly different spectrum of activity in SKBR3 cells. These results may prove useful for breast cancer patients who fall into the HER2 molecular subtype to receive maximum benefit from anti-EGFR/HER2 therapy including EGF, which might be able to be used as an effective strategy to overcome EGFR/HER2 associated breast cancer proliferation, although, more research is warranted to determine whether EGF could be used as a therapy for HER2 overexpressing breast cancer.

4 Chapter 4 - Encapsulation of Gefitinib in H-AFt

4.1 Introduction

At present, although Gefitinib is used as an anti-cancer agent, its therapeutic window is drastically narrowed by poor bioavailability, acquired resistance and systemic toxicity [123]. Gefitinib is a basic compound which demonstrates poor gastrointestinal absorption producing low or variable bioavailability between patients [123] [219]. Most often the systemic toxicities are a result of interactions of drugs with healthy tissues during transmission and distribution of the drugs in the body. Gefitinib resistance may be related to insufficient or ineffective cellular uptake of drug [220]. Treatment with Gefitinib can also result in adverse gastro-intestinal and skin-related toxicities such as diarrhoea, nausea, vomiting, skin rashes, dry skin and acne. Other toxicities include fatigue, weight loss and interstitial lung disease [102] [108] [123] [219] [221]. Therefore, development of a delivery system would minimise disadvantages associated with Gefitinib bioavailability, toxicity and resistance.

Currently, the use of nanotechnology in drug delivery is being widely explored [105]. Many biodegradable NPs are being developed as drug delivery systems [104] [105]. Leaky vasculature which is associated with sustained tumour angiogenesis together with tumour related poor lymphatic drainage can enhance passive targeting of NPs to malignant tissue which results in the EPR effect as mentioned in chapter 1 [222] [223]. Nanoparticulate drug formulations, exploiting this feature of the tumour microenvironment can be used to deliver chemotherapeutic agents to a tumour target

site thereby increasing the therapeutic effect while minimising systemic toxicities [129]. When selecting a delivery system a major consideration is controlled release of the drug to the target site at a therapeutically optimal rate [104] [224]. As a promising targeted delivery system, the native iron storage protein ferritin was chosen. Ferritin is an ideal drug delivery carrier due its nanoscale structure, biocompatible, biodegradable, multifunctional, stable and non-toxic properties [105] [131] [225]. The internal cavity of ferritin stores iron atoms. When the iron is released AFt is formed with a hollow cavity. In this study, Gefitinib was encapsulated into the cavity of H-AFt by diffusion. Prior research has shown that AFt has been used for many successful applications both *in vitro* and *in vivo*. For instance, iron oxide NPs have been encapsulated inside H-AFt to visualise tumour tissues *in vitro* [226]. Further, a gadolinium-loaded AFt displayed system has been used to visualise tumour endothelial cells that could be used for identifying angiogenic blood vessels both *in vitro* and *in vivo*. This system has displayed good *in vivo* stability and tolerability [227]. Liang et al, 2014 has shown that AFt-encapsulated Doxorubicin displayed an excellent safety profile which reduced toxicity in healthy organs *in vivo* murine models compared to free Doxorubicin and also Doxil which is the clinically approved liposomal Doxorubicin nanomedicine formulation which was discussed in chapter 1 [228]. Furthermore, it has been shown that AFt-encapsulated lead sulphide (PbS) quantum dots can be used in anti-tumour activity in both *in vitro* and *in vivo*. *In vitro* breast and colon carcinoma cell growth has been inhibited effectively while *in vivo* this agent has shown to be well tolerated with no behavioural or weight changes in mice [229]. In addition, near-infrared of PbS quantum dots have been used for tumour imaging in the same study [131] [229]. These studies confirm that AFt is efficiently up taken by tissues *in vivo* and that it is a safe and efficient vehicle for Gefitinib drug

delivery. Thus, this chapter describes the characterisation and investigation of functionality of H-AFt-encapsulated-Gefitinib targeting EGFR and HER2 overexpressing breast cancer.

4.2 Results and Discussion

4.2.1 Characterisation of H-AFt-encapsulated-Gefitinib

4.2.1.1 Determining EE, protein concentration of H-AFt and H-AFt:Gefitinib ratio

For efficient entrapment of drug into a delivery system, consideration of physical properties of both the drug and the delivery system is important. Gefitinib is a hydrophobic drug and H-AFt has 6 hydrophobic channels of 0.3 - 0.4 nm in diameter on its surface which will allow the drug molecules to enter the H-AFt cavity by passive diffusion during the mixing of the drug with the protein (Figure 4.1 (a)) [230]. The lateral dimensions of Gefitinib are less than 0.3 nm, allowing Gefitinib intake through the 6 hydrophobic channels by diffusion. Gefitinib has low solubility in aqueous buffers [231]. Thus, Gefitinib was first dissolved in DMSO to make a homogeneous solution which was then diluted with PBS in a 1:1 solution at pH 7.2 to a final solution of 1 mM. This aqueous solution of Gefitinib was mixed with H-AFt where the Gefitinib molecules entered the H-AFt cavity by passive diffusion. The resulting solution was exhaustively dialysed and centrifuged at high speed to remove any un-encapsulated Gefitinib and any impurities. Several groups have reported the use of the assembly and disassembly property of the AFt protein cage to encapsulate drugs using acidic pH levels [129] [220] [224]. However, use of acidic pH such as pH 2.0 to disassemble the AFt cage could damage the AFt by forming defects by means of holes

on the outer surface which eventually will damage the stability and drug delivery effectivity to cells, therefore a diffusion method was utilised [228].

Gefitinib but not H-AFt is fluorescent. The fluorescence of Gefitinib was checked under UV. At the end of the encapsulation process of Gefitinib into H-AFt, the fluorescence of the resulting solution was visualised under UV and it was found that the resulting solution was fluorescent, but not as fluorescent as Gefitinib alone (Figure 4.1 (b1 - b3)). This indicates that Gefitinib is encapsulated within H-AFt. In fact, it has been previously shown that attachment of drug molecules to the AFt surface is very low [232].

Subsequently, the EE of the encapsulated test agent was determined. The EE was analysed using a UV spectrophotometer; 250 nm was chosen as the optimum wavelength to analyse the absorbance of Gefitinib [233]. An example of the spectrum is shown in Figure 4.1 (c). With the use of the Beer-Lambert law, encapsulated Gefitinib was quantified and an average maximum EE of ~ 54.90% was found. It was observed that even though the drug concentration was increased the EE did not increase. This might indicate that there is a maximum amount of drug molecules that the AFt cavity can hold. Protein determination by Bradford assay revealed an average of 1.25 mg H-AFt/ml which is equivalent to 50.58 μM . UV spectrophotometry determined a mean concentration of 604.70 μM Gefitinib. Thus, on average 1 μM of H-AFt was equivalent to 11.96 μM of encapsulated Gefitinib.

4.2.1.2 Mass spectrometry (MALDI)

Mass spectrometry measures the mass to charge ratio of charged particles which can be used to determine the purity and the molar mass of the particles of importance [234]. MALDI studies showed high intensity peaks for H-AFt and Gefitinib, which indicate high abundance of the drug and the protein in the mixture corresponding to a MW of 24,711.9 Da for H-AFt and a MW of 442.6 Da for Gefitinib which is comparable to expected standard values (Figure 4.1 (d)). The standard MW of H-AFt is 21,000 Da, however, the H-AFt which was used for the encapsulation procedure had additional his-and avidin tags and also linker sequences that made it slightly larger [130]. The standard MW of Gefitinib is 446.9 Da [108] [125]. The values obtained by MALDI demonstrate that there was an abundance of H-AFt and Gefitinib in the encapsulated test agent.

4.2.1.3 Confirmation of encapsulation of Gefitinib in H-AFt

In order to confirm whether Gefitinib was encapsulated within the H-AFt NPs, Astrios EQ flow cytometry (Beckman Coulter) analysis was employed. The area occupied by a molecule is proportional to the MW, thus particles more than a certain size could only be analysed by this method. The MW of H-AFt was found to be 24,711.8 Da compared to Gefitinib which has a much smaller MW (442.6 Da), beyond detection by flow cytometry. As Gefitinib is fluorescent under UV, H-AFt-encapsulated-Gefitinib was observed using excitation and emission wavelengths of 355 and 385 nm respectively by the 405/30 band pass filter of the flow cytometer. Fluorescence was detected by the forward scatter and a marker was placed to detect the populations

positive (R3) and negative (R4) for fluorescence. Figure 4.1 (e1) shows a histogram of H-AFt which was not encapsulated, thus showing only a negative population on to the left with very little fluorescence. However, after encapsulation of Gefitinib within the H-AFt cavity, a large positive population, shifted to the right, was detected with a fluorescence population 180 x brighter than H-AFt alone. These data confirm encapsulation of Gefitinib within AFt NPs (Figure 4.1 (e2)).

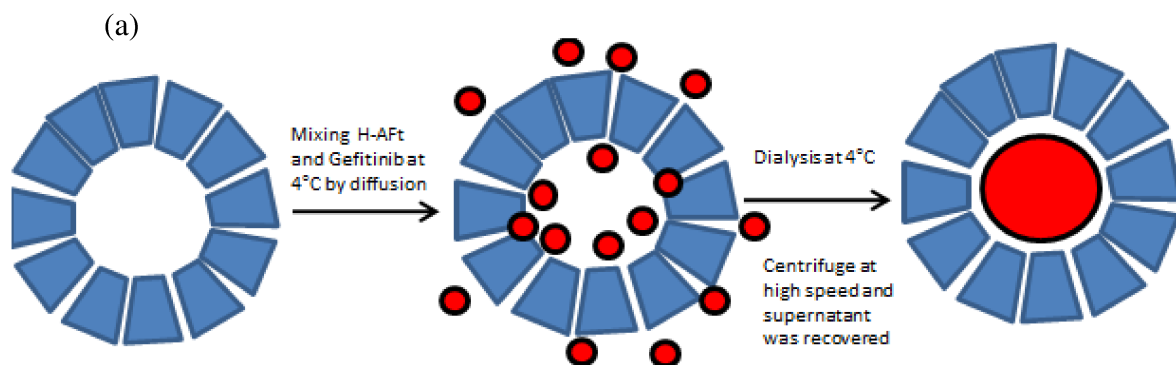
4.2.1.4 Determining stability and structural integrity

Gefitinib was encapsulated in AFt adopting a dialysis method. In order to determine whether the stability and the structural integrity of H-AFt-encapsulated-Gefitinib were altered after encapsulation, SDS-PAGE was carried out (Figure 4.1 (f1)). As depicted, H-AFt-encapsulated-Gefitinib showed a band similar to that of H-AFt only, ~ 24,700 Da. This indicates that AFt protein structure remains unchanged after encapsulation of Gefitinib. The amount of H-AFt was less in the encapsulated test agent which was expected (Figure 4.1 (f2)).

4.2.1.5 TEM

TEM images revealed that encapsulated Gefitinib molecules do not disrupt the structure of H-AFt NPs and confirm that the NPs possess and retain their spherical shape even after encapsulation. The mean outer diameter of the H-AFt NPs was measured to be 12.5 ± 0.46 nm which confirms that the size has not changed following encapsulation. However, specific Gefitinib molecules within the NP could not be determined from the TEM images; the electron density of Gefitinib molecules was

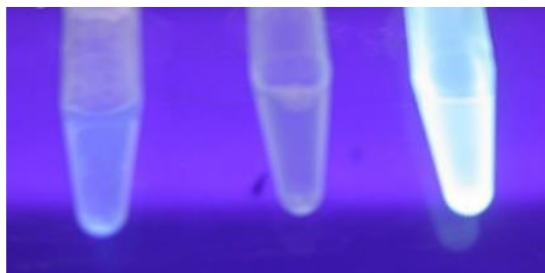
similar to that of H-AFt such that there was insufficient contrast to resolve encapsulated Gefitinib. This may reflect even distribution of Gefitinib molecules within the H-AFt cavity (Figure 4.1 (g1 and g2)).

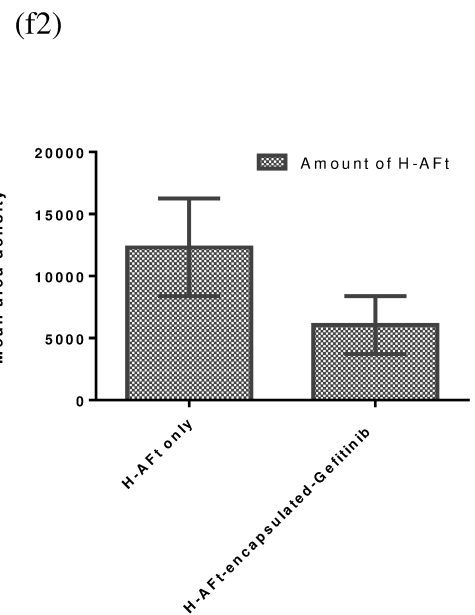
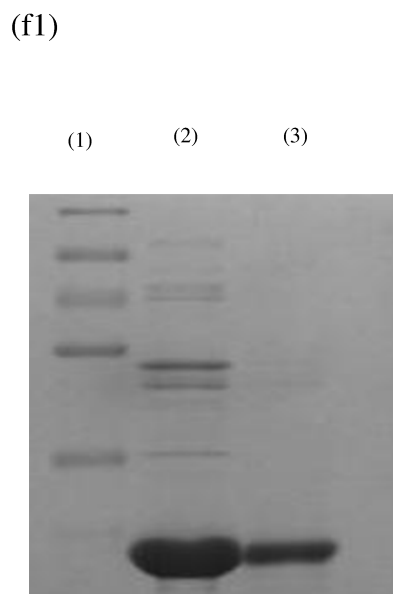
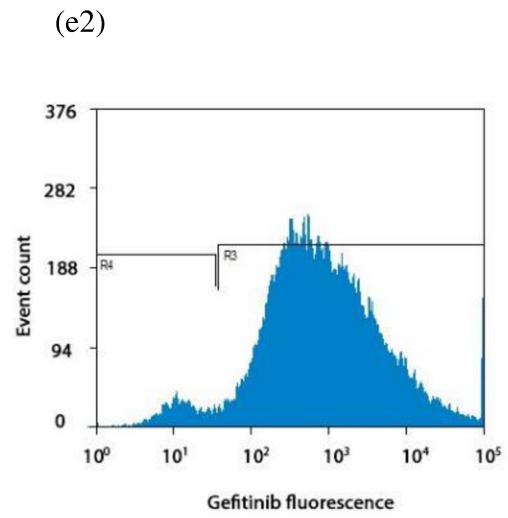
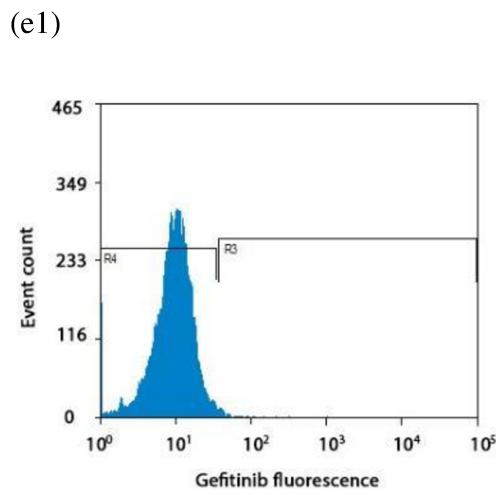
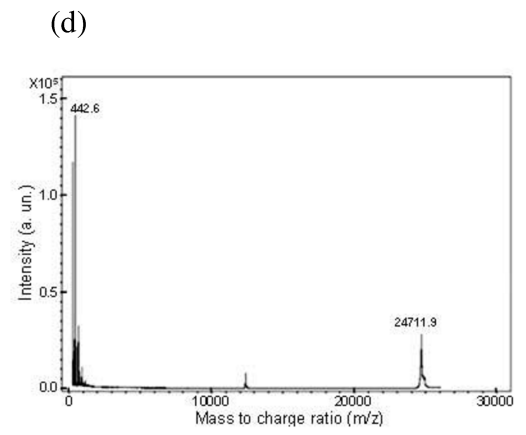
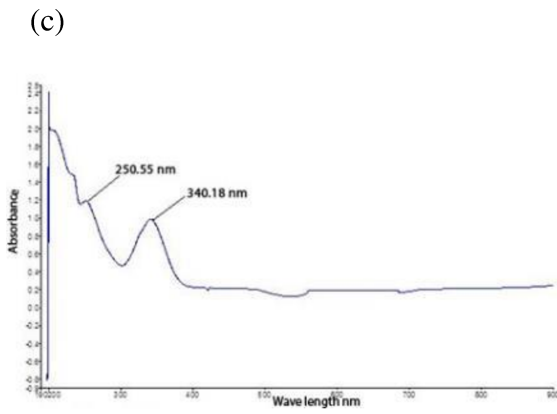


(b1)

(b2)

(b3)





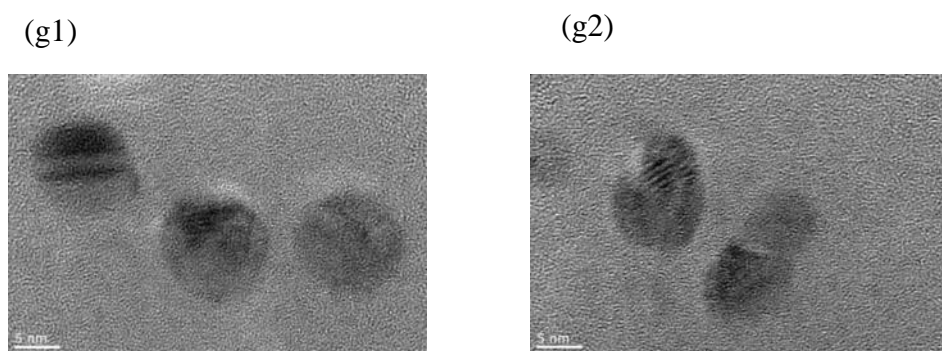


Figure 4.1: Characterisation of H-AFt-encapsulated-Gefitinib. (a) Schematic representation of preparation of H-AFt-encapsulated-Gefitinib NPs. (b) Fluorescence of (b1) H-AFt-encapsulated-Gefitinib, (b2) H-AFt only (b3) Gefitinib only, visualised under UV. (c) Spectrum of Gefitinib at 250 nm using UV spectrometry (d) MALDI spectrum with peaks for Gefitinib and H-AFt of the encapsulated test agent demonstrating the MWs of Gefitinib (442.9 Da) and H-AFt (24,711.9 Da) within the test agent. (e) Flow cytometry histograms confirming the encapsulation of Gefitinib in H-AFt. (e1) H-AFt only and (e2) H-AFt-encapsulated-Gefitinib. (f) Determining stability and structural integrity of H-AFt, (f1) SDS-PAGE - 1) Marker 2) H-AFt only and 3) H-AFt-encapsulated-Gefitinib and (f2) Densitometry analysis of SDS-PAGE. Mean and SD of trials ≥ 3 . (g) TEM Images of H-AFt-encapsulated-Gefitinib (g1) and (g2).

4.2.2 *In vitro* growth inhibitory effects of H-AFt-encapsulated-Gefitinib

The effect of H-AFt-encapsulated-Gefitinib was assessed using the HER2 overexpressing SKBR3 cell line and the MDA-MB 231 cell line that does not express HER2. The SKBR3 cell line expresses low levels of EGFR and the MDA-MB 231 cell line expresses high levels of EGFR [189]. Cells were incubated with H-AFt-encapsulated-Gefitinib, Gefitinib alone and H-AFt alone for 72 h initially. Dose dependent growth inhibition was demonstrated (Table 4.1 (a)), (Figure 4.2 (a - c)). Interestingly, the SKBR3 cell line was sensitive to both Gefitinib alone ($GI_{50} = 0.94 \mu\text{M}$) and H-AFt-encapsulated-Gefitinib ($GI_{50} = 1.44 \mu\text{M}$). However, the GI_{50} value obtained with the SKBR3 cells treated with H-AFt-encapsulated-Gefitinib was

slightly higher compared to Gefitinib alone. This implies that encapsulated Gefitinib requires time to be released from the H-AFt cavity as it is processed by acidic endosomes and lysosome systems within the cell. At early time points, AFt has shown to be restricted in endosomes while with time, AFt is transferred to lysosomes. These systems will facilitate release of the drug and degrade cytosolic AFt by autophagy or proteasomal elimination [130]. Indeed Liang et al, 2014, has shown that Doxorubicin was gradually released from the AFt cavity which was located in the cytoplasm and transferred to acidic lysosomes of cancer cells at 24 h. Subsequently, majority of the encapsulated drug has been in lysosomes [228]. It has been portrayed that late endosomes could reach an acidity of pH 6.0 while lysosomes are highly acidic and can reach an acidic environment of pH 4.5 and 5.0 [235]. This is an ideal environment for AFt to release its cargo because it has been shown that the AFt cage starts to swell and the protein subunits separate at $\text{pH} \leq 5.0$ [129].

This observation was further confirmed by a MTT assay which was used to test the activity of H-AFt-encapsulated-Gefitinib and Gefitinib alone following 24 h exposure. H-AFt-encapsulated-Gefitinib demonstrated a GI_{50} value of 2.24 μM which was higher than the GI_{50} value obtained after 72 h. Gefitinib alone demonstrated a GI_{50} value of 0.74 μM . The MDA-MB 231 cell line demonstrated low sensitivity to both Gefitinib alone ($\text{GI}_{50} = 21.80 \mu\text{M}$) and H-AFt-encapsulated-Gefitinib ($\text{GI}_{50} > 25 \mu\text{M}$) after 72 h exposure (Figure 4.2 (d – f), and also after 24 h exposure where both agents showed a GI_{50} value $> 25 \mu\text{M}$). As it was outlined in the previous chapter, no correlation was observed between EGFR expression and cell sensitivity to Gefitinib alone and H-AFt-encapsulated-Gefitinib although Gefitinib is an EGFR TKI [190]. Gefitinib

activity requires a phosphorylated form of EGFR whereas MDA-MB 231 cells express a non-phosphorylated form of EGFR, hence are not sensitive to this drug [189].

In the current study, transferrin has been exploited for the delivery of H-AFt-encapsulated-Gefitinib into cancer cells by transferrin receptors [220] [228]. Many studies have portrayed modified ferritin with recognition ligands to achieve tumour specific targeting, however, it was thought that it could abolish the intrinsic tumour specific binding and then disrupt the release of encapsulated cargo which will result in an interrupted *in vivo* performance [228] [236] [237].

H-AFt is efficiently taken up by cells transported *via* the cardiovascular system by the use of TfR1[130] [238]. TfR1 receptors are expressed at high levels in cancer cells compared to normal human cells. It has been found that the expression of TfR1s is associated with tumour stage or cancer progression [218]. In fact, malignant breast tissue has been shown to have a 7-fold increase in cytosolic ferritin compared to benign lesions of the breast [237]. Iron is required by many cellular processes such as metabolism and DNA synthesis. Thus, cancer cells have more TfR1s than normal cells [234] [238]. These receptors reside on cell membranes and transport cargo into cells by receptor mediated endocytosis via clathrin-coated pits [126] [218]. Further, the EPR effect may enhance NP drug accumulation at tumour sites compared to normal tissues by passive targeting. Nevertheless the EPR effect would only be achieved in an *in vivo* environment [218]. Further, TfR1 receptors have also shown potential in

the delivery of anti-cancer agents into the brain by overcoming the blood-brain barrier [220]. This is quite important as breast cancer often metastasises into the brain [15].

However, it has been shown that binding of H-AFt occurs in the absence of transferrin and that binding is significantly inhibited by transferrin although not completely since transferrin is the main transport system for iron atoms. Research has depicted that the binding sites for H-AFt and transferrin might not be identical but probably overlap or that transferrin alters TfR1 so that it reduces binding of H-ferritin which could be a limitation to this system. Nonetheless, it has also been shown that high concentrations of H-AFt partially block binding of transferrin to TfR1 [130]. Further, it has been demonstrated that ferritin/AFt binds to an inhibitor of angiogenesis with high affinity and antagonises the effects of this inhibitor thereby increasing cell viability *in vivo* which may suggest competition between endogenous ferritin and H-AFt uptake [239]. However, once again at high concentrations of H-AFt this function might be succeeded *in vivo* as successful delivery of agents encapsulated in AFt has been shown [228]. Another limitation to this delivery system would be that markedly high levels of TfR1 are exhibited on haematopoietic stem cells. However, it is apparent that hyperexpression of TfR1s in haematopoietic stem cells is related to differentiation rather than proliferation. *In vitro* studies have shown that erythroid cells show markedly higher TfR1 levels compared to other progenitor cells at an early differentiation stage to maturation. Thus, H-AFt-encapsulated-Gefitinib may bind to haematopoietic stem cells including erythroid cells which may affect haematopoiesis *in vivo* [240]. Despite its limitations, TfR1 receptors were considered in this study as a targeting molecule due to high levels expressed in tumour cells.

Both SKBR3 and MDA-MB 231 cells express high levels of TfR1s which would assist H-AFt-encapsulated-Gefitinib uptake compared to normal cells [241] [242]. Nevertheless, the SKBR3 cell line showed a lower GI_{50} value to H-AFt alone compared to the MDA-MB 231 cell line (Table 4.1 (a)). The greater SKBR3 growth inhibition in the presence of H-AFt compared to MDA-MB 231 implies greater sequestration of H-AFt by SKBR3 cells. Indeed, it has been shown previously that ferritin was not taken up by MDA-MB 231 cells [243]. Intriguingly, it was observed that the GI_{50} value obtained for MDA-MB 231 with the exposure to H-AFt alone was lower compared to H-AFt-encapsulated-Gefitinib. This could be due to MDA-MB 231 cells being resistant to Gefitinib and with the release of the drug these cells may demonstrate resistant mechanisms by increased proliferation.

To determine whether a longer exposure time to encapsulated drug, will be more effective in cells, MTT assays were performed following 120 h cellular exposure to agents (Table 4.1 (b)) and (Figure 4.3 (a - f)). Interestingly, the GI_{50} value for H-AFt-encapsulated-Gefitinib ($GI_{50} = 0.52 \mu\text{M}$) against the SKBR3 cell line was lower compared to the 72 h and 24 h assays and it was also lower than Gefitinib alone for 120 h ($GI_{50} = 1.66 \mu\text{M}$). There was no apparent significant difference between the GI_{50} values of Gefitinib alone after 72 and 120 h exposure periods ($P > 0.05$). However, from the results it is apparent that the GI_{50} values for Gefitinib alone increased with time, whereas the GI_{50} values for H-AFt-encapsulated-Gefitinib decreased with time for the SKBR3 cell line showing enhanced H-AFt-encapsulated-Gefitinib potency with increased time (Figure 4.4). Consistent with results following 72 h exposure, after 120 h exposure, the MDA-MB 231 cell line did not show any sensitivity to H-AFt-

encapsulated-Gefitinib. Once again the SKBR3 cell line showed a lower GI₅₀ value for H-AFt alone compared to the MDA-MB 231 cell line at 120 h. It should be noted that at H-AFt-encapsulated-Gefitinib GI₅₀ values of 1.44 μM (72 h) and 0.52 μM (120 h), the concentrations of H-AFt were 0.11 μM and 0.04 μM respectively, concentrations which negligibly impacted SKBR3 growth inhibition. These results demonstrate that drug encapsulation enhances the activity of Gefitinib in SKBR3 cells and support the hypothesis that the H-AFt cage allows controlled release of the drug molecules. Sustained drug release is an attractive factor in a drug delivery system and may lead to extended exposure of tumour cells/tissue to therapeutic drug concentrations [104].

Tumour microenvironments exhibit lower extracellular pH than normal tissues while the intracellular pH of cells within normal and tumour cells is similar [129]. The overall pH range within a tumour environment is 6.9 and 7.4 whereas normal cells will have a pH range between 7.2 and 7.6 [244] [245]. This slightly more acidic environment develops within tumour cells when increased glucose break down results in significant production of lactate and H⁺ which is transported to the extracellular environment. Therefore, due to the pH discrepancy, encapsulated drug may preferably be released within this slightly more acidic tumour microenvironment [129]. Hence, it was tested whether a more acidic *in vitro* environment would promote effective release of Gefitinib from its H-AFt cage. (Table 4.1 (c)) and (Figure 4.5). However, preliminary investigations revealed that SKBR3 cells cannot withstand environments < pH 7.0 for > 72 h. Lower GI₅₀ values were observed at pH 7.0 following 72 h exposure compared to normal pH conditions (pH 7.5) for both Gefitinib and H-AFt-

encapsulated-Gefitinib. This could be because Gefitinib ionises progressively as the pH drops, which increases solubility of Gefitinib [123]. It could be also a consequence of compromised cell growth.

(a)	Mean GI ₅₀ ± SD (72 h MTT assay)		
Cell line	Gefitinib alone	H-AFt-encapsulated-Gefitinib	H-AFt alone
SKBR3	0.94 µM ± 0.85	1.44 µM ± 1.20	4.84 µM ± 4.80
MDA-MB 231	21.80 µM ± 0.74	> 25 µM	16.47 µM ± 1.39

(b)	Mean GI ₅₀ ± SD (120 h MTT assay)		
Cell line	Gefitinib alone	H-AFt-encapsulated-Gefitinib	H-AFt alone
SKBR3	1.66 µM ± 1.36	0.52 µM ± 0.29	5.50 µM ± 5.38
MDA-MB 231	19.56 µM ± 0.91	> 25 µM	19.85 µM ± 0.21

(c)	Mean GI ₅₀ ± SD (72 h MTT assay at pH 7.0)	
Cell line	Gefitinib alone	H-AFt-encapsulated-Gefitinib
SKBR3	0.13 µM ± 0.08	0.44 µM ± 0.28

Table 4.1: Mean GI₅₀ ± SD values of Gefitinib, H-AFt, and H-AFt-encapsulated-Gefitinib. It should be noted that the GI₅₀ values for H-AFt-encapsulated-Gefitinib refer to encapsulated Gefitinib concentrations. The amount of Gefitinib encapsulated per H-AFt cage impacts material potency and merits further detailed study. Cells were seeded in 96 well plates at a density of 2.5 x 10³ cells/well. After allowing time to adhere (24 h), cells were exposed to Gefitinib alone, H-AFt-encapsulated-Gefitinib or H-AFt alone (n = 8 for either 72 h or 120 h at pH 7.5). SKBR3 cells were also seeded at a density of 2.5 x 10³ cells/well in 96 well plates at pH 7.0 and treated with Gefitinib alone or H-AFt-encapsulated-Gefitinib. Mean and SD of trials ≥ 3.

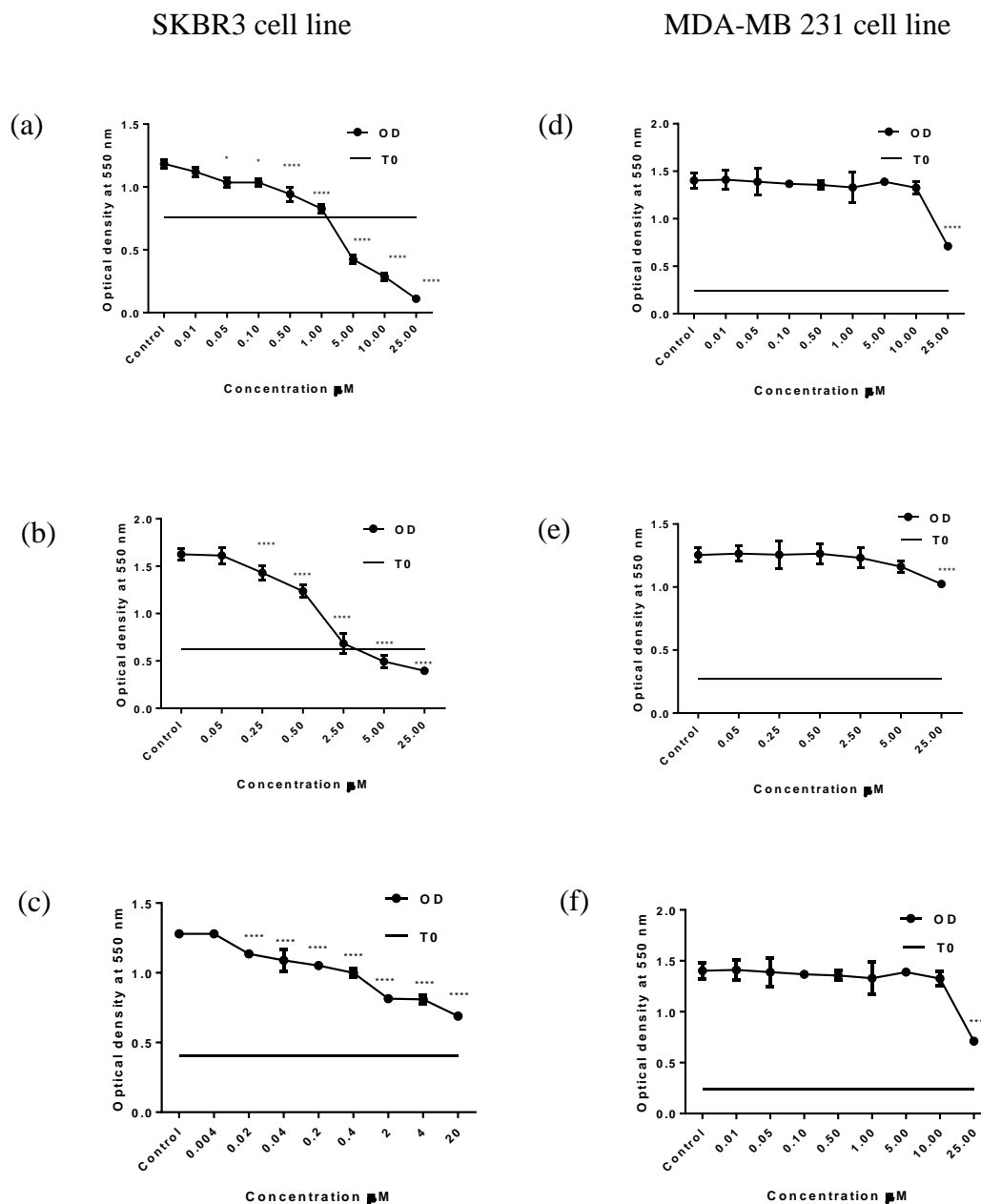


Figure 4.2: Growth inhibitory curves for Gefitinib and H-AFt-encapsulated-Gefitinib after 72 h exposure. (a, b, c) SKBR3 cell line and (d, e, f) MDA-MB 231 cell line. Cells were treated after 24 h and exposed to agents for 72 h ($n = 8$) prior to MTT assay; (a, d) Gefitinib only, (b, e) H-AFt-encapsulated-Gefitinib and (c, f) H-AFt only. Mean and SD of representative experiments are shown ($n = 8$ per trial); trials ≥ 3 . * indicates significant difference compared to control, * ($P < 0.05$), ** ($P < 0.01$), *** ($P < 0.001$), **** ($P < 0.0001$).

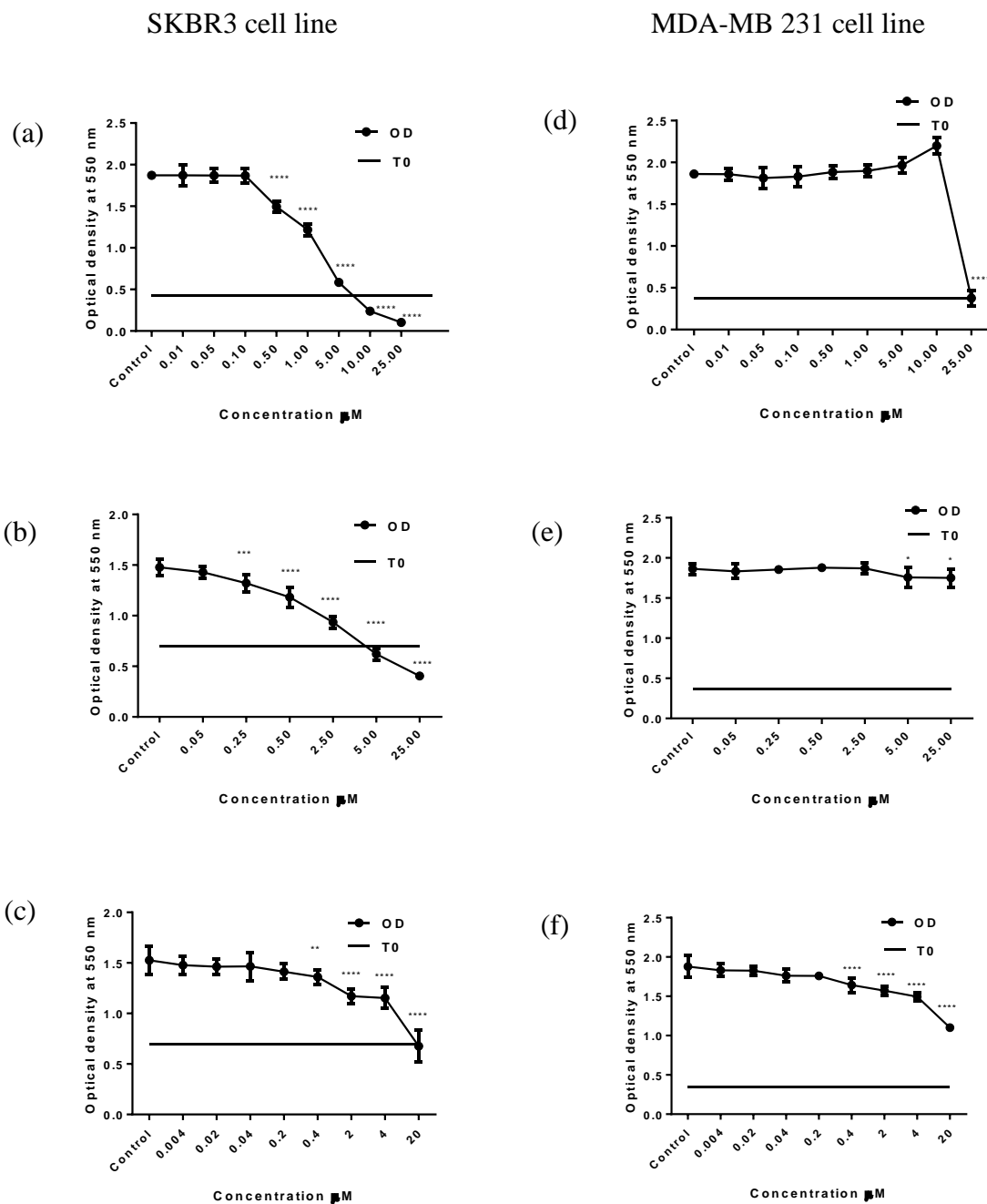


Figure 4.3: Growth inhibitory curves for Gefitinib and H-AFt-encapsulated-Gefitinib after 120 h exposure. (a, b, c) SKBR3 cell line and (d, e, f) MDA-MB 231 cell line. Cells were treated after 24 h and exposed to agents for 120 h prior to MTT assay ($n = 8$); (a, d) Gefitinib only, (b, e) H-AFt-encapsulated-Gefitinib and (c, f) H-AFt only. Mean and SD of representative trials are shown ($n = 8$ per trial); trials ≥ 3 . * indicates significant difference compared to control, * ($P < 0.05$), ** ($P < 0.01$), *** ($P < 0.001$), **** ($P < 0.0001$).

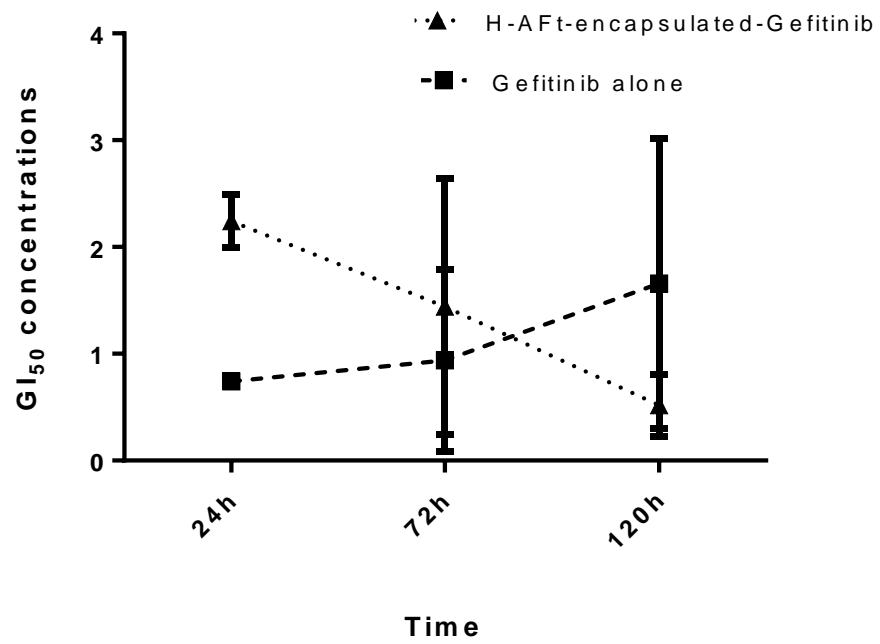


Figure 4.4: GI₅₀ values for Gefitinib alone and H-AFt-encapsulated-Gefitinib at each time point tested in the SKBR3 cell line. Mean and SD of each GI₅₀ value is shown; trials ≥ 3 .

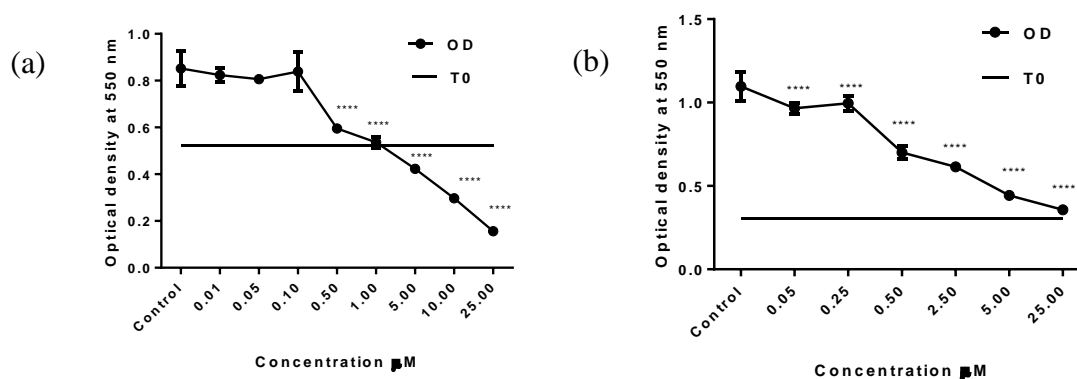


Figure 4.5: Growth inhibitory curves after 72 h exposure at pH 7.0. (a) Gefitinib only and (b) H-AFt-encapsulated-Gefitinib. SKBR3 cells were seeded at a density of 2.5×10^3 cells/well in 96 well plates at pH 7.0. Cells were treated after 24 h and exposed to agents for 72 h ($n = 8$) prior to MTT assay. Mean and SD of representative trials are shown ($n = 8$ per trial); trials ≥ 3 . * indicates significant difference compared to control, * ($P < 0.05$), ** ($P < 0.01$), *** ($P < 0.001$), **** ($P < 0.0001$).

4.2.3 Effects of H-AFt-encapsulated-Gefitinib on SKBR3 colony formation

Clonogenic assays were performed to determine whether single SKBR3 cells were able to survive challenge with Gefitinib alone or H-AFt-encapsulated-Gefitinib (brief exposure of 24 h vs. continuous exposure to agents for 14 days) and subsequently form progeny colonies, indicative of tumour repopulation [147]. Cells were treated with 1 μM (equivalent to 1x GI_{50} of Gefitinib) and 5 μM (equivalent of 5x GI_{50} of Gefitinib) (Figure 4.6).

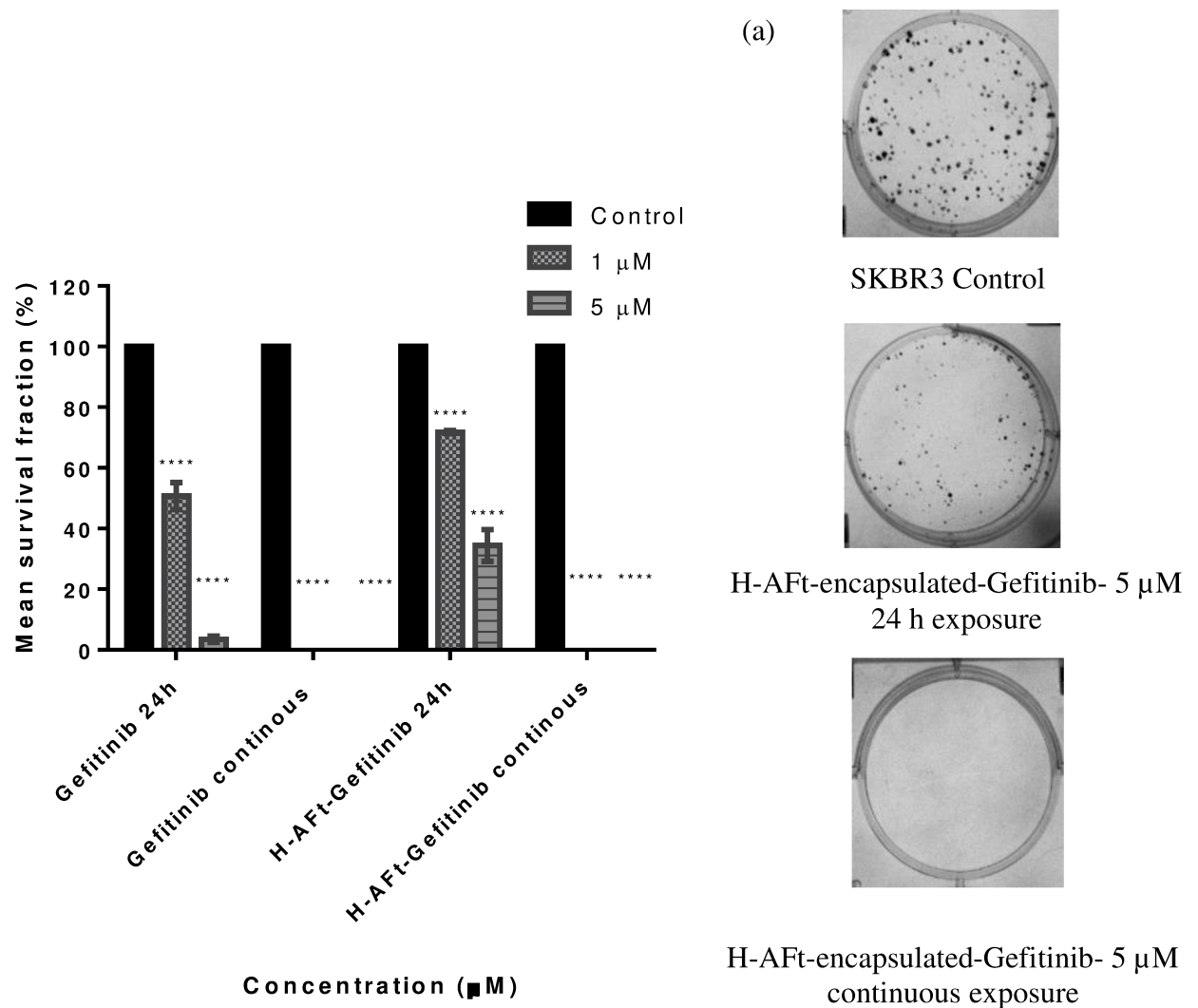


Figure 4.6: Effects of Gefitinib and H-AFt-encapsulated-Gefitinib on colony formation. (a) Representative images of colony formation after exposure to agents. Mean SF as a % of plating efficiency of control represented as the mean and SD of trials ≥ 3 , (n = 3 per trial). **** indicates significant difference compared to control (P < 0.0001) in colony formation.

The clonogenic assay results concur with those of the MTT assays. H-AFt-encapsulated-Gefitinib was less potent than Gefitinib alone after 24 h exposure. The SF of cells treated with H-AFt-encapsulated-Gefitinib was 34.40% (5 μ M) compared to control whereas SF of cells treated with Gefitinib was 3.48% (5 μ M) compared to control. It was noted that an increased concentration such as 5 μ M which is equivalent to 5x GI₅₀ of Gefitinib demonstrated a highly cytotoxic effect compared to 1x and 2x GI₅₀ concentrations of the same agent which resulted in cytostatic and moderate cytotoxic effects showed in the previous chapter. Further, it was also observed in chapter 3, that 2x GI₅₀ was more cytotoxic than 1x GI₅₀ following a same trend to the results within this chapter. Interestingly, following continuous exposure to both agents, no colonies could be detected after 14 days, compared to control. Results infer that continuous exposure allows Gefitinib molecules to escape from the H-AFt cavity and endorse the premise of sustained drug release from an efficient drug delivery system.

4.2.4 Release of Gefitinib from H-AFt

The AFt NPs disassemble into protein subunits under acidic conditions and release the encapsulated cargo [129]. In order to verify this, a pH dependent drug release profile was carried out. The release of H-AFt-encapsulated-Gefitinib was examined over a period of 24 h by analysing the buffer released from the dialysis bags and buffer retained within the dialysis bags. UV spectrometry was adopted to compare Gefitinib release from H-AFt at pH 2, 4 and 7.5. At pH 2, the AFt cage completely disassembles, at pH 4, the AFt cage will swell and the protein subunits will separate, at pH 7.5, the AFt cage retains its assembled structure [129]. Release of Gefitinib alone was

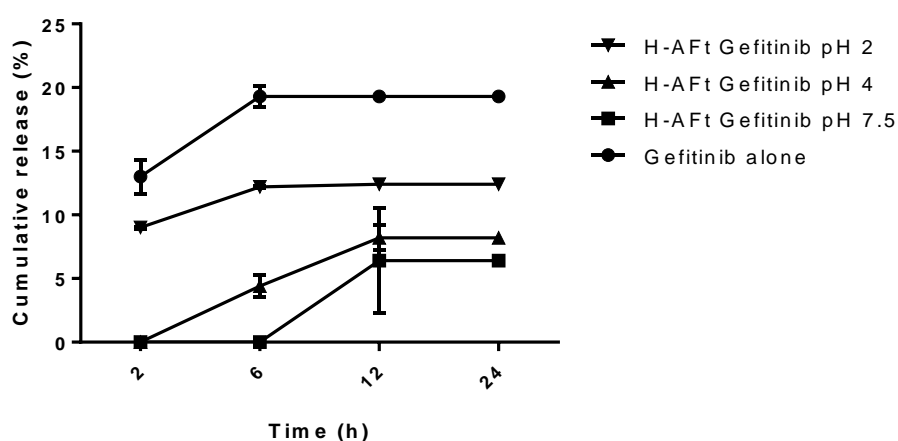
observed only at pH 7.5. By analysing the buffer released from the dialysis bag it was observed that Gefitinib alone showed a rapid release profile with a higher percentage of drug release. Gefitinib release reached a plateau at 6 h. In comparison at pH 2, 4 and 7.5, H-AFt-encapsulated-Gefitinib showed a slower cumulative release profile and a lower percentage of drug release due to being encapsulated in the AFt cavity. Among the pH levels the fastest cumulative release profile was observed for H-AFt-encapsulated-Gefitinib at pH 2. This is consistent with the AFt cage disassembling completely and releasing more Gefitinib molecules to diffuse into the buffer. (Figure 4.7 (a)).

In figure 4.7, it was observed that only a low percentage of Gefitinib was detected as released, for all 4 release profiles. The buffer used was 20 mM Tris buffer and Gefitinib is not soluble in aqueous buffers such as Tris. Thus, Gefitinib would have been degraded or precipitated in the released buffer after 24 h as the samples were incubated for more than 24 h before analysing them with the UV spectrometry. Therefore only a maximum of 19% was detected in 24 h for Gefitinib alone as released and the rest which was released would have been degraded or reformed precipitates.

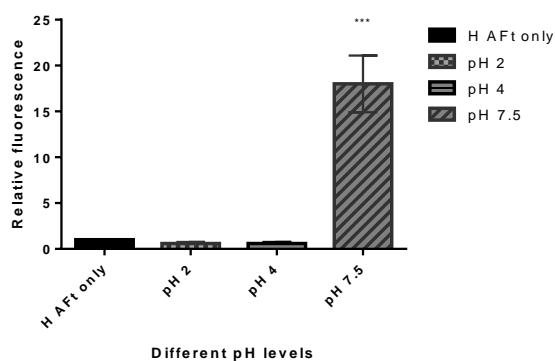
The residual buffer with NPs remaining in the dialysis bags at all studied pH levels was analysed by flow cytometry and compared to H-AFt only (control), also placed in a dialysis bag (Figure 4.7 (c)). At pH 2 and 4, residual dialysis bag buffer revealed only 2 negative (R4) populations exposing no fluorescence in the histograms relative to control. This implies that there was no Gefitinib left in the dialysis bags; drug had

been released over the 24 h period (Figure 4.7 (d and e)). However at pH 7.5, a small population positive for fluorescence remained (R3): 18.0 ± 3.1 x brighter fluorescence was detected compared to H-AFt alone, which corroborated with the results obtained by UV spectrometry examining Gefitinib released from the H-AFt-capsule (Figure 4.7 (f)). These results further confirm sustained release of Gefitinib from H-AFt which maximises the efficacy of the drug, especially at physiological pH levels. Nevertheless, in an acidic environment such as stomach cancers where the pH reaches as low as pH 1.5, a higher percentage of drug might be observed [228] [245] [246] (Figure 4.7 (b)).

(a)



(b)



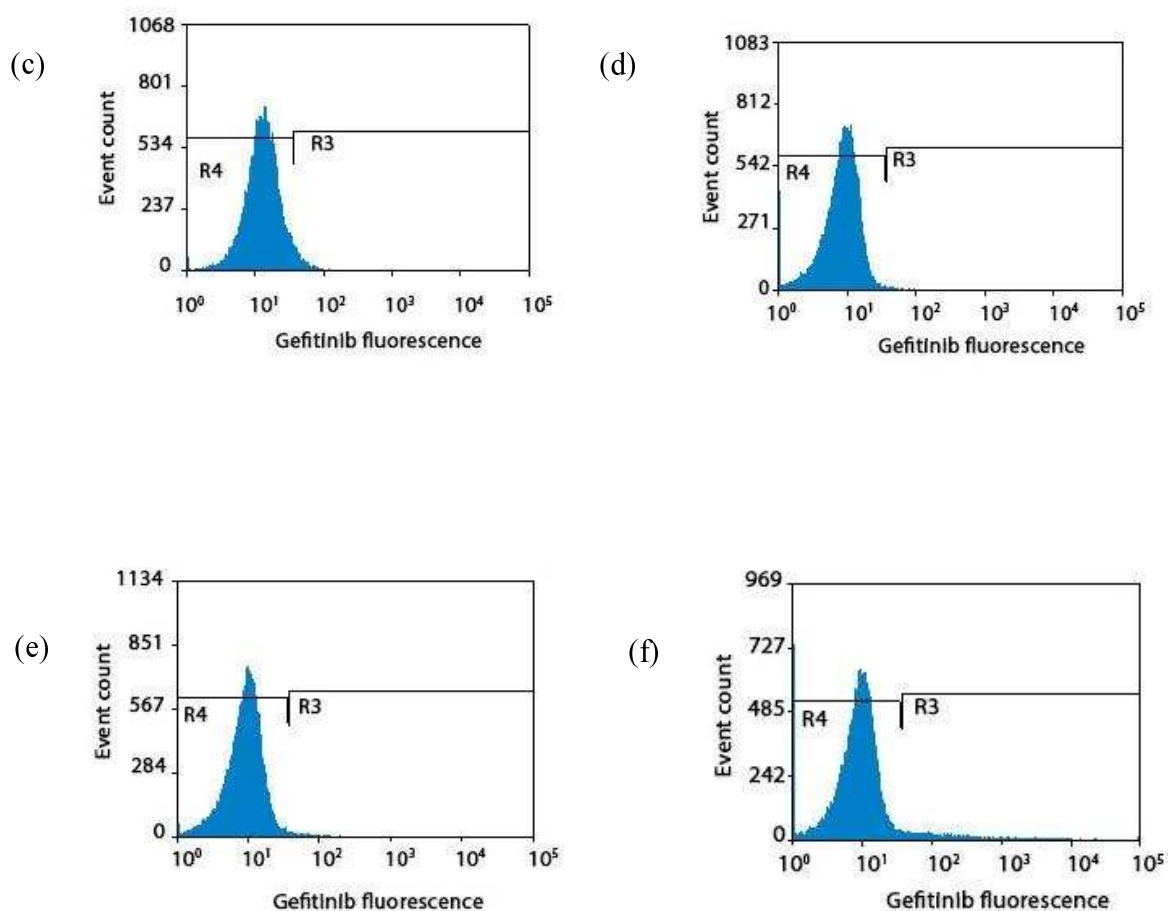


Figure 4.7: Detection of Gefitinib release from the H-AFt cavity. (a) Cumulative release of Gefitinib alone at pH 7.5 and from H-AFt-encapsulated-Gefitinib at pH 2, 4 and 7.5 at 2, 6, 12 and 24 h observed by UV spectrometry. (b) Relative total fluorescence emitted by Gefitinib retained within the dialysis bags at pH 2, 4 and 7.5 after a period of 24 h detected by flow cytometry. (c - f): Representative histograms representing fluorescence emitted by Gefitinib. A marker was placed to detect the positive (R3) and the negative (R4) populations for fluorescence. (c) Residual H-AFt alone, (d) Residual H-AFt-encapsulated-Gefitinib (pH 2), (e) Residual H-AFt-encapsulated-Gefitinib (pH 4) and (f) Residual H-AFt-encapsulated-Gefitinib (pH 7.5). Mean and SD of trials ≥ 3 , ($n = 3$ per trial). * indicates significant difference compared to control, *** ($P < 0.001$).

4.2.5 Cellular uptake of H-AFt-encapsulated-Gefitinib by confocal microscopy

Cellular uptake and internalisation of H-AFt-encapsulated-Gefitinib or Gefitinib alone was measured by confocal microscopy. SKBR3 and MDA-MB 231 cells were treated with H-AFt-encapsulated-Gefitinib (5 μ M), or Gefitinib alone (5 μ M) for 24 h. The fluorescence of Gefitinib is environmentally sensitive – peak excitation and emission depends upon environment polarity and is intense in nonpolar solvents [153]. Intracellular fluorescence was punctuate and was localised in cytoplasmic vesicles such as acidic lysosomes and endosomes. Fluorescence was excluded from nuclei [153]. It was evident from the bright fluorescence within the cytoplasm of H-AFt-encapsulated-Gefitinib and Gefitinib treated cells that H-AFt-encapsulated-Gefitinib was internalised in a manner similar to Gefitinib alone. However, the punctuate fluorescence pattern was slightly less within the cells treated with H-AFt-encapsulated-Gefitinib compared to Gefitinib alone (Figure 4.8 (b - e)). SKBR3 cells that were treated with 5 μ M H-AFt alone (Figure 4.8 (f)) appeared to be identical to control cells (Figure 4.8 (a)) and did not show bright fluorescence as expected. The MDA-MB 231 cells that were treated with (5 μ M) H-AFt-encapsulated-Gefitinib did not show visible cellular uptake compared to MDA-MB 231 cells that were treated with Gefitinib alone indicating negligible uptake in these cells (Figure 4.8 (h - k)). Further, neither MDA-MB 231 control (Figure 4.8 (g)) nor MDA-MB 231 cells treated with 5 μ M H-AFt alone (Figure 4.8 (l)) fluoresced.

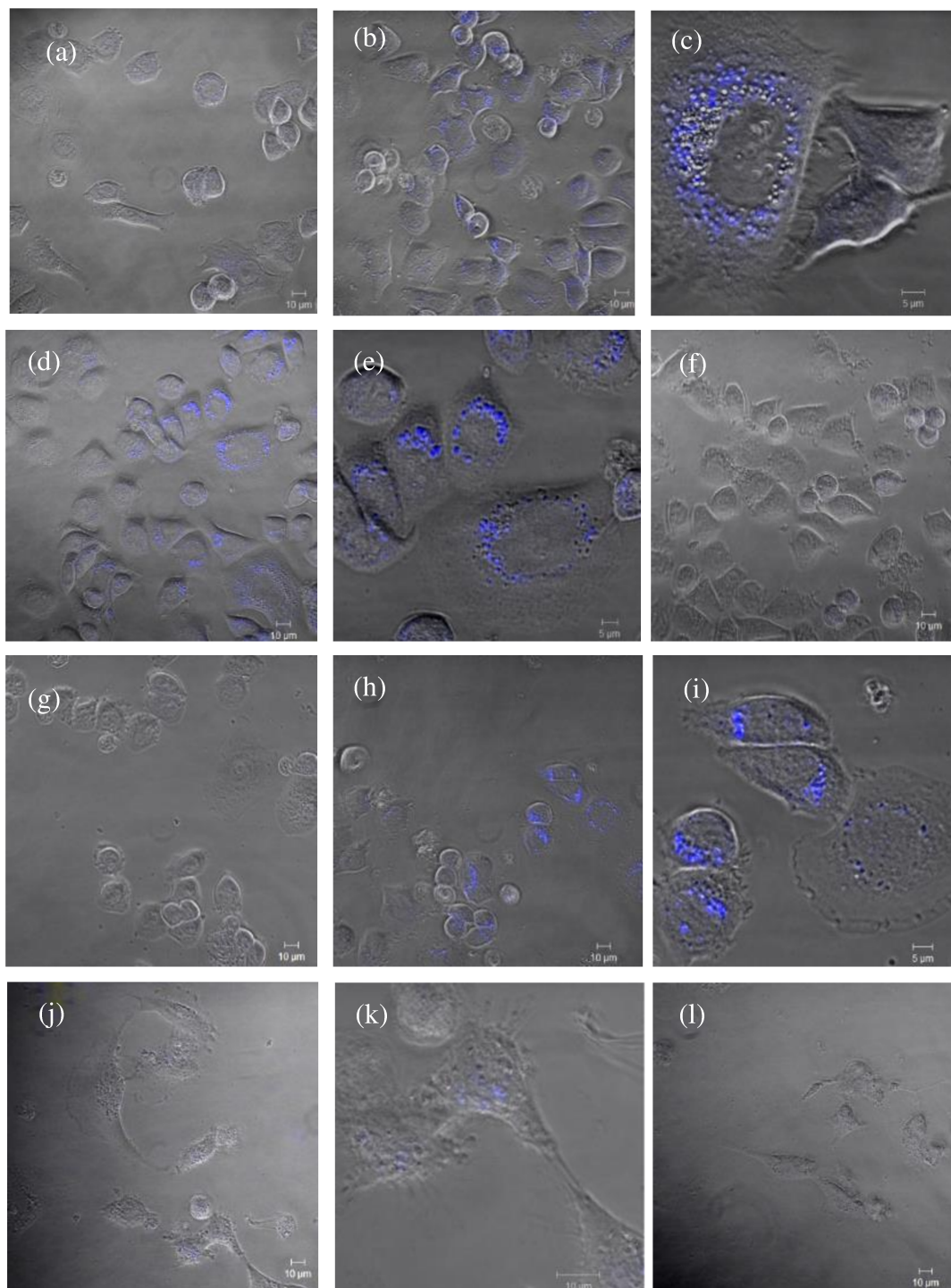


Figure 4.8: Confocal microscopy images of SKBR3 and MDA-MB 231 cells following exposure to Gefitinib and H-AFt-encapsulated-Gefitinib. (a – f) SKBR3 and (g – l) MDA-MB 231 cells demonstrating cellular uptake of Gefitinib after 24 h exposure of cells to: (a, g) control, (b, c, h, i) Gefitinib alone, (d, e, j, k) H-AFt-encapsulated-Gefitinib, (f, l) H-AFt alone. Representative images of trials ≥ 3 , ($n = 2$ per trial).

4.2.6 Cellular uptake of H-AFt-encapsulated-Gefitinib by flow cytometry

Cellular uptake of H-AFt-encapsulated-Gefitinib was measured quantitatively using flow cytometry. SKBR3 and MDA-MB 231 cells were treated with H-AFt-encapsulated- Gefitinib or Gefitinib alone (5 μ M) for 24 h and compared to control. Mean fluorescence was used as a measure of Gefitinib uptake by cells and compared to control (Figure 4.9). The uptake of Gefitinib alone by SKBR3 cells ($P < 0.001$) and MDA-MB 231 cells ($P < 0.0001$) was extremely significant compared to control. The uptake of H-AFt-encapsulated-Gefitinib by SKBR3 cells was also significant ($P < 0.05$) compared to control. However, uptake of H-AFt-encapsulated-Gefitinib by MDA-MB 231 cells was not significant compared to control corroborating confocal microscopy results. Thus, the qualitative observations of confocal microscopy were reinforced by flow cytometry analyses. Together, results suggest that H-AFt-encapsulated-Gefitinib is internalised by HER2 overexpressing SKBR3 cells successfully.

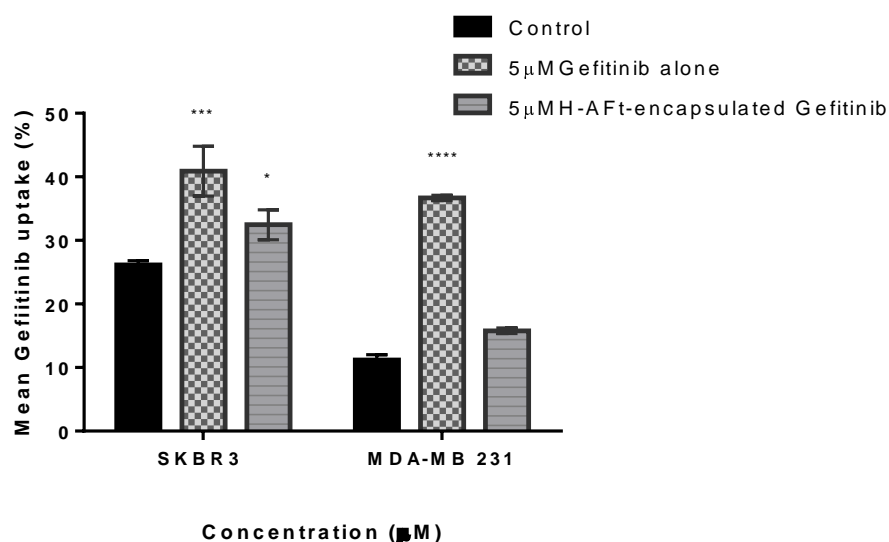


Figure 4.9: Mean fluorescence uptake by SKBR3 and MDA-MB 231 cells using flow cytometry. Mean and SD of trials ≥ 3 , ($n = 2$ per trial). * indicates significant difference compared to control, * ($P < 0.05$), ** ($P < 0.01$), *** ($P < 0.001$), **** ($P < 0.0001$).

4.3 Conclusion

This chapter describes successful encapsulation of Gefitinib within the H-AFt cavity by diffusion, sustained release of cargo and subsequent anti-cancer activity selectively in HER2 overexpressing SKBR3 breast carcinoma cells. Prior research has shown liposomal encapsulation of Gefitinib. However, these studies are at an early developmental phase [247]. Thus, testing further NPs where Gefitinib could be encapsulated may support to diminish the toxic effects of Gefitinib in the clinic. The unique properties of H-AFt have inspired many researchers to investigate its potential as a vehicle to encapsulate and deliver anti-cancer drugs. One such property is that it can be recognised and sequestered by TfR1 of cancer cells; encapsulated drug can thus be internalised into cancer cells *via* TfR1 mediated endocytosis and subsequently processed by acidic lysosome systems [222] [223] [228]. Utilising the fluorescent property of Gefitinib, it was able to confirm intracellular localisation of Gefitinib following exposure of SKBR3 cells to H-AFt-encapsulated-Gefitinib. Potent, dose dependent growth inhibition of cancer cells sensitive to EGFR and HER2 inhibition was observed. Clonogenic assays further provided evidence supporting sustained Gefitinib release and significant *in vitro* anti-cancer activity of H-AFt-encapsulated-Gefitinib. This system could reduce off target toxicities of Gefitinib and diminish drug deposition in normal tissues. The controlled and sustained release of Gefitinib from H-AFt, demonstrated potent activity with time compared to Gefitinib alone, which is a feature of a successful nanotechnology drug delivery system. As future work, an AFt drug delivery system could be utilised in stomach cancers with low pH ranges which would be ideal for AFt to disassemble and release its cargo efficiently [246].

5 Chapter 5 - Anti-proliferative effects of novel HER2 targeting heavy (H) and light (L) chain AFt-fusion proteins

5.1 Introduction

New agents that target HER2 are essential, especially agents which are associated with nanotechnology because a large fraction of patients have shown to develop resistance to existing clinical agents such as Trastuzumab [55]. With the development of recombinant DNA technology, multivalent fusion proteins have become a promising therapeutic approach for HER2+ cancers. Thus, an affibody molecule (targeting protein) genetically fused to H or L-AFt NPs was tested against HER2 overexpressing breast cancer cells. Genetic fusion proteins provide simpler therapeutic options compared to protein conjugates that comprise laborious chemical conjugation steps [248]. Affibody molecules compared to antibodies such as Trastuzumab, represent a more appropriate targeting moiety because of their smaller sizes (~ 10,000 Da) compared to monoclonal antibodies that typically have a size of ~ 150,000 Da. Further, excellent cell penetration ability with an endocytosis dependent internalisation mechanism and high binding affinity to the recombinant extracellular domain of the protein HER2 are significant features of these peptides [249] [250] [251]. However, small peptides have their limitations such as short plasma circulation time and fast blood clearance. Therefore, affibody fusion proteins may extend plasma half-life [248]. Thus, a fusion protein, of the affibody peptide (targeting protein) and H or L-AFt NPs becomes an attractive advantage to target HER2 overexpression in breast

cancer. This chapter describes the activity and mechanism of action of these novel fusion proteins compared to activity and mechanism of action of Trastuzumab.

5.2 Results and Discussion

5.2.1 *In vitro* growth inhibitory effects of H and L-AFt-fusion proteins, H and L-AFt only, targeting protein and Trastuzumab

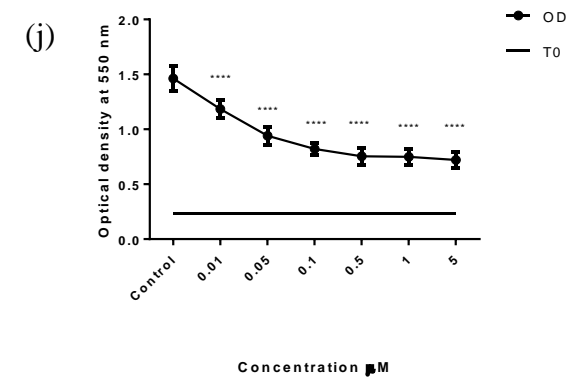
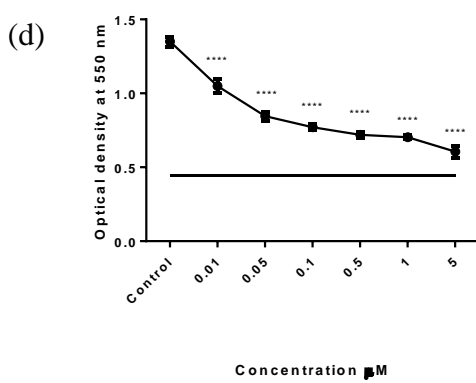
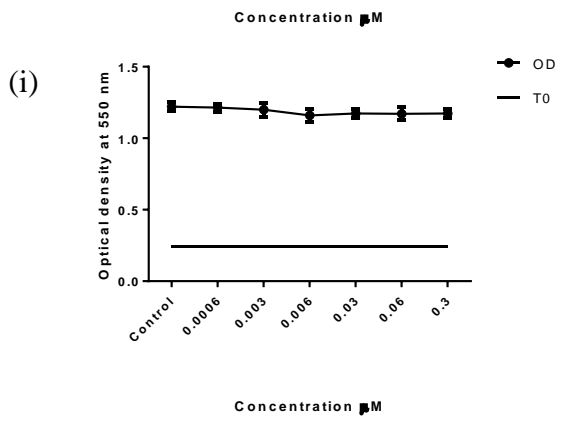
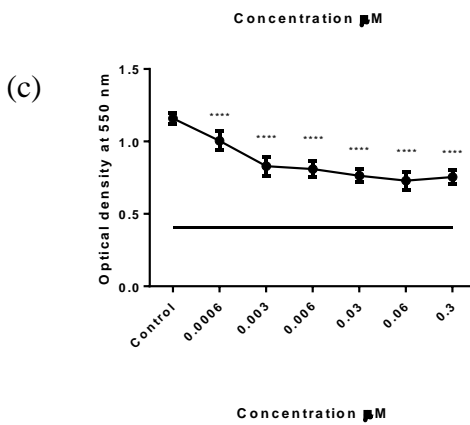
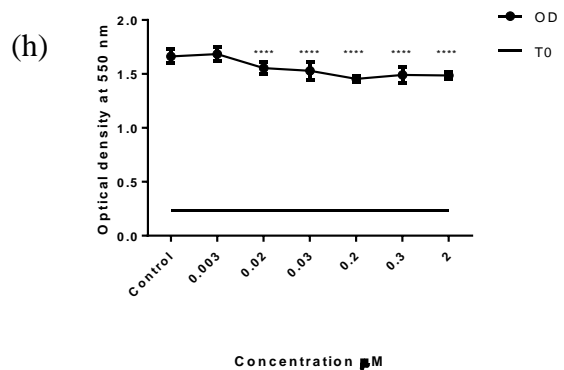
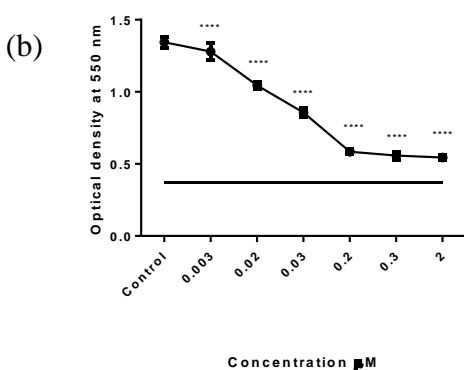
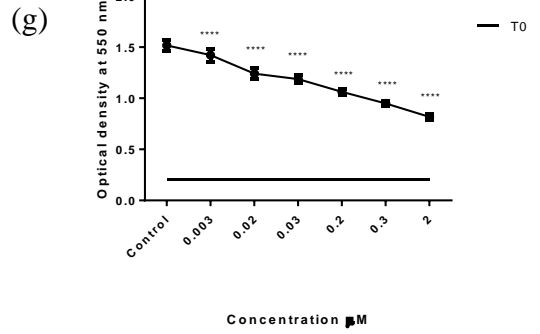
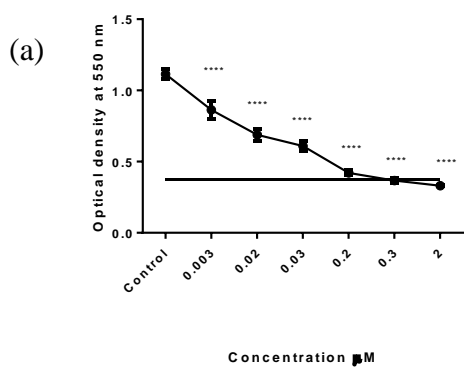
The anti-proliferative effects of the above mentioned agents were investigated using MTT viability assays against 2 cell lines; the HER2 overexpressing SKBR3 cell line and the HER2 lacking MDA-MB 231 cell line (negative control). The MTT results for all agents tested are summarised in Table 5.1.

Mean GI ₅₀ ± SD (72 h MTT assays)						
Cell line	H-AFt-fusion protein	L-AFt-fusion protein	Trastuzumab	Targeting protein	H-AFt only	L-AFt only
SKBR3	18.26 nM ± 8.54	103.60 nM ± 76.14	27.00 nM ± 5.83	34.69 nM ± 4.45	4.84 µM ± 4.80	7.50 µM ± 5.10
MDA-MB 231	986.04 nM ± 316.89	> 2 µM	> 3 µM	386.15 nM ± 283.27	16.47 µM ± 1.39	> 20 µM

Table 5.1: Mean GI₅₀ ± SD values of H and L-AFt-fusion proteins, Trastuzumab, targeting protein, H and L-AFt only. Cells were seeded in 96 well plates at a density of 2.5 x 10³ cells/well. Allowing time to adhere (24 h), cells were exposed to agents mentioned above (72 h; n = 8). Mean and SD of ≥ 3 trials.

SKBR3 cell line

MDA-MB 231 cell line



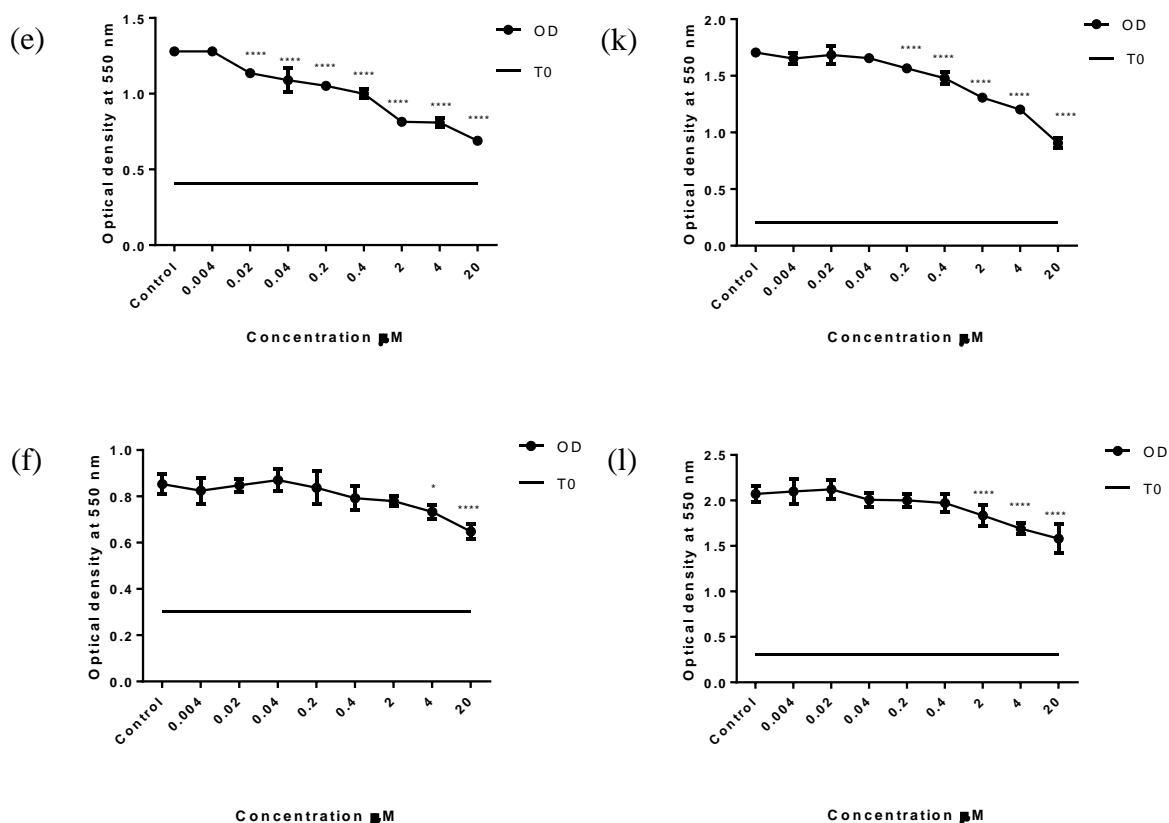


Figure 5.1: Growth inhibitory curves of H and L-AFt-fusion proteins, Trastuzumab, targeting protein, H and L-AFt only. (a, b, c, d, e and f) SKBR3 and (g, h, i, j, k and l) MDA-MB 231 cells; (a, g) H-AFt-fusion protein, (b, h) L-AFt-fusion protein, (c, i) Trastuzumab, (d, j) targeting protein, (e, k) H-AFt only and (f, l) L-AFt only. Mean and SD of representative experiments are shown ($n = 8$ per trial); trials ≥ 3 . * indicates significant difference compared to control, * ($P < 0.05$), ** ($P < 0.01$), *** ($P < 0.001$), **** ($P < 0.0001$).

From the results obtained it was observed that the novel HER2 targeting H-AFt-fusion protein was the most potent agent among all agents tested against the SKBR3 cell line ($GI_{50} = 18.26$ nM). The L-AFt-fusion protein was less potent (~ 5 -fold) ($GI_{50} = 103.60$ nM) than the H-AFt-fusion protein against the same cell line. Both agents elicited dose dependent growth inhibition and all concentrations tested showed a significant growth inhibitory effect compared to untreated SKBR3 cells ($P < 0.0001$). The difference in

the potency of H and L-AFt-fusion proteins could be a consequence of the high uptake of H-AFt by the SKBR3 cells which expresses high levels of TfR1. As it was outlined in chapter 4, binding of ferritin to TfR1s consists only of H ferritins illustrating that binding of ferritin to cells is facilitated by the H chain but not by the L chain [130].

Interestingly, the HER2 targeting protein alone displayed potency against the SKBR3 cell line ($GI_{50} = 34.69$ nM). These results showed that the HER2 targeting protein elicited potent activity against the SKBR3 cell line, which was higher than that for the L-AFt-fusion protein. This may be because the targeting protein has very high affinity for the HER2 receptor which would facilitate immediate binding to the cell surface of HER2 receptors of SKBR3 cells, which would decrease heterodimerisation and thereby induce cell death [53]. This could also happen particularly in the absence of other required growth factors and nutrients during an incubation period of 72 h, thus inducing cell death [34] [132].

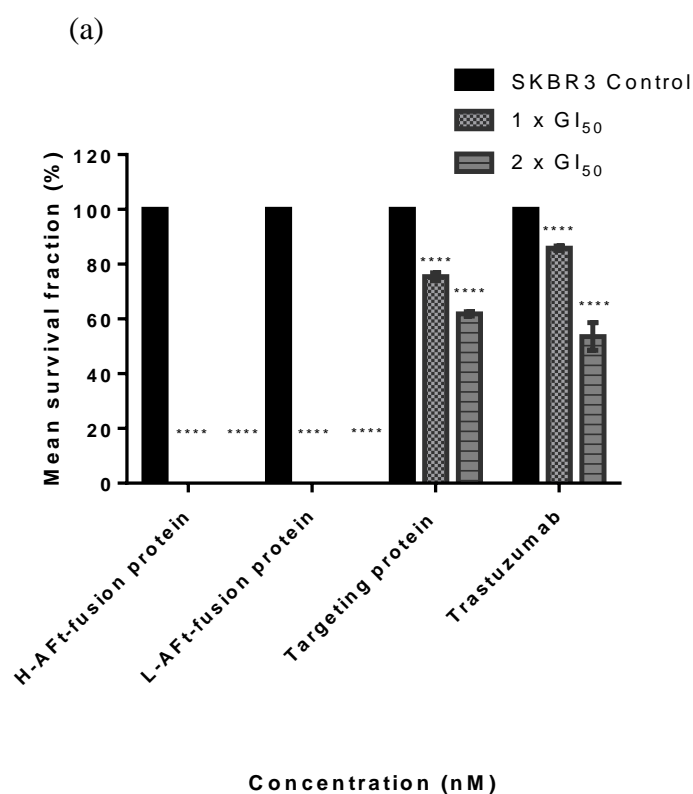
Each AFt subunit is fused to a targeting protein in a 1:1 ratio to develop the H-AFt-fusion protein. However the toxicity profile of different combinations of H-AFt alone with H-AFt-fusion proteins were determined against the SKBR3 and MDA-MB 231 cell lines as the H-AFt-fusion protein was quite toxic. This experiment was carried out in collaboration with a PhD student M. Zygouropoulou under the supervision of the author. Results are shown in appendix II.

From the results obtained it was observed that the different combinations of H-AFt alone with H-AFt-fusion proteins were not as potent compared to the H-AFt-fusion protein which comprises a targeting protein fused to each subunit of the H-AFt, against the SKBR3 cell line. Hence, all experiments were carried out with the H-AFt-fusion protein which had targeting proteins fused to each subunit of H-AFt.

As expected, H-AFt and L-AFt by themselves did not show good potency against the SKBR3 cell line. H-AFt only was slightly more potent than L-AFt possibly as a consequence of H-AFt being up taken more readily by the cells compared to L-AFt. Trastuzumab demonstrated potency against the SKBR3 cell line ($GI_{50} = 27.00$ nM), however, compared to the H-AFt-fusion protein it was slightly less potent illustrating that the H-AFt-fusion protein is more effective in the SKBR3 cell line ($GI_{50} = 18.26$ nM) ($P < 0.05$), (Figure 5.1 (a - f)). Enhanced potency of H-AFt-fusion protein relative to Trastuzumab may be related to the size of the proteins where H-AFt-fusion protein is smaller than Trastuzumab. In addition, excellent cell penetration and high affinity binding characteristics of the H-AFt-fusion protein would have been beneficial [249] [250]. Furthermore, H-AFt-fusion protein binds to a different epitope of the HER2 receptor in contrast to Trastuzumab [249]. Thus, the activity of the 2 agents could be distinct. None of the agents were highly potent against the MDA-MB 231 cell line which lacks HER2 expression compared to the SKBR3 cell line (Figure 5.1 (g-l)). Although, the MDA-MB 231 cell line was not sensitive to the fusion proteins, the H-AFt-fusion protein was slightly more potent against the MDA-MB-231 cell line compared to the L-AFt-fusion protein, a probable consequence of high expression of TfR1s on the cell surface of these cells [241]. Further, the MDA-MB 231 cell line

showed moderate levels of sensitivity towards the HER2 targeting protein compared to all other agents tested on this cell line. In contrast, MDA-MB 231 cell growth was unaffected by Trastuzumab at all observed concentrations. It should be noted that the MTT assays were carried out using different batches of the agents; hence, the GI_{50} values for each agent were slightly inconsistent which is reflected on the SDs.

5.2.2 Effects of H and L-AFt-fusion proteins, targeting protein and Trastuzumab on SKBR3 and MDA-MB 231 colony formation



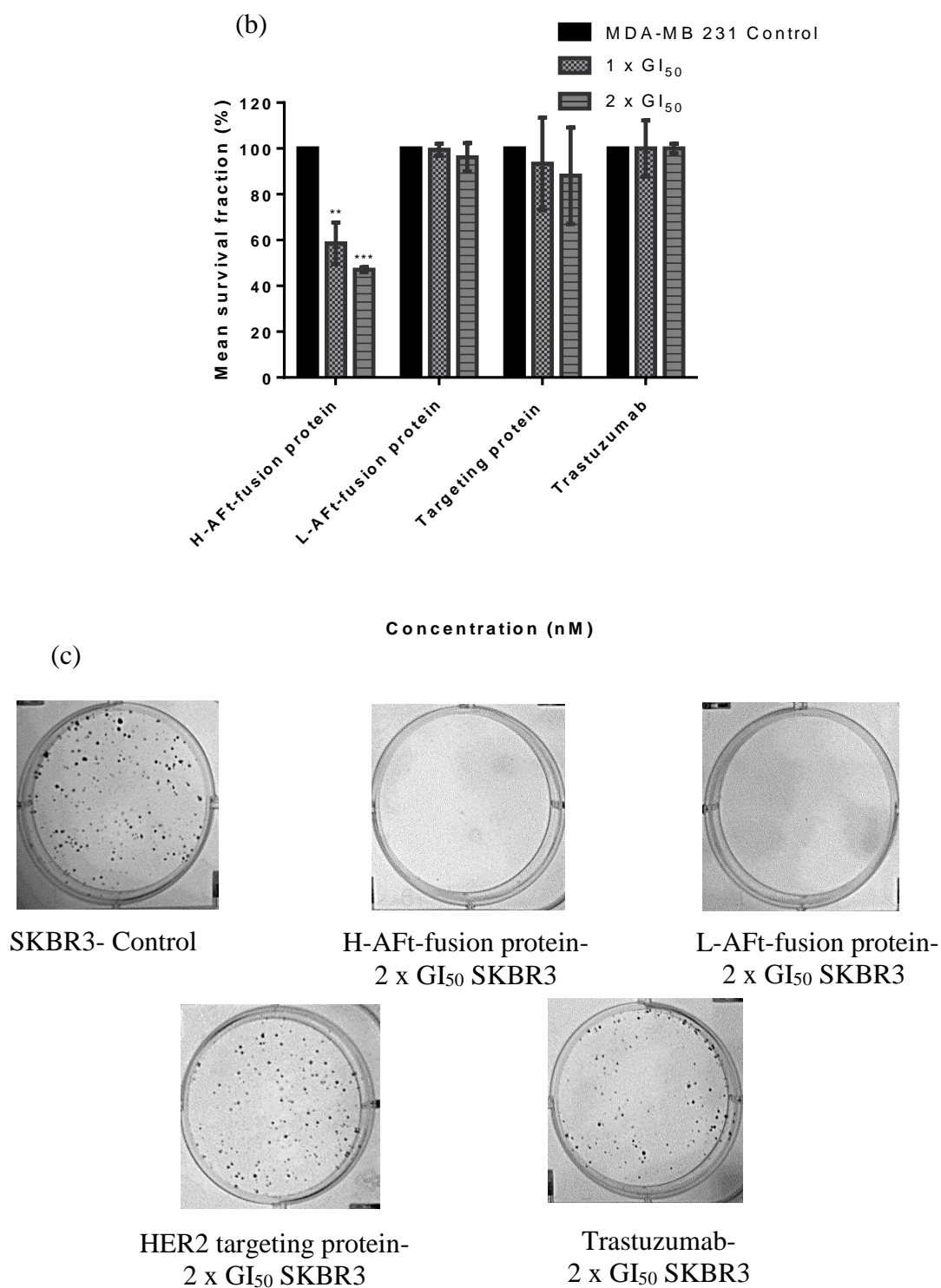


Figure 5.2: Effects of H and L-AFt-fusion proteins, targeting protein and Trastuzumab on colony formation. (a) SKBR3 (b) MDA-MB 231. (c) Representative images of colony formation after exposure to agents. Mean SF as % plating efficiency of control represented as the mean \pm SD of trials \geq 3, (n = 3 per trial). * indicates significant difference compared to control, * (P < 0.05), ** (P < 0.01), *** (P < 0.001), **** (P < 0.0001).

To analyse whether individual SKBR3 and MDA-MB 231 cells were able to retain their ability to reproduce after a short exposure (24 h) to H and L-AFt-fusion proteins, HER2 targeting protein and Trastuzumab, clonogenic assays were carried out. The results of H and L-AFt-fusion proteins were remarkable showing that SKBR3 cells were not able to meet the challenge of both H and L-AFt-fusion proteins. The SF of SKBR3 cells after exposed to 1x GI₅₀ and 2x GI₅₀ of the H-AFt-fusion protein showed no colonies after 14 days ($P < 0.0001$). Similarly, SKBR3 cells failed to form colonies after exposure to 1x and 2x GI₅₀ concentrations of L-AFt-fusion protein ($P < 0.0001$) suggesting that these agents are highly cytotoxic and that the effect is irreversible. The results for both agents against the MDA-MB 231 cell line corroborated the results of the MTT assays; H-AFt-fusion protein showed a lower SF than the L-AFt-fusion protein probably due to uptake of H-AFt by the TfR1 receptors of MDA-MB 231 cells (Figure 5.2).

Following treatment of SKBR3 cells with 1x and 2x GI₅₀ concentrations of the HER2 targeting protein, SFs of 75.44% and 61.84% respectively were obtained (compared to control; $P < 0.0001$). Although the targeting protein showed potent activity (GI₅₀ = 34.69 nM) against the SKBR3 cell line in MTT assays, it is apparent that the SKBR3 cells were able to resume growth after a brief exposure to the agent, suggesting that the HER2 targeting protein is nontoxic to cells compared to the fusion proteins. Previous research done by Lee et al, 2008, has shown similar results. They have shown that the targeting protein did not significantly affect the clonogenic survival in SKBR3 cells and that it is not toxic [249].

Interestingly Trastuzumab resulted in SFs of 85.87% and 53.57% with 1x and 2x GI₅₀ concentrations respectively (compared to control; $P < 0.0001$) indicating that the SKBR3 cells survived the brief exposure compared to the fusion proteins. MDA-MB 231 colony formation was uninhibited after exposure of cells to Trastuzumab. These results suggests that Trastuzumab is more of a cytostatic agent with moderate cytotoxic effects and also that it is highly selective to the HER2 overexpressing SKBR3 cell line. These results are consistent with *in vivo* data [55] [252].

5.2.3 Confocal microscopy imaging of SKBR3 cells treated with H-AFt-fusion protein

The H-AFt-fusion protein was shown to be the most potent agent among the 2 fusion proteins hence, the uptake of H-AFt-fusion protein by SKBR3 cells was visualised by fluorescence confocal microscopy. Strong fluorescence was observed in treated SKBR3 cells compared to control cells (Figure 5.3 (b)). After a 2 h time period, localisation of the agent was observed (Figure 5.3 (c)). After 6 h exposure, a sufficient amount of H-AFt-fusion protein had been internalised into SKBR3 cells. This could be most likely by receptor mediated endocytosis according to previous literature [131] [222] [253]. Taken together these results indicate that a short exposure period (2 to 6 h) is sufficient for H-AFt-fusion protein to recognise and bind to HER2 receptors on the surface of SKBR3 cells and to be internalised (Figure 5.3 (d)). It was observed that fluorescence was present in both the cytoplasm and nuclei by the superimposition of green (H-AFt-fusion protein) on blue (DAPI) staining. These results may suggest that the H-AFt-fusion protein is accessing the DNA within the nucleus. The internalisation of the agent was still detectable at 24 h (Figure 5.3 (f)). This experiment was carried out in collaboration with Dr. Lei Zhang and the author extends her appreciation.

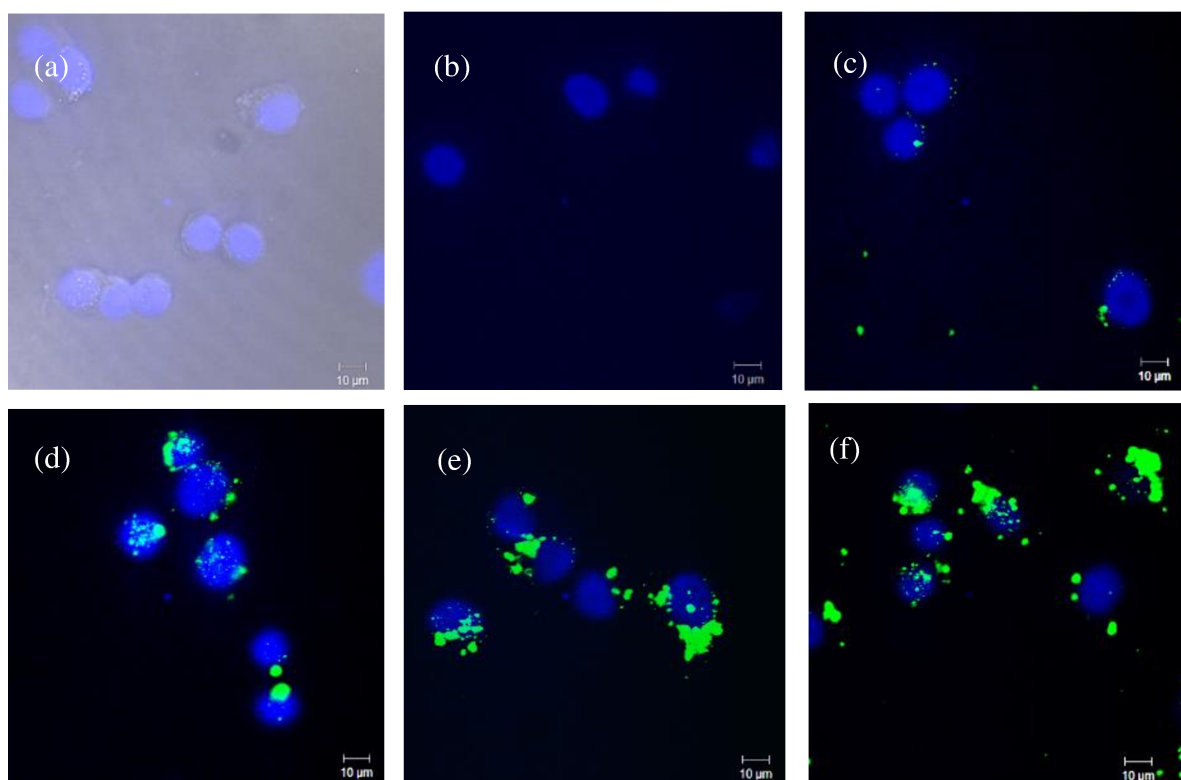


Figure 5.3: Confocal microscopy images of SKBR3 cells following exposure to H-AFt-fusion protein. SKBR3 cells were treated with 20 μ l of H-AFt-fusion protein labelled with Alexa 488 fluorophore *via* a thiol maleimide conjugation. Treated cells were exposed to 4 time points. (a) Control in bright field (b) Control (c) 2 h (d) 6 h (e) 12 h (f) 24 h. Blue – DAPI - nucleus, green - H-AFt-fusion protein. Trials \geq 3, (n = 2 per trial).

5.2.4 Effects of H and L-AFt-fusion proteins and Trastuzumab on SKBR3 and MDA-MB 231 cell cycle

It was examined whether H and L-AFt-fusion proteins and Trastuzumab treatments target specific phases of SKBR3 and MDA-MB 231 cell cycling. Both H and L-AFt-fusion proteins caused significant accumulation of events in the G1 phase relative to SKBR3 control (65.10%) after 24 h. Further it was observed that the H-AFt-fusion

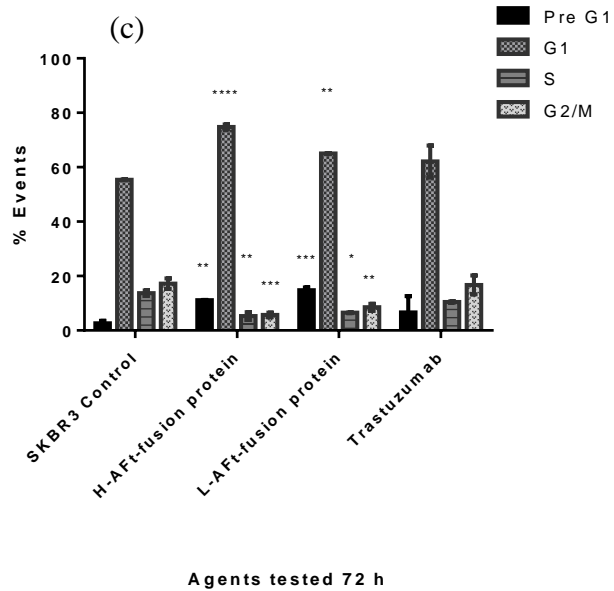
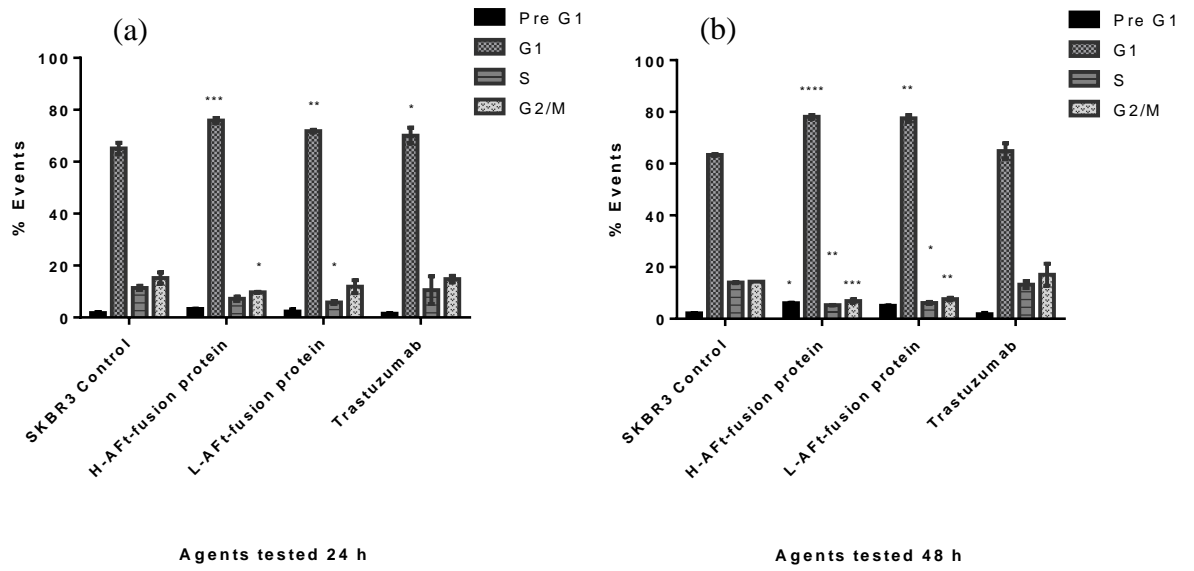
protein induced a higher accumulation in the G1 phase (75.90%) ($P < 0.001$) compared to L-AFt-fusion protein (71.79%) ($P < 0.01$). Trastuzumab also caused a significant accumulation of the G1 phase (70.08%) relative to SKBR3 control after 24 h ($P < 0.05$), which was consistent with previous research [55] (Figure 5.4 (a)).

Interestingly, 48 h exposure of SKBR3 cells to both H and L-AFt-fusion proteins, resulted in a significant increase in the G1 phase, and resulted in depleted S and G2/M phases. Moreover, the H-AFt-fusion protein induced a significant pre-G1 accumulation which is indicative of apoptotic cells (6.00%) compared to control (2.00%) ($P < 0.05$). It was observed that the H-AFt-fusion protein demonstrated a much greater effect compared to the L-AFt-fusion protein at all 3 phases at 48 h in SKBR3 cells, although the difference was not significant (Figure 5.4 (b)).

Following 72 h exposure, it was found that both H and L-AFt-fusion proteins caused significant pre-G1 accumulations (H-AFt-fusion protein 11.10% ($P < 0.01$), L-AFt-fusion protein 14.80% ($P < 0.001$) and SKBR3 control, 2.60%. Further, both fusion proteins caused an enhanced G1 peak (H-AFt-fusion protein – 74.80%; $P < 0.0001$ and L-AFt-fusion protein – 65.00%; $P < 0.01$) and reduced cell populations in S phase (H-AFt-fusion protein – 5.30%; $P < 0.01$ and L-AFt-fusion protein – 6.50%; $P < 0.05$) and G2/M phase (H-AFt-fusion protein – 5.70%; $P < 0.001$ and L-AFt-fusion protein – 8.50%; $P < 0.01$) significantly compared to SKBR3 control (G1 phase – 55.40%, S phase – 13.70% and G2/M – 17.20%) (Figure 5.4 (c)) and (Figure 5.5 (a)). It was observed that the H-AFt-fusion protein demonstrated a much greater significant effect

at the G1 phase $P < 0.0001$ and G2/M phase $P < 0.05$ compared to the L-AFt-fusion protein at 72 h.

In contrast, MDA-MB 231 cells were resistant to both H and L-AFt-fusion proteins and did not display cell cycle perturbations compared to the untreated cells at all 3 time points (Figure 5.4 (d, e and f)) and (Figure 5.5 (b)). Trastuzumab did not demonstrate a significant accumulation of the pre-G1 phase or a significant depleted S and G2/M phase compared to the H-AFt and L-AFt fusion proteins at all investigated time points against the SKBR3 cell line (Figure 5.4 (a, b and c)) and (Figure 5.5 (a)). Similar to the results obtained for the fusion proteins, the MDA-MB 231 cell line was mostly resistant towards Trastuzumab, however this agent showed a significant enhanced G1 peak in MDA-MB 231 cells at 24 h ($P < 0.01$) and 48 h ($P < 0.05$).



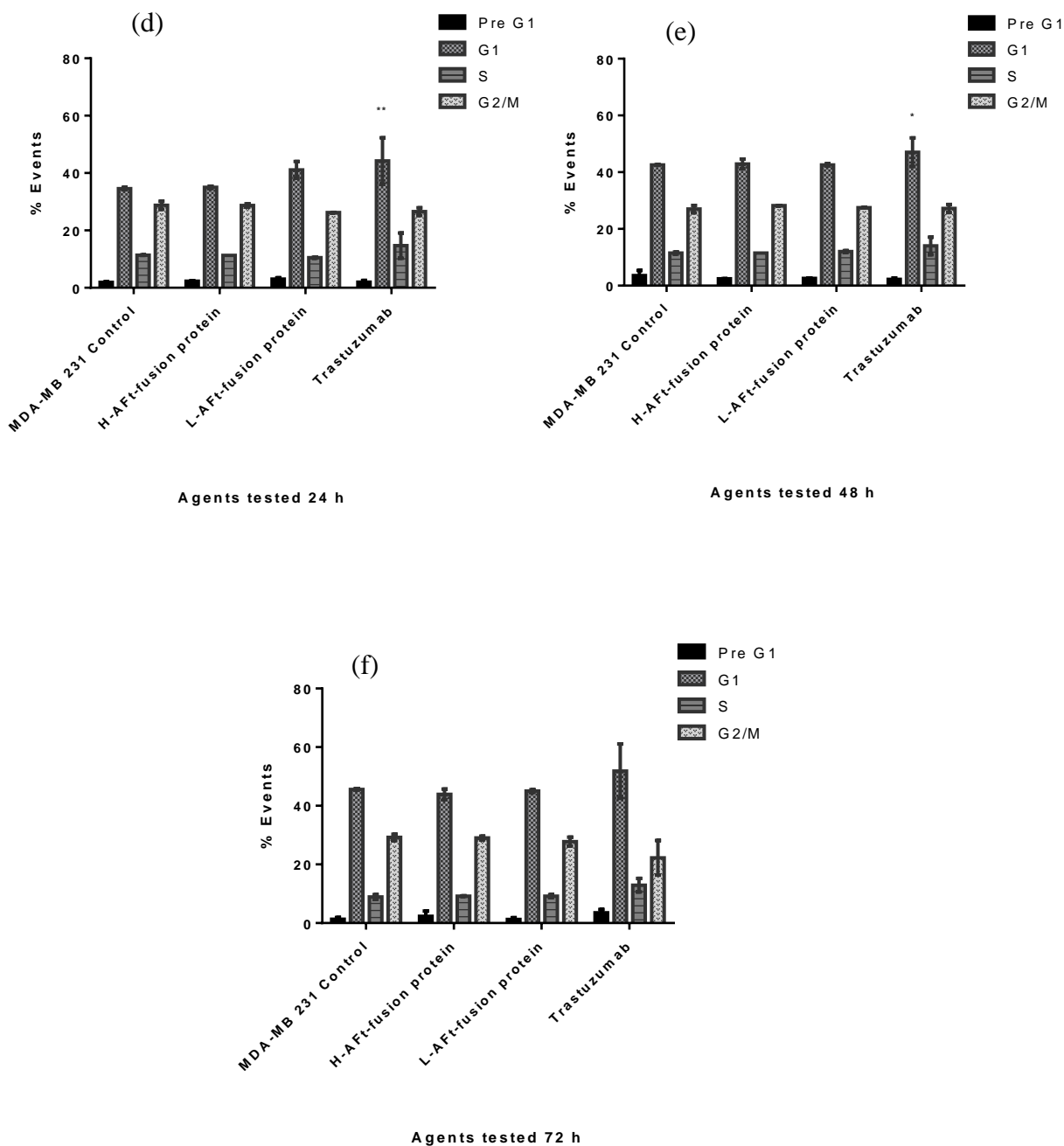
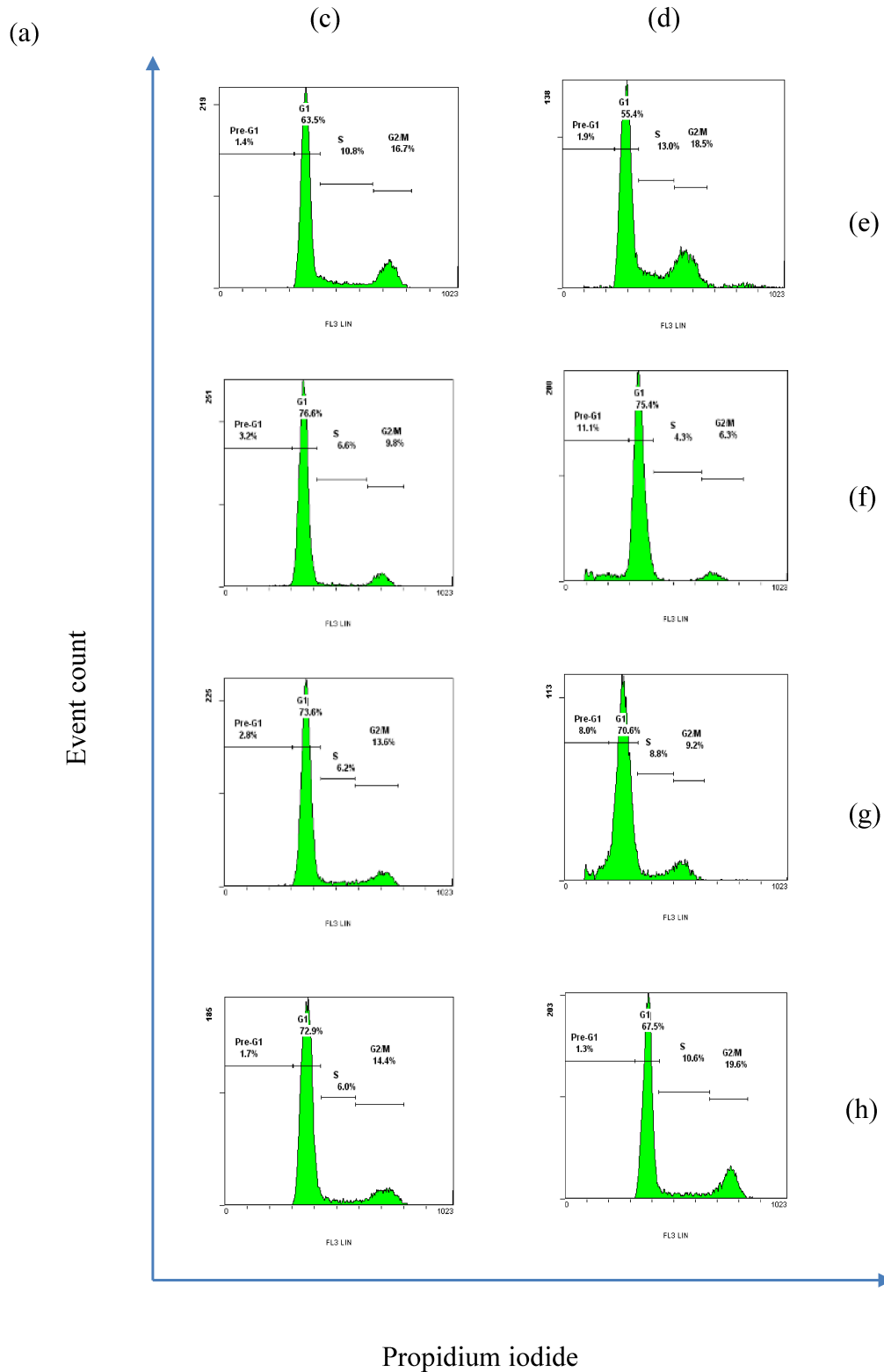


Figure 5.4: Effects of H-AFt-fusion protein, L-AFt-fusion protein and Trastuzumab on SKBR3 and MDA-MB 231 cell cycle. (a, b, c)- SKBR3 and (d, e, f)- MDA-MB 231 cells were treated with 2x GI₅₀ concentrations of these agents for 3 time points 24, 48 and 72 h. Mean and SD of trials ≥ 3 , (n = 2 per trial). * indicates significant difference compared to control, * (P < 0.05), ** (P < 0.01), *** (P < 0.001), **** (P < 0.0001).



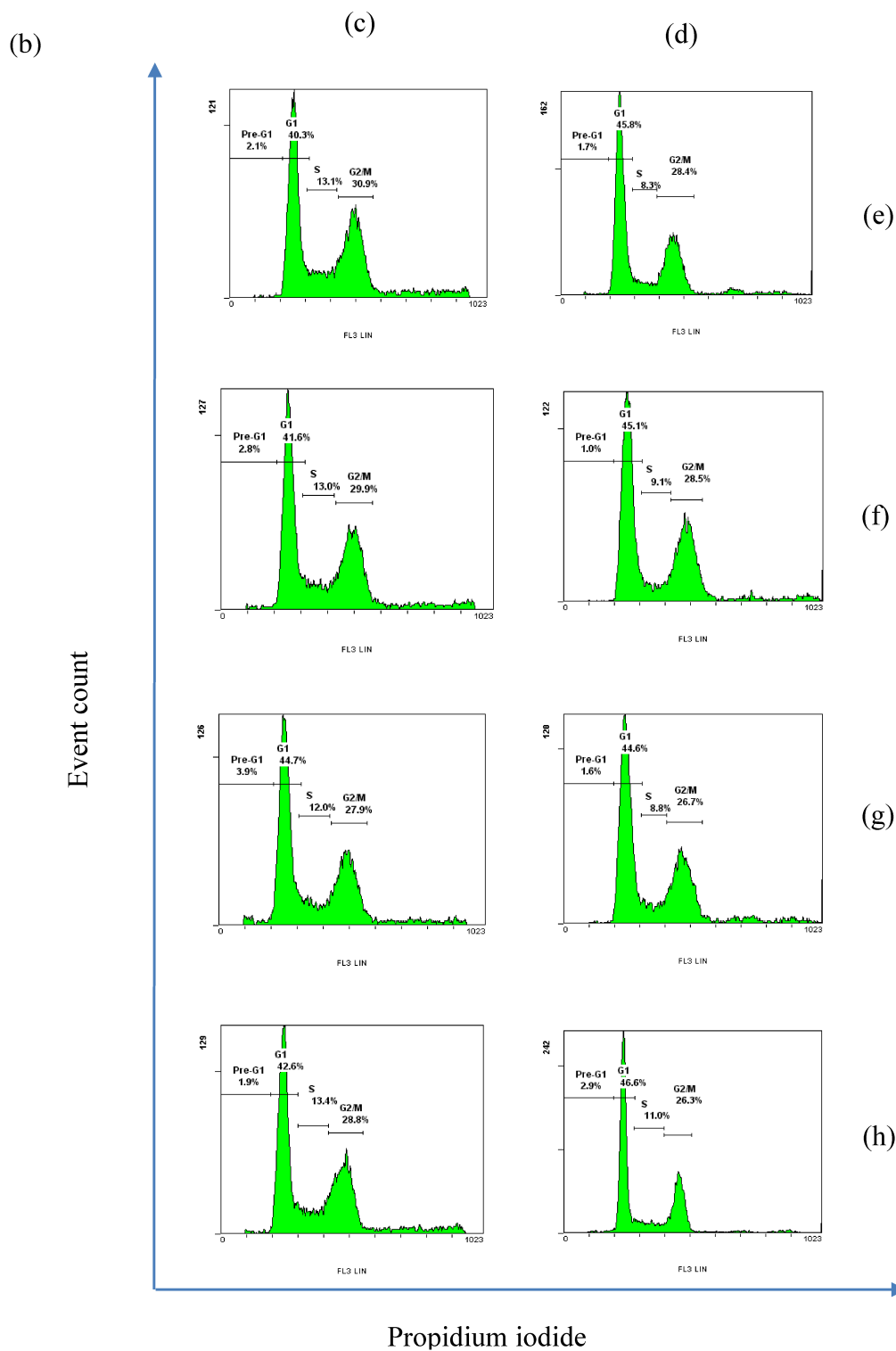


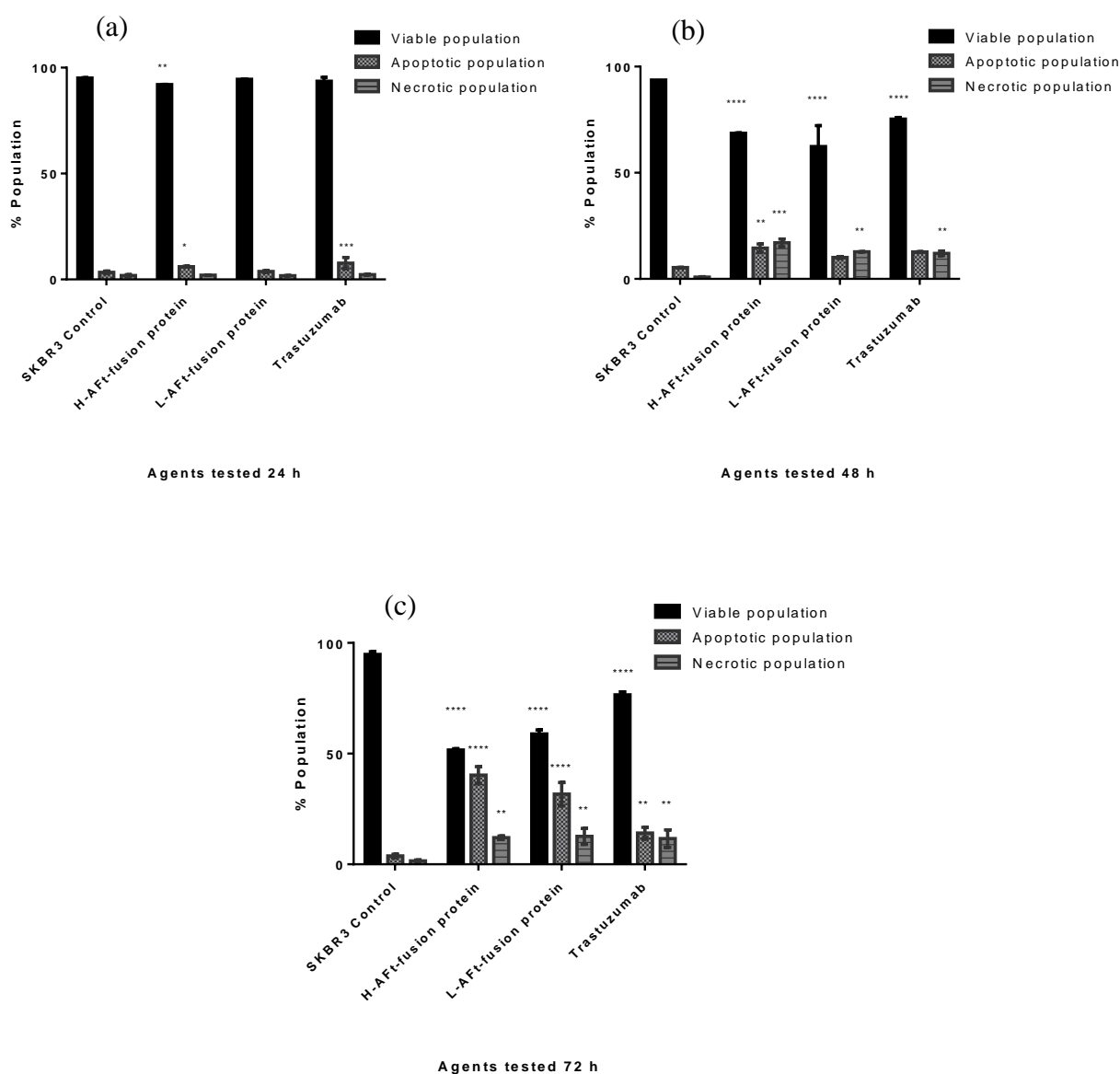
Figure 5.5: Representative cell cycle histograms of cells treated with HER2 targeting agents (a) SKBR3, (b) MDA-MB 231 cells. Cells were treated with 2x GI_{50} concentrations of these agents, (c) 24 h, (d) 72 h, (e) Control, (f) H-AFt-fusion protein, (g) L-AFt-fusion protein and (h) Trastuzumab. These are representative histograms, 15,000 events were analysed in each experiment.

From the results obtained it is evident that the H-AFt-fusion protein induced significant SKBR3 G1 accumulations at all 3 time points investigated. In addition, this agent showed a depleted S and a G2/M phase at 48 and 72 h. The L-AFt-fusion protein also showed similar results although not as significant as the H-AFt-fusion protein. This effect may suggest that the H-AFt-fusion protein blocks cells in the G1 phase or in the G1/S transition phase and selectively inhibits cells that are actively proliferating in the S phase probably by manipulating their DNA since it was observed that the H-AFt-fusion protein was stained within the nucleus in the confocal microscopy images. Previous literature has shown that cytosolic signalling activates different genes and how small differences in signal strength can generate qualitative differences in gene expression. Thus, inhibition of signalling pathways may inhibit gene transcription [254]. Indeed, as discussed in section 5.2.6, it was observed that the H-AFt-fusion protein inhibited signalling pathways that would have resulted in a reduced orchestration of cell cycle events that causes reduced cell proliferation. Further, the results reveal that both fusion proteins were able to induce a marked increase in pre-G1 phase events. The pre-G1 phase is indicative of apoptosis and it shows that SKBR3 cells are susceptible to H-AFt-fusion protein induced cytotoxicity [255]. Furthermore, the SKBR3 cell line expresses mutant *TP53*, which may allow abnormal proliferation [209] [256]. Thus, these results suggest that H-AFt-fusion protein is able to overcome *TP53* mutant mechanisms in SKBR3 cells by inhibiting abnormal proliferation in SKBR3 cells. Trastuzumab was only able to cause G1 accumulations in cells and it is shown to be associated with increased p27^{kip1} levels [55]. It has been demonstrated previously that anti-HER2 monoclonal antibodies exert inhibitory effects on HER2 overexpressing breast cancers by enhancing levels of p27^{kip1} causing proliferating cells

to exit from the cell cycle [257]. Further, investigations are warranted to determine whether the H-AFt-fusion protein possesses a similar mechanism within the cell cycle.

5.2.5 Effects of H and L-AFt fusion proteins, targeting protein and Trastuzumab on SKBR3 and MDA-MB 231 cellular apoptosis

In order to identify whether the agents described in this chapter induced cell death following treatment, an annexin V-FITC/PI assay was carried out.



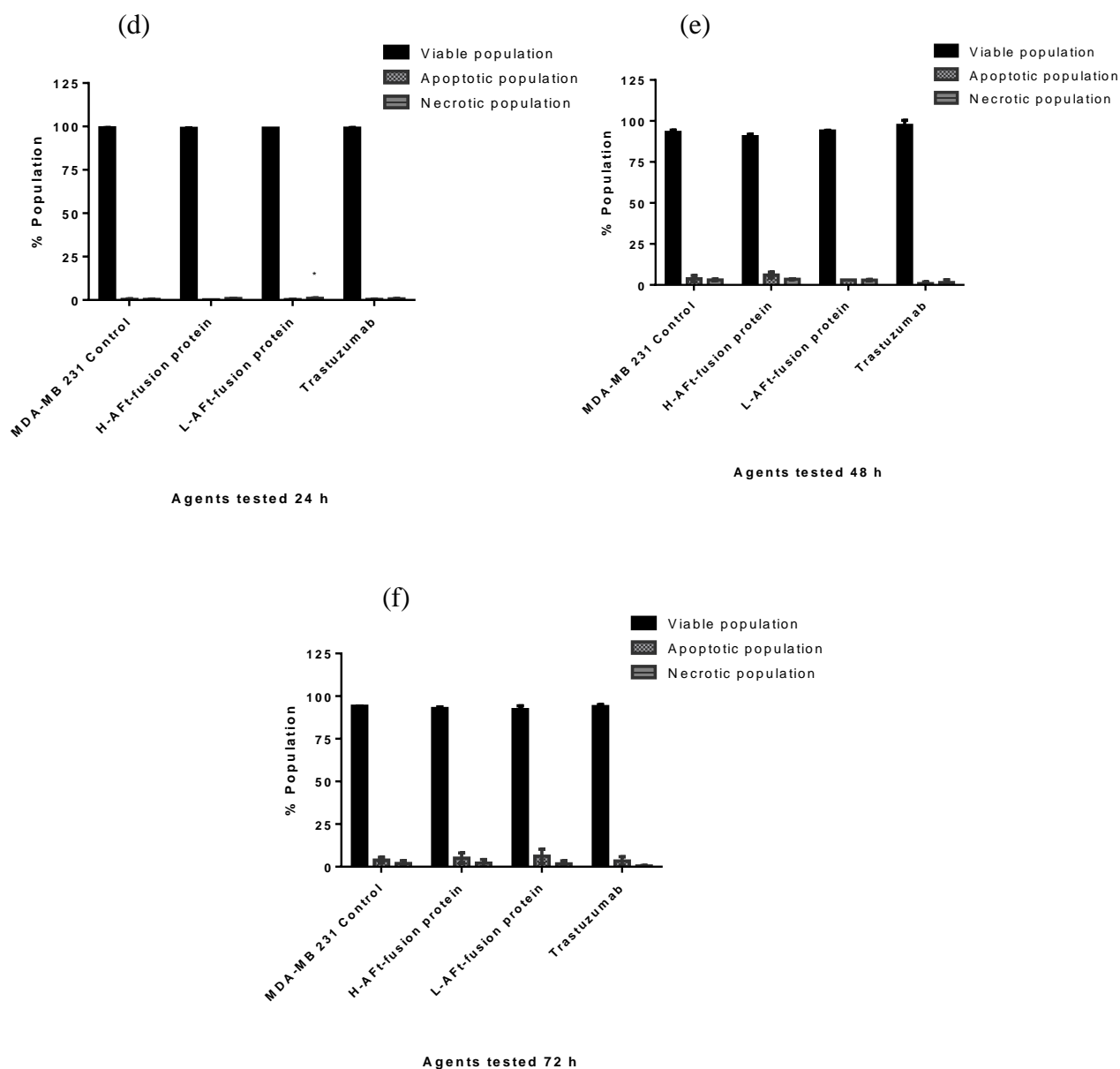
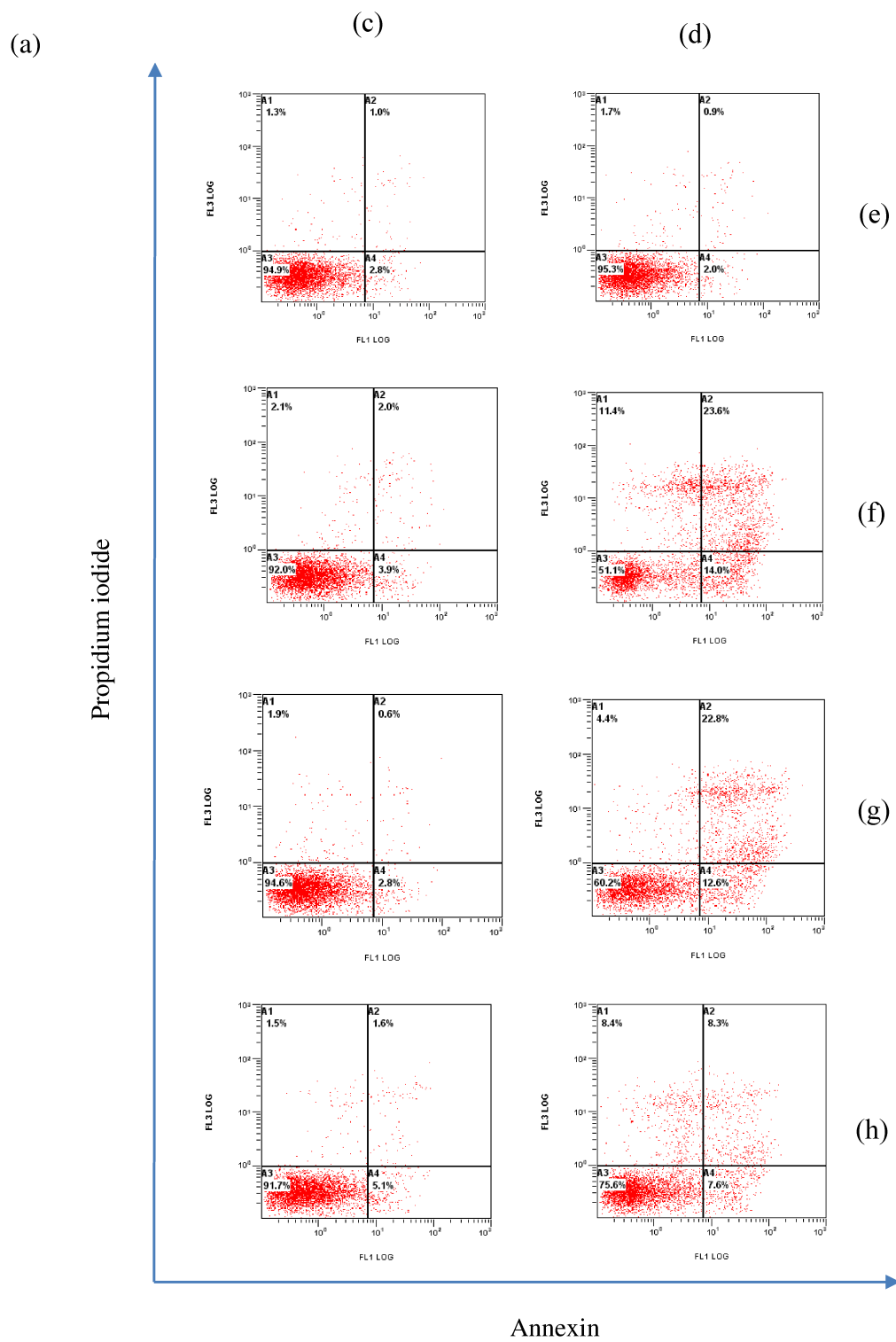


Figure 5.6: Effects of H-AFt-fusion protein, L-AFt-fusion protein and Trastuzumab on SKBR3 and MDA-MB 231 cellular apoptosis. (a, b, c)- SKBR3 and (d, e, f)- MDA-MB 231 cells were treated with 2 x GI_{50} concentrations of these agents for 3 time points 24, 48 and 72 h. Mean and SD of trials ≥ 3 , (n = 2 per trial). * indicates significant difference compared to control, * ($P < 0.05$), ** ($P < 0.01$), *** ($P < 0.001$), **** ($P < 0.0001$).



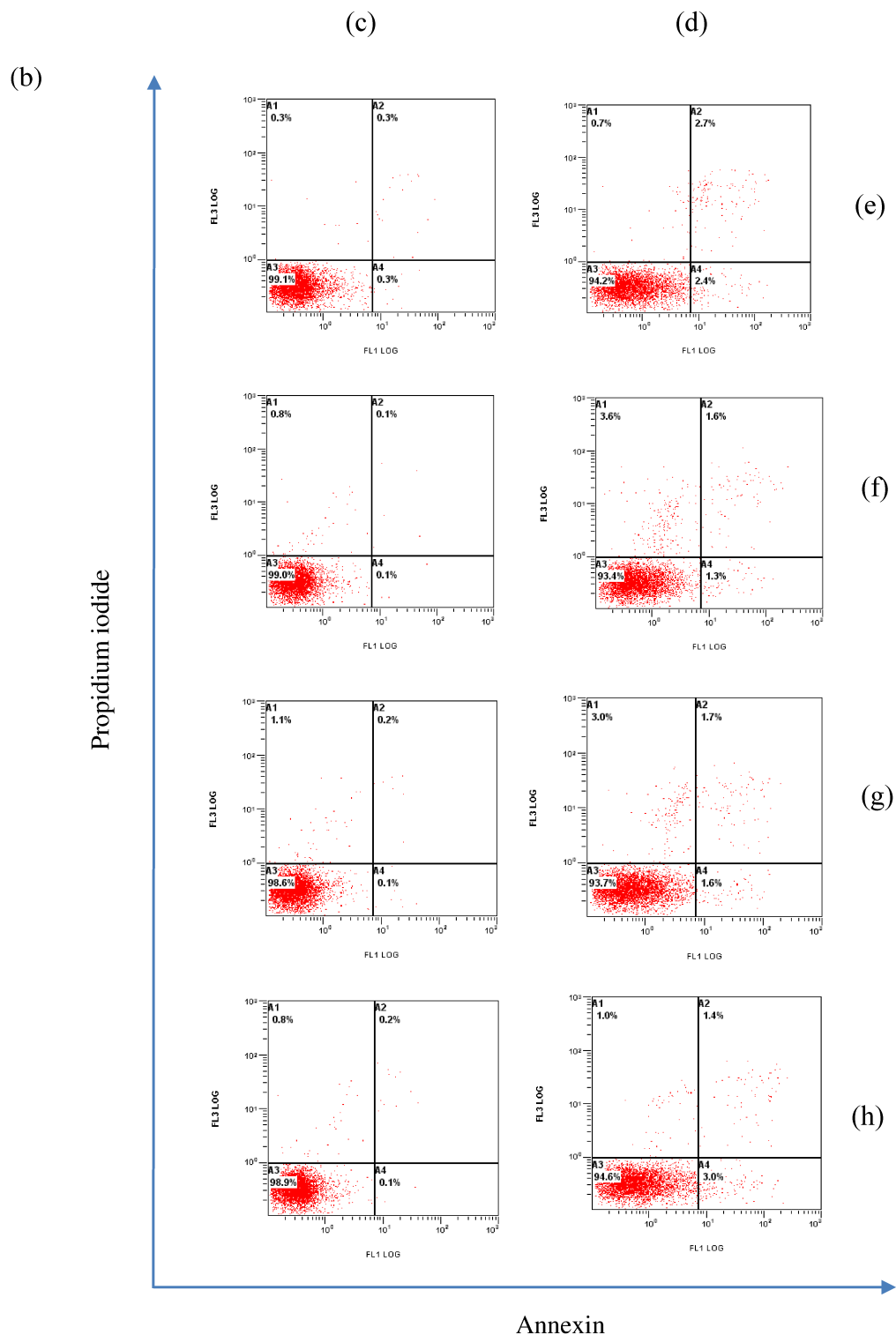


Figure 5.7: Representative apoptotic quadrant plots of cells treated with HER2 targeting agents (a) SKBR3, (b) MDA-MB 231 cells. (c) Control, (d) H-AFt-fusion protein, (e) L-AFt-fusion protein and (f) Trastuzumab. Cells were treated with 2x GI₅₀ concentrations of these agents, (c) 24 h, (d) 72 h, (e) Control, (f) H-AFt-fusion protein, (g) L-AFt-fusion protein and (h) Trastuzumab. These are representative quadrant plots analysed by flow cytometry, 10,000 events were recorded for each experiment.

SKBR3 and MDA-MB 231 cells were treated with 2x GI₅₀ concentrations of the H and L-AFt-fusion proteins for a time course of 24, 48 and 72 h. Early and late apoptotic populations were summed to determine the total apoptotic population in cells following treatment. The results obtained were then compared to results obtained with Trastuzumab treatment.

H-AFt-fusion protein induced a significant apoptotic population relative to control SKBR3 cells at 24 h ($P < 0.05$). On the contrary, L-AFt-fusion protein did not induce a significant apoptotic population in SKBR3 cells in 24 h. Trastuzumab caused a significant apoptotic population in SKBR3 cells in 24 h ($P < 0.001$), (Figure 5.6 (a)). After 48 h, the H-AFt-fusion protein caused an increased apoptotic population relative to control ($P < 0.01$). All agents induced significant necrotic populations compared to control at 48 h (Figure 5.6 (b)). Interestingly, after 72 h there was a dramatic increase in the total apoptotic population in SKBR3 cells after treatment with H-AFt-fusion protein (40.30%) and L-AFt-fusion protein (31.70%) compared to control SKBR3 cells (3.75%). Out of the total apoptotic population the late apoptotic population was increased compared to the early apoptotic population ($P < 0.0001$). When SKBR3 cells were visualised microscopically following 72 h, it was observed that cells treated with these 2 novel agents showed morphological changes indicative of apoptosis. Cells were shrunk and showed cell fragmentations. At 72 h in contrast, Trastuzumab, induced a smaller apoptotic population (14.10%) compared to control SKBR3 cells ($P < 0.01$). All agents at 72 h, also caused significant necrotic populations, H-AFt-fusion protein (12.00%), L-AFt-fusion protein (12.60%), Trastuzumab (11.60%) compared to SKBR3 control (1.50%), ($P < 0.01$), (Figure 5.6 (c)) and (Figure 5.7(a)). MDA-MB 231 cells were extremely resistant to treatment and no significant apoptosis was

observed in all 3 time points with all tested agents (Figure 5.6 (d, e and f)) and (Figure 5.7 (b)).

From the results, it was observed that H and L-AFt-fusion proteins induced apoptosis and necrosis and that the H-AFt-fusion protein was more toxic than the L-AFt-fusion protein causing increased apoptosis. SKBR3 cells progressed to apoptosis and also necrosis at 72 h. These results confirmed the results of the cell cycle analysis which showed a stark pre-G1 accumulation at 72 h which is indicative of apoptotic cells.

In the current study, it was observed by Western blots that SKBR3 cells treated with 2x GI₅₀ of H-AFt-fusion protein down-regulated total PARP at 24 h (Figure 5.12). In addition, protein microarray analyses (section 5.2.7) following 24, 48 and 72 h exposure of SKBR3 cells to H-AFt-fusion protein confirmed these results obtained for PARP expression levels. These results may imply that the H-AFt-fusion protein may activate apoptotic pathways at an earlier time point than 24 h and the level of PARP may be reduced due to post-apoptotic degradation; and activating secondary necrosis afterwards [258]. Certainly, it has been shown that cell death occurs by alternative methods and more than one apoptotic cascade may be activated at the same time [208]. One of the main methods of cell death in the case of H-AFt-fusion proteins is necrosis, as a high percentage of necrosis was observed in this investigation. This could be secondary necrosis taking place. However, it has been shown that programmed necrosis can also participate in cell killing when apoptotic pathways are abrogated [259]. Furthermore, it was observed by Western blotting that the H-AFt-fusion protein is able to down-regulate proteins of the RAS/MAPK, PI3K/AKT and JAK/STAT pathways by direct blockade of the HER2 receptor. Inhibition of proteins of these anti-

apoptotic pathways sensitises SKBR3 cells to apoptosis [248]. Trastuzumab also caused apoptosis in SKBR3 cells and it has been previously shown that Trastuzumab is able to mediate apoptosis by inhibiting the PI3K/AKT signalling pathway. Further, Trastuzumab is able to mediate apoptosis by inhibiting cellular DNA repair mechanisms and by antibody dependent cellular cytotoxicity *in vivo* [55]. As future studies, it would be interesting to determine whether the H-AFt-fusion protein possesses a similar mechanism.

5.2.6 Effects of H-AFt-fusion protein, targeting protein and Trastuzumab on HER2/P-HER2, RAS/MAPK, PI3K/AKT and JAK/STAT signalling pathways and PARP in SKBR3 and MDA-MB 231 cells by Western blotting

SKBR3 and the MDA-MB 231 cells had been treated with H-AFt-fusion protein, targeting protein and Trastuzumab for 24 h by 1x and 2x GI_{50} concentrations. Following treatment both cell lines were examined for protein expression levels of HER2, P-HER2 and for the expression levels of key proteins of RAS/MAPK, PI3K/AKT and JAK/STAT pathways. Initially, it was found that HER2 and P-HER2 expression was significantly reduced in SKBR3 cells after treating the cells with H-AFt-fusion protein ($P < 0.0001$) (HER2 - ARD - 1x GI_{50} – 22.88% and 2x GI_{50} – 8.99% and P-HER2 - ARD - 1x GI_{50} – 76.41% and 2x GI_{50} – 19.02% compared to SKBR3 control). In contrast, it was observed that the targeting protein was not able to decrease HER2 or P-HER2 protein expression levels in SKBR3 cells. Further, HER2 expression levels were not decreased in response to Trastuzumab, however P-HER2 expression levels were slightly reduced ($P < 0.05$) (Figure 5.8) and (Figure 5.9 (a) and (b)).

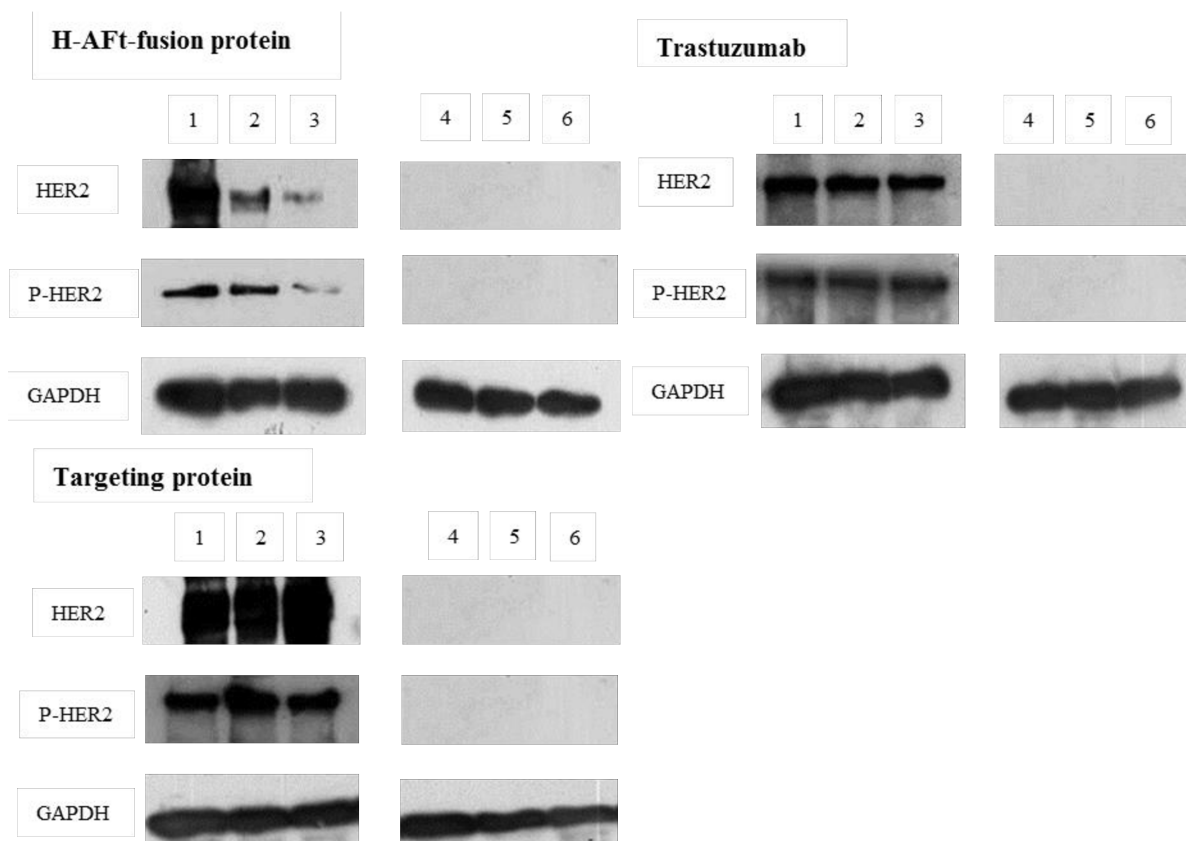


Figure 5.8: Western blot analysis of HER2 and P-HER2 following exposure of SKBR3 and MDA-MB 231 cells to H-AFt-fusion protein, Trastuzumab and targeting protein. HER2, P-HER2 (185 kDa) and GAPDH (37 kDa). GAPDH was probed as a loading control and adjusted relative densities (ARD) were calculated. (1) SKBR3 control, (2) 1x GI₅₀, (3) 2x GI₅₀, (4) MDA-MB 231 control, (5) 1x GI₅₀, (6) 2x GI₅₀. Representative blots are shown; experiments were conducted ≥ 3 times. SKBR3 and MDA-MB 231 whole cell protein lysates (50 μ g) were subjected to 10% SDS-polyacrylamide gel electrophoresis.

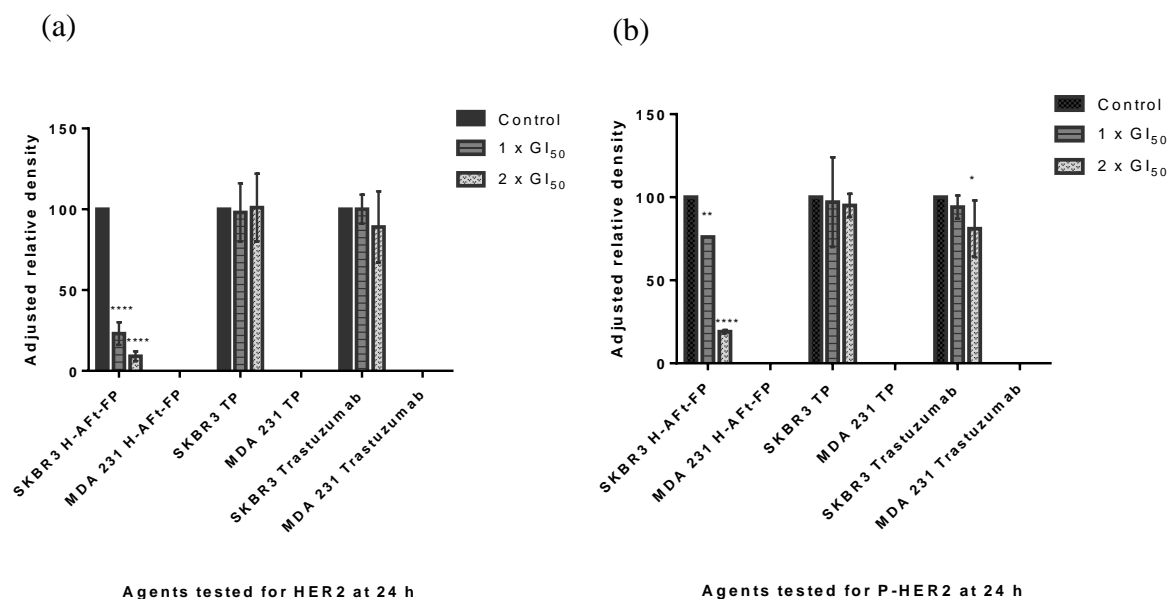


Figure 5.9: ARD levels for HER2 and P-HER2 of HER2 targeting agents. (a) HER2 and (b) P-HER2 expression levels in SKBR3 and MDA-MB 231 cells. Cells were treated with H-AFt-fusion protein, targeting protein or Trastuzumab for 24 h. Mean and SD of trials ≥ 3 . * indicates significant difference compared to control, * ($P < 0.05$), ** ($P < 0.01$), *** ($P < 0.001$), **** ($P < 0.0001$).

Previous research has shown that some anti-HER2 monoclonal antibodies are able to reduce the amount of total HER2 receptor expressed on the cell surface [260]. H-AFt-fusion protein decreased the levels of total HER2. This may be a result of accelerated internalisation of the H-AFt-fusion protein after binding to cell surface HER2 receptors by endocytosis followed by intracellular routing to lysosomes where degradation occurs [261]. Further, suppression of HER2 receptor levels will further reduce homodimerisation and heterodimerisation of HER receptors which in turn will reduce phosphorylation levels [49]. However, the amount of phosphorylation observed in this study was not as low as the amount of total HER2 in response to H-AFt-fusion protein treatment. This could be due to certain amount of dimerisation and

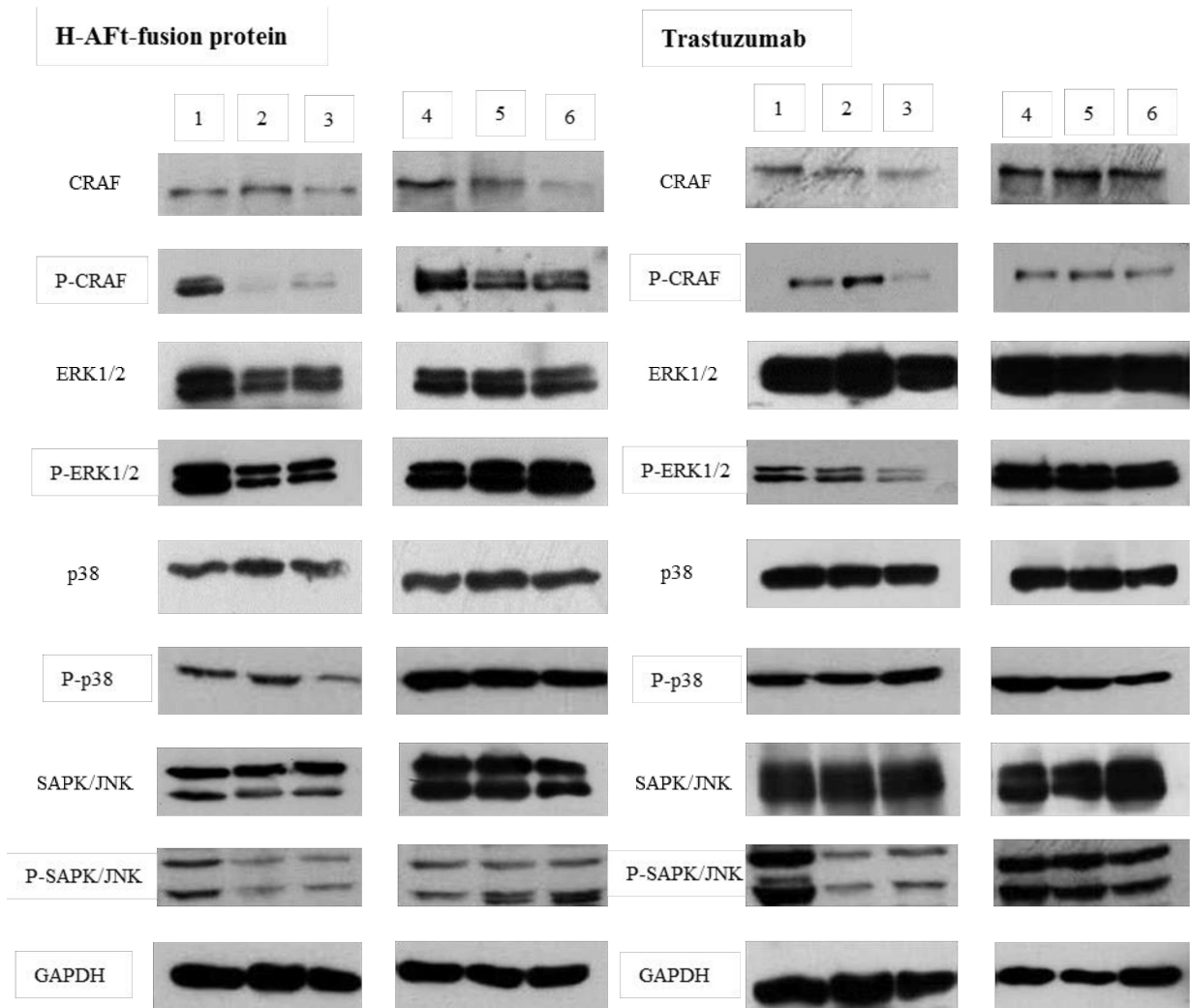
subsequent autophosphorylation. Nevertheless, down-regulation of downstream pathways were observed in SKBR3 cells after exposure to H-AFt-fusion protein which is discussed below.

In contrary, the targeting protein did not show any alterations of total and phosphorylated HER2 levels which was expected as it was merely used as a targeting molecule. Further, complying with the results of this study, previously it has been shown that total HER2 receptor levels were unchanged in SKBR3 cells and that phosphorylation of HER2 was inhibited slightly by Trastuzumab treatment and the efficacy of this agent is largely related to down-regulation of the PI3K/AKT pathway and inducing an immune response [103] [262].

Next, the protein expression levels of some of the key proteins of the RAS/MAPK pathway was investigated following exposure with the agents mentioned above. It was observed that both total CRAF (ARD – 50.95%) and P-CRAF (Ser259) (ARD - 10.88%) and similarly total ERK1/2 (ARD - 76.99%) and P-ERK1/2 (ARD – 51.60%) of the RAS/MAPK pathway were extremely suppressed in SKBR3 cells following treatment with 2x GI₅₀ of H-AFt-fusion protein compared to SKBR3 control (P < 0.0001). Phosphorylation at Ser259 of CRAF (ARD – 14.54%) and ERK 1/2 (ARD – 65.61%) was significantly reduced with 1x GI₅₀ of H-AFt-fusion protein as well (P < 0.0001). In comparison, the targeting protein did not cause significant perturbations in the phosphorylated forms of the same proteins. Nonetheless, significant down-regulation of total CRAF after exposure to 2x GI₅₀ targeting protein was observed (ARD – 42.43%) (P < 0.0001). Trastuzumab (2x GI₅₀) showed similar results to the H-AFt-fusion protein, where all 4 proteins of the RAS/MAPK pathway investigated

showed significant depletion. Conversely, a lower concentration of Trastuzumab (1x GI₅₀) did not cause significant down-regulation compared to H-AFt-fusion protein. Protein expression in MDA-MB 231 cells was not significantly affected other than total CRAF following exposure to 2x GI₅₀ H-AFt-fusion protein (P < 0.001).

It was also found that H-AFt-fusion protein (2x GI₅₀ concentrations) down-regulated phosphorylated levels of p38 (Thr180/Tyr182) (ARD – 55.02%) (P < 0.0001). Furthermore, it down-modulated P-SAPK/JNK (Thr183/Tyr185) at both 1x and 2x GI₅₀ concentrations in SKBR3 cells (ARD – 44.61% and 37.55% respectively) (P < 0.001). Trastuzumab did not perturb P-p38 (Thr180/Tyr182) but inhibited P-SAPK/JNK (Thr183/Tyr185) significantly in SKBR3 cells (P < 0.01). Targeting protein alone did not cause any perturbations in these proteins (Figure 5.10). Densitometry analysis with the ARD values for the significant results are shown in appendix I under section 9.1.2.1.



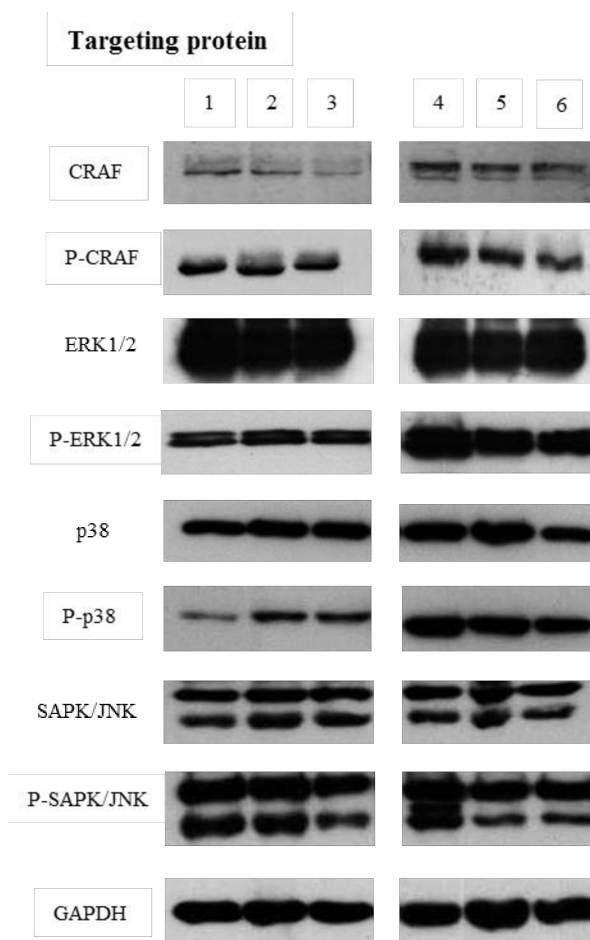


Figure 5.10: Western blot analysis of RAS/MAPK pathway following exposure of SKBR3 and MDA-MB 231 cells to H-AFt-fusion protein, Trastuzumab and targeting protein. CRAF, P-CRAF (74kDa), ERK 1/2, P-ERK 1/2 (44 and 42 kDa), p38, P-p38 (43 kDa), SAPK/JNK, P-SAPK/JNK (46 and 54 kDa) and GAPDH (37 kDa). GAPDH was probed as a loading control and adjusted relative densities (ARD) were calculated. (1) SKBR3 control, (2) 1x GI₅₀, (3) 2 x GI₅₀, (4) MDA-MB 231 control, (5) 1 x GI₅₀, (6) 2 x GI₅₀. SKBR3 and MDA-MB 231 whole cell protein lysates (50 μg) were subjected to 10% SDS-polyacrylamide gel electrophoresis.

CRAF is one of the 3 RAF members of the RAS/MAPK pathway, and CRAF is the major mediator of RAS activity in this pathway [63] [263]. Thus, it was interesting to observe that the H-AFt-fusion protein was able to abolish phosphorylation of CRAF (Ser259) and also reduce total levels of CRAF remarkably which would result in a

reduced active form. It was also observed that protein expression levels of ERK1/2 which in turn is phosphorylated by MEK were also down-modulated in this study, nevertheless the measured levels of total and phosphorylated ERK1/2 were higher than that observed for CRAF and P-CRAF. Although the RAF–MEK–ERK cascade is typically drawn as a linear cascade of protein kinases, it is actually a key core component of a complex signalling network, with many other interactions as mentioned before. As such, different alternations of protein expression levels could be expected. Further, in line with previous research it was found that Trastuzumab inhibited phosphorylation of CRAF and ERK at 2x GI₅₀ concentrations [116] [135].

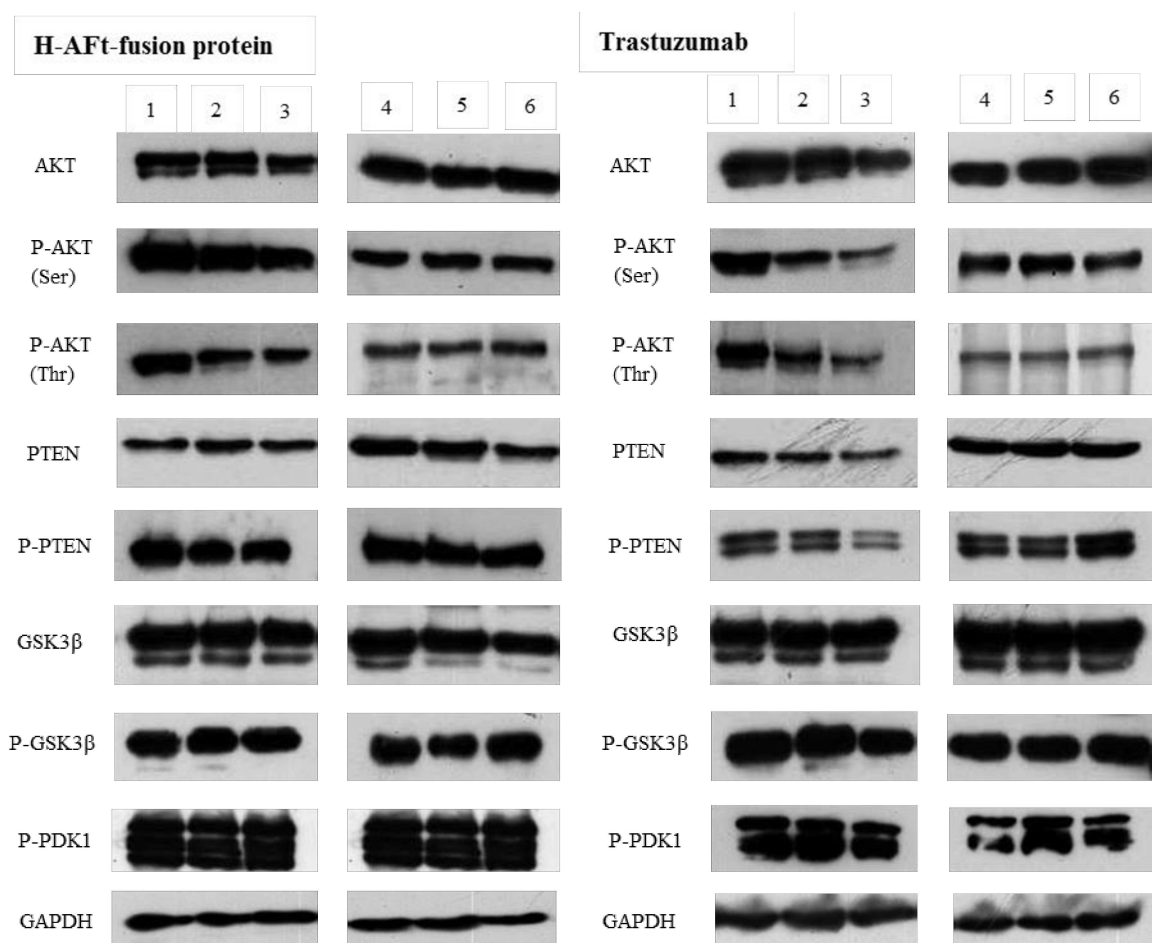
H-AFt-fusion protein caused suppression of phosphorylation of p38 and SAPK/JNK but not the total protein expression levels. Donnelly et al, 2014, has shown increased phosphorylation of p38 in the RAS/MAPK pathway was associated with acquired resistance to Trastuzumab and that inhibition of p38 rescued Trastuzumab sensitivity in cells with acquired resistance. Thus, reduction in phosphorylation of p38 may enhance the effect of the H-AFt-fusion protein. However, controversies exist regarding the activity of this pathway and regulation of this pathway may involve many upstream and downstream signals that will coordinate cellular processes such as cell growth, apoptosis and survival [67]. Thus, more investigations are warranted to find out the exact function of p38 in cells treated with H-AFt-fusion protein.

As far as the role of SAPK/JNK is concerned, debates exist over its precise function in cell proliferation and apoptosis. Thus, this pathway has been shown to have a pro-apoptotic and an anti-apoptotic role or a neutral role depending on the stimuli [65]

[66]. In the current investigation, inhibition of P-SAPK/JNK was observed in SKBR3 cells exposed to H-AFt-fusion protein. Similar results were observed in response to Trastuzumab as well. Previously, Dokmanovic et al, 2009, has shown that a Trastuzumab resistant SKBR3 cell line was restored by down-regulating P-ERK1/2 and P-SAPK/JNK by a Rac1 inhibitor [264]. Hence, it could be suggested that these agents are enhancing the pro-apoptotic role of SAPK/JNK in SKBR3 cells in the current study. Nevertheless, further investigations are needed to confirm the exact mechanism. The targeting protein did not affect these protein expression levels.

It was further examined whether the H-AFt-fusion protein is able to abolish protein expression levels of the PI3K/AKT pathway. It was found that P-AKT (Thr308) (ARD – 65.68%) was significantly suppressed by 2x GI₅₀ H-AFt-fusion protein (P < 0.05) compared to SKBR3 control. Although the same agent (2x GI₅₀) showed reduction in P-AKT (Ser473) and total AKT, the results were not significant. The targeting protein did not show alterations in these proteins in SKBR3 cells. However, Trastuzumab (2x GI₅₀) demonstrated significant depletion of total AKT (P < 0.05), P-AKT (Ser473) (P < 0.05) and P-AKT (Thr308) (P < 0.001) compared to SKBR3 control. Phosphorylation of PTEN (Ser380) was slightly reduced by 1x and 2x GI₅₀ concentrations of H-AFt-fusion protein (P < 0.01). Nevertheless, total PTEN protein expression was unaffected. Targeting protein did not affect the PTEN expression levels, however, it was observed that Trastuzumab also caused reduction in phosphorylated PTEN (Ser380) protein expression levels (P < 0.001). Further, total GSK 3 β , P-GSK 3 β (Ser9) and P-PDK1 (Ser241) protein levels were unaffected in SKBR3 cells by the effect of H-AFt-fusion protein and Trastuzumab. Thus, the effect

of the targeting protein on these 3 proteins on SKBR3 cells were not investigated. The PI3K/AKT protein expression levels of MDA-MB 231 cells were also unaffected following treatment with all agents tested (Figure 5.11). Densitometry analysis with the ARD values for the significant results are shown in appendix I under section 9.1.2.2.



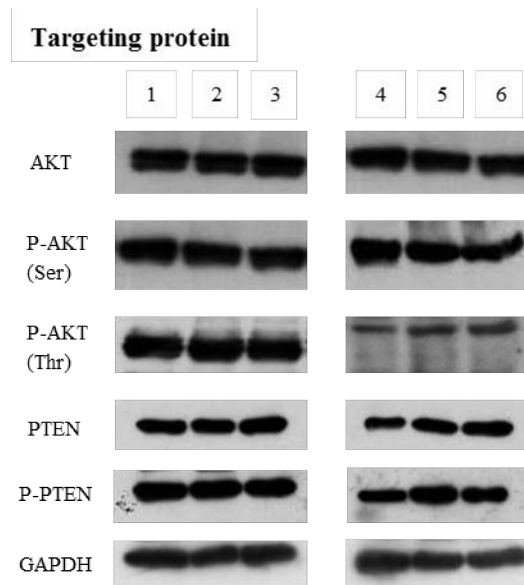


Figure 5.11: Western blot analysis of PI3K/AKT pathway following exposure of SKBR3 and MDA-MB 231 cells to H-AFt-fusion protein, Trastuzumab and targeting protein. AKT, P-AKT (Ser473), P-AKT (Thr308) (60 kDa), PTEN, P-PTEN (54 kDa), GSK3 β , P- GSK3 β (46 kDa), P-PDK1 (58-68 kDa) and GAPDH (37 kDa). GAPDH was probed as a loading control and adjusted relative densities (ARD) were calculated. (1) SKBR3 control, (2) 1x GI₅₀, (3) 2 x GI₅₀, (4) MDA-MB 231 control, (5) 1 x GI₅₀, (6) 2 x GI₅₀. Representative blots are shown; experiments were conducted ≥ 3 times. SKBR3 whole cell protein lysates (50 μ g) were subjected to 10% SDS-polyacrylamide gel electrophoresis.

Although the H-AFt-fusion protein only significantly down-regulated P-AKT (Thr308) by Western blot analysis, the results of the protein microarray experiment revealed significant down-regulation for total AKT, P-AKT (Thr308) and P-AKT (Ser473) against the SKBR3 cell line after exposed to H-AFt-fusion protein (2x GI₅₀). Reduction of total AKT levels prevents the generation of its activated phosphorylated form. Activated AKT is known to stimulate intracellular signalling in cancer and block apoptosis [265]. Thus, these results show that the H-AFt-fusion protein is able to suppress the AKT function and promote growth inhibitory effects and apoptosis against the SKBR3 cells. In concordance with previous studies, Trastuzumab reduced

both P-AKT (Thr308) and (Ser473) levels. It has been reported that as a result Trastuzumab causes accumulation of cells in the G1 phase of the cell cycle, which was observed in this study [262].

PTEN negatively regulates the PI3K/AKT pathway. Intriguingly, previous literature has shown that reduction of total PTEN and increased phosphorylation of the PTEN protein especially at Ser380 causes to lose its tumour suppressor function which is controversial to some of the other published reports [266]. Multiple phosphorylation sites of the PTEN protein has been identified such as Ser380, Thr382, and Thr383, that leads to loss of phosphatase activities or a gain of PTEN stability which may in turn result in loss of tumour suppressor function and increased cancer susceptibility. However, out of the phosphorylation sites of the PTEN protein, according to previous reports, Ser380 is the most critical for regulation of PTEN function, and this form was investigated in the current study [266]. Further, it has been shown that unphosphorylated forms of PTEN can act to down-regulate AKT activity, rather than the phosphorylated forms which may also demonstrate a suppressed form. Thus, in this regard, reduction of phosphorylation by the H-AFt-fusion protein in SKBR3 cells may be advantageous and promotes AKT down-regulation [267] [268]. P-PTEN was down-regulated significantly in SKBR3 cells after Trastuzumab treatment as well. However, prior reports have shown that loss or reduced PTEN activity caused blocked Trastuzumab mediated growth inhibition due to continuous activation of the PI3K/AKT pathway which results in resistance to the agent [55] [103]. Therefore, more investigations are warranted to state the exact mechanism of the H-AFt-fusion protein and Trastuzumab in SKBR3 cells with regards to the PTEN status in the

current study as it was observed that both agents down-regulated phosphorylated AKT.

Interestingly, 1x and 2x GI₅₀ concentrations of H-AFt-fusion protein degraded phosphorylated STAT5 (Tyr694) significantly compared to SKBR3 control (ARD – 1x GI₅₀ - 46.84% and 2x GI₅₀ - 17.42%) ($P < 0.0001$). However, phosphorylation of JAK2 (Tyr1007) in the JAK/STAT pathway was not inhibited by the H-AFt-fusion protein. Trastuzumab also evoked slight down-regulation of P-STAT5 in SKBR3 cells ($P < 0.001$) but did not deplete the protein expression levels of P-JAK2.

P-STAT5 was not detected in MDA-MB 231 cells and no significant change in the protein expression levels of MDA-MB 231 cells was detected for P-JAK2. Furthermore, it was observed that protein expression levels of PARP were depleted by both 1x ($P < 0.001$) and 2x GI₅₀ concentrations ($P < 0.0001$) of H-AFt-fusion protein and Trastuzumab ($P < 0.0001$) in SKBR3 cells. No cleaved PARP was observed in this experiment. Likewise, 2x GI₅₀ concentrations of H-AFt-fusion protein also caused down-regulation of PARP in MDA-MB 231 cells ($P < 0.0001$). Trastuzumab also induced a slight effect in MDA-MB 231 cells ($P < 0.05$). Further, the targeting protein did not cause an effect in the protein expression levels of P-STAT5 and PARP (Figure 5.12). Densitometry analysis with the ARD values for the significant results are shown in appendix I under section 9.1.2.3.

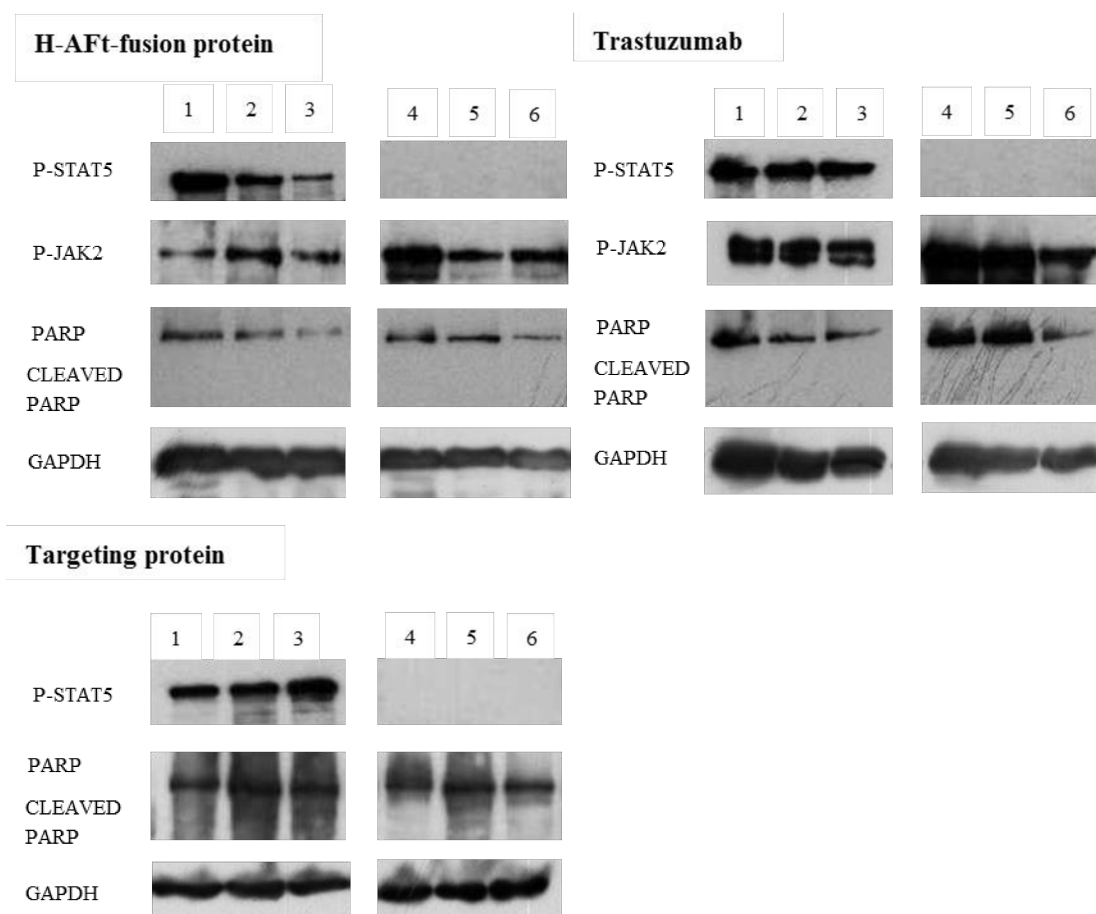


Figure 5.12: Western blot analysis of JAK/STAT pathway and PARP following exposure of SKBR3 and MDA-MB 231 cells to H-AFt-fusion protein, Trastuzumab and targeting protein. P-JAK2 (125 kDa), P-STAT5 (90 kDa), PARP (116 kDa), CLEAVED PARP (89 kDa) and GAPDH (37 kDa). GAPDH was probed as a loading control and adjusted relative densities (ARD) were calculated. (1) SKBR3 control, (2) 1x GI₅₀, (3) 2 x GI₅₀, (4) MDA-MB 231 control, (5) 1 x GI₅₀, (6) 2 x GI₅₀. Representative blots are shown; experiments were conducted ≥ 3 times. SKBR3 and MDA-MB 231 whole cell protein lysates (50 μ g) were subjected to 10% SDS-polyacrylamide gel electrophoresis.

Studies have shown that STAT5 is activated *via* JAK2 within the JAK/STAT pathway. STAT5 has been shown a prominent role in breast cancer. However, this role is found to be controversial depending on the breast cancer subtype. Thus, determining the activity of JAK2/STAT5 in HER2 overexpressing SKBR3 cells after exposure to the 3 agents was thought to be interesting [84]. It has been shown that STAT5 activity restores phosphorylated AKT and blocks cellular apoptosis, thereby off-setting the impact of cell viability [83]. Thus, reduction of P-STAT5 by the H-AFt-fusion protein and Trastuzumab may cause reduction in phosphorylated AKT thereby increasing apoptosis in SKBR3 cells. Further, as mentioned above SKBR3 cells treated with H-AFt-fusion protein and Trastuzumab showed depleted PARP activity, with no cleaved PARP identified. *TP53* loss in SKBR3 cells has shown to cause non-apoptotic cell death by impairing PARP activity. However, depleted PARP activity observed in the current study could be because of post-apoptotic degradation and secondary necrosis taking place in SKBR3 cells after exposure to H-AFt-fusion protein [258] [269].

Taken together the results of the Western blots suggest that the novel H-AFt-fusion protein is able to down-regulate most of the key proteins of all 3 pathways investigated in this study. Nonetheless, the protein expression levels tested are not isolated proteins and they all exist in the presence of other proteins and among a plethora of many signalling pathways. As such, cross talk may influence the results of this study largely.

5.2.7 Effects of H-AFt-fusion protein, targeting protein and Trastuzumab on EGFR/P-EGFR, HER2/P-HER2, HER3/P-HER3, RAS/MAPK, PI3K/AKT and JAK/STAT signalling pathways and PARP in SKBR3 and MDA-MB 231 cells by reverse phase protein microarray (RPMA)

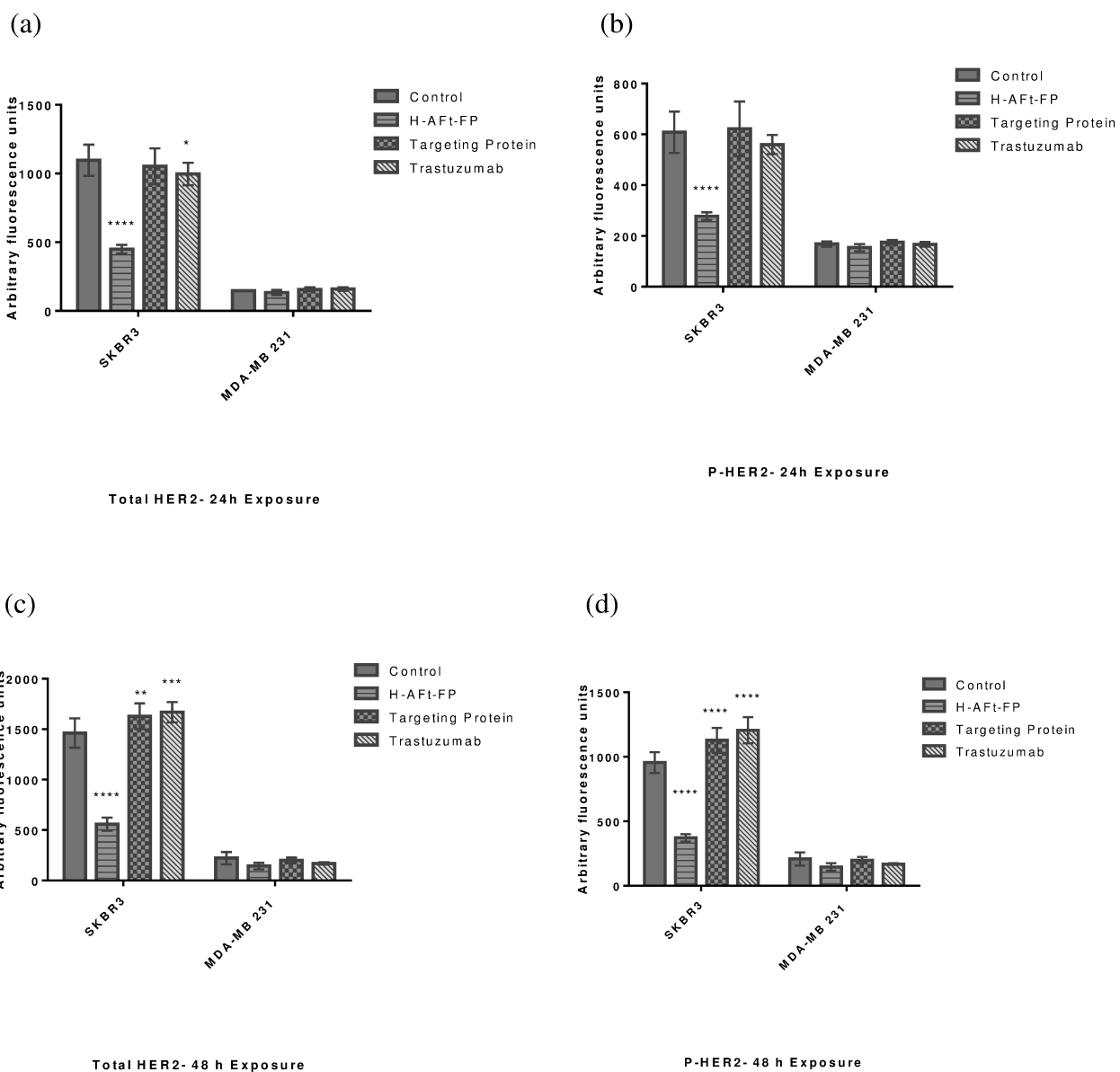
The results of the protein microarray (RPMA) strongly corroborated with the results of the Western blots. As in the above Western blot experiments, 2x GI₅₀ concentrations of H-AFt-fusion protein, targeting protein and Trastuzumab were evaluated for all protein expression levels tested in the Western blots by RPMA against SKBR3 and MDA-MB 231 cells. A time course of 24, 48 and 72 h was adopted to test the ability of all 3 agents to perturb signal transduction cascades. H-AFt-fusion protein down-regulated total HER2 and P-HER2 in SKBR3 cells significantly during the time course ($P < 0.0001$) (Figure 5.13). Protein expression levels of other HER family members; EGFR and HER3 and their phosphorylated forms were also tested after SKBR3 cells had been treated with H-AFt-fusion protein. Extremely significant down-regulation of the expression levels of P-EGFR was observed with H-AFt-fusion protein treatment at all 3 time points ($P < 0.0001$). However, total EGFR was not down-regulated. Further, both total HER3 and P-HER3 were inhibited significantly by the H-AFt-fusion protein ($P < 0.01$).

Total CRAF and P-CRAF were also down-regulated by H-AFt-fusion protein at all 3 time points in SKBR3 cells ($P < 0.05$). However, the H-AFt-fusion protein showed slight down-regulation of total and phosphorylated ERK1/2 in 24 h but surprisingly did not show inhibition of total and phosphorylated ERK1/2 in 48 and 72 h in SKBR3

cells. In fact, it showed up-regulation of P-ERK1/2 at 48 and 72 h ($P < 0.01$). In contrast, the same agent down-regulated P-p38, total SAPK/JNK and P-SAPK/JNK in SKBR3 cells at all 3 time points ($P < 0.05$). H-AFt-fusion protein was also able to perturb the PI3K/AKT pathway significantly. Total AKT, P-AKT (Thr308) and P-AKT (Ser473) were down-regulated significantly at 24 and 72 h ($P < 0.01$). However, no significance was observed at 48 h. This could be due to the large variances in the results obtained. Further, the same agent inhibited protein expression levels of P-STAT5 and PARP in SKBR3 cells significantly at all 3 time points ($P < 0.0001$). Trastuzumab elicited similar results to the H-AFt-fusion protein, however, showed significant up-regulation of HER2 and P-HER2 in 48 h, while the protein expression levels dropped at 72 h significantly ($P < 0.0001$). Trastuzumab did not cause down-regulation in HER3 and P-HER3 but showed slight down-regulation in EGFR and P-EGFR ($P < 0.05$). Further, the targeting protein was unable to cause a significant effect in this experiment. Furthermore, MDA-MB 231 cells were unaffected significantly with all tested proteins. This experiment was conducted in collaboration with Dr. Lei Zhang, Dr. Ola Negm and Dr. Paddy Tighe, and the author extends her appreciation.

EGFR, HER2 and HER3 are all implicated in the development and progression of breast cancer [270]. Indeed, it has been shown that HER receptor family members interact with each other as a highly interactive signalling group [49]. As such, these results elicit that the H-AFt-fusion protein is able to bind to HER2 and suppress its signalling capability, and in addition inhibit the function of EGFR and HER3 as well. Further, HER2/HER3 heterodimer is considered the most potent HER receptor pair with respect to strength of interaction [270]. Thus, down-regulation of HER3 and also

EGFR will prevent heterodimerisation of HER2/HER3 and HER2/EGFR which might provide promising results in the clinic. Furthermore, it has also been shown that down-regulation of HER3 results in G1 arrest of the cell cycle and decreased phosphorylation of AKT in SKBR3 cells, which further explains the results of the current study [271].



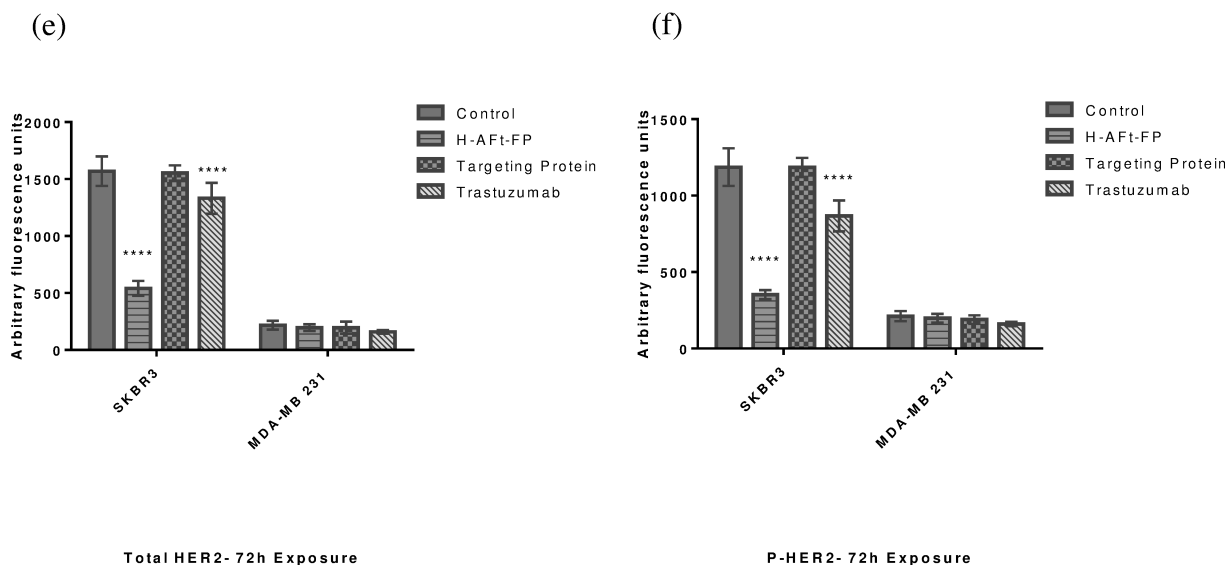


Figure 5.13: RPA analysis for HER2 and P-HER2 following exposure of SKBR3 and MDA-MB 231 cells to H-AFt-fusion protein, Trastuzumab and targeting protein. A time course was carried out (24, 48 and 72 h) to test the effect of HER2 targeting agents (H-AFt-fusion protein, Trastuzumab and targeting protein) and their ability to alter total HER2 and P-HER2 (185 kDa). β -actin (45 kDa) was probed as a loading control and normalised using RPPanalyzer. Mean and SD of trials ≥ 3 , ($n = 2$ per trial). * indicates significant difference compared to control, * ($P < 0.05$), ** ($P < 0.01$), *** ($P < 0.001$), **** ($P < 0.0001$).

5.3 Conclusion

There is a significant unmet medical need for the development of novel effective therapies that can stabilise or slow the progression of HER2+ breast cancer. In the current study, 2 novel H and L-AFt-fusion proteins targeting the HER2 receptor in breast cancer were investigated. From the results obtained, it was apparent that the H-AFt-fusion protein was potent against the HER2 overexpressing SKBR3 cell line compared to the L-AFt-fusion protein. Clonogenic assays revealed that the H-AFt-fusion protein significantly abolished SKBR3 colony formation completely which exemplified that this fusion protein is highly cytotoxic. This agent induced an

extremely significant G1 accumulation phase at all 3 time points investigated. Furthermore, the H-AFt-fusion protein induced a large apoptotic population in SKBR3 cells corroborating the cytotoxic effect it demonstrated in the clonogenic assay and also with the pre-G1 phases of the cell cycle. It has been shown that therapies leading to HER2 receptor down-regulation of its total and phosphorylation forms improve sensitivity in breast cancer cells. As such, the H-AFt-fusion protein evoked remarkable down-regulation of HER2 and P-HER2 proteins in SKBR3 cells. Protein microarray studies revealed, that the H-AFt-fusion protein is also able to down-regulate P-EGFR, HER3 and P-HER3 which may inhibit mitogenic receptor heterodimerisation. Inhibition of these receptors resulted in down-regulation of RAS/MAPK, PI3K/AKT and JAK/STAT pathways significantly thereby ultimately leading to SKBR3 apoptosis. However, further studies are warranted to understand the mechanism by which H-AFt-fusion protein alters some of the protein levels in the studied signalling pathways. Nevertheless, this agent could be a promising nanodrug for the treatment of HER2 overexpressing breast cancer in the future.

6 Chapter 6 - Agent combination studies

6.1 Introduction

Breast cancer is a multi-factorial disease and involves many activated molecular pathways that demonstrate cross talk, which in turn increases cell growth and survival [272]. Although there have been many novel therapeutics reaching the clinic, the success rate is low. This could be due to compensatory and alternative pathways that cancer cells use to thrive and gain acquired resistance to these agents [143] [272]. In order to address this issue, a combination strategy could be used. Anti-cancer agents in combination may provide better efficacy in combating breast cancer than agents alone. Agents in combination which target similar molecular pathways may provide synergistic effects. Further, agents that target different pathways may increase potency over any agent used alone and overcome resistance by reducing the activity of compensatory pathways thereby similarly resulting in synergistic effects. Furthermore, a combination strategy may also help to overcome metastatic breast cancer [143] [272]. In this setting, there would be multiple sites that need to be targeted to inhibit tumour growth, where a combinatorial approach would provide a better therapeutic effect [272].

Thus, this chapter explores concurrent inhibition of major signalling pathways pertinent to breast tumourigenesis such as EGFR, RAS/MAPK, PI3K/AKT, mTOR and AhR. The interactions of several agent combinations such as Sirolimus and

CGP57380, Raloxifene and 5F 203, Gefitinib and 5F 203 and novel dual PI3K/mTOR inhibitors alone and in combination with 5F 203 have been investigated.

Agent interactions were evaluated as, synergistic, additive or antagonistic according to the Chou and Talalay method [273] [274]. Synergism can be concluded if agent combinations demonstrate greater than the additive activity expected from each agent alone. Antagonism can be concluded if agent combination results in activity that is less than the additive activity of each agent alone [275]. The combination index (CI) theorem of Chou and Talalay quantitatively depicts synergism as $CI < 0.9$, additivity as $0.9 > CI < 1.1$, and antagonism as $CI > 1.1$ of the agent combinations. The CI values were evaluated for each cell line tested with the 2 agent combinations using the equation below. The mutually nonexclusive model was used based on the assumption that the 2 agents act through entirely different mechanisms. [Agent1] and [Agent2] were 50% inhibitory concentrations (IC_{50}) of agent 1 and agent 2 in combination. $[Agent1]_x$ and $[Agent2]_x$ were IC_{50} concentrations of agent 1 and agent 2 alone. IC_{50} concentrations were used for calculation purposes as mentioned in the Chou and Talalay, CI method [273] [274].

$$CI = \frac{[Agent1]}{[Agent1]_x} + \frac{[Agent2]}{[Agent2]_x} - \frac{[Agent1] \times [Agent2]}{[Agent1]_x \times [Agent2]_x}$$

6.2 Results and Discussion

6.2.1 Effects of Sirolimus and CGP57380 alone and in combination

6.2.1.1 *In vitro* growth inhibitory effects of Sirolimus and CGP57380 alone and in combination

It has been shown that the mTOR inhibitor, Sirolimus inhibits mRNA translation induced by mTOR which is a downstream target of the PI3K/AKT pathway [276]. Similarly CGP57380, a MNK inhibitor inhibits mRNA translation induced by the MNK kinases that act downstream of ERK and p38 of the RAS/MAPK pathway [80]. Thus, anti-proliferative effects of the 2 agents were investigated using MTT viability assays against the panel of breast cancer cell lines. The MTT results for the 2 agents tested alone are summarised in Table 6.1.

Mean GI ₅₀ ± SD (72 h MTT assays)		
Cell line	Sirolimus	CGP57380
MCF7	> 1 µM	47.38 µM ± 1.99
T47D	0.62 nM ± 0.24	9.22 µM ± 0.59
ZR-75-1	0.65 nM ± 0.17	39.51 µM ± 6.31
SKBR3	1.49 nM ± 1.02	13.32 µM ± 3.91
MDA-MB 468	3.42 nM ± 2.19	48.31 µM ± 5.31
MDA-MB 231	> 1 µM	93.59 µM ± 5.76

Table 6.1: Mean GI₅₀ ± SD values of Sirolimus and CGP57380. Cells were seeded in 96 well plates at a density of 2.5 x 10³ cells/well. After allowing time to adhere (24 h), cells were exposed to agents (72 h; n = 8). Mean and SD of trials ≥ 3.

As shown in Table 6.1, T47D and ZR-75-1, cell lines were sensitive to Sirolimus while SKBR3 and MDA-MB 468 showed moderate sensitivity. In contrast, MCF7 and

MDA-MB 231 cell lines were resistant to Sirolimus alone. Once again T47D showed highest sensitivity to CGP57380 while SKBR3 also demonstrated somewhat high sensitivity to this agent. ZR-75-1, MCF7 and MDA-MB 468 depicted moderate sensitivity to CGP57380. MDA-MB 231 cell line was resistant to CGP57380 with a ~10-fold higher GI_{50} value compared to the T47D cell line (Table 6.1). Sirolimus showed a dose dependent growth inhibitory effect that appeared cytostatic in the MTT experiments with all cell lines tested. CGP57380 also showed dose dependent growth inhibition in all cell lines tested.

One of the main downstream effectors of the mTOR pathway is known to be 4E-BP1. Hyperphosphorylated 4E-BP1 is shown to dissociate from eIF4E thereby increasing the amount of functional eIF4E. Thus, Sirolimus inhibits mTOR signalling by suppressing mainly 4E-BP1 phosphorylation [276] [277]. Further, p70S6K1 is also phosphorylated by mTOR which is also inhibited by Sirolimus [276]. Previous observations on potency of Sirolimus have been contentious. Some researchers have reported various factors that are required for Sirolimus inhibition such as high levels of total p70S6K1 or loss of *PTEN* [117] [278]. In contrast, some have reported that loss of *PTEN* can facilitate a negative feedback loop leading to activation of the PI3K/AKT pathway in response to Sirolimus treatment and thereby resistance to this agent as mentioned in chapter 1 [279]. MDA-MB 468 cells are *PTEN* deficient, and in the present study, this cell line showed moderate sensitivity to Sirolimus compared to ZR-75-1 which is also *PTEN* deficient. ZR-75-1 cells showed high sensitivity, compared to MDA-MB 468 cells to Sirolimus ($P < 0.01$) [72] [117] [183]. Nevertheless, T47D was the most sensitive to Sirolimus in this study ($GI_{50} = 0.62$ nM).

T47D cells harbour wildtype *PTEN* and demonstrate a mutated *PIK3CA* gene [72]. According to previous observations, breast cancer cells that have a mutant *PIK3CA* gene are selectively sensitive to mTOR inhibitors such as Sirolimus [73]. In addition, it has been also shown previously that T47D and ZR-75-1 cell lines show high levels of total and phosphorylated p70S6K1 which could be the reason for high sensitivity to Sirolimus in this study [117].

Further, cells expressing aberrant HER2 which regulates mTOR signalling have also shown sensitivity to mTOR inhibition thus, SKBR3 cells that fall into the HER2 molecular subtype showed sensitivity to Sirolimus. On the other hand, MDA-MB 231 cells were resistant. These cells express wild type *PTEN* and low levels of p70S6K1 [117]. Further, MDA-MB 231 cells consists of a mutant form of the *RAS* gene (*K-RAS*) [72]. Thus, the RAS/MAPK pathway is constitutively activated in these cells as well. Although, many reports have shown that MCF7 cells are sensitive to this agent due to having high levels of phosphorylated p70S6K1, a mutant *PIK3CA* gene and low levels of phosphorylated AKT, this cell line showed resistance to this agent in this study [72] [117] [183].

Existing research has shown that although Sirolimus reduces phosphorylation of 4E-BP1 and p70S6K1, paradoxically it increases phosphorylation of eIF4E and AKT [79]. In fact, it has been revealed that Sirolimus only blocks mTORC1 but not mTORC2 which mediates AKT phosphorylation [77]. However, it has been also shown that phosphorylated AKT levels are not increased in cell lines with wild type *PTEN* [279].

Further, it has been portrayed that enhanced eIF4E phosphorylation is independent of p70S6K1 inhibition [277]. Some researchers have shown that Sirolimus treatment can up-regulate the RAS/MAPK pathway in certain cell lines [280] [281]. Thus, these factors could contribute to different levels of sensitivity to Sirolimus in the breast cancer cell line panel.

eIF4E also targets the RAS/MAPK pathway. ERK and p38 phosphorylate MNK1 leading to eIF4E phosphorylation which can be inhibited by CGP57380. This agent is in fact a potent inhibitor of both MNK1 and MNK2 [78]. Interestingly, T47D was the most sensitive cell line to CGP57380 as well ($GI_{50} = 9.22 \mu\text{M}$). The HER2 overexpressing SKBR3 cell line also depicted high sensitivity to CGP57380. These cells have portrayed high levels of MNK1 and MNK2 activity and additionally high levels of basal and phosphorylated eIF4E, and are therefore sensitive to CGP57380 [187] [282]. Further, Wheater et al, 2010, has shown that T47D, ZR-75-1 and MDA-MB 231 cell lines were inhibited by CGP57380 due to high or moderate levels of phosphorylated eIF4E. Nevertheless, these researchers have shown differential phosphorylated eIF4E levels by CGP57380 within these cell lines and that it is most likely to reflect variations of metabolism of the agent or up-regulation of agent insensitive kinases [187]. Further, it has been also shown that MCF7 and MDA-MB 468 cell lines depict low amounts of phosphorylated eIF4E which makes it less sensitive to CGP57380 [187] [283].

Interestingly, it has been found that enhanced eIF4E phosphorylation induced by Sirolimus is dependent on the MNK activation [79] [277]. As outlined above MNK1 regulates eIF4E activation. Wang et al, 2007, has shown that knocking down MNK1 activation reduced phosphorylated eIF4E levels but could not prevent its phosphorylation being increased by Sirolimus treatment. This suggests that MNK1 silencing is not sufficient to prevent eIF4E phosphorylation by Sirolimus. Thus, it may imply that both MNK1 and MNK2 may be responsible for Sirolimus induced eIF4E phosphorylation because loss of MNK1 function may be compensating for MNK2 [277]. Thus, it was hypothesised that combining both Sirolimus and CGP57380 would lead to reduced eIF4E phosphorylation thereby inhibition of mRNA translation.

In order to determine the effect of the agent combination, 3 concentrations were selected from each agent depending on how effective the agents were in the cell line panel. The concentrations selected for CGP57380 were 1 μ M, 5 μ M and 10 μ M while the concentrations for Sirolimus were selected as 0.1 nM, 0.5 nM and 1 nM for T47D, ZR-75-1, SKBR3 and MDA-MB 468 cell lines and 100 nM, 500 nM and 1 μ M for MCF7 and MDA-MB 231 cell lines.

Unexpectedly, it was found that all 6 cell lines with the agent combination showed a CI value of > 1.1 which indicated an antagonistic effect. These findings could be due to up-regulation of AKT of the PI3K/AKT pathway. Further, mTOR exerts influence on PI3K/AKT signalling through the mTOR-p70S6K1-insulin receptor substrate feedback loop in normal cells. However, it has been shown that inhibition of mTORC1

by mTOR inhibitors, relieves this negative feedback, by activating AKT. It has been reported that activated AKT extends a direct effect on pro-apoptotic and anti-apoptotic proteins of the Bcl-2 family which enhances cell survival [77] [284]. These findings can also be due to up-regulation of the RAS/MAPK pathway in the breast cancer cell lines. Upstream effectors of MNK such as ERK1/2 could be playing a role in these cell lines since it has been shown that CGP57380 does not affect the phosphorylated levels of ERK [285]. Further, prolonged treatment with Sirolimus has shown to add complexity to the extensive signal transduction cross talk by increasing ERK1/2 signalling in certain cancer cells by a feedback activation [286].

In parallel to this study, an undergraduate student H. K. Sin supervised by the author carried out a study with Sirolimus and CGP57380 alone and in combination using pancreatic Mia PaCa-2 cells. Mia PaCa-2 cells represents a type of pancreatic ductal adenocarcinoma which is very aggressive [287]. Results were similar to the present study with antagonistic results. The results are shown in appendix III.

Despite the efficacy of mTOR inhibitors, these agents have shown to induce eIF4E phosphorylation in a PI3K dependent mechanism. Intriguingly, Wang et al, 2007, has demonstrated that a PI3K inhibitor (LY294002) was able to block Sirolimus induced eIF4E phosphorylation in lung cancer cells. Furthermore, the same research group has depicted that mTOR inhibitors activate PI3K leading to an increase in eIF4E phosphorylation [277]. Therefore, it was investigated whether dual PI3K/mTOR inhibitors would be more effective in the panel of breast cancer cell lines.

6.2.2 Effects of dual PI3K/mTOR inhibitors

6.2.2.1 *In vitro* growth inhibitory effects of dual PI3K/mTOR inhibitors

Dual PI3K/mTOR inhibitors have an advantage over single target inhibitors since they are able to target PI3K, AKT and mTOR simultaneously. It has been shown previously that agents which fall into dual PI3K/mTOR inhibitors target both mTORC1 and mTORC2 which will inhibit negative feedback activation of PI3K/AKT signalling in cancer cells. This may completely abrogate PI3K/AKT and mTOR pathways which is beneficial but as a shortcoming these agents could be highly toxic [77].

In the current study, 3 dual PI3K/mTOR inhibitors - MS-73, MS-74 and MS-76 have been tested in the panel of breast cancer cell lines. MS-74 and MS-76 are novel analogues of MS-73 as mentioned in chapter 1 [140]. MS-73 has been shown to be a pan PI3K inhibitor portraying potency against PI3K isoforms (p110 α , p110 β , p110 γ , and p110 δ) [70]. Among the isoforms, the gene encoding the p110 α isoform, which is *PIK3CA* is mostly mutated in breast cancer [70] [140]. As outlined in chapter 1, the 2 novel analogues MS-74 and MS-76 have been developed to investigate the structural activity relationships with MS-73 and to increase solubility, because MS-73 is found to be poorly soluble. The MTT results for the 3 agents tested are summarised in Table 6.2.

Mean GI ₅₀ ± SD (72 h MTT assays)			
Cell line	MS-73	MS-74	MS-76
MCF7	36.53 nM ± 0.37	458.65 nM ± 13.13	5.16 µM ± 0.85
T47D	25.16 nM ± 1.35	277.92 nM ± 8.38	2.77 µM ± 0.49
ZR-75-1	16.94 nM ± 2.12	229.21 nM ± 5.46	2.13 µM ± 1.15
SKBR3	29.70 nM ± 2.34	283.95 nM ± 20.99	2.80 µM ± 0.73
MDA-MB 468	15.97 nM ± 1.64	233.03 nM ± 9.48	1.31 µM ± 0.41
MDA-MB 231	52.14 nM ± 1.07	823.72 nM ± 16.86	7.32 µM ± 0.70

Table 6.2: Mean GI₅₀ ± SD values of MS agents. Cells were seeded in 96 well plates at a density of 2.5×10^3 cells/well. After allowing time to adhere (24 h), cells were exposed to agents (72 h; n = 8). Mean and SD of trials ≥ 3 .

MS-73 had the highest potency across all the cell lines and MS-76 had the least potency. It was observed that MDA-MB 468 which is the *PTEN* deficient cell line was the most sensitive towards all 3 agents. Interestingly, it was observed that there was a 15-fold decrease in the potency of MS-74 compared to MS-73 ($P < 0.0001$) while there was a 5-fold decrease in the potency of MS-76 compared to MS-74 ($P < 0.01$) in the activity against the MDA-MB 468 cell line.

ZR-75-1 also showed high sensitivity towards MS-73 and MS-74 while this cell line showed less sensitivity to MS-76 compared to MDA-MB 468 cells. T47D and SKBR3 cell lines portrayed moderate sensitivity to MS-73, MS-74 and MS-76. MCF7 also showed moderate sensitivity to MS-73, however, this cell line showed less sensitivity

to MS-74 and MS-76. In contrast, the MDA-MB 231 cell line was resistant to all 3 agents.

According to prior literature, loss of the tumour suppressor gene *PTEN* and also mutations of the *PIK3CA* oncogene results in dysregulated PI3K/mTOR signalling [288]. In the current study 2 cell lines that are *PTEN* deficient; MDA-MB 468 and ZR-75-1 portrayed similar sensitivity to MS-73 and MS-74. However, the MDA-MB 468 cell line was the most sensitive to MS-76 as mentioned above.

In contrast, an earlier study has reported that dual PI3K/mTOR inhibitors are potent in ER+ and HER2 overexpressing cell lines [288]. In fact, a study performed previously on MS-73 revealed that this agent showed enhanced potency with a HER2+ and ER+ breast cancer cell line - MDA-MB 361 [140]. However, HER2 overexpressing SKBR3 cell line exhibited moderate sensitivity towards these agents in the present study. It could be due to SKBR3 harbouring wild type *PTEN* and *PI3K* [73] [288]. Moreover, T47D also showed moderate sensitivity. The reasons for the sensitivity could be; T47D harbouring a mutant *PIK3CA* gene and being HER2+ as depicted in chapter 3, figure 3.1 and figure 3.2 [73] [117]. Further, ligand independent ER activation has been shown by the mTOR pathway through phosphorylation of 4E-BP1 and p70S6K1 [142]. T47D demonstrated high levels of ER as depicted in chapter 3, figure 3.1 and figure 3.2. Thus, inhibition of T47D and ZR-75-1 cell growth by these novel agents would be beneficial. MCF7 which also harbours a mutated *PIK3CA* gene, did not show sensitivity to these agents compared to T47D [72]. Conversely, MCF7 cells did not express HER2 as shown in chapter 3, figure 3.1 and figure 3.2,

unlike T47D cells which could be the reason for reduced sensitivity. MDA-MA 231 was resistant to these agents. These cells are shown to harbour wildtype *PTEN* and mutant *RAS* [72] [117]. Further, these cells do not harbour a mutated *PIK3CA* gene or have HER2 as depicted in chapter 3, figure 3.1 and figure 3.2 [72]. Thus, not sensitive to these agents. A significant dose dependent reduction of viable cell numbers was observed in MDA-MB 468, ZR-75-1, SKBR3 and T47D cell lines with the 3 agents. As depicted in the dose response curves, MS-73 and MS-74 showed cytotoxicity at higher concentrations while MS-76 showed cytotoxicity only at the highest concentration tested which was 10 μ M (Figure 6.1).

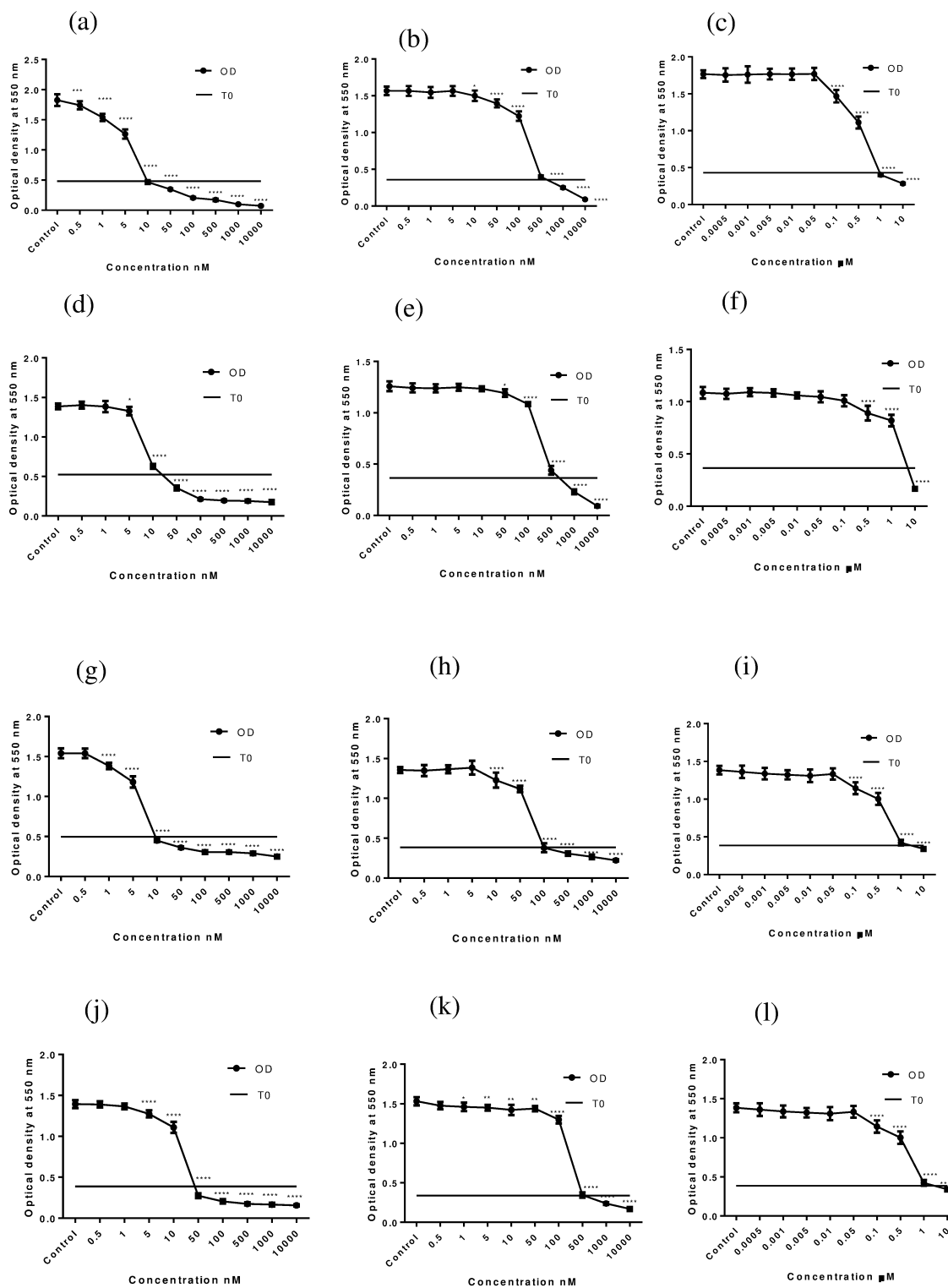
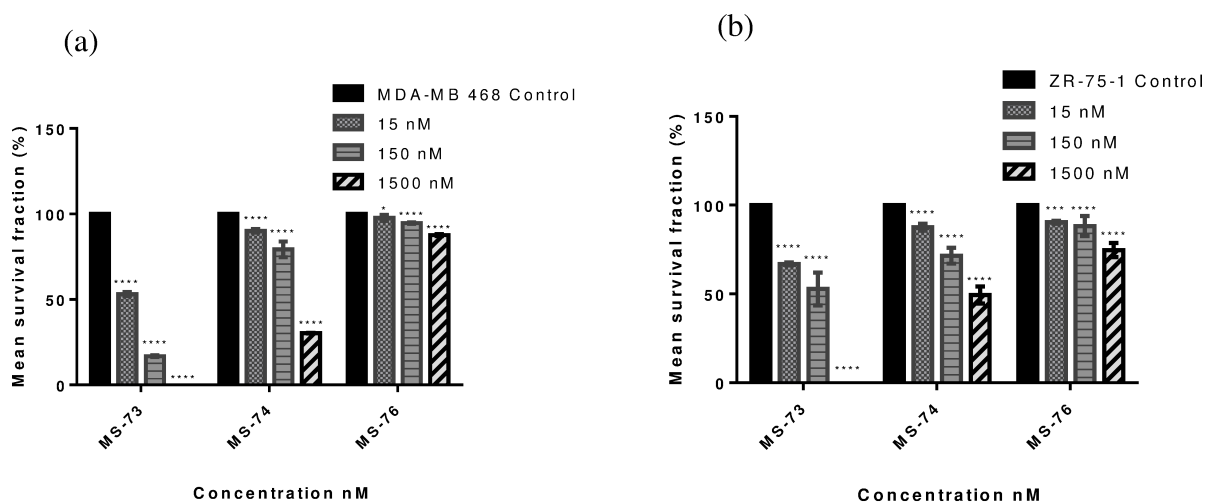


Figure 6.1: Growth inhibitory curves of MS-73, MS-74 and MS-76. (a, b and c) - MDA-MB 468, (d, e and f) - SKBR3, (g, h and i) - ZR-75-1 and (j, k and l) - T47D cells; MS-73 (a, d, g and j), MS-74 (b, e, h and k) and MS-76 (c, f, i and l). Mean and SD of representative experiments are shown (n = 8 per trial); trials ≥ 3 . * indicates significant difference compared to control, * (P < 0.05), ** (P < 0.01), *** (P < 0.001), **** (P < 0.0001).

6.2.2.2 Effects of dual PI3K/mTOR inhibitors on MDA-MB 468, ZR-75-1 and SKBR3 colony formation

In order to further evaluate these agents on survival and proliferation of breast cancer cells, 3 concentrations were selected which corresponded ~ with the lowest GI₅₀ value of each agent. Thus, 15 nM, 150 nM and 1500 nM (1.5 μ M) were selected. To determine whether single cells were able to survive and form colonies after a 24 h exposure to the 3 agents' clonogenic assays were carried out. MDA-MB 468 and ZR-75-1 cell lines were chosen, as these 2 cell lines were highly sensitive to the agents while the SKBR3 cell line was also chosen as it showed moderate sensitivity in the MTT experiment (Figure 6.2).



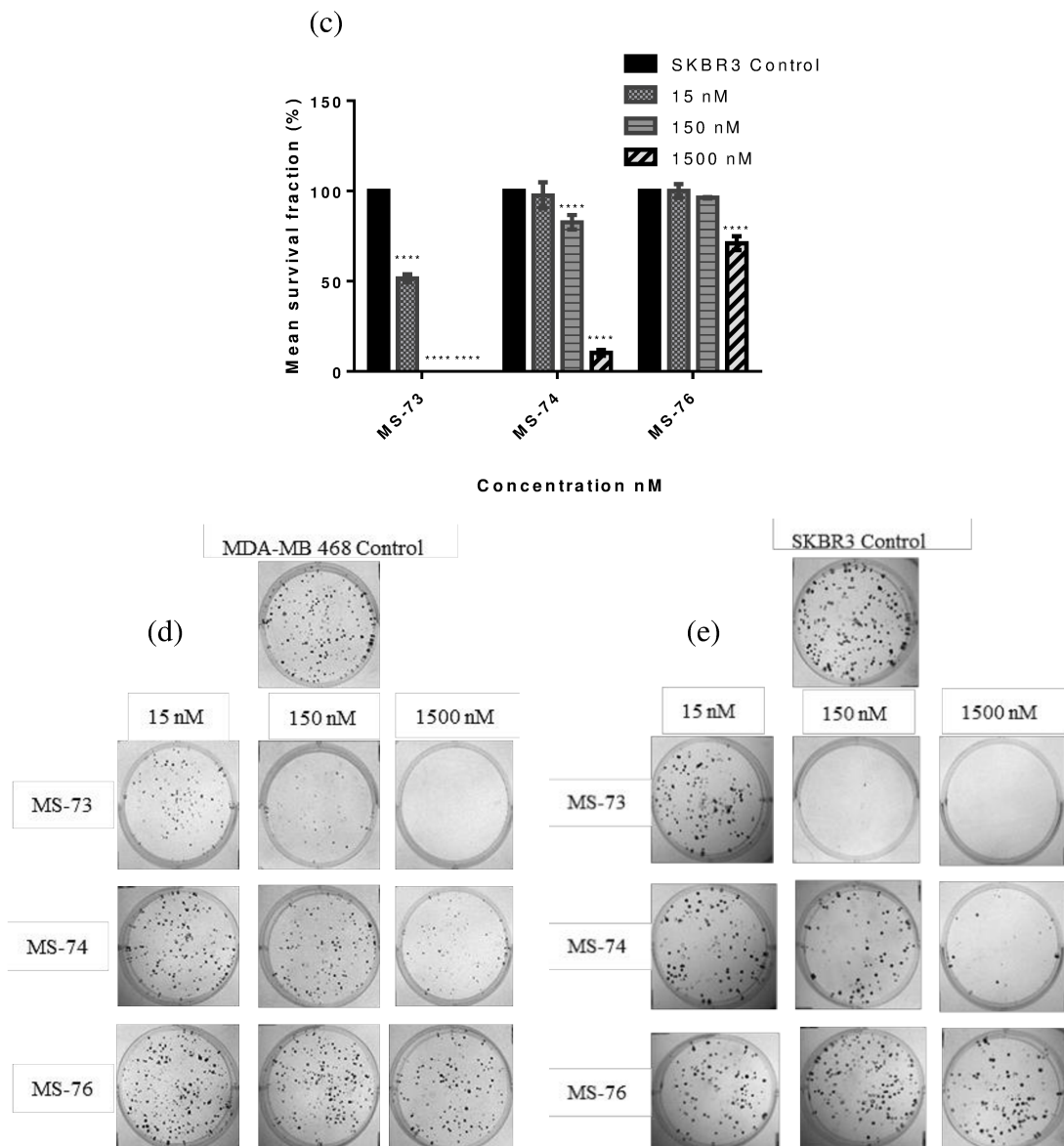


Figure 6.2: Effects of MS-73, MS-74 and MS-76 on colony formation. (a) MDA-MB 468, (b) ZR-75-1 and (c) SKBR3. Representative images of colony formation after exposure to MS agents - (d) MDA-MB-468 and (e) SKBR3. Mean SF as % plating efficiency of control represented as the mean \pm SD of trials ≥ 3 , ($n = 3$ per trial). * indicates significant reduction * ($P < 0.05$), ** ($P < 0.01$), *** ($P < 0.001$), **** ($P < 0.0001$) in colony formation.

MDA–MB 468 cell line portrayed a strikingly low SF compared to control at all tested concentrations of the 3 agents. Interestingly, it was observed that at 150 nM MS-73, the number of colonies were less and the size of the colonies were reduced compared to control. At 1500 nM (~ 94 fold GI₅₀), MS-73 completely abolished colony formation ($P < 0.0001$). The results for ZR-75-1 were very similar to MDA-MB 468 and showed a very low SF ($P < 0.0001$).

Remarkably, both 150 nM and 1500 nM of MS-73 completely eradicated survival of SKBR3 cells ($P < 0.0001$). It was noticed that, SFs of SKBR3 colonies were significantly reduced at 1500 nM MS-74 (10.27%) and MS-76 (71.12%) compared to MDA-MB 468 cells (MS-74 - 30.30% and MS-76 - 87.66%) which was remarkable ($P < 0.0001$). Similarly, SKBR3 cells at the highest concentration (1500 nM) of MS-74 showed significantly less survival compared to ZR-75-1 cells (49.40%) ($P < 0.0001$).

Hence, it can be stated that the results of the clonogenic assay corroborates with the results of the MTT assay by demonstrating that MS-73 was the most potent while MS-74 was moderately potent and MS-76 was the least potent among the tested agents. Further, evidence presented herein suggests that all 3 agents, especially MS-73 and MS-74 were highly cytotoxic in these cell lines at high concentrations. Interestingly, these results depict that the HER2 overexpressing SKBR3 cell line was unable to reproduce and form many colonies in the presence of the novel analogue - MS-74 at

the highest concentration which is 1500 nM. Therefore, SKBR3 and the MDA-MB 468 cells lines were chosen to further investigate the activity of these 3 agents.

6.2.2.3 Effects of dual PI3K/mTOR inhibitors on MDA-MB 468 and SKBR3 cell cycle

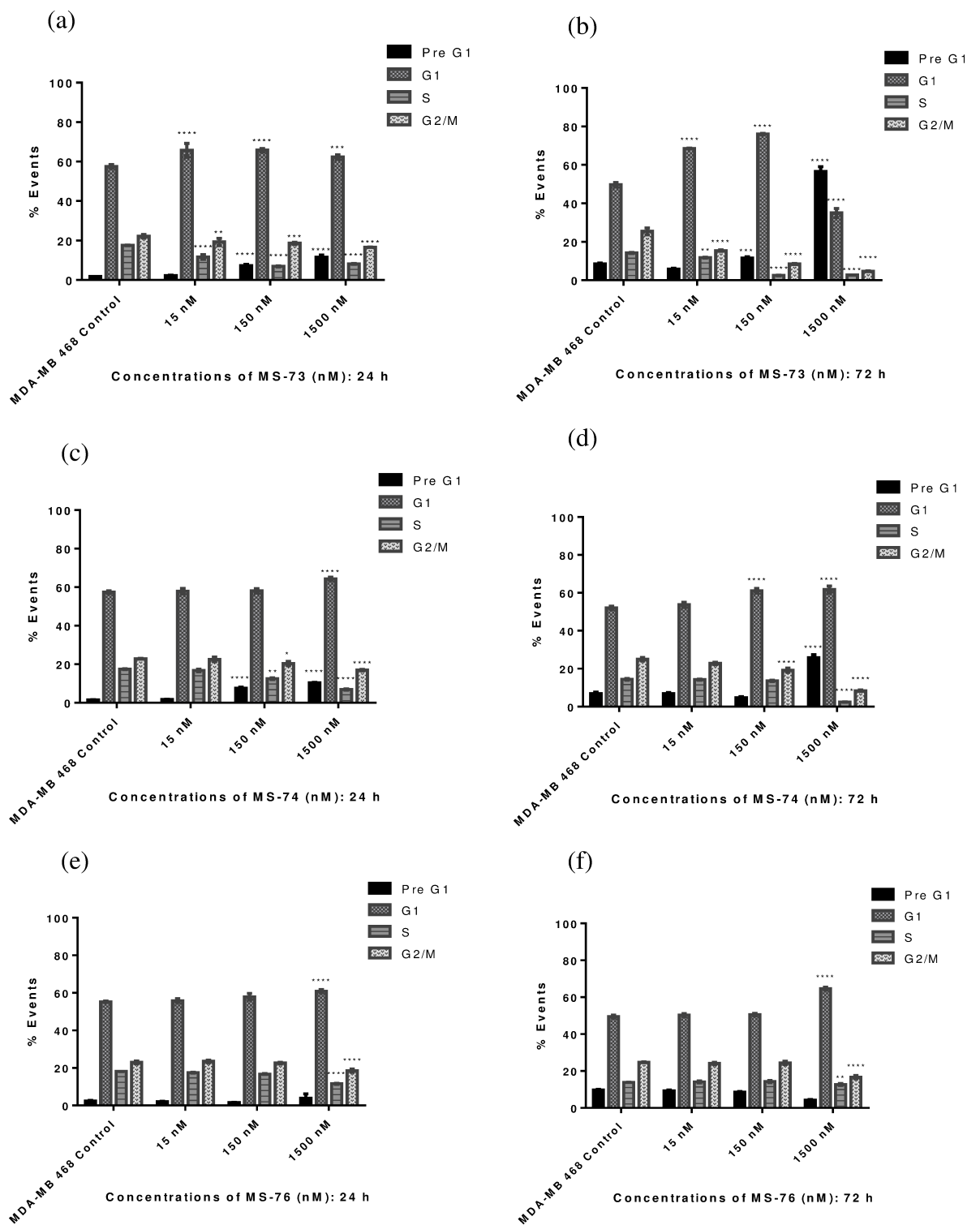
To further examine the effect of the 3 agents on cell cycling; flow cytometric analysis were carried out. Cells were treated with 15 nM, 150 nM and 1500 nM of the agents for 24 and 72 h. The highest 2 concentrations; 150 nM and 1500 nM of MS-73 and 1500 nM of the new analogue MS-74 showed extremely significant pre-G1 accumulations against the MDA-MB 468 cell line compared to control at 24 and 72 h ($P < 0.0001$) which is indicative of apoptosis. Interestingly, the pre-G1 accumulations in the SKBR3 cell line was stark. The results at 1500 nM of MS-73 (81.35%) and MS-74 (80.45%) were remarkably high at 72 h in the SKBR3 cell line compared to control (9.90%) ($P < 0.0001$). These results corroborated the results of the clonogenic assay, although in this experiment, cells were exposed to agents for a period of 72 h. On the contrary, MS-76 did not evoke a significant pre-G1 population at all tested concentrations against both cell lines (Figure 6.3) and (Figure 6.4).

Further, it was found that MS-73 caused a significant G1 phase arrest at all 3 concentrations tested at 24 h and also at 15 and 150 nM at 72 h in the MDA-MB 468 cell line ($P < 0.0001$) with corresponding diminished S and G2/M phases ($P < 0.0001$). However, 1500 nM MS-73, at 72 h showed a decreased G1 phase compared to control, due to a high apoptotic population (pre-G1) ($P < 0.0001$). The novel analogues, MS-

74 (1500 nM) and MS-76 (1500 nM) also caused a G1 accumulation at both 24 h and 72 h together with reduced S and G2/M phases in MDA-MB 468 cells compared to control cells ($P < 0.0001$).

SKBR3 cells were significantly arrested in the G1 phase after treatment with all 3 concentrations of MS-73 which was followed with decreased S and G2/M phases at 24 h ($P < 0.0001$). In contrast, only 1500 nM MS-74 induced a G1 arrest at 24 h, which again resulted in reduced S and G2/M populations ($P < 0.0001$). Contrariwise, MS-76 did not cause significant alterations in the cell cycle at 24 h in SKBR3 cells although this agent caused significant G1 accumulations in the MDA-MB 468 cell line.

However, at 72 h the SKBR3 cell line portrayed reduced G1 populations with all 3 agents compared to untreated cells ($P < 0.0001$). Among these results the highest concentrations of MS-73 and MS-74 caused an enhanced pre-G1 population which would have caused the reduced G1 phase at 72 h. MS-76 did not induce a discernible pre-G1 accumulation compared to MS-73 and MS-74 but still portrayed a reduced G1 phase ($P < 0.0001$) that was followed by an increased G2/M phase ($P < 0.0001$) compared to control at 72 h. These results suggested that MS-76 did not perturb the cell cycle distribution in SKBR3 cells (Figure 6.3).



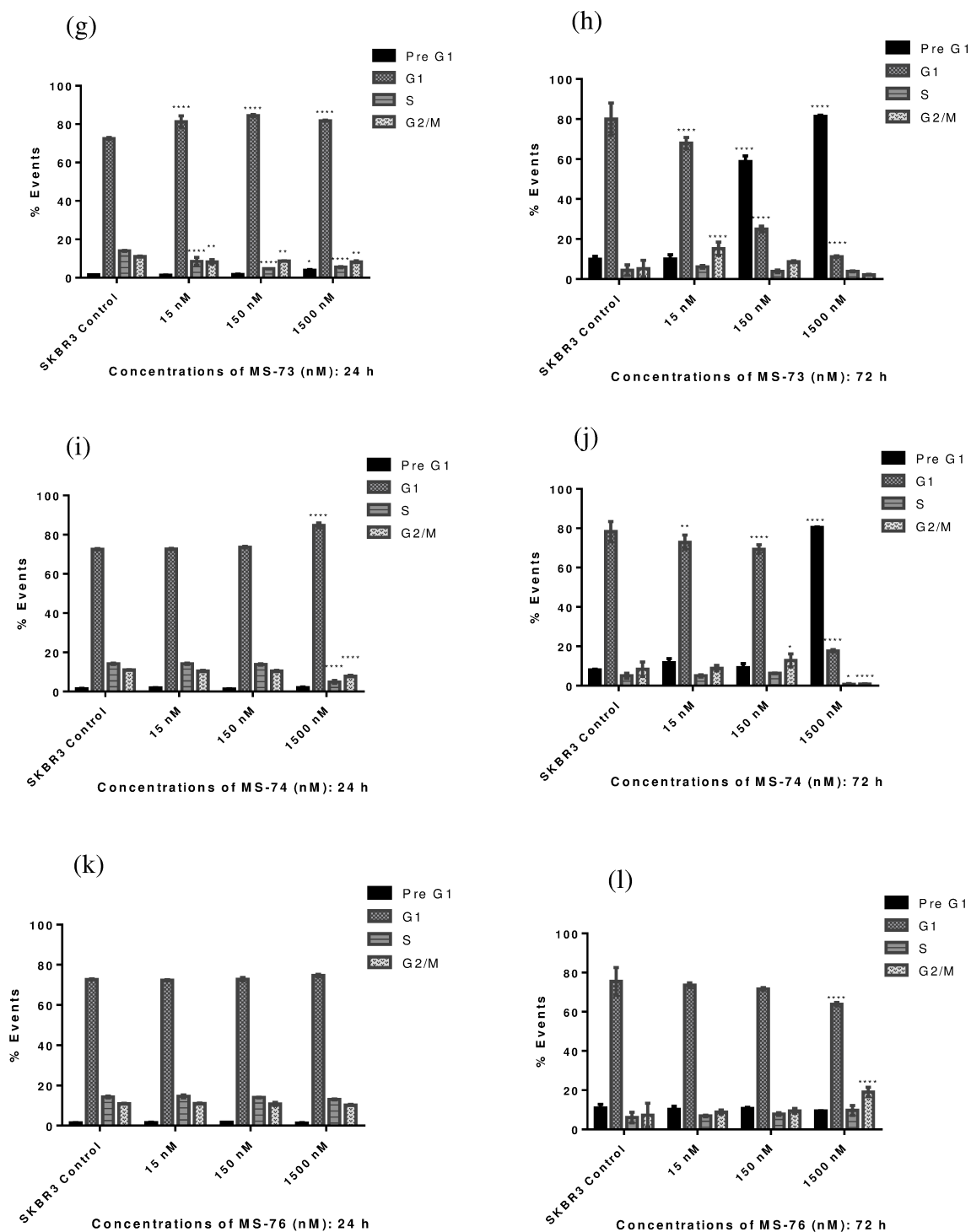


Figure 6.3: Cell cycle analysis following treatment of cells with MS-73, MS-74 and MS-76. (a, b, c, d, e and f) - MDA-MB 468 and (g, h, i, j, k and l) - SKBR3 cells were treated with 15 nM, 150 nM and 1500 nM concentrations of these agents for 2 time points 24 and 72 h. Mean and SD of trials ≥ 3 , ($n = 3$ per trial). * indicates significant difference compared to control, * ($P < 0.05$), ** ($P < 0.01$), *** ($P < 0.001$), **** ($P < 0.0001$).

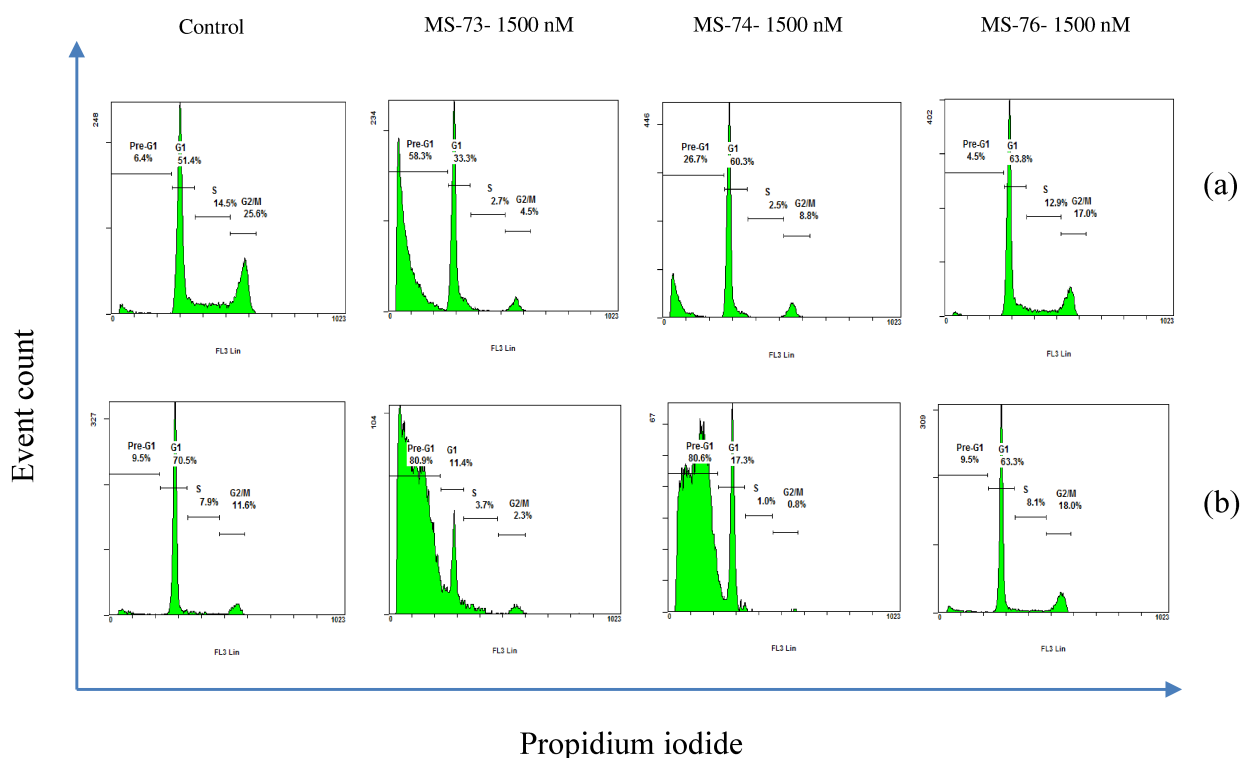


Figure 6.4: Representative cell cycle histograms at the highest concentration (1500 nM) tested of MS-73, MS-74 and MS-76. (a) MDA-MB 468 and (b) SKBR3 cells were treated for 72 h. These are representative histograms, 15,000 events were analysed in each experiment.

The results of the cell cycle analysis would suggest that the new analogue MS-74 at 1500 nM which was equivalent to $\sim 5x$ GI_{50} , caused apoptosis in MDA-MB 468 cells and especially caused high levels of apoptosis in SKBR3 cells. Further, MS-74 was able to evoke a G1 arrest which resulted in an inhibition of the transition from G1 phase to S and then to G2/M phase which would contribute to inhibiting cell cycling in both cell lines. MS-76 at the highest concentration tested (equivalent to $\sim 1x$ GI_{50} in the MDA-MB 468 cell line) elicited a G1 accumulation that was followed by decreased S and G2/M phases in MDA-MB 468 cells but this agent did not demonstrate inhibition of cycling SKBR3 cells. This could be due to this agent being less potent. Further, SKBR3 cells possess mutant *TP53* [209]. It has been shown that

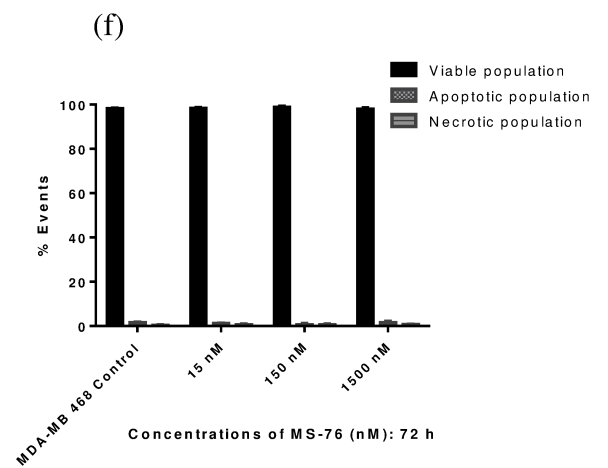
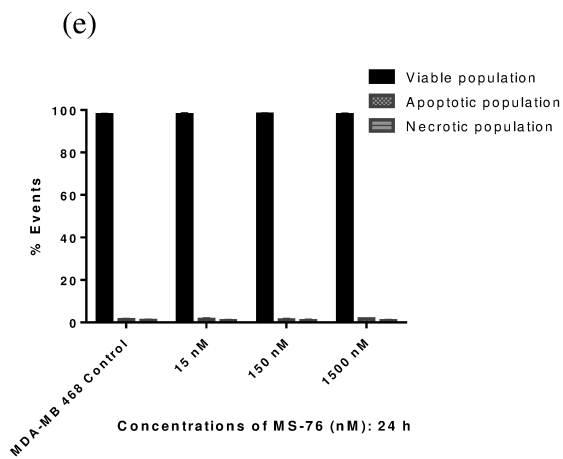
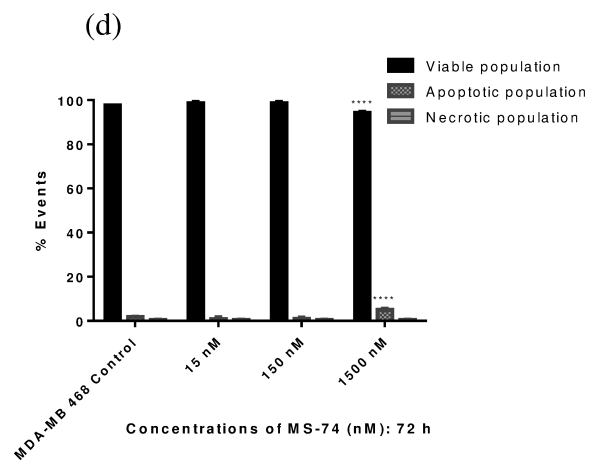
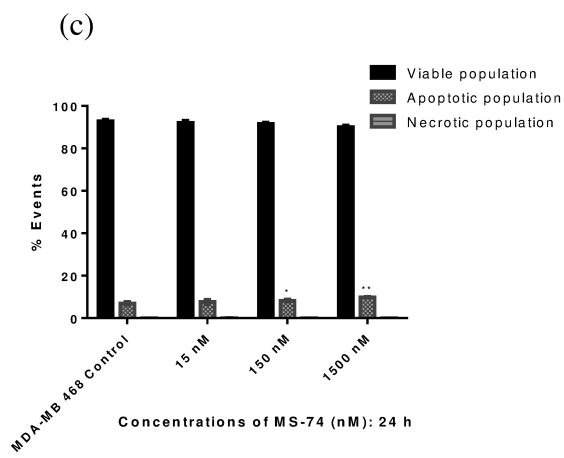
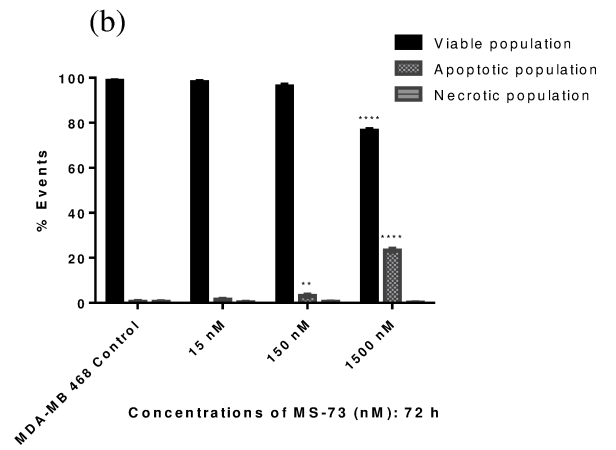
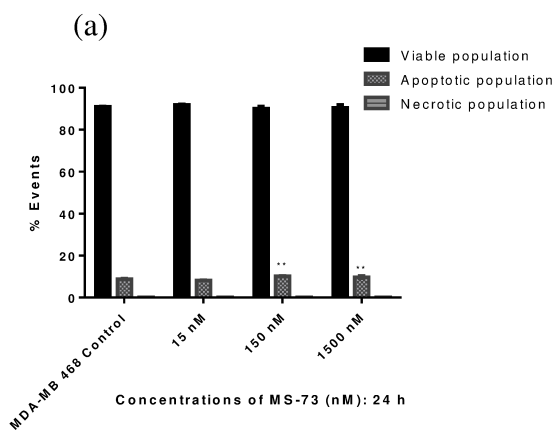
TP53 plays a prominent role as a checkpoint protein in cells at the transition from G1 to S phase in the cell cycle. However, this function is defective in SKBR3 cells, thus at the concentration tested (1500 nM), MS-76 would have failed to inhibit cycling SKBR3 cells [41]. Subsequently, the effect of apoptosis in cells by these agents were evaluated, in order to confirm whether the pre-G1 phases observed were actually due to apoptosis.

6.2.2.4 Effects of dual PI3K/mTOR inhibitors on MDA-MB 468 and SKBR3 cellular apoptosis

Induction of apoptosis by the 3 agents was analysed by flow cytometry. The early and late apoptotic populations were summed to determine the total apoptotic population. It was found that MS-73 caused a small significant apoptotic population with 150 nM and 1500 nM at 24 h and with 150 nM at 72 h ($P < 0.01$) in MDA-MB 468 cells. Nevertheless, at 72 h this agent caused a large total apoptotic population (23.33%) which was extremely significant compared to control (0.60%) ($P < 0.0001$). The early apoptotic population (19.73%) was higher than the late apoptotic population (3.60%) ($P < 0.0001$). MS-74 caused a small significant apoptotic populations at 150 nM ($P < 0.05$) and 1500 nM ($P < 0.01$) at 24 h in MDA-MB 468 cells. However, no significant apoptosis was observed following treatment of cells with 150 nM at 72 h but only with 1500 nM ($P < 0.0001$) at the same time point. These results corroborated with the results of cell cycle analysis of MDA-MB 468 cells, and the results may suggest that MDA-MB 468 cells would be able to resume growth after a longer incubation period at low concentrations such as 150 nM MS-74, due to being *PTEN* deficient [117]. MS-76 did not induce prominent apoptosis in this cell line which again corroborated results

of the cell cycle analysis and the clonogenic assay where MS-76 showed reduced activity.

None of the agents were found to cause apoptosis at 24 h in SKBR3 cells, although cell cycling results in the same cell line showed small significant pre-G1 populations with 1500 nM MS-73. In contrast at 72 h, 150 nM (37.27%) and 1500 nM (57.37%) MS-73 induced stark extremely significant apoptotic populations compared to SKBR3 control (10%) ($P < 0.0001$) which corroborated the cell cycle results. It was observed that at 1500 nM of MS-73, there was no significant difference between the early (28.43%) and late (28.93%) apoptotic populations in SKBR3 cells. In addition, a small significant necrotic population (7.53%) was also observed compared to untreated SKBR3 cells (0.30%) with 1500 nM of MS-73 ($P < 0.0001$) at 72 h. There was no other significant necrotic populations identified in this experiment. MS-74 (1500 nM) at 72 h caused an extremely significant apoptotic population (33.05%) compared to SKBR3 control (8.63%) ($P < 0.0001$) which again was consistent with the cell cycle results. Interestingly, MS-76 (1500 nM) portrayed a slight but significant apoptotic population (12.70%) compared to SKBR3 control cells (10.60%) ($P < 0.05$), which was not apparent with the cell cycle results. However, the results obtained for SKBR3 cells treated with 1500 nM of MS-76 corresponded with the clonogenic results where these cells depicted less survival of colonies at the same concentration compared to MDA-MB 468 cells.



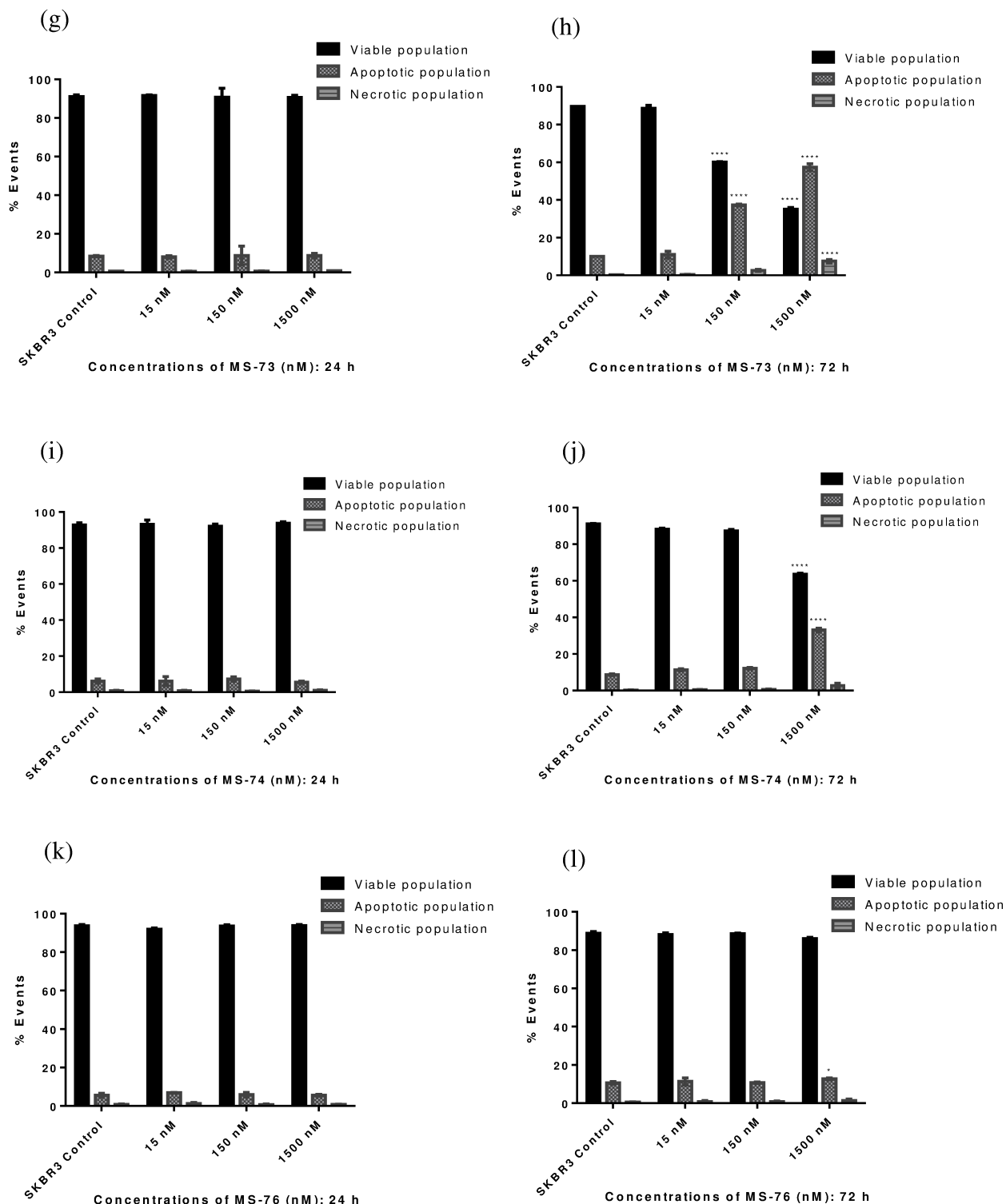


Figure 6.5: Apoptosis analysis of cells following exposure to MS-73, MS-74 and MS-76. (a, b, c, d, e and f) - MDA-MB 468 and (g, h, i, j, k and l) - SKBR3 cells were treated with 15 nM, 150 nM and 1500 nM concentrations of these agents for 2 time points 24 and 72 h. Mean and SD of trials ≥ 3 , ($n = 3$ per trial). * indicates significant difference compared to control, * ($P < 0.05$), ** ($P < 0.01$), *** ($P < 0.001$), **** ($P < 0.0001$).

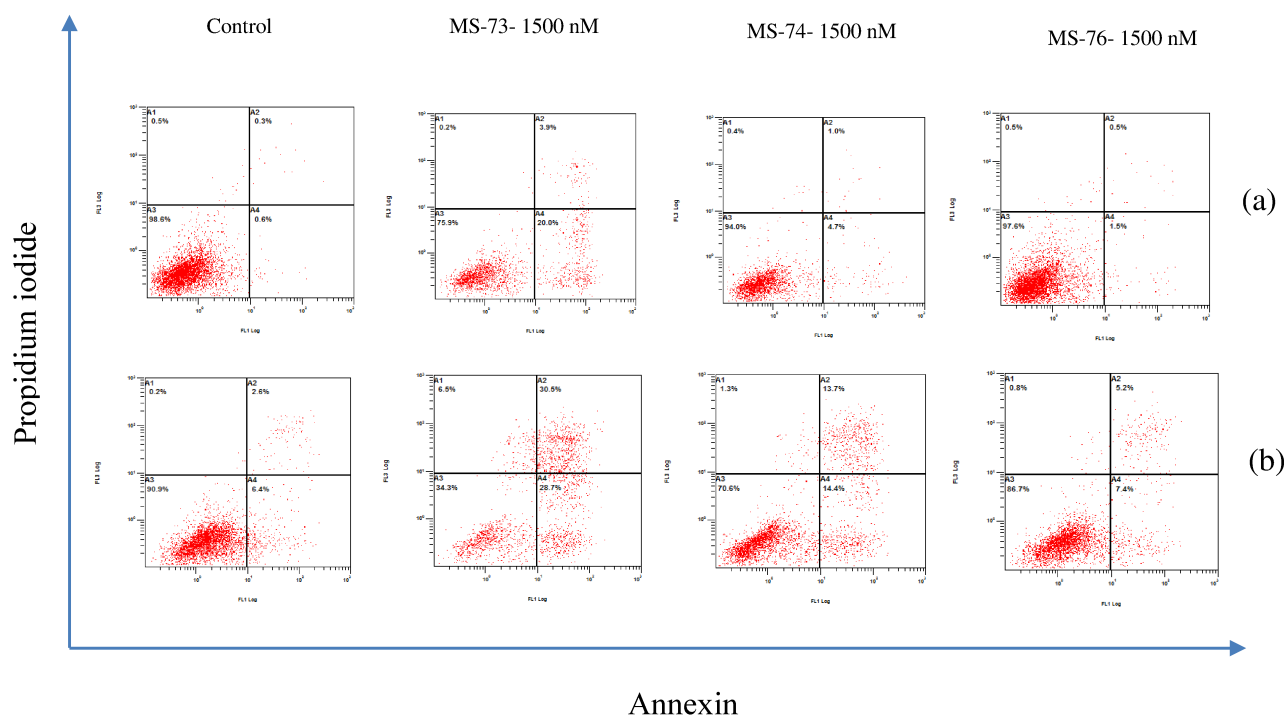


Figure 6.6: Representative apoptotic quadrant plots at the highest concentration (1500 nM) tested of MS-73, MS-74 and MS-76. (a) MDA-MB 468 and (b) SKBR3 cells were treated for 72 h. These are representative quadrant plots, 10,000 events were analysed in each experiment.

Apoptotic analyses would suggest that MS-73 and MS-74 are highly cytotoxic. However, it was noted that although these 2 agents caused apoptosis, it was caused at high concentrations only which was also observed in MTT and clonogenic assays. While MS-74 caused apoptosis in both cell lines, interestingly, MS-76 caused apoptosis only in SKBR3 cells but not in MDA-MB 468 cells. This could be due to MS-76 being less potent and also due to *PTEN* deficiency in MDA-MB 468 cells that contributes to constitutive signalling through the PI3K/AKT pathway [117]. In addition the results indicated that these agents did not evoke necrosis except when a large apoptotic population was induced such as when MS-73 evoked a comprehensive

apoptotic population at 1500 nM in SKBR3 cells. This could be secondary necrosis taking place when a large late apoptotic population is induced [206].

6.2.2.5 Effects of dual PI3K/mTOR inhibitors on PI3K/AKT and mTOR pathways in MDA-MB 468 and SKBR3 cells by Western blotting

The described effects on cell cycling and apoptosis in MDA-MB 468 and SKBR3 cells by the 3 agents, prompted an investigation into the key proteins which these agents would target within the PI3K/AKT and mTOR pathway. The effect of 1x and 2x GI₅₀ concentrations of the 3 agents within the MDA-MB 468 cell line was used to assess the activity of the proteins in the PI3K/AKT and mTOR pathways. Thus, both MDA-MB 468 and SKBR3 cells were exposed for 24 h to 1x and 2x GI₅₀ concentrations of the agents. As it has been shown that phosphorylation of 4E-BP1 results in eIF4E release which increases cap dependent translation, the effect of the agents on these 2 proteins of the mTOR pathway were investigated. Further, phosphorylation of AKT of the PI3K/AKT pathway was also investigated [117] [276] [277].

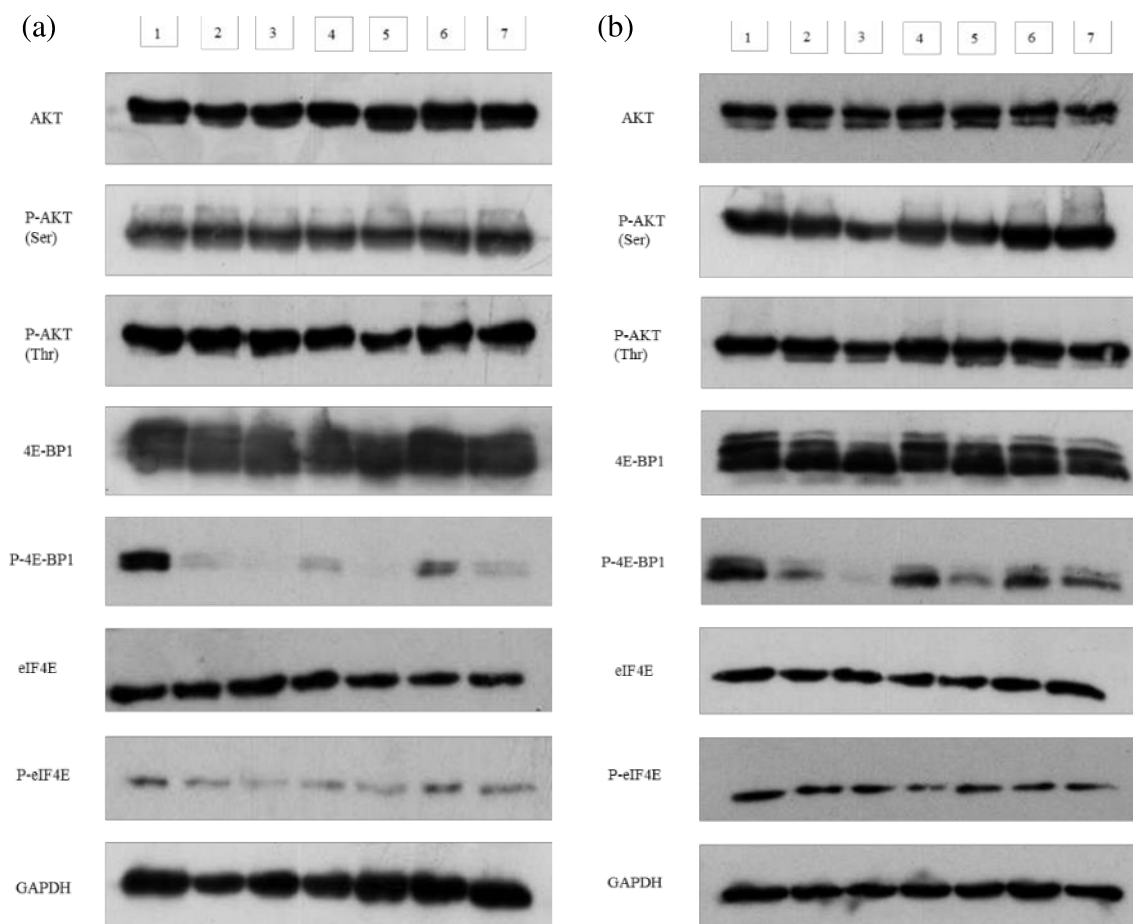


Figure 6.7: Western blot analysis of PI3K/AKT and mTOR pathways following exposure of cells to MS-73, MS-74 and MS-76. AKT, P-AKT (Ser473), P-AKT (Thr308) (60 kDa), 4E-BP1, P-4E-BP1 (15-20 kDa), eIF4E and P-eIF4E (25 kDa) and GAPDH (37 kDa). GAPDH was probed as a loading control and adjusted relative densities (ARD) were calculated. (a) MDA-MB 468 cell line and (b) SKBR3 cell line. (1) Control, (2) 1x GI₅₀ - MS-73, (3) 2x GI₅₀ - MS-73, (4) 1x GI₅₀ - MS-74, (5) 2x GI₅₀ - MS-74, (6) 1x GI₅₀ - MS-76, (7) 2x GI₅₀ - MS-76. MDA-MB 468 and SKBR3 whole cell protein lysates (50 µg) were subjected to 10% SDS-polyacrylamide gel electrophoresis.

It was found that all 3 agents down-regulated phosphorylated 4E-BP1 (Ser65) extremely significantly at all concentrations tested in MDA-MB 468 cells ($P < 0.0001$). Interestingly, as shown by figure 6.7, the novel analogue MS-74 (1x GI_{50} - ARD - 9.89% and 2x GI_{50} - ARD - 1.92%) showed a similar effect to MS-73 (1x GI_{50} - ARD - 8.33% and 2x GI_{50} - ARD - 2.00%). MS-76 also exhibited down-regulation (1x GI_{50} - ARD - 33.32% and 2x GI_{50} - ARD - 11.78%), although the effect was not as apparent as MS-74.

The SKBR3 cell line also portrayed significant down-regulation of P-4E-BP1 ($P < 0.0001$). Nevertheless, it was observed that the down-regulation was not as low compared to MDA-MB 468 cells ($P < 0.001$) except for 2x GI_{50} MS-73 where it was not significantly different compared to MDA-MB 468 cells (MDA-MB 468 - 2x GI_{50} MS-73 - ARD - 2.00% and SKBR3 - 7.82%). Moreover, in SKBR3 cells, MS-74 did not cause a similar down-regulation of P-4E-BP1 compared to MS-73, unlike in MDA-MB 468 cells (SKBR3 - MS-73-1x GI_{50} - ARD - 39.48% and 2x GI_{50} - ARD - 7.82%, MS-74 - 1x GI_{50} - ARD - 58.12% and 2x GI_{50} - ARD - 33.56% and MS-76 - 1x GI_{50} - ARD - 71.77% and 2x GI_{50} - ARD - 59.99%).

As shown in figure 6.7, MS-73 and similarly MS-74 down-regulated P-eIF4E (Ser209) significantly in MDA-MB 468 cells ($P < 0.0001$). On the contrary, the down-regulation of eIF4E phosphorylation was not as efficient as P-4E-BP1 in MDA-MB 468 cells. Interestingly, SKBR3 cells did not show any significant down-regulation of P-eIF4E. In contrast, SKBR3 cells after exposure to 2x GI_{50} concentrations of MS-73

down-regulated P-AKT (Ser473) ($P < 0.01$) and P-AKT (Thr308) ($P < 0.01$) which was the only alternation observed for phosphorylated AKT with the agents and their concentrations tested in this study. Densitometry analysis with the ARD values for the significant results are shown in appendix I under section 9.1.3.1.

A parallel study carried out by 3 undergraduate students under the supervision of the author, found that a higher concentration of MS-73 (10 μ M), completely abolished P-AKT (Ser473) and P-AKT (Thr308) in MCF7 and HCT116 colon cancer cells. Additionally, the same agent at 10 μ M down-regulated P-AKT (Ser473) and P-AKT (Thr308) levels significantly in MDA-MB 468 cells but failed to completely abolish P-AKT levels due to these cells being *PTEN* deficient. These results are shown in appendix IV.

All 3 agents did not affect the total expression levels of AKT, 4E-BP1 and eIF4E within the current study. It has been shown earlier that MS-73 did not affect the total protein expression levels of AKT [26].

These results indicate that MS-73 and MS-74 inhibited the mTOR pathway significantly by down-regulating phosphorylation of 4E-BP1 and eIF4E in MDA-MB 468 cells and also down-regulating P-4E-BP1 in SKBR3 cells. In fact, it was interesting to observe that all agents inhibited P-4E-BP1 in the *PTEN* deficient MDA-MB 468 cell line which has been shown to have high levels of P-4E-BP1 [283]. This

is an interesting finding as it has been shown that Sirolimus decreases P-4E-BP1 and paradoxically increases eIF4E phosphorylation [277]. This increase of P-eIF4E has been shown to be PI3K dependent through MNK activation. In fact, Wang et al, 2007 has shown that LY294002 which is a PI3K inhibitor was able to block Sirolimus induced eIF4E phosphorylation [277]. Thus, it was interesting to observe that there was no increase of eIF4E phosphorylation in MDA-MB 468 and SKBR3 cells after exposure to all 3 MS agents. These results suggest that there may be no or insignificant MNK activation in these cells with MS agent treatment. Further, this implies that these MS agents are in fact functioning as dual PI3K/mTOR inhibitors. Yet, the P-eIF4E expression levels did not correspond to P-4E-BP1 levels, which could suggest low activity of mRNA translation. These results may indicate that MS agent treatment is generating conflicting signals to cap dependent protein translation. This could be due to cross talk with compensatory and alternative signalling pathways involving P-eIF4E in breast cancer cells. Previously, it has been shown that ERK signalling is associated with enhanced eIF4E activation by feedback activity with the treatment of a mTORC1/2 inhibitor which could be one of the mechanisms for higher P-eIF4E expression [289]. Indeed, a previous study has shown that MS-73 does not inhibit the RAS/MAPK pathway [290]. However, more investigations are warranted to find the exact mechanism of these agents.

Further, it was observed that all 3 agents failed to down-regulate the PI3K/AKT pathway in the MDA-MB 468 cell line at the tested concentrations. This could be due to *PTEN* deficiency in this cell line and the inability to inhibit AKT phosphorylation [77] [283]. Thus, these results may suggest that mTORC2 is not completely inhibited

by these agents at the tested concentrations in MDA-MB 468 cells [77]. mTORC2 is shown to contribute to complete AKT activation by phosphorylation of AKT (Ser473), therefore no inhibition of phosphorylated AKT was observed in MDA-MB 468 cells [291]. It has been shown that Sirolimus increases P-AKT (Ser473) by inhibiting mTORC1, but interestingly there was no increase of P-AKT (Ser473) observed in both cell lines tested following exposure to MS agents [292] [293]. Nevertheless, as outlined above, if higher concentrations of these agents were used, then down-regulation of P-AKT would have been observed in MDA-MB 468 cells, as it was shown that 10 μ M of MS-73 down-regulated P-AKT levels in MDA-MB 468 cells.

In fact, HER2 overexpressing SKBR3 cells after exposure to MS-73 (2x GI_{50}) inhibited P-AKT (Ser473) slightly which coincided with previous results in MDA-MB 361 cells which is also HER2+ [140]. This could be the reason this cell line completely eradicated survival of SKBR3 cells preventing colony formation at 150 nM and 1500 nM ($P < 0.0001$). Prior studies have also shown that MS-73 has little effect on upstream elements such as AKT in most cell lines although this agent down-regulated P-AKT (Ser473) and P-AKT (Thr308) in the MDA-MB 361 cell line [294]. The MDA-MB 361 cell line may show high sensitivity because it is *PIK3CA* mutant and also HER2+ [290]. This could be the reason less potent MS-74 and MS-76 did not demonstrate significant P-AKT inhibition in the SKBR3 cell line compared to MS-73. Once again, if higher concentrations were used down-regulation of this pathway would have been observed. Nevertheless, sensitivity of *PTEN* deficient cells and HER2 overexpressing cells to dual PI3K/mTOR inhibitors may be dependent on interactions between other survival pathways such as the RAS/MAPK pathway [286]. Previously,

MS-73 has been shown to inhibit P-P70S6K1 which is also a downstream target of mTOR that is mainly responsible of phosphorylating 40S ribosomal protein S6 leading to mRNA translation that encodes for ribosomal proteins and elongation factor-1 [140]. However, the expression of P70S6K1 was not investigated in this study, as it has been shown that eIF4E phosphorylation was independent P70S6K1 [277].

Thus, taken together these results would suggest that MS agents, do function as dual PI3K/mTOR inhibitors and they would be more therapeutically effective in breast tumours lacking *PTEN* or breast tumours which are HER2 overexpressing if used at higher concentrations or combined with a different class of inhibitors. For instance, previously MS-73 has portrayed enhanced potency in resistant head and neck cancer models with the combination of Cetuximab an EGFR inhibitor [295]. Furthermore, MS-73 in combination with PD0325901 which is a MEK inhibitor has shown enhanced growth inhibition in a HCT116 model [290].

6.2.3 *In vitro* growth inhibitory effects of AhR ligand - 5F 203

The underlying anti-tumour mechanism of action of potent benzothiazoles (AhR ligands) in breast cancer has been previously explored by Dr. Tracey D. Bradshaw and her group [92] [94] [296]. Many signal transduction pathways such as the EGFR, ER and RAS/MAPK pathways have shown cross talk with the AhR pathway [297]. Further, signalling molecules downstream of EGFR such as PI3K, cross talks with pathways such as RAS/MAPK. Thus, PI3K may be responsive to AhR [61]. Furthermore, the AhR pathway influences a variety of cellular processes such as

mitogenesis, hypoxia response and vascularisation as mentioned in chapter 1 [92] [94]. AhR has been shown to be expressed in both ER+ and ER- cell lines [141]. Thus, studies were performed following combination of MS agents with a potent AhR ligand.

5F 203, which is an AhR ligand, binds to cytosolic AhR which is translocated to the nucleus, followed by dimerisation with ARNT. Consequently, xenobiotic response elements on the CYP1A1 promoter is induced by driving gene transcription [296]. Induction of CYP1A1 gene expression is reflected as one of the most sensitive indicators of exposure to AhR ligands. Subsequently, CYP1A1 metabolises 5F 203 to a reactive electrophilic species which binds to nucleophilic regions of DNA that results in formation of DNA adducts and DNA strand breaks, ultimately causing cell death [92] [138] [296]. It has been previously shown that this agent is able to cause anti-cancer effects in certain breast cancer cells (ER+ and ER-), thus the effect of this agent was tested in the panel of breast cancer cell lines [296] (Table 6.3).

Cell line	Mean GI ₅₀ ± SD (72 h MTT assay)
MCF7	31.30 nM ± 2.72
T47D	22.15 nM ± 1.35
ZR-75-1	40.87 nM ± 0.01
SKBR3	20.41 nM ± 0.90
MDA-MB 468	22.94 nM ± 2.75
MDA-MB 231	> 10 μM

Table 6.3: Mean GI₅₀ ± SD values of 5F 203. Cells were seeded in 96 well plates at a density of 2.5×10^3 cells/well. After allowing time to adhere (24 h), cells were exposed to 5F 203 (72 h; (n = 8)). Mean and SD of trials ≥ 3 .

Interestingly, it was found that the HER2 overexpressing SKBR3 cell line was the most sensitive towards 5F 203, out of the panel of breast cancer cell lines tested (GI₅₀ = 20.41 nM). MDA-MB 468 and T47D cell lines were also sensitive. It has been shown previously that this agent is very active in ER+ cell lines and also in TNBC MDA-MB 468 cells [92] [95] [141]. In contrast, TNBC MDA-MB 231 was resistant to 5F 203 and similar insensitivity to benzothiazoles has been shown by this cell line previously [95]. However, the sensitivity of all cell lines is shown to be based on cytosolic AhR expression levels [141]. Further, mutations in the CYP1A1 promoter may also lead to agent insensitivity [92]. As SKBR3 and MDA-MB 468 cell lines were highly sensitive to 5F 203, these cell lines were selected to analyse the combination effect of 5F 203 with MS agents.

6.2.4 Effects of 5F 203 and MS agents in combination

6.2.4.1 *In vitro* growth inhibitory effects of 5F 203 and MS agents in combination

All 3 MS agents were combined with 5F 203 and 3 concentrations were selected of each agent according to activity in the most sensitive cell line. The concentrations selected for 5F 203 were 4 nM, 10 nM and 20 nM equivalent to 0.2, 0.5 and 1x GI₅₀ concentrations respectively in the SKBR3 cell line.

Concentrations for MS-73 were selected as 6 nM, 15 nM and 30 nM. Concentrations for MS-74 were selected as 60 nM, 150 nM and 300 nM while for MS-76 were selected as 600 nM, 1500 nM and 3000 nM equivalent to GI₅₀ values in the MDA-MB 468 cell line. It was determined that both MDA-MB 468 and SKBR3 cell lines with the agent combinations showed a CI value of > 1.1 which indicated an antagonistic result.

It has been shown that AhR ligands are able to stimulate ERK activity *via* the RAS/MAPK pathway [297] [298]. Further RAS/MAPK family members such as SAPK/JNK and p38 are also activated by AhR ligands [97]. Both SAPK/JNK and p38 have been implicated in many cellular processes including apoptosis. However, their role is shown to be cell type specific [65] [67]. Indeed, it has been demonstrated that 5F 203 is able to increase phosphorylation of ERK, JNK and p38 in ovarian cancer cells [137]. Moreover, MS agents do not inhibit the RAS/MAPK pathway [290]. Although both 5F 203 and MS agents were potent as single agents in both MDA-MB 468 and SKBR3 cells; in combination it could be suggested that an alternative pathway such as RAS/MAPK may be highly activated in these cells which would have

increased their proliferation and survival. Nonetheless, it has been found clinically that multi kinase blockade may lead to increased toxicity, therefore dual PI3K/mTOR inhibitors may not be well suited for combination therapy [299].

6.2.5 Effects of 5F 203 and Raloxifene in combination

6.2.5.1 *In vitro* growth inhibitory effects of 5F 203 and Raloxifene in combination

Raloxifene, a SERM has found to be an AhR ligand as mentioned before [115]. Raloxifene has been shown to activate AhR and induce apoptosis in MDA-MB 231 cells compared to non-transformed mammary epithelial cells, implying that AhR is a molecular target of Raloxifene which helps this agent to induce apoptosis in the absence of ER. Further, the induction of apoptosis in MDA-MB 231 cells has shown to be dependent upon the AhR expression levels within the cells and the levels of sensitivity to Raloxifene [141]. The activity of Raloxifene was tested in the panel of breast cancer cell lines (Chapter 3, table 3.1). All cell lines tested showed similar GI₅₀ values in medium supplemented with 10% FBS (MCF7 - 18.88 μ M, T47D - 16.76 μ M, ZR-75-1 - 15.75 μ M, SKBR3 - 19.22 μ M, MDA-MB 468 - 15.00 μ M and MDA-MB 231 - 16.81 μ M).

AhR, unlike most ligand-dependent transcription factors can be bound and activated by structurally varied ligands and these differences contribute to a variety of responses. These different responses elicited by the ligands have been linked to alterations in gene expression [300]. Thus, Raloxifene was combined with 5F 203 to determine activity

in ER- cell lines. Therefore, MDA-MB 468 and SKBR3 cell lines were chosen to determine the combined effect.

As before, the concentrations selected for 5F 203 were 4 nM, 10 nM and 20 nM equivalent to 0.2, 0.5 and 1x GI₅₀ concentrations respectively in the SKBR3 cell line. The concentrations selected for Raloxifene were 4 μM, 10 μM and 20 μM equivalent to 0.2, 0.5 and 1x GI₅₀ concentrations respectively in the SKBR3 cell line. The concentrations selected for Raloxifene were based on the effectiveness of the agent in the entire cell line panel, as all cell lines showed a similar sensitivity profile in medium supplemented with 10% FBS. It was found that both MDA-MB 468 and SKBR3 with the agent combination showed a CI value of > 1.1 which indicated an antagonistic result.

As both 5F 203 and Raloxifene are AhR ligands, it was postulated that there may be competitive binding to the AhR ligand binding pocket [300]. It has been shown that 5F 203 is a high affinity ligand to AhR [138]. One of the most high affinity AhR ligands is found to be TCDD [138]. Interestingly, the affinity of 5F 203 is similar to TCDD and the difference between 5F 203 and TCDD for AhR affinity is shown to be within 10-fold. [92] [138]. However, Raloxifene has shown a lower binding affinity compared to TCDD and high concentrations of Raloxifene are shown to be needed to activate AhR which suggests that 5F 203 is a higher affinity AhR ligand than Raloxifene [141].

The antagonistic effect of the combination of 5F 203 and Raloxifene could be due to Raloxifene exhibiting an antagonistic activity in the presence of a full agonist such as 5F 203, as Raloxifene is shown to have a low binding affinity to AhR [300]. Bazzi et al, 2009, has shown that TCDD in the presence of 5F 203 showed reduced potency for AhR compared to TCDD alone [138]. Further, they showed that in the presence of TCDD, 5F 203 acted as a partial agonist and showed decreased bioavailability [138]. A similar scenario could have taken place with the combination of 5F 203 and Raloxifene due to competition and perhaps the effect of Raloxifene is blocked after being competed out in the ER- cell lines tested.

6.2.6 Effects of 5F 203 and Gefitinib in combination

Cross talk between AhR and EGFR pathways has been identified [61] [301]. The AhR ligand, TCDD has shown to activate EGFR in certain cells that overexpress EGFR [61]. In addition, Sutter et al, 2009, has shown that EGFR ligands such as EGF could block AhR signalling by decreasing TCDD-induced CYP1A1 levels to basal levels in human keratinocytes by preventing recruitment of p300 (A histone acetyltransferase) coactivator [96]. Studies have shown that p300 which interacts with a variety of transcription factors, binds to ARNT in the AhR-ARNT complex and it plays a role in control of gene transcription [96]. In contrast, the EGFR inhibitor, Gefitinib that blocks EGFR expression is shown to activate p300 in skin carcinoma cells and is able to induce cell death [301]. However, these effects of TCDD, EGF and Gefitinib and the associated ability of induction of CYP1A1 could be cell type specific [61] [96]. CYP1A1 has shown to play a role in breast cancer. It has been found as a candidate gene for low penetrance of breast cancer susceptibility as CYP1A1 metabolises

xenobiotics, carcinogens and as well as oestrogen [61] [302]. Further, around 8 genetic polymorphisms of CYP1A1 have been identified [303]. It has been reported that these CYP1A1 polymorphisms function as predictors of the clinical outcome to EGFR inhibitors in patients with advanced lung cancer. Therefore, these genetic polymorphisms could be associated with CYP1A1 inducibility which would determine the outcome of the metabolised agent [301] [303].

Interestingly, it has been shown that Gefitinib induces CYP1A1 activity which is associated with bioactivation of the drug through drug metabolism in Gefitinib sensitive cells [301]. Other EGFR inhibitors such as Erlotinib, Cetuximab and Lapatinib have also shown induction of CYP1A1 activity, however, Gefitinib has shown much higher induction than the other EGFR inhibitors in sensitive cells [301]. Although, Gefitinib and Erlotinib share similar chemical structures, it has been shown that these agents are metabolised by slightly different CYP enzymes [304]. For instance CYP1A2 and CYP1B1 are not shown to be involved in Gefitinib metabolism whereas CYP1A2 has shown to have a slight impact on Erlotinib metabolism [301] [304]. Further, MEK inhibitors of the RAS/MAPK pathway have demonstrated induction of high levels of CYP1A1 activity whereas PI3K/AKT/mTOR inhibitors have not shown any CYP1A1 induction in drug metabolism which could further explain the reason for antagonistic results of the MS agents and 5F 203 in combination [301].

It has been implied that induction of CYP1A1 expression by Gefitinib may be associated with inhibition of downstream EGFR signalling such as RAS/MAPK signal transduction, because agents inhibiting the RAS/MAPK pathway have been shown to induce high levels of CYP1A1. This is not the case for inhibitors of the PI3K/AKT/mTOR pathway. Indeed it was found that 1x and 2x GI₅₀ concentrations of Gefitinib abolished phosphorylated ERK1/2 in SKBR3 cells and this was described in chapter 3 which would be a good indicator that this agent may induce CYP activity (Chapter 3, figure 3.12). In this context inhibition of the RAS/MAPK pathway might represent an association between EGFR inhibition and induction of CYP1A1 [301]. Further, as it was outlined before hypoxia increases ERK activation which thereby suppresses CYP1A1 activity. Hypoxia is mediated through HIF-1. HIF-1 helps hypoxic tumour cells to maintain energy production [305]. Moreover, HIF-1 has shown a strong correlation between elevated levels of tumour metastasis, angiogenesis and poor patient prognosis and resistance to anti-cancer therapy. HIF-1 is a heterodimeric transcription factor composed of HIF-1 α and HIF-1 β [305]. HIF-1 β which is also known as ARNT is an important AhR binding partner [92] [298]. As such, under hypoxia, HIF-1 β (aka ARNT) is dimerised to HIF-1 α and presumably not available for dimerisation with AhR [305]. Inhibition of ERK will reverse this effect. Furthermore, 5F 203 is shown to induce CYP1A1 activity and promote anti-tumour activity [94]. Thus, Gefitinib and 5F 203 were combined to determine their activity. To carry out this task, 2 sensitive cell lines to both Gefitinib and 5F 203 were selected - SKBR3 and MDA-MB 468. In addition a cell line which was sensitive to 5F 203 but resistant to Gefitinib was selected, which was MCF7 and another cell line that was resistant to both agents were also selected - MDA-MB 231.

6.2.6.1 *In vitro* growth inhibitory effects of 5F 203 and Gefitinib in combination

Initially, *in vitro* growth inhibitory activity was determined. For combination studies, the concentrations selected for 5F 203 were 4 nM, 10 nM and 20 nM and the concentrations selected for Gefitinib were 0.2 μ M, 0.5 μ M and 1 μ M. The selected concentrations were based on 0.2x, 0.5x and 1x GI₅₀ concentrations of both agents against the SKBR3 cell line, since it was the most sensitive cell line to 5F 203 and Gefitinib alone among the cell lines tested.

Interestingly, it was found that both agents in combination showed a CI value of 0.64 \pm 0.08 in SKBR3 cells, which is indicative of synergism according to the Chou and Talalay theorem [273]. In contrast, MDA-MB 468, MCF7 and MDA-MB 231 cell lines showed a CI value of > 1.1 which was antagonistic. SKBR3 cells demonstrated extremely significant sensitivity to the agents alone at the 2 highest concentrations tested of 5F 203 (20 nM) and Gefitinib (1 μ M) ($P < 0.0001$). Further, agents in combination resulted in extremely significant growth inhibition of SKBR3 cells (observed growth) compared to the expected growth inhibition with all tested concentrations of the agent combination ($P < 0.0001$). Further in combination, 5F 203 and Gefitinib demonstrated a dose dependent growth inhibition where increasing concentrations of the 2 agents resulted in increased growth inhibition in sensitive SKBR3 cells. (Figure 6.8 (a) and (b)).

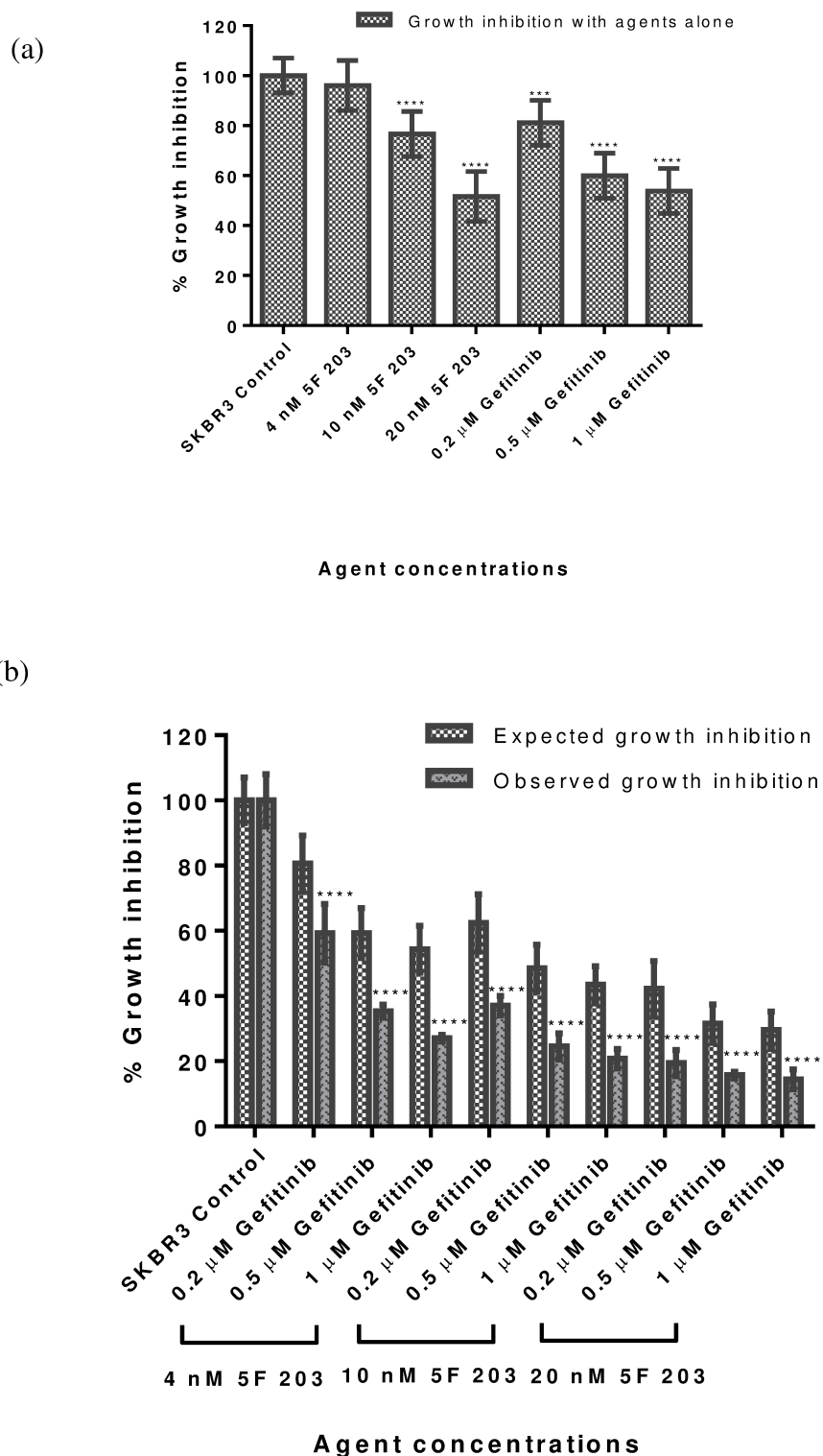


Figure 6.8: *In vitro* growth inhibitory effects of 5F 203 and Gefitinib (a) alone and (b) in combination against the SKBR3 cell line. Mean and SD of representative experiments are shown (n = 8 per trial); trials ≥ 3 . * indicates significant difference compared to control, * (P < 0.05), ** (P < 0.01), *** (P < 0.001), **** (P < 0.0001).

6.2.6.2 Effects of 5F 203 and Gefitinib alone and in combination on SKBR3 colony formation

In order to further investigate the synergistic effects of the agent combination on SKBR3 colony formation, a clonogenic assay was carried out. SKBR3 cells were treated with agents alone (0.5x GI₅₀ and 1x GI₅₀ which is equivalent to 0.5 μM and 1 μM of Gefitinib respectively and 0.5x GI₅₀ and 1x GI₅₀ which is equivalent to 10 nM and 20 nM of 5F 203 respectively). SKBR3 cells were also treated with agents in combination as shown below for 24 h (Figure 6.9).

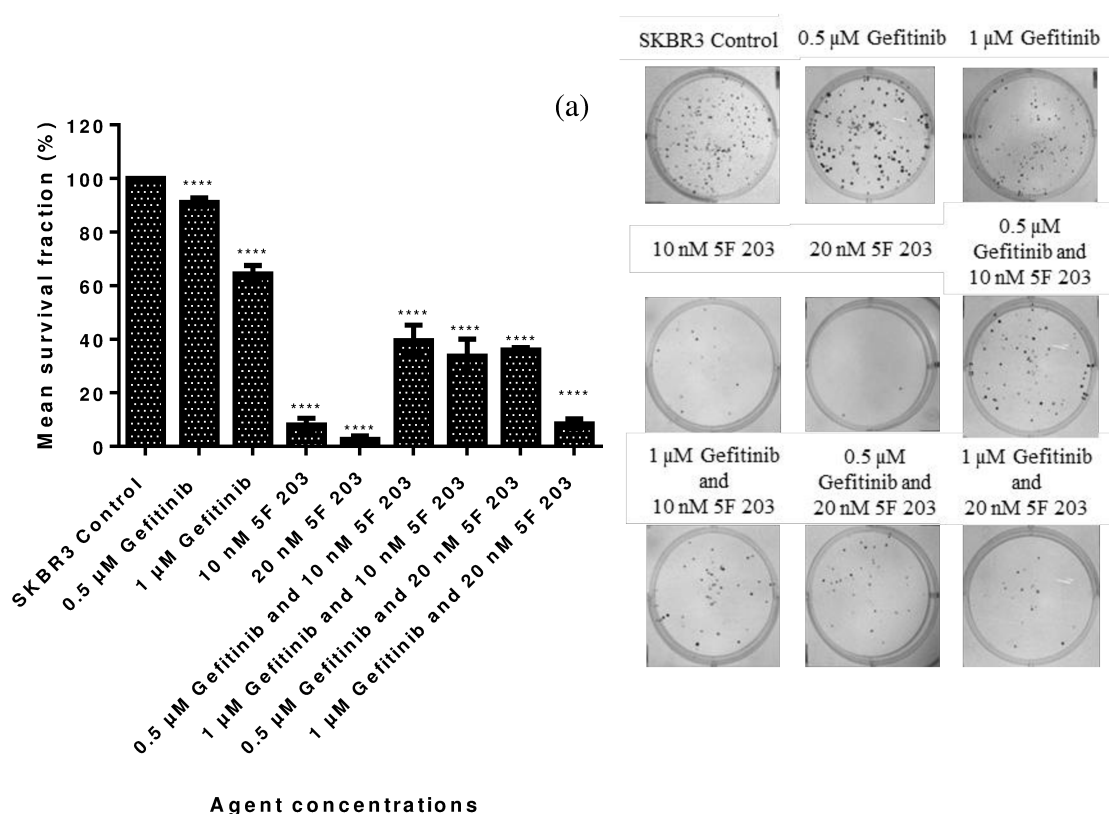


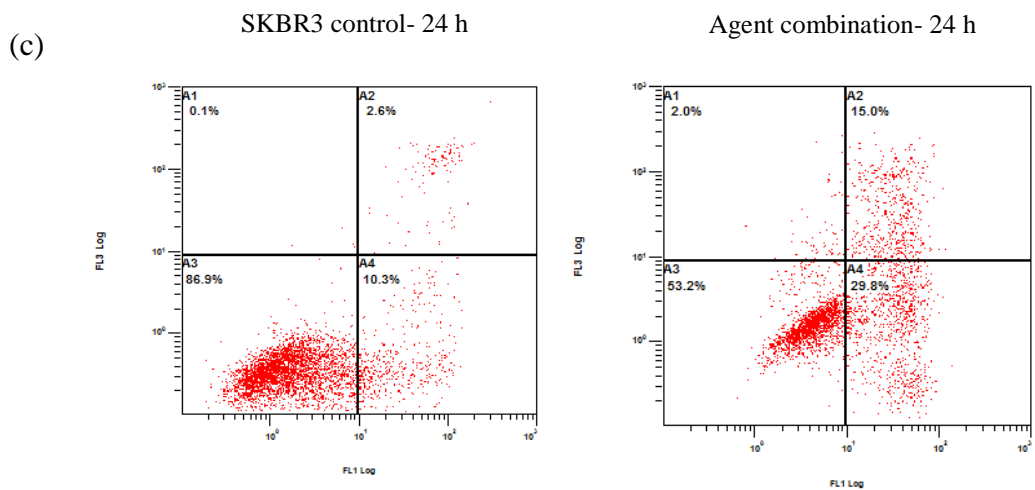
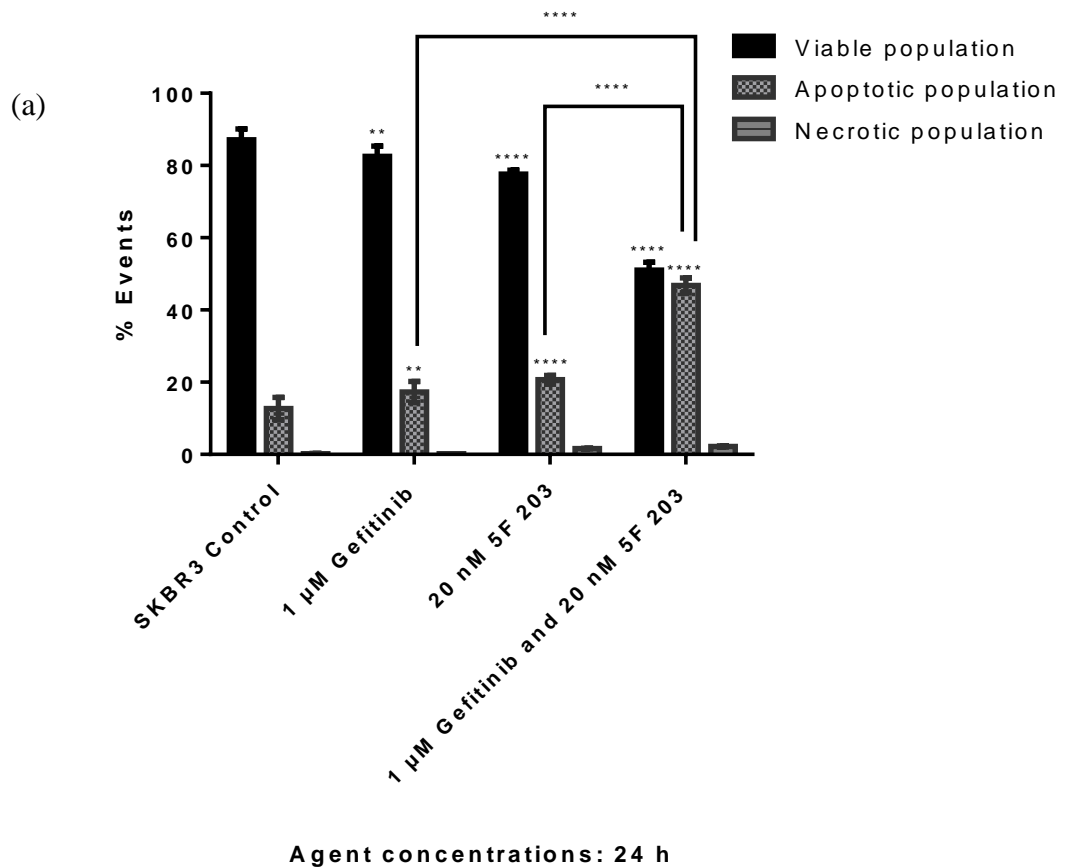
Figure 6.9: Effects of 5F 203 and Gefitinib in combination on SKBR3 colony formation. (a) Representative images of colony formation after exposure to 5F 203 and Gefitinib alone and in combination. Mean SF as % plating efficiency of control represented as the mean \pm SD of trials \geq 3, (n = 3 per trial). * indicates significant reduction, * (P < 0.05), ** (P < 0.01), *** (P < 0.001), **** (P < 0.0001) in colony formation.

Gefitinib alone at 0.5 μM demonstrated a SF of 91.11% and 1 μM of the same agent demonstrated a SF of 64.44% compared to control ($P < 0.0001$). In contrast 5F 203 alone at 10 nM (SF = 8%) and 20 nM (SF = 2.67%) demonstrated very potent cytotoxic effects compared to control ($P < 0.0001$). Agents in combination showed a significant reduction in SKBR3 colony formation at the tested concentrations compared to Gefitinib alone (both 0.5 μM and 1 μM) ($P < 0.0001$). Surprisingly agents in combination of 0.5 μM Gefitinib and 10 nM 5F 203 (SF = 39.56%) and also 1 μM Gefitinib and 10 nM 5F 203 (SF = 33.78%) did not demonstrate a reduction in colony formation compared to 10 nM of 5F 203 alone, which illustrated antagonistic results ($P < 0.0001$). Similarly, 0.5 μM Gefitinib and 20 nM of 5F 203 (SF = 36%) failed to demonstrate a reduction in colony formation compared to 20 nM 5F 203 alone ($P < 0.0001$), once again showing an antagonistic result. However, there was no significant difference seen between the colony formation of 20 nM 5F 203 alone and the combination of 1 μM Gefitinib and 20 nM 5F 203 (SF = 8.44%). Thus, among the combinations tested, 1 μM Gefitinib and 20 nM of 5F 203 were selected for further investigations as this combination also showed high potency in the MTT assay as well. Although, it was anticipated, synergism was not observed with this assay as 5F 203 alone was extremely potent in SKBR3 colony inhibition. However, colony formation at all tested concentrations were significantly reduced compared to SKBR3 control ($P < 0.0001$).

6.2.6.3 Effects of 5F 203 and Gefitinib alone and in combination on SKBR3

cellular apoptosis

To determine the cytotoxic effect in detail, flow cytometric analysis was carried out using an annexin V-FITC/PI assay with 24 h and 72 h exposure points which coincides with the exposure times of the clonogenic and MTT assays respectively. It was found that at 24 h, Gefitinib alone (17.27%) and 5F 203 alone (20.70%) showed a greater apoptotic population compared to SKBR3 control (12.73%) ($P < 0.0001$). Interestingly, it was found that at 24 h the agents combination (1x GI_{50} of both agents, equivalent to 1 μ M Gefitinib and 20 nM 5F 203) showed an extremely significant total apoptotic population (46.83%) compared to both agents alone and SKBR3 control ($P < 0.0001$). Intriguingly, at 24 h the expected apoptotic population was 25.24% while the observed was 46.83% endorsing the synergistic effect observed within the *in vitro* growth inhibitory MTT assays. At 72 h, Gefitinib alone demonstrated a significant apoptotic population (25.33%) compared to SKBR3 control (16.90%) ($P < 0.001$). Interestingly, 5F 203 alone demonstrated a high apoptotic population (63.93%) compared to control ($P < 0.0001$). Agents in combination also showed a high apoptotic population (67.95%) compared to control and Gefitinib alone ($P < 0.0001$). However there was no significant observed difference between the apoptotic populations evoked by 5F 203 alone and agents in combination at 72 h. Further, it was found that the expected apoptotic population for the agent combination was 72.36% while the observed was only 67.95% which is suggestive of an antagonistic apoptotic effect at 72 h. In addition, there was no significant necrosis identified at both time points tested (Figure 6.10).



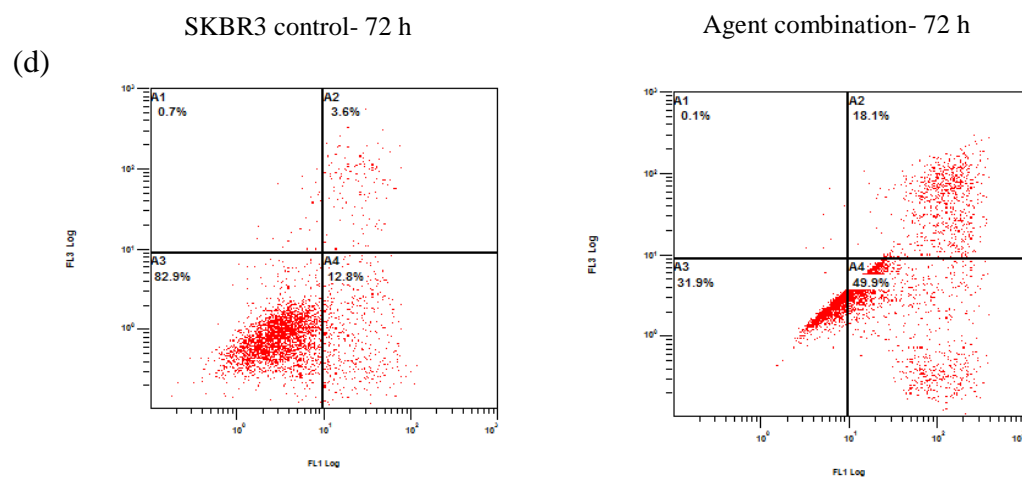
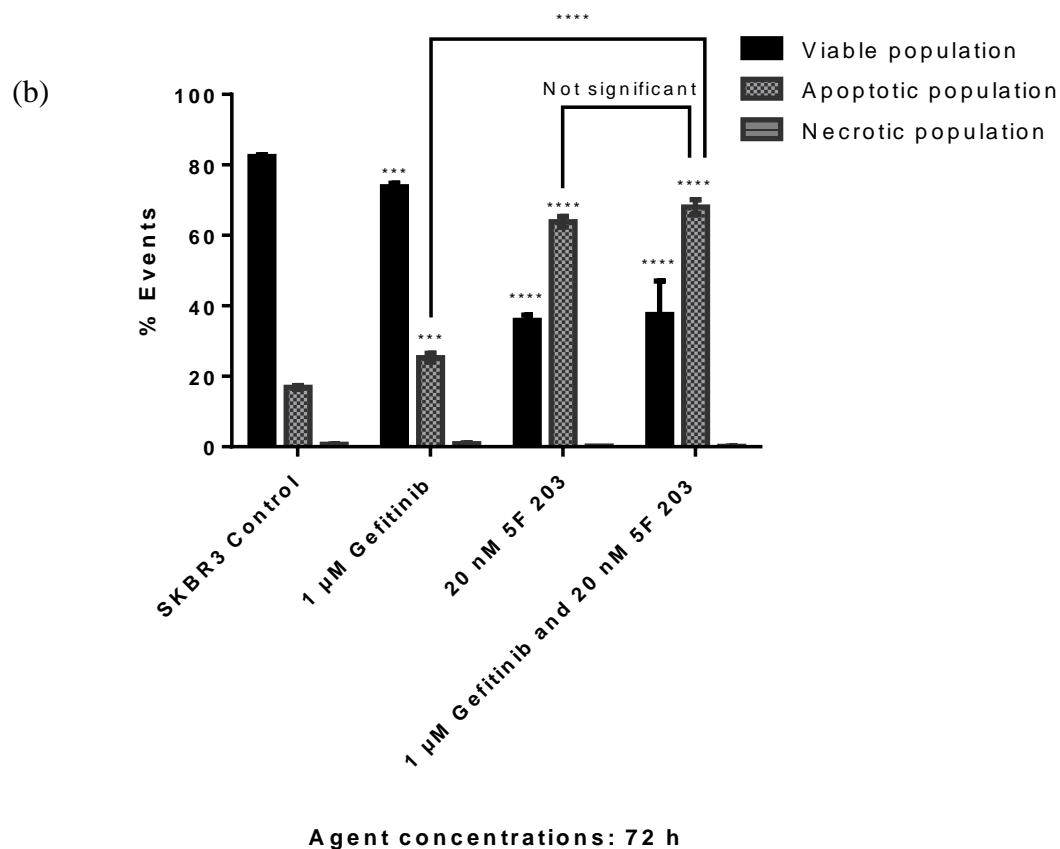


Figure 6.10: Apoptosis analysis of SKBR3 cells following exposure to 5F 203 and Gefitinib alone and in combination. (a) 24 h and (b) 72 h. Mean and SD of trials ≥ 3 , ($n = 2$ per trial). * indicates significant difference compared to control and agents alone, * ($P < 0.05$), ** ($P < 0.01$), *** ($P < 0.001$), **** ($P < 0.0001$). (c) and (d) are representative quadrant plots of control and agent combination, 10,000 events were analysed in each experiment.

These results confirm that 5F 203 alone and in combination evoked apoptosis in SKBR3 cells synergistically at 24 h. However, at 72 h the observed levels were less than expected for the agent combination. It was found that the effect of 1x and 2x GI₅₀ values of Gefitinib evoked a largely cytostatic and a moderate cytotoxic response in sensitive SKBR3 cells in chapter 3. Only at 48 h, a small significant apoptotic population was emerging with a 9.33% increase compared to control by Gefitinib alone as described in chapter 3. Further, at 72 h, a 12.93% increase was observed than control in Gefitinib treated SKBR3 cells. Results described within this chapter corroborate with these results, although, there is a slight difference which could be due to different passage numbers of SKBR3 cells used. At 24 h, 1x GI₅₀ Gefitinib evoked only 4.54% greater apoptosis than control, and at 72 h, Gefitinib evoked an increase of 8.43% in apoptosis. Thus, these results demonstrate that the effect of Gefitinib was potentiated by combining 5F 203 with it in the apoptotic assay. Indeed, it has been demonstrated that activation of the AhR signalling pathway by 5F 203 triggers metabolic transformation of the drug through CYP1A1 into reactive species damaging DNA that ultimately results in apoptosis in sensitive cells [92] [93]. This was an interesting finding because it has been portrayed that *TP53* mutant cells such as SKBR3 cells show greater resistance against DNA manipulating agents [209] [269] [306]. Nevertheless, it was noted that 5F 203 activity is independent of *TP53* status since this agent has demonstrated its potent activity in *TP53* mutant MDA-MB 468 cells [137].

As it was mentioned above induction of CYP1A1 by 5F 203 can lead to generation of ROS which results in DNA damage and then successively apoptosis in sensitive cells

[137]. On the other hand as outlined in chapter 3, it was shown that Gefitinib is able to down-regulate EGFR and RAS/MAPK pathways, thereby inhibiting cellular proliferation and causing apoptosis in SKBR3 cells. Therefore, the mechanism of action of the agents in combination was examined in detail as the agent combination evoked a high level of apoptosis in SKBR3 cells. Thus, the level of mRNA translation (CYP1A1 and EGFR), the effects of ROS generation, induction of DNA damage and protein expression levels of the main targets of EGFR and RAS/MAPK signalling, in agent combination treated SKBR3 cells were investigated.

6.2.6.4 Effects of 5F 203 and Gefitinib alone and in combination on CYP1A1 and EGFR mRNA translation

It has been shown that CYP1A1 protein inducibility is strongly associated with its genetic expression [301]. Thus, QPCR was incorporated to produce quantitative data of the gene expression levels of *CYP1A1*. Further, because Gefitinib was responsible of inhibition of EGFR, the genetic expression of *EGFR* was also determined by QPCR. SKBR3 cells were treated with agents alone (1x GI₅₀) and in combination (1x GI₅₀ of each agent) prior to QPCR analysis (Figure 6.11).

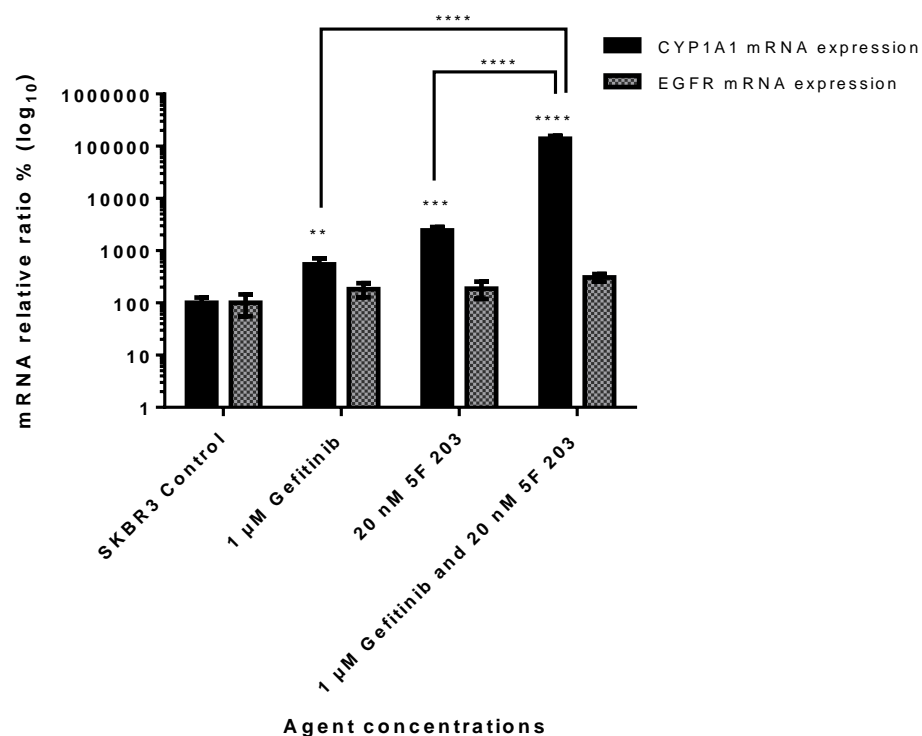


Figure 6.11: mRNA expression levels of *CYP1A1* and *EGFR* after exposure to 5F 203 and Gefitinib alone and in combination for 24 h in SKBR3 cells. Fluorescence was recorded and normalised to the expression of *GAPDH* and the relative expression of each gene's mean and SD was calculated; trials ≥ 3 , ($n = 3$ per trial). * indicates significant difference compared to control and agents alone, * ($P < 0.05$), ** ($P < 0.01$), *** ($P < 0.001$), **** ($P < 0.0001$).

It was observed that Gefitinib caused a slight increase in CYP1A1 mRNA expression (~ 5-fold higher than control) although not significant. These results were interesting and confirmed that Gefitinib induces CYP1A1 activity in relation to drug metabolism in Gefitinib sensitive SKBR3 cells [301]. For 5F 203 alone, CYP1A1 mRNA translation was increased by ~ 24-fold relative to control. On the other hand, the agents in combination enhanced CYP1A1 mRNA translation remarkably with ~ 1385-fold relative to SKBR3 control ($P < 0.0001$). Further, agents in combination also showed enhanced CYP1A1 mRNA translation compared to agents alone ($P < 0.0001$). On the

contrary, mRNA levels of EGFR among treated SKBR3 cells were not significantly different compared to control. Protein expression levels of CYP1A1 and EGFR were also investigated by Western blotting to determine the correlation between mRNA and protein expression levels. These results are shown in section 6.2.6.7.

These results strongly confirm that the synergism observed with Gefitinib and 5F 203 in combination was possibly due to the induction of CYP1A1 expression in SKBR3 cells. This observation would propose that monitoring CYP1A1 induction in HER2 overexpressed breast tumours may provide a biomarker for identification of sensitive tumour phenotypes to 5F 203 inhibition in the clinic.

6.2.6.5 Effects of 5F 203 and Gefitinib alone and in combination on induction of ROS

As it was outlined before, 5F 203 has shown to generate ROS in sensitive cells by induction of CYP1A1 [137]. Thus, the effects of ROS generation was determined. A moderate increase of ROS is known to evoke malignant transformation of cells, but the development of cancer may depend on many more factors including the extent of DNA damage [307]. Nevertheless, ROS can act as a double edged sword in a malignant state where very high levels of ROS is shown to be therapeutically beneficial by inducing cancer cell apoptosis [269] [308]. For instance, Paclitaxel induces ROS in breast cancer cells [309]. Hence, the induction of ROS was investigated by 1x GI₅₀ of Gefitinib and 5F 203 alone and in combination (Figure 6.12).

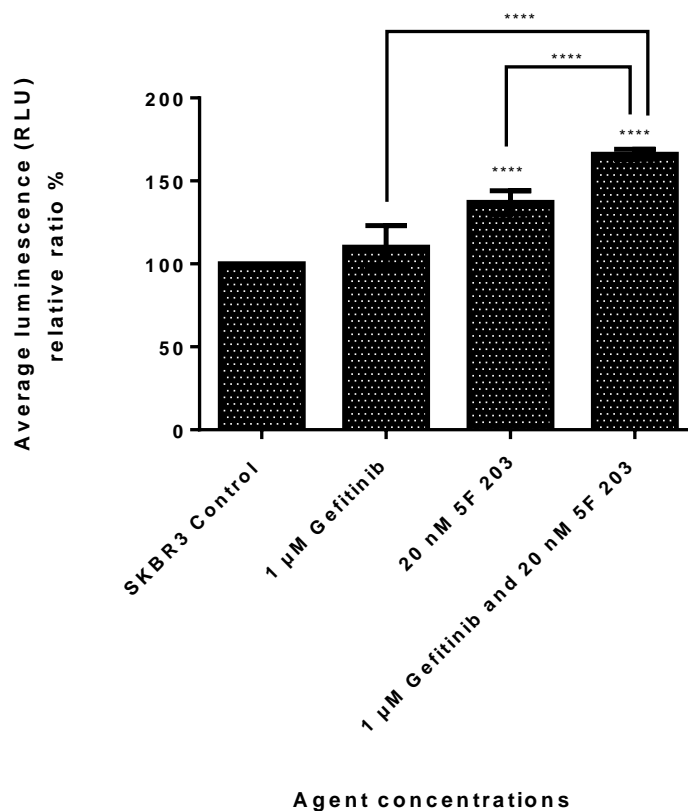


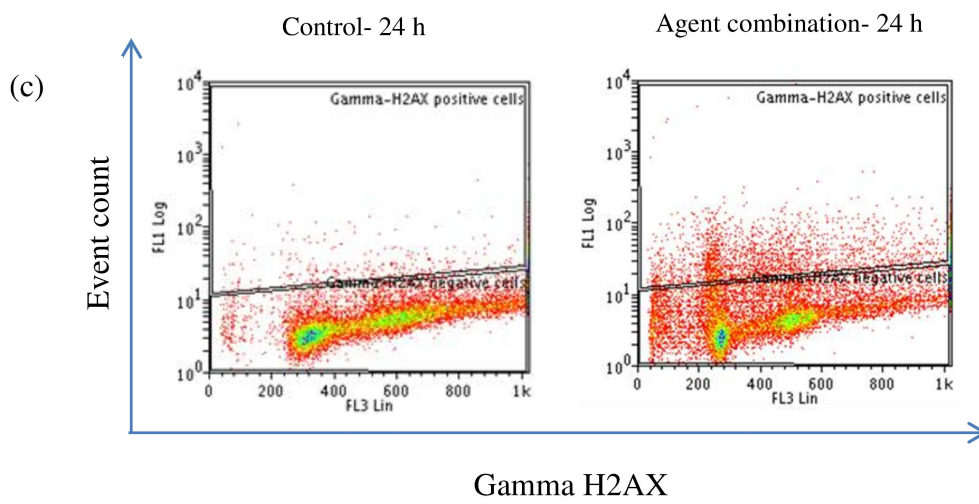
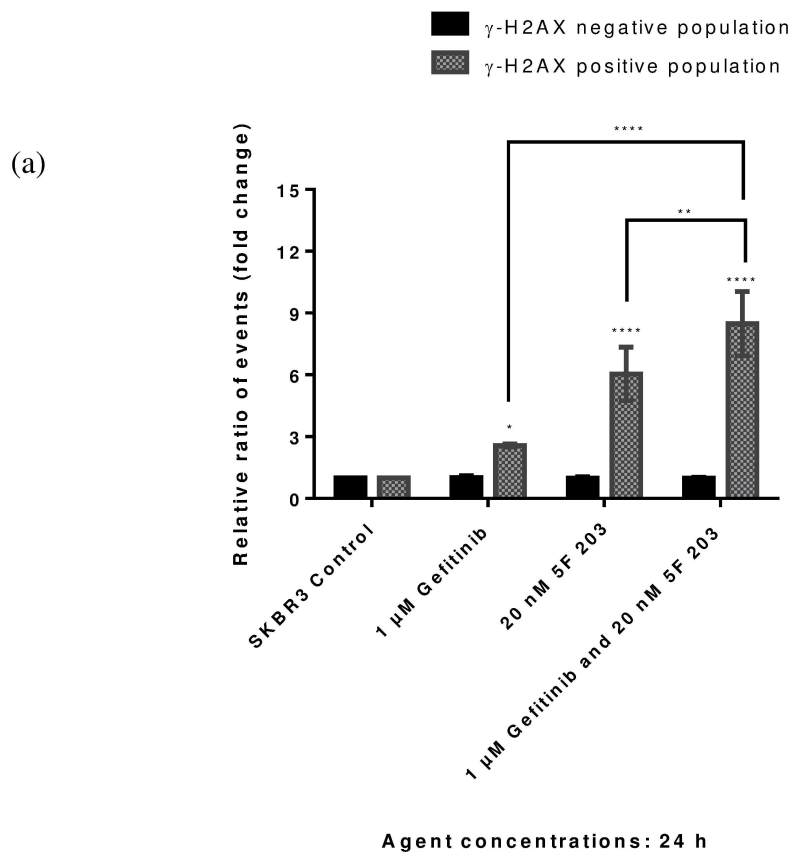
Figure 6.12: Induction of ROS following exposure to 5F 203 and Gefitinib alone and in combination for 24 h in SKBR3 cells. Mean luminescence was recorded in relative light units (RLU) and relative ratios were calculated. SD were also calculated of trials ≥ 3 , ($n = 4$ per trial). * indicates significant difference compared to control and agents alone, * ($P < 0.05$), ** ($P < 0.01$), *** ($P < 0.001$), **** ($P < 0.0001$).

As shown in figure 6.12, agents in combination generated a larger level of ROS (166%) compared to control after 24 h which was significant ($P < 0.0001$). As stated in previous literature, it was observed that 1x GI_{50} of 5F 203 also generated ROS (137%) significantly ($P < 0.0001$) compared to control [137]. There was no significant ROS generation was observed for Gefitinib (110%) compared to control. Further, it was observed that agents in combination showed significant generation of ROS compared to Gefitinib alone and 5F 203 alone at 24 h ($P < 0.0001$) confirming the synergy observed within the MTT assay and the apoptosis assay. Subsequently, it was

determined whether the agents alone and in combination induced DNA damage in SKBR3 cells.

6.2.6.6 Effects of 5F 203 and Gefitinib alone and in combination on induction of γ -H2AX positive populations

It was investigated whether the agents alone and in combination would cause DDSBs. Thus, γ -H2AX expression was measured in SKBR3 cells following exposure to 1x GI₅₀ concentrations of Gefitinib and 5F 203 alone and in combination for 24 h and 72 h (Figure 6.13).



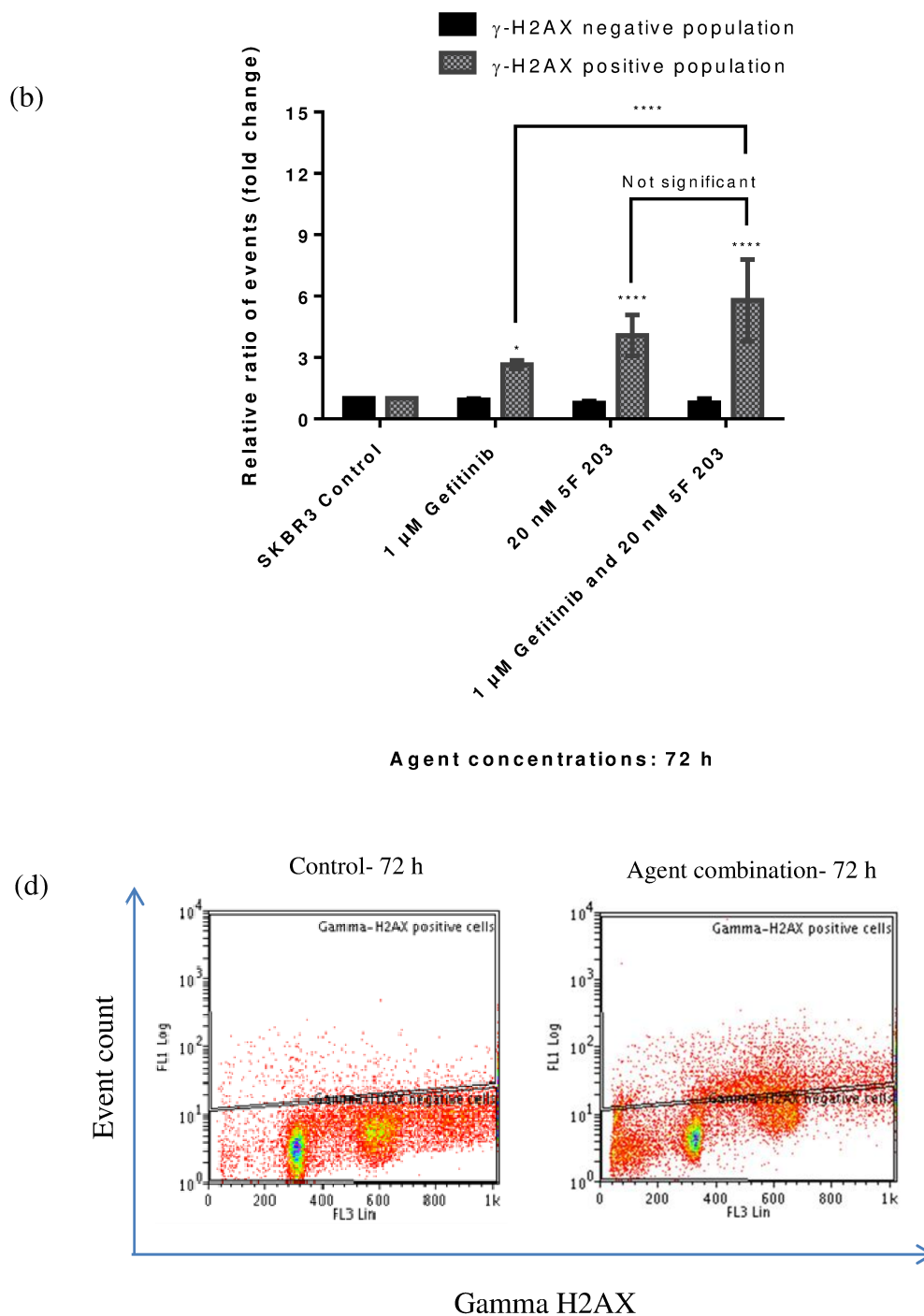


Figure 6.13: γ -H2AX analysis of SKBR3 cells following exposure to 5F 203 and Gefitinib alone and in combination. (a) 24 h and (b) 72 h. Relative ratio of events and SD of trials ≥ 3 , ($n = 2$ per trial). * indicates significant difference compared to control and agents alone, * ($P < 0.05$), ** ($P < 0.01$), *** ($P < 0.001$), **** ($P < 0.0001$). (c) and (d) are representative graphs of control and agent combination, 10,000 events were analysed in each experiment.

As shown in figure 6.13, 5F 203 alone showed an increased positive population for DDSBs at 24 h (~ 6-fold) and 72 h (~ 4-fold) relative to control ($P < 0.0001$). Gefitinib alone also showed a slight increase in DNA damage relative to control at both 24 h (~ 2.6-fold) and 72 h (~ 2.7-fold) in SKBR3 cells. Agents in combination demonstrated an enhanced positive population for DDSBs at 24 h (~ 8.5-fold) and 72 h (~ 5.8-fold) relative to SKBR3 control ($P < 0.0001$). However, these findings show that the agents in combination induced a slightly higher level of DNA damage at 24 h which would have led to high level of SKBR3 cell death at 24 h. Agents in combination showed significant DNA damage compared to Gefitinib at both time points ($P < 0.0001$). Further, the agents in combination showed a significant difference between the levels of DDSBs compared to 5F 203 alone only at 24 h ($P < 0.01$) and not at 72 h which validates the results observed with the apoptosis assay.

6.2.6.7 Effects of 5F 203 and Gefitinib alone and in combination on EGFR, HER2, RAS/MAPK and c-MET signalling pathways by Western blotting

The effect of Gefitinib and 5F 203 (1x GI₅₀ concentrations) alone and in combination (1x GI₅₀ concentrations of each agent) on protein expression of EGFR, RAS/MAPK and c-MET signalling pathways were investigated further through Western blot analysis. As it was demonstrated in chapter 3, Gefitinib is extremely active in inhibiting the SKBR3 cell line that overexpresses HER2, with the presence of EGFR. In addition it was also found that AhR ligands could enhance the activity of EGFR. Thus, the effect of the agents in combination were investigated on the protein expression of EGFR and HER2 levels [61] [189]. Further, the protein expression of CYP1A1 was evaluated. These protein expression results helped to validate the mRNA expression levels of the QPCR analysis. Protein expression levels of ERK1/2 of the RAS/MAPK pathway was also investigated as ERK1/2 was shown to be associated with the induction of CYP1A1 expression [301].

Furthermore, there has been evidence of cross talk between EGFR and c-MET. EGFR ligands are found to activate c-MET which results in synergistic activation of EGFR and c-MET pathways [310]. In addition c-MET and HER2 have also shown to synergise in promoting tumour growth. Overexpression and activation of c-MET is an independent predictor of poor prognosis in breast cancer [75] [310]. From a therapeutic point, inhibition of EGFR and HER2 by Gefitinib could provide cancer cells to shift their growth dependence to alternative receptor mediated pathways such as c-MET and demonstrate resistant mechanisms [75]. In actual fact, amplification of

c-MET has found to lead to Gefitinib resistance [101]. Furthermore, previous research has shown that hypoxic conditions can induce c-MET expression in many cancer cells which is mediated through HIF-1. In fact, 2 different binding sites for HIF-1 have been identified on the promoter of c-MET [311]. This demonstrates the association of c-MET and AhR signalling since HIF-1 β is also known as ARNT [305]. Moreover, hypoxia is shown to induce ERK activation as well [298]. Therefore, the effect of agents alone and in combination on these modulators were investigated by Western blots (Figure 6.14). Densitometry analysis with the ARD values for the significant results are shown in appendix I under section 9.1.3.2.

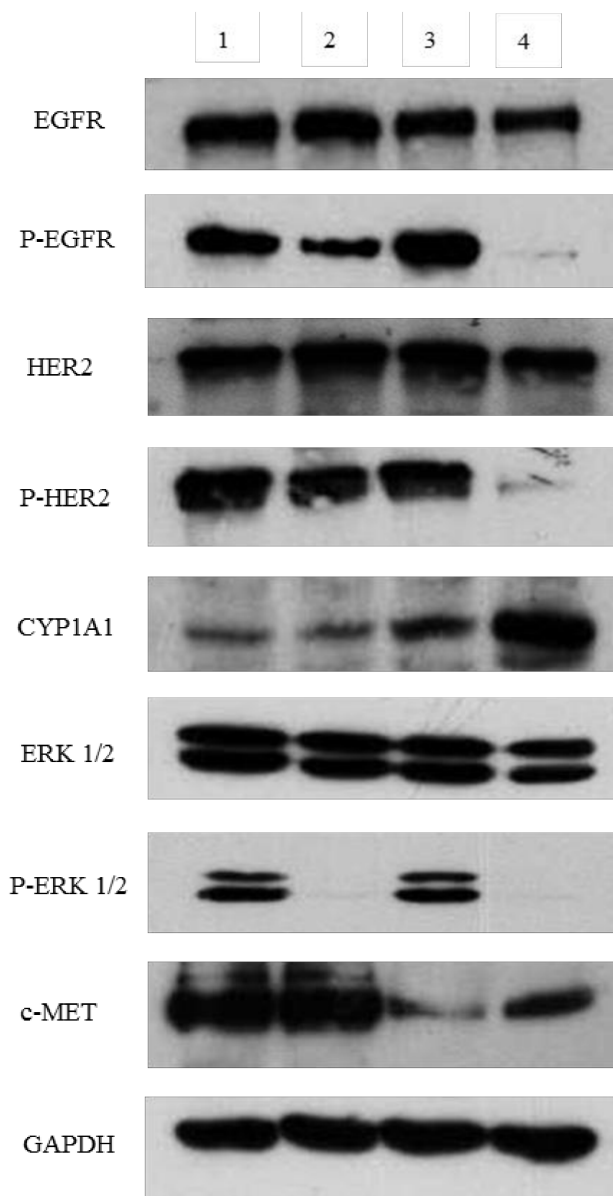


Figure 6.14: Western blot analysis of the effects of 5F 203 and Gefitinib alone and in combination for 24 h in SKBR3 cells. EGFR, P-EGFR (175 kDa), HER2, P-HER2 (185 kDa), CYP1A1 (58 kDa), ERK1/2, P-ERK1/2 (44 and 42 kDa), c-MET (140 and 170 kDa) and GAPDH (37 kDa). GAPDH was probed as a loading control and adjusted relative densities (ARD) were calculated. (1) Control, (2) 1x GI₅₀ - Gefitinib (3) 1x GI₅₀ - 5F 203 (4) Gefitinib and 5F 203 in combination (1x GI₅₀ each). Representative blots are shown; experiments were conducted ≥ 3 times. SKBR3 whole cell protein lysates (50 μ g) were subjected to 10% SDS-polyacrylamide gel electrophoresis.

It was observed that Gefitinib alone decreased P-EGFR levels (ARD – 57.49%) ($P < 0.0001$) whereas 5F 203 alone slightly increased P-EGFR levels (ARD – 115.89%) compared to control ($P < 0.05$). Interestingly, there was a remarkable reduction in P-EGFR levels (ARD – 5.36%) by the agents in combination compared to agents alone and control ($P < 0.0001$). Further, agents alone did not demonstrate a significant reduction in P-HER2 levels, in stark contrast the agents in combination portrayed a remarkable reduction in P-HER2 levels (ARD – 5.25%) compared to SKBR3 control ($P < 0.0001$). However, there was no significant difference observed in the protein expression levels of total EGFR and HER2 by agents alone or by the combination.

As expected CYP1A1 protein expression was increased with exposure of cells to 5F 203 (1x GI_{50} concentration) compared to control (ARD – 141.82%) ($P < 0.05$). In contrast, Gefitinib did not show a significant increase of CYP1A1 expression levels compared to control cells in the Western blot analysis, compared to QPCR analysis. Agents in combination, remarkably enhanced the CYP1A1 protein expression levels (ARD – 385.40%) compared to control ($P < 0.0001$). It has been stated that the quantification of both mRNA and protein levels are complementary and is not redundant; measurements taken from both are necessary for a complete understanding of how the cell works [312]. Although mRNA is eventually translated into protein, and it can be assumed that there should be an association between the level of mRNA and that of protein, it has been depicted that, complicated and varied posttranscriptional mechanisms are most often involved in turning mRNA into protein, and there can be differences between mRNA translation and protein expression [312]. In fact, although, these results correspond with the results of the

mRNA expression levels of CYP1A1 confirming that the mRNA levels have been transferred into proteins, there is a slight difference between the 2 levels. For instance, there was no difference between the CYP1A1 protein expression levels for Gefitinib treatment and control.

As portrayed in chapter 3, results within this chapter showed that Gefitinib alone completely abolished P-ERK1/2 expression (ARD – 1.40%) in relative to control ($P < 0.0001$). Although the results are not significant, it was also observed that 5F 203 alone reduced P-ERK1/2 expression very faintly (ARD – 89.15%) compared to control. Intriguingly, the agents in combination almost abolished P-ERK1/2 expression levels (ARD – 1.18%) ($P < 0.0001$). Total ERK1/2 levels were not altered.

In addition, it was found that 5F 203 alone was able to extremely significantly decrease the expression levels of c-MET in SKBR3 cells compared to control (ARD – 16.77%) ($P < 0.0001$) and the agents in combination also reduced c-MET levels compared to control but the reduction was not as low as 5F 203 alone (ARD – 37.61%) ($P < 0.0001$). In contrast, Gefitinib alone was not able to alter c-MET levels in SKBR3 cells.

These findings were extremely interesting, as outlined before induction of CYP1A1 by Gefitinib is shown to be associated with increased drug metabolism. However, this increased metabolism has been shown to reduce the level of intracellular Gefitinib in

sensitive cells [301]. Hence, from the results of this study it can be suggested that in the presence of 5F 203 which induces CYP1A1 activity, the rate of Gefitinib metabolism increases to a level where Gefitinib could persist for a longer period of time within the cells and increase Gefitinib's pharmacological action. Indeed, this strategy leads to enhanced inhibition of phosphorylation of EGFR and HER2 in SKBR3 cells by the agents in combination which works synergistically compared to Gefitinib alone [101]. These results add to a body of data which suggests synergism between 5F 203 and Gefitinib.

In addition, it was interesting to observe that 5F 203 alone slightly increased P-EGFR that corroborates with previous literature, which describes that AhR ligands enhances EGFR expression levels [61]. Thus, these results demonstrate the importance of the combination of Gefitinib and 5F 203 which could work synergistically to inhibit cross talk between EGFR and AhR. Further, an association was stated between inhibition of this RAS/MAPK pathway and CYP1A1 induction [301]. Thus, inhibition of P-ERK1/2 by Gefitinib would induce CYP1A1 expression which would synergistically work together with 5F 203 which also induces expression of CYP1A1 that ultimately leads to apoptosis of SKBR3 cells.

Western blot results showed that 5F 203 alone down-regulated c-MET expression in SKBR3 cells significantly. These results suggest that 5F 203 treatment may be preventing ARNT's activity as HIF-1 β [305]. Depletion of ARNT impedes HIF-1 composition which is induced by hypoxic conditions, increasing expression and

activity of c-MET and also ERK1/2 [305]. This could be also the reason for observing a slight reduction of P-ERK1/2 in SKBR3 cells after exposure to 5F 203 alone, although not significant. In addition, it has been found that Gefitinib inhibits events induced by hypoxia in Gefitinib sensitive cells [301]. However, there was no reduction of c-MET observed with Gefitinib treatment alone. In point of fact, Gefitinib is not known to be a c-MET inhibitor. Nevertheless, the agent combination effectively down-regulated c-MET expression significantly. This may certainly prevent resistant mechanisms due to up-regulation of compensatory pathways. Inhibition of EGFR and HER2 by Gefitinib alone may provide cancer cells with an 'escape hatch' enabling cancer cells to move their growth dependence to a different receptor activated pathway such as c-MET and evade therapy enabling therapeutic resistance [75]. In cancer it is most unlikely that inhibition of one molecular target alone will provide substantial therapeutic benefit. Thus, this combination undoubtedly minimises cross talk and feedback loops that comprises in the complex HER family associated signalling network [143]. Thus, experimental evidence from this study suggests that, combining 5F 203 with Gefitinib may demonstrate synergistic effects in the inhibition of HER2 overexpressing SKBR3 breast cancer cells.

6.3 Conclusion

Cellular pathways have been shown to have complex interactions which when perturbed demonstrate redundant mechanisms for survival. Therefore, targeting just one overexpressed protein in breast cancer may not always result in an optimal outcome [143] [272]. Thus, this chapter explored 4 combination options for breast cancer.

Although, Sirolimus and CGP57380 as single agents have shown to be effective in breast cancer, Sirolimus together with CGP57380 showed an antagonistic result in the panel of breast cancer cell lines [117] [187]. In order to obtain a better effect of Sirolimus or CGP57380 it could be combined with another PI3K/AKT or RAS/MAPK inhibitor.

MS agents showed potent inhibitory effects both in *PTEN* deficient MDA-MB 468 and HER2 overexpressing SKBR3 cells. MS-73 was the most potent, while MS-74 was moderately potent and MS-76 was the least potent. It was found that all 3 agents tested significantly inhibited P-4E-BP1 of the mTOR pathway but was not able to inhibit the PI3K/AKT pathway in MDA-MB 468 cells at the tested concentrations. In contrast MS-73 down-regulated P-AKT while all 3 agents down-regulated P-4E-BP1 in SKBR3 cells.

An abundance of evidence demonstrates the importance of AhR in dictating tumorigenic outcomes, suggesting that therapeutic manipulation of AhR in human cancer is on the horizon [91]. For instance, aminoflavone an AhR ligand has shown potent inhibitory effects in breast cancer cell lines and these agents have reached clinical trials [313]. In the current study the AhR ligand, 5F 203 was tested in the panel of breast cancer cell lines and it was found to be potent in the HER2 overexpressing SKBR3 cell line. This agent was combined with MS agents, Raloxifene and Gefitinib. MS agents together with 5F 203 and Raloxifene together with 5F 203 showed an antagonistic effect in MDA-MB 468 and SKBR3 cell lines. In contrast, the

combination of 5F 203 and Gefitinib elicited synergy in SKBR3 growth inhibition, mainly by 5F 203 potentiating the effect of Gefitinib. The mechanism involved enhanced induction of CYP1A1 mRNA and protein expression. Subsequently it was observed that the agents in combination generated ROS which led to DNA damage (DDSB) in SKBR3 cells at 24 h. This ultimately resulted in a large apoptotic response in SKBR3 cells which inhibited SKBR3 cell growth at 24 h. Thus, 5F 203 in combination with Gefitinib may offer a potential novel treatment for HER2 overexpressing breast cancer.

7 Chapter 7 - General discussion, Conclusion and Future directions

7.1 General discussion

The genetic heterogeneity of breast cancer has led to the clinical development of a large number of targeted therapeutics including TKIs and monoclonal antibodies that target the HER family. One of the major challenges in the clinical development of these therapies is to identify the appropriate patient populations most likely to benefit from these therapies. The currently identified molecular subtypes of breast cancer sets the stage to identify breast cancer patient populations who may respond to these specific targeted treatment options. Although, this molecular classification is still evolving and has a lack of standardised molecular class prediction method, it is indeed a powerful new classification system which can be incorporated in the clinic [18]. Further, this classification could be used to retool existing clinical therapies. Many agents that show initial promising activity against a particular biological target may be discarded due to low efficacy and toxicity. Thus, identifying specific subgroups that will benefit from these existing clinical therapies would be ideal. The effect of EGF which is the ligand of EGFR, was evaluated using the panel of breast cancer cell lines that represent the molecular subtypes of breast cancer. This is because it has been previously shown that many growth factors including EGF, play a role in the development of the mammary gland and also in both ER+ and ER- breast cancer [51] [120] [170]. Culture medium and serum are supplemented with biomolecules associated with growth promoting effects [169]. These growth promoting effects are essential for the growth and regulation of cancer cells *in vitro*. It has been shown

previously that certain cancer cells, invariably demonstrate a reduced dependence on exogenous mitogenic growth factors since they are able to generate many of their own mitogenic growth stimulatory signals [172]. Therefore, initially the effect of medium supplemented with depleted (2%) and normal (10%) levels of FBS on the breast cancer cell line panel were evaluated to understand how each cell line would behave in culture. MCF7 (ER+) and MDA-MB 468 (ER-) cell lines showed significant growth in serum depleted (2% FBS) medium suggesting no correlation with ER status and that these cells are able to stimulate their own growth factors even in a harsh environment compared to the rest of the cell lines. Out of all the cell lines tested, the HER2 overexpressing, *TP53* deficient SKBR3 cell line which is categorised under the HER2 molecular subtype appeared to be the most sensitive to EGF in medium supplemented with 10% FBS. Further, the SKBR3 cell line was found to be the most sensitive to the EGFR TKI, Gefitinib in medium supplemented with 10% FBS. However, Erlotinib which is also an EGFR TKI, was not effective in any of the cell lines tested in the current study, although both Gefitinib and Erlotinib share similar chemical structures [304]. There is evidence of cross talk between the HER family and ER [87]. Thus, the effect of Raloxifene which is a second generation SERM which has shown to have fewer side effects than Tamoxifen was evaluated against the panel of breast cancer cell lines [115]. However, it was found that Raloxifene did not exert growth inhibitory effects in the breast cancer cell line panel. This agent is also found to function as an AhR ligand [10]. Thus, its action as an AhR ligand was evaluated which is discussed further below.

As EGF and Gefitinib were potent in the HER2 overexpressing SKBR3 cell line, the effect of these agents were evaluated in more detail using this cell line. Clonogenic assays demonstrated that both agents induced a moderate cytotoxic effect together with a cytostatic effect at 1x and 2x GI₅₀ concentrations of EGF and Gefitinib by reducing colony size and inhibiting SKBR3 colony formation. Both EGF and Gefitinib treatment down-regulated P-EGFR in SKBR3 cells significantly while only Gefitinib down-regulated P-HER2 levels significantly. Further, downstream RAS/MAPK and PI3K/AKT pathways were down-regulated with EGF and Gefitinib treatment leading to cell cycle arrest and small significant apoptotic populations in SKBR3 cells with prolonged treatment. The rational selection of breast cancer patients for EGFR TKIs still remains a challenge. Thus, these results may provide experimental evidence that EGF and Gefitinib could improve outcomes of breast cancer patients that fall into the HER2 molecular subtype. However, the effect of EGF on HER2 overexpressing breast cancer merits additional studies.

Although, Gefitinib is used in the clinic to treat patients currently, its therapeutic window is drastically narrowed by poor bioavailability, acquired resistance and systemic toxicity [123]. Thus, to minimise these effects this agent was encapsulated within H-AFt NPs by diffusion. TfR1 is highly expressed in cancer cells compared to normal human cells and these receptors are found to be associated with the uptake of H-AFt [222]. Thus, TfR1 receptors were considered as a targeting molecule. This novel agent was tested against the Gefitinib sensitive SKBR3 cell line and it was found that H-AFt-encapsulated-Gefitinib demonstrated slightly reduced potency compared to Gefitinib alone at 72 h which implied that encapsulated Gefitinib may require time

to be released from the H-AFt cavity. Interestingly, a longer exposure time showed increased anti-tumour activity in the SKBR3 cell line compared to Gefitinib alone supporting the hypothesis that the H-AFt cage allows controlled release of drug molecules which is a characteristic of a successful nanotechnology drug delivery system. Further, H-AFt-encapsulated-Gefitinib was successfully taken up by SKBR3 cells in a manner similar to Gefitinib alone. Thus, encapsulation of Gefitinib in H-AFt may reduce off target toxicities and decrease drug deposition in normal tissues. This agent might be a promising agent in the clinic.

HER2 overexpression in breast cancer is mostly associated with an aggressive phenotype [51]. Although Trastuzumab improved the outcome of HER2+ breast cancer, it is associated with the development of resistance [55]. Thus, novel targeting therapies especially agents that fall into the category of nanomedicine will be beneficial to treat HER2+ breast cancers. The mechanism of action of 2 novel HER2 targeting agents - H-AFt-fusion protein and L-AFt-fusion protein was explored and it was found that the H-AFt-fusion protein was more effective in inhibiting SKBR3 cell growth and proliferation compared to the L-AFt-fusion protein. SKBR3 cells failed to proliferate and form colonies in the presence of the H-AFt-fusion protein suggesting that this agent has a highly cytotoxic effect compared to Trastuzumab which showed a moderate cytotoxic and a cytostatic effect. Further, this novel agent inhibited the expression levels of total and phosphorylated HER2 extremely significantly which resulted in significant down-regulation of RAS/MAPK, PI3K/AKT and JAK/STAT pathways. This again, led to reduced orchestrations of cell cycle events and a high level of apoptosis in SKBR3 cells. Further, co-expression of 2 or more HER family

members has shown to be correlated with an aggressive phenotype in breast cancer. Interestingly, it was found by protein microarray analysis, that this novel H-AFt-fusion protein is able to inhibit not just HER2 but also P-EGFR, HER3 and P-HER3. This suggests inhibition of mitogenic heterodimerisation of the HER receptors. Thus, this novel agent is an attractive nanodrug for HER2 overexpressing breast cancer.

The heterogeneity of breast cancer rarely depends on the aberrant expression or function of a single receptor or a signalling pathway but depends on a considerable capacity for compensatory cross talk between signalling pathways. Thus, a combination therapy approach was explored and several agents in combination were tested [143]. As outlined before, eIF4E of the mTOR pathway plays a key regulatory role in initiating mRNA translation. mTOR directly phosphorylates 4E-BP1 which thereby increases functional eIF4E [79]. Sirolimus which is known as an mTOR inhibitor, is found to inhibit 4E-BP1 phosphorylation resulting in suppression of cap dependent mRNA translation [277]. Paradoxically, it has also been shown that, Sirolimus in fact increases eIF4E phosphorylation secondary to inhibition of 4E-BP1 phosphorylation. Additionally, MNK1 and MNK2 which are activated by the RAS/MAPK pathway are also found to phosphorylate eIF4E. Previously, it has been shown that eIF4E phosphorylation by mTOR inhibitors is abolished only when both MNK1 and MNK2 were knocked out, suggesting that mTOR inhibitors increase MNK dependent phosphorylation of eIF4E [277]. Thus, a strategy to improve the efficacy of Sirolimus would be to combine it with a MNK inhibitor. Thus, the activity of Sirolimus together with CGP57380 which is an inhibitor of MNK1 and MNK2, was

tested on the panel of breast cancer cell lines. Unexpectedly, agents in combination, showed an antagonistic result according to the CI method of Chou and Talalay.

The PI3K/AKT pathway is commonly deregulated in cancer with the most common events being mutations or increased gene copy numbers of the *PIK3CA* gene or mutations or loss of expression of the *PTEN* gene [314]. Thus, inhibiting PI3K, in cancer remains an attractive strategy. Furthermore, it has been demonstrated that the PI3K/AKT pathway is paradoxically activated following mTOR inhibition [277]. Therefore, inhibition of both PI3K and mTOR together provides a compelling rationale for testing dual PI3K/mTOR kinase inhibitors in breast cancer [77]. Hence, 3 dual PI3K/mTOR agents (MS-73, MS-74 and MS-76) were tested against the panel of breast cancer cell lines. MS-73 currently has entered clinical trials, while MS-74 and MS-76 are novel analogues of MS-73. MS-73 showed the highest potency while MS-74 showed moderate potency and MS-76 showed the least potency against the panel of breast cancer cell lines. Interestingly, MDA-MB 468 cell line which is TNBC, *PTEN* and *TP53* deficient (categorised under the basal molecular subtype) was the most sensitive towards all 3 agents tested. Further, it was also found that HER2 overexpressing SKBR3 cells were unable to form large number of colonies in the presence of 1500 nM of MS-73 and MS-74. In this regard, the activity of the 3 agents were further evaluated by using MDA-MB 468 and SKBR3 cell lines. MS-73 caused large significant apoptotic populations in both MDA-MB 468 and SKBR3 cell lines. Interestingly the novel analogue, MS-74 also caused similar significant apoptotic populations in both cell lines which was observed in cell cycle and apoptosis experiments as well. All 3 agents significantly down-regulated P-4E-BP1 in MDA-

MB 468 and SKBR3 cells confirming that these agents inhibited the mTOR pathway by down-regulating P-4E-BP1. However, all 3 agents failed to down-regulate the PI3K/AKT pathway in MDA-MB 468 cells at the tested concentrations. In contrast, 2x GI₅₀ MS-73, down-regulated P-AKT (Ser473) and P-AKT (Thr308) marginally in SKBR3 cells. However, higher concentrations of these agents may down-regulate this pathway significantly. Thus, these results would suggest that, indeed these novel agents function as dual PI3K/mTOR inhibitors and also that the novel analogues MS-74 and MS-76 have similar activity to MS-73, but with reduced potency.

AhR is the main transcriptional regulator of CYP1A1 and it has been shown previously that 5F 203 which is an experimental AhR ligand induces AhR signalling in sensitive breast cancer cells [92]. The effect of 5F 203 was tested against the panel of breast cancer cell lines; the HER2 overexpressing SKBR3 cell line was the most sensitive towards 5F 203. AhR is shown to cross talk with a number of key signalling pathways in breast cancer including EGFR and RAS/MAPK. Alternately, signalling molecules down stream of EGFR such as PI3K is known to be involved in cross talk with the RAS/MAPK pathway and may be responsive to AhR ligands [61] [297]. Thus, a number of agents were combined with 5F 203 to determine the combination effect. The effect of MS agents in combination with 5F 203 demonstrated an antagonistic effect according to the CI method of Chou and Talalay. In addition, Raloxifene which is found to function as an AhR ligand was tested in combination with 5F 203. It has been previously shown that Raloxifene, activates AhR and induces apoptosis in ER- cell lines such as MDA-MB 231 cells [141]. Therefore, the activity of Raloxifene was tested in combination with 5F 203 in ER- cell lines in this study. MDA-MB 468 and

SKBR3 cell lines were chosen. An antagonistic result was found according to the CI method of Chou and Talalay. As mentioned above AhR and EGFR cross talk has been identified [61]. It has been demonstrated that the EGFR inhibitor Gefitinib induces CYP1A1 activity which is associated with drug metabolism in Gefitinib sensitive cells [301]. 5F 203 also induces CYP1A1 activity [92]. Thus, the effects of the agents in combination were determined by MTT assays. Intriguingly, it was found that the agents in combination showed a CI value of 0.68 ± 0.08 which is indicative of synergism according to the Chou and Talalay method in sensitive SKBR3 cells. It was found that agents in combination showed a remarkable level of CYP1A1 induction by QPCR analysis which was ~ 1385-fold higher, relative to control SKBR3 cells. These results corroborated with the results of the protein expression levels of CYP1A1. Further, the agents in combination generated ROS which resulted in greater DDSBs in SKBR3 cells at 24 h. This led to a large apoptotic population at 24 h. In fact, the total apoptotic population observed (46.83%) was higher than the expected total population (25.24%) at 24 h confirming the synergistic effect observed within the MTT assay results. Furthermore, the agents in combination portrayed a greater inhibition of phosphorylation of EGFR and HER2 in SKBR3 cells compared to Gefitinib alone which would have been associated with enhanced persistence of Gefitinib in SKBR3 cells with the agents in combination; potentiating the effect of Gefitinib by 5F 203 [301]. c-MET expression was also down-regulated in SKBR3 cells treated with both Gefitinib and 5F 203 compared to Gefitinib alone, which certainly would minimise resistance, as it has been demonstrated previously that amplification of c-MET is correlated to Gefitinib resistance [101]. The agents in combination may offer a potent approach to controlling HER2 overexpressing breast tumours and could also help to delay or avoid acquired resistance to Gefitinib alone.

7.2 Conclusion

The work presented in this thesis analysed the activity of several pharmacological agents that targets the HER receptor family and the associated signal transduction network in relation to breast cancer. These agents included clinically available agents, experimental and completely novel agents. Inhibition of EGFR, HER2 and HER3 and the associated signalling pathways were achieved by existing clinical agents such as EGF and Gefitinib and novel agents such as H-AFt-fusion protein. Gefitinib was successfully encapsulated in H-AFt NPs to reduce toxicities associated with this agent and also to increase its bioavailability. HER2 overexpressing SKBR3 cell line was found to be the most sensitive towards all these agents which may indicate that breast cancer patients who fall into the HER2 molecular subtype may benefit from these therapies in the clinic. In line with the complexity of the signalling network a personalised combination therapy approach was explored. Thus, it was found that dual PI3K/mTOR inhibitor, MS-74 which is a novel analogue of MS-73 demonstrated potent activity similar to MS-73, against the MDA-MB 468 and SKBR3 cell lines, which may indicate that patients who fall into the basal or HER2 molecular subtypes will benefit from these MS agents. Further, an experimental AhR ligand, 5F 203 in combination with Gefitinib portrayed synergistic growth inhibition, mainly by 5F 203 potentiating the effect of Gefitinib in SKBR3 cells. This agent combination may also help to control HER2+ breast tumours in the clinic. These results are promising and may help to improve the understanding of the HER signalling network further. Similarly, it may also help to enhance the outcome of breast cancer patients with aggressive phenotypes by personalising the way in which these patients receive these therapies described, according to molecular subtypes of breast cancer.

7.3 Future directions

- In order to gain better understanding about the therapeutic window and also to determine the toxicity profile towards normal tissues, H-AFt-encapsulated-Gefitinib, H-AFt-fusion protein, MS agents and 5F 203 in combination with Gefitinib could be tested in human normal cell lines.
- Additional *in vitro* studies could be carried out, to understand the mechanism in which certain proteins of the HER family associated signalling network, such as PTEN, SAPK/JNK and p38 are perturbed by the agents tested in the study, especially EGF and H-AFt-fusion protein in breast cancer cells including SKBR3 cells.
- H-AFt disassembles completely at pH 2.0. As such, the effect of H-AFt-encapsulated-Gefitinib can be determined by disassembly of the H-AFt and the release of Gefitinib molecules with the use of stomach cancer cells since these cells may be accustomed to an acidic environment where the pH reaches low as pH 1.5 [246].
- The agents that demonstrated potent anti-cancer activity *in vitro*, including H-AFt-encapsulated-Gefitinib, H-AFt-fusion protein, MS agents and 5F 203 in combination with Gefitinib should be integrated into the clinical routine as the next step. Therefore, in order to integrate these agents into the clinical routine, these agents should be evaluated in 3-dimensional cultures or they should be evaluated using *in vivo* studies. In fact *in vivo*

models may provide a native microenvironment in which the tumour resides and these models might be more advantageous compared to studies carried out *in vitro* or in 3-dimensional cultures [315] [316].

- A combination therapy approach is shown to be potent in controlling and delaying acquired resistance. However, multi kinase blockade may lead to increased toxicities in the clinic [299]. Thus, nanoformulations can help avoid such limitations by carrying several therapies in combination. Therefore, agents such as 5F 203 and Gefitinib which has different pharmacological behaviour could be encapsulated in one NP and tested for its functionality. These NPs may carry an optimised synergistic drug ratio in a single NP to the targeted tumour.
- NP drug delivery systems offer revolutionary opportunities to develop highly effective personalised targeted therapy. As NPs are foreign materials the immune system may result in immunosuppression or immune stimulation which may at times bring unwanted responses [317]. However, AFt NPs have shown excellent activity *in vivo* with reduced toxicities, nevertheless the lack of human clinical trials regarding AFt associated agents may suggest insufficient information regarding its activity in humans as yet [228]. Thus, it could be investigated whether, ferritin from each breast cancer patient's body could be extracted, and carry out the process of removing the iron atoms and subsequently encapsulating with the pharmacological agent/s and testing for its functionality. This system would certainly enable personalisation of therapeutic regimens for each

breast cancer patient and ideally improve the field of nanomedicine which yet remains to reach its full potential.

8 References

1. Timothy J. Key, P.K.V.a.E.B., *Epidemiology of breast cancer*. The Lancet Oncology, 2001. **2**: p. 133-140.
2. Chiun-Sheng Huang, C.-H.L., Yen-Shen Lub and Chen-Yang Shen, *Unique features of breast cancer in Asian women—Breast cancer in Taiwan as an example*. Journal of Steroid Biochemistry & Molecular Biology, 2010. **118**: p. 300-303.
3. Mohammad Sorowar Hossain, S.F.a.H.E.K.-K., *Breast cancer in South Asia: A Bangladeshi perspective*. Cancer Epidemiology, 2014. **38**: p. 465-470.
4. Jacques Ferlay, I.S., Rajesh Dikshit, Sultan Eser, Colin Mathers, Marise Rebelo, Donald Maxwell Parkin, David Forman and Freddie Bray, *Cancer incidence and mortality worldwide: Sources, methods and major patterns in GLOBOCAN 2012*. International Journal of Cancer, 2014. **136**: p. E359-E386.
5. J. Ferlay, I.S., M. Ervik, D. Forman, F. Bray, R. Dikshit, S. Elser, C. Mathers, M. Rebelo and DM. Parkin. *GLOBOCAN 2012: Estimated cancer incidence, mortality and prevalence worldwide in 2012*. [cited 2015 01-08-2015]; Available from: <http://globocan.iarc.fr/>.
6. Nirmala Bhoo-Pathy, C.-H.Y., Mikael Hartman, Cuno S.P.M. Uiterwaal, Beena C.R. Devi, Petra H.M. Peeters, Nur Aishah Taib, Carla H. van Gils and Helena M. Verkooijen, *Breast cancer research in Asia: Adopt or adapt Western knowledge?* European Journal of Cancer, 2013. **49**: p. 703-709.
7. Joachim Schuz, C.E., Patricia Villain, Rolando Herrero, Maria E. Leon, Silvia Minozzi, Isabelle Romieu, Nereo Segnan, Jane Wardle, Martin Wiseman, Filippo Belardelli, Douglas Bettcher, Franco Cavalli, Gauden Galea, Gilbert Lenoir, Jose M. Martin-Moreno, Florian Alexandru Nicula, Jørgen H. Olsen, Julietta Patnick, Maja Primic-Zakelj, Pekka Puska, Flora E. van Leeuwen, Otmar Wiestler, Witold Zatonski and Working Groups of Scientific Experts, *European code against cancer 4th edition: 12 ways to reduce your cancer risk*. Cancer Epidemiology, 2015. **39**: p. S1–S10.
8. UK, C.R. *Breast cancer incidence*. [cited 2015 01-08-2015]; Available from: <http://www.cancerresearchuk.org/health-professional/cancer-statistics/>.
9. Ahmedin Jemal, F.B., Melissa M. Center, Jacques Ferlay, Elizabeth Ward and David Forman, *Global cancer statistics*. CA: A Cancer Journal for Clinicians, 2011. **61**: p. 69-90.
10. Washbrook, E., *Risk factors and epidemiology of breast cancer*. Women's Health Medicine, 2006. **3**: p. 1.
11. Libby M. Morimoto, E.W., Z. Chen, Rowan T. Chlebowski, Jennifer Hays, Lewis Kuller, Ana Marie Lopez, JoAnn Manson, Karen L. Margolis, Paola C. Muti, Marcia L. Stefanick and Anne McTiernan, *Obesity, body size, and risk of postmenopausal breast cancer: the Women's Health Initiative (United States)*. Cancer Causes and Control, 2002. **13**: p. 741-751.

12. K. McPherson, C.M.S.a.J.M.D., *ABC of breast diseases breast cancer-epidemiology, risk factors, and genetics*. British Medical Journal, 2000. **321**: p. 624-628.
13. Overmoyer, B., *Breast cancer screening*. Medical Clinics of North America, 1999. **83**: p. 1443-1466.
14. Thomas, J.M.D.a.J., *Breast cancer*, in *ABC of breast diseases*, J.M. Dixon, Editor. 2012, Wiley Blackwell.
15. Britta Weigelt, J.L.P.a.L.J.v.t.V., *Breast cancer metastasis: Markers and models*. Nature Reviews Cancer, 2005. **5**: p. 591-602.
16. Sina Kasraeian, D.C.A., Elke R. Ahlmann, Alexander N. Fedenko and Lawrence R. Menendez, *A Comparison of fine-needle aspiration, core biopsy, and surgical biopsy in the diagnosis of extremity soft tissue masses*. Clinical Orthopaedics and Related Research, 2010. **468**: p. 2992-3002.
17. Emad A Rakha, J.S.R.-F., Frederick Baehner, David J Dabbs, Thomas Decker, Vincenzo Eusebi, Stephen B Fox, Shu Ichihara, Jocelyne Jacquemier, Sunil R Lakhani, Jose Palacios, Andrea L Richardson, Stuart J Schnitt, Fernando C Schmitt, Puay-Hoon Tan, Gary M Tse, Sunil Badve and Ian O Ellis, *Breast cancer prognostic classification in the molecular era: the role of histological grade*. Breast Cancer Research, 2010. **12**: p. 207.
18. Michelle Alizart, J.S., Margaret Cummings and Sunil R Lakhani, *Molecular classification of breast carcinoma*. Diagnostic Histopathology, 2012. **18**: p. 97-103.
19. Baselga, M.J.H.a.J., *Targeted therapies for breast cancer*. The Journal of Clinical Investigation, 2011. **121**: p. 3797-3803.
20. Reed, L.W.a.M., *The role of surgery in the management of older women with breast cancer*. European Journal of Cancer, 2007. **43**: p. 2253-2263.
21. Curigliano, G., *New drugs for breast cancer subtypes: Targeting driver pathways to overcome resistance*. Cancer Treatment Reviews, 2012. **38**: p. 303-310.
22. Allison, K.H., *Molecular pathology of breast cancer, what a pathologist needs to know*. American Society for Clinical Pathology, 2012. **138**: p. 770-780.
23. Lajos Pusztai, C.M., Keith Anderson, Yun Wu and W. Fraser Symmans, *Molecular classification of breast cancer: Limitations and potential*. The Oncologist, 2006. **11**: p. 868-877.
24. Speirs, D.L.H.a.V., *Choosing the right cell line for breast cancer research*. Breast Cancer Research, 2011. **13**: p. 215.
25. Seho Park, J.S.K., Min Suk Kim, Hyung Seok Park, Jun Sang Lee, Jong Seok Lee, Seung Il Kim and Byeong-Woo Park, *Characteristics and outcomes according to molecular subtypes of breast cancer as classified by a panel of four biomarkers using immunohistochemistry*. The Breast, 2012. **21**: p. 50-57.
26. Parvin F. Peddi, M.J.E.a.C.M., *Molecular basis of triple negative breast cancer and implications for therapy*. International Journal of Breast Cancer, 2011. **2012**: p. 1-7.

27. Richard M. Neve, K.C., Jane Fridlyand, Jennifer Yeh, Frederick L. Baehner, Tea Fevr, Laura Clark, Nora Bayani, Jean-Philippe Coppe, Frances Tong, Terry Speed, Paul T. Spellman, Sandy DeVries, Anna Lapuk, Nick J. Wang, Wen-Lin Kuo, Jackie L. Stilwell, Daniel Pinkel, Donna G. Albertson, Frederic M. Waldman, Frank McCormick, Robert B. Dickson, Michael D. Johnson, Marc Lippman, Stephen Ethier, Adi Gazdar and Joe W. Gray, *A collection of breast cancer cell lines for the study of functionally distinct cancer subtypes*. *Cancer Cell*, 2006. **10**: p. 515-527.
28. Jordan, A.S.L.a.V.C., *MCF-7: The first hormone-responsive breast cancer cell line*. *Cancer Research*, 1997. **57**: p. 3071-3078.
29. Roger R. Beerli, D.G.-P., Kathie Woods-Cook, Xiaomei Chen, Yosef Yarden and Nancy E. Hynes, *Neu differentiation factor activation of ErbB-3 and ErbB-4 is cell specific and displays a differential requirement for ErbB-2*. *Molecular and Cellular Biology*, 1995. **15**: p. 6496-6505.
30. J. F. Glover, J.T.I.a.P.D.D., *Interaction of phenol red with estrogenic and antiestrogenic action on growth of human breast cancer cells ZR-75-1 and T-47-D*. *Cancer Research*, 1988. **48**: p. 3693-3697.
31. Kristina Subik, J.-F.L., Laurie Baxter, Tamera Strzepak, Dawn Costello, Patti Crowley, Lianping Xing, Mien-Chie Hung, Thomas Bonfiglio, David G. Hicks and Ping Tang, *The Expression patterns of ER, PR, HER2, CK5/6, EGFR, Ki-67 and AR by immunohistochemical analysis in breast cancer cell lines*. *Breast Cancer: Basic and Clinical Research*, 2010. **4**: p. 35-41.
32. ATCC. ZR-75-1. 2015 02-09-2015]; Available from: <http://www.lgcstandards-atcc.org/>.
33. Hurvitz, D.J.L.W.a.S.A., *Recent advances in the development of anti-HER2 antibodies and antibody-drug conjugates*. *Annals of Translational Medicine*, 2014. **12**: p. 1-14.
34. Deborah K. Armstrong, S.H.K., Yvonne L. Ottaviano, Yuzo Furuya, Julie A. Buckley, John T. Isaacs and Nancy E. Davidson, *Epidermal Growth Factor-mediated Apoptosis of MDA-MB-468 Human Breast Cancer Cells*. *Cancer Research*, 1994. **54**: p. 5280-5283.
35. Raymond M. Reilly, R.K., Jasbir Sandhu, Ying Wai Lee, Ross G. Cameron, Aaron Hendler, Katherine Vallis and Jean Garipey, *A comparison of EGF and mAb 528 labeled with 111 infor imaging human breast cancer*. *Journal of Nuclear Medicine*, 1999. **41**: p. 903-911.
36. Fabricio F. T. Barros, D.G.P., Ian O. Ellis and Andrew R. Green, *Understanding the HER family in breast cancer: interaction with ligands, dimerization and treatments*. *Histopathology*, 2010. **56**: p. 560-572.
37. Weinberg, D.H.a.R.A., *The hallmarks of cancer*. *Cell*, 2000. **100**: p. 57-70.
38. Kinzler, B.V.a.K.W., *Cancer genes and the pathways they control*. *Nature Medicine*, 2004. **10**: p. 789-799.
39. Weinberg, D.H.a.R.A., *Hallmarks of cancer: The next generation*. *Cell*, 2011. **144**: p. 646-674.

40. Schafer, K.A., *The cell cycle: A review*. Veterinary Pathology, 1998. **35**: p. 461-478.
41. Manfredi, L.E.G.a.J.J., *The p53 tumor suppressor participates in multiple cell cycle checkpoints*. Journal of Cellular Physiology, 2006. **209**: p. 13-20.
42. Ashley L. Hein, M.M.O.a.Y.Y., *Radiation-induced signaling pathways that promote cancer cell survival (Review)*. Journal of Oncology, 2014. **45**: p. 1813-1819.
43. Bhardwaj, N., *Harnessing the immune system to treat cancer*. The Journal of Clinical Investigation, 2007. **117**: p. 1130-1136.
44. Jr., R.R., *The ErbB/HER family of protein-tyrosine kinases and cancer*. Pharmacological Research, 2014. **79**: p. 34-74.
45. Rowinsky, J.S.d.B.a.E.K., *The ErbB receptor family: a therapeutic target for cancer*. Trends in Molecular Medicine, 2002. **8**: p. S19-S26.
46. Thomas Holbro, G.C.a.N.E.H., *The ErbB receptors and their role in cancer progression*. Experimental Cell Research, 2003. **284**: p. 99-110.
47. Gibson, E.S.H.a.S.B., *Surviving cell death through epidermal growth factor (EGF) signal transduction pathways: Implications for cancer therapy*. Cellular Signalling, 2006. **18**: p. 2089-2097.
48. Evans, A.K.K.a.T.R.J., *The epidermal growth factor receptor family in breast cancer*. OncoTargets and Therapy, 2008. **1**: p. 5-19.
49. Mina D. Marmor, K.B.S.a.Y.Y., *Signal transduction and oncogenesis by ErbB/HER receptors*. International Journal of Radiation Oncology, Biology, Physics, 2004. **58**: p. 903-913.
50. Hongtao Zhang, A.B., Qiang Wang, Geng Zhang, Jeffrey Drebin, Ramachandran Murali and Mark I. Greene, *ErbB receptors: from oncogenes to targeted cancer therapies*. The Journal of Clinical Investigation, 2007. **117**: p. 2051-2058.
51. I. Uberall, Z.K., R. Trojanec, J. Berkovcova and M. Hajduch, *The status and role of ErbB receptors in human cancer*. Experimental and Molecular Pathology, 2008. **84**: p. 79-89.
52. Stern, D.F., *ERBB3/HER3 and ERBB2/HER2 duet in mammary development and breast cancer*. Journal of Mammary Gland Biology and Neoplasia, 2008. **13**: p. 215-223.
53. N. Normanno, C.B., A. De Luca, M. R. Maiello and D. S. Salomon, *Target-based agents against ErbB receptors and their ligands: A novel approach to cancer treatment*. Endocrine-Related Cancer, 2003. **10**: p. 1-21.
54. J. Papewalis, A.Y.N.a.M.F.R., *G to A polymorphism at amino acid codon 655 of the human erbB-2/HER2 gene*. Nucleic Acids Research, 1991. **19**: p. 5452.
55. Jasniz, G.L.F.a.M.A., *Molecular mechanisms of Trastuzumab resistance in HER2 overexpressing breast cancer*. International Journal of Breast Cancer, 2011. **2011**: p. 1-11.

56. Anderson, G.S.a.L.M., *The ERBB3 receptor in cancer and cancer gene therapy*. Cancer Gene Therapy, 2008. **15**: p. 1-64.
57. Desbois-Mouthon, C., *The HER3/ErbB3 receptor: A promising target in cancer drug therapy*. Gastroenterologie Clinique et Biologique, 2010. **34**: p. 255-259.
58. D. M. Abd El-Rehim, S.E.P., C. E. Paish, J. A. Bell, R. S. Rampaul, R. W. Blamey, J. F. R. Robertson, R. I. Nicholson and I. O. Ellis, *Expression and co-expression of the members of the epidermal growth factor receptor (EGFR) family in invasive breast carcinoma*. British Journal of Cancer, 2004. **91**: p. 1532-1542.
59. Mass, R.D., *The HER receptor family: A rich target for therapeutic development*. International Journal of Radiation Oncology*Biology*Physics, 2004. **58**: p. 932-940.
60. Jiang Shou, S.M., C. Kent Osborne, Alan E. Wakeling, Simale Ali, Heidi Weiss and Rachel Schiff, *Mechanisms of Tamoxifen resistance: Increased estrogen receptor-HER2/neu cross-talk in ER/HER2-positive breast cancer*. Journal of the National Cancer Institute, 2004. **96**: p. 926-935.
61. Guofeng Xie, Z.P.a.J.-P.R., *Src-mediated aryl hydrocarbon and epidermal growth factor receptor cross talk stimulates colon cancer cell proliferation*. American journal of Physiology Gastrointestinal and Liver Physiology, 2012. **302**: p. 1006-1015.
62. A. S. Dhillon, S.H., O. Rath and W. Kolch, *MAP kinase signalling pathways in cancer*. Oncogene, 2007. **26**: p. 3279-3290.
63. Richard J. Santen, R.X.S., Robert McPherson, Rakesh Kumar, Liana Adam, Meei-Huey Jeng and Wei Yue, *The role of mitogen-activated protein (MAP) kinase in breast cancer*. Journal of Steroid Biochemistry and Molecular Biology, 2002. **80**: p. 239-256.
64. Sparano, T.L.a.J.A., *Inhibiting Ras signaling in the therapy of breast cancer*. Clinical Breast Cancer, 2003. **3**: p. 405-416.
65. Hiroshi Nishina, T.W.a.T.K., *Physiological roles of SAPK/JNK signaling pathway*. The Journal of Biochemistry, 2004. **136**: p. 123-126.
66. Lin, J.L.a.A., *Role of JNK activation in apoptosis: A double-edged sword*. Cell Research, 2005. **15**: p. 36-42.
67. Han, T.Z.a.J., *Activation and signaling of the p38 MAP kinase pathway*. Cell Research, 2005. **15**: p. 11-18.
68. Press, C.U. *The organisation and function of the Ras-Raf-Mek-Erk pathway*. 2002 [cited 2015 01-10-2015]; Available from: <http://journals.cambridge.org/>.
69. Shira Peleg Hasson, T.R., Larysa Ryvo and Ido Wolf, *Endocrine resistance in breast cancer: Focus on the phosphatidylinositol 3-kinase/akt/mammalian target of rapamycin signaling pathway*. Breast Care (Basel), 2013. **8**: p. 248-255.

70. Geoffrey I. Shapiro, K.M.B.-M., Julian R. Molina, Johanna Bendell, James Spicer, Eunice L. Kwak, Susan S. Pandya, Robert Millham, Gary Borzillo, Kristen J. Pierce, Lixin Han, Brett E. Houk, Jorge D. Gallo, Maria Alsina, Irene Brana and Josep Tabernero, *First-in-human study of PF-05212384 (PKI-587), a small-molecule, intravenous, dual inhibitor of PI3K and mTOR in patients with advanced cancer*. *Clinical Cancer Research*, 2015. **21**: p. 1-8.
71. MacDonald, N.E.H.a.G., *ErbB receptors and signaling pathways in cancer*. *Current Opinion in Cell Biology*, 2009. **21**: p. 177-184.
72. Antoinette Hollestelle, F.E., Jord H.A. Nagel, Wouter W. Kallemeijn and Mieke Schutte, *Phosphatidylinositol-3-OH kinase or RAS pathway mutations in human breast cancer cell lines*. *Molecular Cancer Research*, 2007. **5**: p. 195-201.
73. B. Weigelt, P.H.W.a.J.D., *PIK3CA mutation, but not PTEN loss of function, determines the sensitivity of breast cancer cells to mTOR inhibitory drugs*. *Oncogene*, 2011. **30**: p. 3222-3233.
74. Boulay, N.E.H.a.A., *The mTOR pathway in breast cancer*. *Journal of Mammary Gland Biology and Neoplasia*, 2006. **11**: p. 53-61.
75. David L. Shattuck, J.K.M., Kermit L. Carraway III and Colleen Sweeney, *Met receptor contributes to Trastuzumab resistance of Her2-overexpressing breast cancer cells*. *Cancer Research*, 2008. **68**: p. 1471-1477.
76. Tbatan. *The PI3K-AKT pathway proteins involved in tumourigenesis*. 2015 [cited 2015 01-10-2015]; Available from: https://en.wikipedia.org/wiki/File:PI3K-Akt_Pathways_with_a_role_in_Cancer.png.
77. Azab, S.S., *Targeting the mTOR signaling pathways in breast cancer: More than the rapalogs*. *Journal of Biochemical and Pharmacological Research*, 2013. **1**: p. 75-83.
78. Jinqiang Hou, F.L., Christopher Proud and Shudong Wang, *Targeting MNKs for cancer therapy*. *Oncotarget*, 2012. **3**: p. 118-131.
79. Shi-Yong Sun, L.M.R., Xuerong Wang, Zhongmei Zhou, Ping Yue, Haiyan Fu and Fadlo R. Khuri, *Activation of Akt and eIF4E survival pathways by rapamycin-mediated mammalian target of rapamycin inhibition*. *Cancer Research*, 2005. **65**: p. 7052-7058.
80. Plataniias, S.J.a.L.C., *Mnk kinase pathway: Cellular functions and biological outcomes*. *World Journal of Biological Chemistry*, 2014. **5**: p. 321-333.
81. reviews, A.p.s. *Introduction/Basic of AKT biology*. 2015 [cited 2015 01-10-2015]; Available from: <http://physrev.physiology.org/content/91/3/1023>.
82. S. J. Thomas, J.A.S., M. P. Zeidler and S. J. Danson, *The role of JAK/STAT signalling in the pathogenesis, prognosis and treatment of solid tumours*. *British Journal of Cancer*, 2015. **113**: p. 365-371.
83. Adrian Britschgi, R.A., Heike Brinkhaus, Ina Klebba, Vincent Romanet, Urs Muller, Masato Murakami, Thomas Radimerski and Mohamed Bentires-Alj, *JAK2/STAT5 inhibition circumvents resistance to PI3K/mTOR blockade: A*

- rationale for cotargeting these pathways in metastatic breast cancer*. *Cancer Cell*, 2012. **22**: p. 796-811.
84. Jennifer E. Yeh, P.A.T.a.D.A.F., *JAK2-STAT5 signaling: A novel mechanism of resistance to targeted PI3K/mTOR inhibition*. *Jak-Stat*, 2013. **2**: p. e24635-1-4.
85. Immunodeficiencies, E.S.f. *Protein phosphorylation and cell signaling by flow cytometry*. 2012 [cited 2015 01-10-2015]; Available from: <http://esid.org/Working-Parties/ESID-Juniors/Young-Researcher-corner/detecting-protein-phosphorylation-and-cell-signaling-by-flow-cytometry>.
86. Vadlamudi, S.S.R.a.R.K., *Role of estrogen receptor signaling in breast cancer metastasis*. *International Journal of Breast Cancer*, 2012. **2011**: p. 1-8.
87. C. Kent Osborne, J.S., Suleiman Massarweh and Rachel Schiff, *Crosstalk between estrogen receptor and growth factor receptor pathways as a cause for endocrine therapy resistance in breast cancer*. *Clinical Cancer Research*, 2005. **11**: p. 865s–870s.
88. Parsons, S.J.P.a.J.T., *Src family kinases, key regulators of signal transduction*. *Oncogene*, 2004. **23**: p. 7906-7909.
89. Rachel Schiff, S.A.M., Jiang Shou, Lavina Bharwani, Syed K. Mohsin and C. Kent Osborne, *Cross-talk between estrogen receptor and growth factor pathways as a molecular target for overcoming endocrine resistance*. *Clinical Cancer Research*, 2004. **10**: p. 331s.
90. Barton, E.R.P.a.M., *The G protein-coupled estrogen receptor GPER in health and disease*. *Nature Reviews Endocrinology*, 2011. **12**: p. 715–726.
91. Iain A. Murray, A.D.P.a.G.H.P., *Aryl hydrocarbon receptor ligands in cancer: Friend and foe*. *Nature Reviews Cancer*, 2014. **14**: p. 801-814.
92. T. D. Bradshaw, V.T., D. A. Vasselin and A. D. Westwell, *The Aryl Hydrocarbon Receptor in Anticancer Drug Discovery: Friend or Foe?* *Current Pharmaceutical Design*, 2002. **8**: p. 2475-2490.
93. Bell, T.D.B.a.D.R., *Relevance of the aryl hydrocarbon receptor (AhR) for clinical toxicology*. *Clinical Toxicology*, 2009. **47**: p. 632-642.
94. T.D. Bradshaw, C.G.M.a.A.D.W., *Update to: The aryl hydrocarbon receptor in anticancer drug discovery: Friend or foe?* *Medicinal Chemistry Reviews - Online*, 2005. **2**: p. 1-9.
95. Loaiza-Perez, M.A.C.a.A.I., *The role of aryl hydrocarbon receptor and crosstalk with estrogen receptor in response of breast cancer cells to the novel antitumor agents benzothiazoles and aminoflavone*. *International Journal of Breast Cancer*, 2011. **2011**: p. 1-9.
96. Carrie Hayes Suttera, H.Y., Yunbo Lib, Jennifer S. Mammenb, Sridevi Bodreddigaria, Gaylene Stevensa, Judith A. Colea and Thomas R. Sutter, *EGF receptor signaling blocks aryl hydrocarbon receptor-mediated transcription and cell differentiation in human epidermal keratinocytes*. *Proceedings of the National Academy of Sciences of the United States of America*, 2009. **106**: p. 4266-4271.

97. Alvaro Puga, C.M.a.J.L.M., *The aryl hydrocarbon receptor cross-talks with multiple signal transduction pathways*. *Biochemical Pharmacology*, 2009. **77**: p. 713-722.
98. Alison Reid, L.V., Heather Shaw and Johann de Bono, *Dual inhibition of ErbB1 (EGFR/HER1) and ErbB2 (HER2/neu)*. *European Journal of Cancer*, 2007. **43**: p. 481-489.
99. Giuseppe Bronte, C.R., Elisa Giovannetti, Giuseppe Cicero, Patrick Pauwels, Francesco Passiglia, Marta Castiglia, Sergio Rizzo, Francesca Lo Vullo, Eugenio Fiorentino, Jan Van Meerbeeck and Antonio Russo, *Are erlotinib and gefitinib interchangeable, opposite or complementary for non-small cell lung cancer treatment? Biological, pharmacological and clinical aspects*. *Critical Reviews in Oncology/Hematology*, 2014. **89**: p. 300-313.
100. Harari, P.M., *Epidermal growth factor receptor inhibition strategies in oncology*. *Endocrine-Related Cancer*, 2004. **11**: p. 689-708.
101. Salgia, N.P.a.R., *Synergism of EGFR and c-Met pathways, cross-talk and inhibition, in non-small cell lung cancer*. *Journal of Carcinogenesis*, 2008. **7**: p. 1-8.
102. Roy S. Herbst, M.F.a.J.B., *Gefitinib - a novel targeted approach to treating cancer*. *Nature Reviews*, 2004. **4**: p. 956-965.
103. Rita Nahta, D.Y., Mien-Chie Hung, Gabriel N. Hortobagyi and Francisco J. Esteva, *Mechanisms of Disease: Understanding resistance to HER2-targeted therapy in human breast cancer*. *Nature Clinical Practice Oncology*, 2006. **3**: p. 269-280.
104. Kumares S. Soppimath, T.M.A., Anandrao R. Kulkarni and Walter E. Rudzinski, *Biodegradable polymeric nanoparticles as drug delivery devices*. *Journal of Controlled Release*, 2001. **70**: p. 1-20.
105. Borm, W.H.D.J.a.P.J.A., *Drug delivery and nanoparticles: Applications and hazards*. *International Journal of Nanomedicine*, 2008. **3**: p. 133-149.
106. Swen Hoelder, P.A.C.a.P.W., *Discovery of small molecule cancer drugs: Successes, challenges and opportunities*. *Molecular Oncology*, 2012. **6**: p. 155-176.
107. Ruibing Wang, P.S.B.a.W.M.M., *Nanomedicine in action: An overview of cancer nanomedicine on the market and in clinical trials*. *Journal of Nanomaterials*, 2012. **2013**: p. 1-12.
108. Wandena S. Siegel-Lakhai, J.H.B.a.J.H.M.S., *Current knowledge and future directions of the selective epidermal growth factor receptor inhibitors Erlotinib (Tarceva®) and Gefitinib (Iressa®)*. *The Oncologist*, 2005. **8**: p. 579-589.
109. Jose Baselga, J.A., Amparo Ruiz, Ana Lluch, Pere Gascon, Vicente Guillem, Sonia Gonzalez, Silvia Sauleda, Irene Marimon, Josep M. Taberner, Maria T. Koehler and Federico Rojo, *Phase II and tumor pharmacodynamic study of gefitinib in patients with advanced breast cancer*. *Journal of Clinical Oncology*, 2005. **23**: p. 5323-5333.

110. Hurvitz, A.D.a.S.A., *HER2-positive breast cancer: Update on new and emerging agents*. The American Journal of Hematology/Oncology, 2015. **11**: p. 17-23.
111. Oncology, E.S.f.M., *ESMO 2014: Final Overall Survival Analysis from the CLEOPATRA Study in Patients with HER2-Positive Metastatic Breast Cancer*. 2014.
112. Xiaoyang Xu, W.H., Xueqing Zhang, Nicolas Bertrand and Omid Farokhzad, *Cancer nanomedicine: From targeted delivery to combination therapy*. Trends in Molecular Medicine, 2015. **21**: p. 223-232.
113. Langer, O.C.F.a.R., *Nanomedicine: Developing smarter therapeutic and diagnostic modalities*. Advanced Drug Delivery Reviews, 2006. **58**: p. 1456-1459.
114. Masaki Uchida, S.K., Courtney Reichhardt, Kevin Harlen and Trevor Douglas, *The ferritin superfamily: Supramolecular templates for materials synthesis*. Biochimica et Biophysica Acta, 2010. **1800**: p. 834-845.
115. Jordan, P.F.a.V.C., *Acquired resistance to selective estrogen receptor modulators (SERMs) in clinical practice (tamoxifen & raloxifene) by selection pressure in breast cancer cell populations*. Steroids, 2014. **90**: p. 44-52.
116. Syed K. Mohsin, H.L.W., M. Carolina Gutierrez, Gary C. Chamness, Rachel Schiff, Michael P. DiGiovanna, Chun-Xia Wang, Susan G. Hilsenbeck, C. Kent Osborne, D. Craig Allred, Richard Elledge and Jenny C. Chang, *Neoadjuvant trastuzumab induces apoptosis in primary breast cancers*. Journal of Clinical Oncology, 2005. **23**: p. 2460-2468.
117. Woo-Chul Noh, W.H.M., Junying Peng, Weiguo Jian, Haixia Zhang, JinJiang Dong, Gordon B. Mills, Mien-Chie Hung and Funda Meric-Bernstam, *Determinants of rapamycin sensitivity in breast cancer cells*. Clinical Cancer Research, 2004. **10**: p. 1013-1023.
118. Goodsell, D.S., *The molecular perspective: Epidermal growth factor*. The Oncologist, 2003. **8**: p. 496-497.
119. Delbert A. Fisher, E.C.S.a.L.B., *Epidermal growth factor and the kidney*. Annual Review of Physiology, 1989. **51**: p. 67-80.
120. C. Kent Osborne, B.H., Grace Titus and Robert B. Livingston, *Epidermal growth factor stimulation of human breast cancer cells in culture*. Cancer Research, 1980. **40**: p. 2361-2366.
121. Calbiochem. *Epidermal growth factor (EGF), human, recombinant, E. coli* 2012 [cited 2015 10-08-2015]; Available from: http://www.merckmillipore.com/GB/en/product/EGF,-Human,-Recombinant,-E.-coli,EMD_BIO-324831.
122. PubChem. *Open chemistry database*. 2015 [cited 2015 31-08-2015]; Available from: <https://pubchem.ncbi.nlm.nih.gov/>.
123. Martin H. Cohen, G.A.W., Rajeshwari Sridhara, Gang Chen, W. David McGuinn, Jr., David Morse, Sophia Abraham, Atiqur Rahman, Chenyi Liang, Richard Lostritto, Amy Baird and Richard Pazdur, *United States food and drug*

- administration drug approval summary: Gefitinib (ZD1839; Iressa) tablets*. Clinical Cancer Research, 2004. **10**: p. 1212–1218.
124. AstraZeneca. *Iressa*. 2015 [cited 2015 01-09-2015]; Available from: <https://www.iressa-usa.com/>.
125. NIH U.S. National Library of Medicine, T.D.N. *ChemIDplus*. 2015 [cited 2015 31-08-15]; Available from: <http://chem.sis.nlm.nih.gov/chemidplus/>.
126. Institute, N.C. *FDA approval for Erlotinib Hydrochloride*. 2013 [cited 2015 03-09-2015]; Available from: <http://www.cancer.gov/about-cancer/treatment/drugs/fda-erlotinib-hydrochloride>.
127. Brown, Y.S.a.M., *Molecular determinants for the tissue specificity of SERMs*. Science, 2002. **295**: p. 2465-2468
128. Institute, N.C. *FDA approval for Raloxifene Hydrochloride*. 2013 [cited 2015 03-09-2015]; Available from: <http://www.cancer.gov/about-cancer/treatment/drugs/fda-raloxifene-hydrochloride>.
129. Aihui Ma-Ham, H.W., Jun Wang, Xinhuang Kang, Youyu Zhang and Yuehe Lin, *Apo ferritin-based nanomedicine platform for drug delivery: Equilibrium binding study of daunomycin with DNA*. Journal of Materials Chemistry, 2011. **21**: p. 8700–8708.
130. Li Li, C.J.F., James C. Ryan, Erene C. Niemi, Jose A. Lebron, Pamela J. Bjorkman, Hisashi Arase, Frank M. Torti, Suzy V. Torti, Mary C. Nakamura and William E. Seaman, *Binding and uptake of H-ferritin are mediated by human transferrin receptor-1*. Proceedings of the National Academy of Sciences of the United States of America, 2010. **107**: p. 3505–3510.
131. Zbynek Heger, S.S., Ondrej Zitka, Vojtech Adam and Rene Kizek, *Apo ferritin applications in nanomedicine*. Nanomedicine, 2014. **9**: p. 2233–2245.
132. Rafal Zielinski, I.L., Moinuddin Hassan, Monika Kuban, Kimberly Shafer-Weaver, Amir Gandjbakhche and Jacek Capala, *HER2-Affitoxin: A potent therapeutic agent for the treatment of HER2-overexpressing tumors*. Clinical Cancer Research, 2011. **17**: p. 5071-5081.
133. J. Lofblom, J.F., V. Tolmachev, J. Carlsson, S. Stahl and F.Y. Frejd, *Affibody molecules: Engineered proteins for therapeutic, diagnostic and biotechnological applications*. FEBS Letters, 2010. **584**: p. 2670-2680.
134. Jens Sorensen, D.S., Mattias Sandstrom, Anders Wennborg, Joachim Feldwisch, Vladimir Tolmachev, Gunnar Astrom, Mark Lubberink, Ulrike Garske-Roman, Jorgen Carlsson and Henrik Lindman, *First-in-human molecular imaging of HER2 expression in breast cancer metastases using the 111 In-ABY-025 affibody molecule*. The Journal of Nuclear Medicine, 2014. **55**: p. 730-735.
135. Ritwik Ghosh, A.N., Shizhen Emily Wang, Shuying Liu, Anindita Chakrabarty, Justin M. Balko, Ana Maria Gonzalez-Angulo, Gordon B. Mills, Elicia Penuel, John Winslow, Jeff Sperinde, Rajiv Dua, Sailaja Pidaparathi, Ali

- Mukherjee, Kim Leitzel, Wolfgang J. Kostler, Allan Lipton, Michael Bates and Carlos L. Arteaga, *Trastuzumab has preferential activity against breast cancers driven by HER2 homodimers*. HHS Author Manuscripts, 2011. **71**: p. 1871-1882.
136. Institute, N.C. *FDA approval for Trastuzumab*. 2013 [cited 2015 03-09-2015]; Available from: <http://www.cancer.gov/about-cancer/treatment/drugs/fda-trastuzumab>.
137. Mariana A. Callero, G.A.L., Diana O. De Dios, Tracey D. Bradshaw and Andrea I. Loaiza Perez, *Biomarkers of sensitivity to potent and selective antitumor 2-(4-Amino-3-Methylphenyl)-5-fluorobenzothiazole (5F203) in ovarian cancer*. Journal of Cellular Biochemistry, 2013. **114**: p. 2392-2404.
138. Rana Bazzi, T.D.B., J. Craig Rowlands, Malcolm F.G. Stevens and David R. Bell, *2-(4-Amino-3-methylphenyl)-5-fluorobenzothiazole is a ligand and shows species-specific partial agonism of the aryl hydrocarbon receptor*. Toxicology and Applied Pharmacology, 2009. **237**: p. 102-110.
139. Sigma-Aldrich. *5F 203*. 2015 [cited 2015 01-09-2015]; Available from: <http://www.sigmaaldrich.com/catalog/product/>.
140. Aranapakam M. Venkatesan, C.M.D., Efren Delos Santos, Zecheng Chen, Osvaldo Dos Santos, Semiramis Ayril-Kaloustian, Gulnaz Khafizova, Natasja Brooijmans, Robert Mallon, Irwin Hollander, Larry Feldberg, Judy Lucas, Ker Yu, James Gibbons, Robert T. Abraham, Inder Chaudhary and Tarek S. Mansour, *Bis (morpholino-1,3,5-triazine) derivatives: Potent adenosine 50-triphosphate competitive phosphatidylinositol-3-kinase/mammalian target of rapamycin inhibitors: Discovery of compound 26 (PKI-587), a highly efficacious dual inhibitor*. Journal of Medicinal Chemistry, 2010. **53**: p. 2636-2645.
141. E. F. O'Donnell, D.C.K., W. H. Bisson, H. S. Jang and S. K. Kolluri, *The aryl hydrocarbon receptor mediates raloxifene induced apoptosis in estrogen receptor-negative hepatoma and breast cancer cells*. Cell Death and Disease, 2014. **5**: p. 1-12.
142. Xiaosong Chen, M.Z., Mingang Hao, Xueqing Sun, Jinglong Wang, Yan Mao, Lidong Zu, Junjun Liu, Yandong Shen, Jianhua Wang and Kunwei Shen, *Dual inhibition of PI3K and mTOR mitigates compensatory AKT activation and improves tamoxifen response in breast cancer*. Molecular Cancer Research, 2013. **11**: p. 1269-1278.
143. Timothy A. Yap, A.O.a.J.S.d.B., *Development of therapeutic combinations targeting major cancer signaling pathways*. Journal of Clinical Oncology, 2013. **31**: p. 1592-1605.
144. Bjare, U., *Serum-free cell culture*. Pharmacology and Therapeutics, 1992. **53**: p. 355-374.
145. S. B. Iloki Assanga, A.A.G.-S., L. M. Lewis Lujan, A. Rosas-Durazo, A. L. Acosta-Silva, E. G. Rivera-Castaneda, and J. Rubio-Pino, *Cell growth curves for different cell lines and their relationship with biological activities*. International Journal for Biotechnology and Molecular Biology Research, 2013. **4**: p. 60-70.

146. Cree, I.A., *Cancer cell culture methods and protocols*. 2nd ed. 2011: Humana Press.
147. Nicolaas A P Franken, H.M.R., Jan Stap, Jaap Haveman and Chris van Bree, *Clonogenic assay of cells in vitro*. Nature Protocols, 2006. **1**: p. 2315-2319.
148. Mike Leach, M.D.a.A.D., *Practical flow cytometry in haematology diagnosis*. 1st ed. 2013: Wiley-Blackwell.
149. Zhao, Z.D.a.H., *Cell cycle analysis by flow cytometry*. eLS: Cell Biology: John Wiley & Sons, Ltd, 2014: p. 1-8.
150. Istvan Vermes, C.H., Helga Steffens-Nakken and Chris Reutelingsperger A novel assay for apoptosis flow cytometric detection of phosphatidylserine early apoptotic cells using fluorescein labelled expression on Annexin V. *Journal of Immunological Methods*, 1995. **184**: p. 39-51.
151. Dane Avondoglio, T.S., Whoon Jong Kil, Mary Sproull, Philip J Tofilon and Kevin Camphausen, *High throughput evaluation of gamma-H2AX*. *Radiation Oncology*, 2009. **4**: p. 1-5.
152. Aida Muslimovic, I.H.I., Yue Gao and Ola Hammarsten, *An optimized method for measurement of gamma-H2AX in blood mononuclear and cultured cells*. *Nature Protocols*, 2008. **3**: p. 1187-1193.
153. Brian J. Trummer, V.I., Sathy V. Balu-Iyer, Robert O'Connor and Robert M. Straubinger, *Physicochemical properties of EGF receptor inhibitors and development of a nanoliposomal formulation of gefitinib*. *Journal of pharmaceutical sciences*, 2012. **101**: p. 2763-2776.
154. Hanry Yu, P.-C.C., Pao-Chun Lin and Fu-Jen Kao, *Multi-modality microscopy*. 2006: World Scientific.
155. Bradford, M.M., *A rapid and sensitive method for the quantitation of microgram quantities of protein utilizing the principle of protein-dye binding*. *Analytical Biochemistry*, 1976. **72**: p. 248-254.
156. Arianna Rath, M.G., Vincent G. Nadeau, Gong Chen and Charles M. Deber, *Detergent binding explains anomalous SDS-PAGE migration of membrane proteins*. *Proceedings of the National Academy of Sciences of the United States of America*, 2009. **106**: p. 1760-1765.
157. Joseph Fernandez, F.G.a.S.M.M., *Routine identification of proteins from sodium dodecyl sulfate-polyacrylamide gel electrophoresis (SDS-PAGE) gels or polyvinyl difluoride membranes using matrix assisted laser desorption/ionization-time of flight-mass spectrometry (MALDI-TOF-MS)*. *Electrophoresis*, 1998. **19**: p. 1036-1045.
158. Donghoon Kang, Y.S.G., Myungkoo Suh and Chulhun Kang, *Highly sensitive and fast protein detection with coomassie brilliant blue in sodium dodecyl sulfate-polyacrylamide gel electrophoresis*. *Bulletin of the Korean Chemical Society*, 2002. **23**: p. 1511-1512.
159. Brydson, R., *RMS - Royal microscopical society : Aberration-corrected analytical transmission electron microscopy*. 2011: USA: John Wiley & Sons.

160. Y. Yang, S.K., J. Werner and A.V. Bazhin, *Reactive oxygen species in cancer biology and anticancer therapy*. Current Medicinal Chemistry, 2013. **20**: p. 3677-3692.
161. Anders Stahlberg, N.Z., Pierre Aman and Mikael Kubista, *Quantitative real-time PCR for cancer detection: The lymphoma case*. Expert Review of Molecular Diagnostics, 2005. **5**: p. 221-230.
162. Claudius Mueller, L.A.L.a.V.E., *Reverse phase protein microarrays advance to use in clinical trials*. Molecular Oncology, 2010. **4**: p. 461-481.
163. Heiko A. Mannsperger, S.G., Frauke Henjes, Tim Beissbarth and Ulrike Korf, *RPPanalyzer: Analysis of reverse-phase protein array data*. Bioinformatics, 2010. **26**: p. 2202-2203.
164. Ola H. Negm, H.A.M., Elizabeth M. McDermott, Elizabeth Drewe, Richard J. Powell, Ian Todd, Lucy C. Fairclough and Patrick J. Tighe, *A pro-inflammatory signalome is constitutively activated by C33Y mutant TNF receptor 1 in TNF receptor-associated periodic syndrome (TRAPS)*. European Journal of Immunology, 2014. **44**: p. 2096-2110.
165. Viale, F.P.-L.a.G., *Pathological and molecular diagnosis of triple-negative breast cancer: A clinical perspective*. Annals of Oncology, 2012. **23**: p. vi19-vi22.
166. David C. Spink, B.C.S., Joan Q. Cao, Joseph A. DePasquale, Brian T. Pentecost, Michael J. Fasco, Ying Li and Thomas R. Sutter, *Differential expression of CYP1A1 and CYP1B1 in human breast epithelial cells and breast tumor cells*. Carcinogenesis, 1998. **19**: p. 191-298.
167. Richard S. Finn, J.D., Dylan Conklin, Ondrej Kalous, David J. Cohen, Amrita J. Desai, Charles Ginther, Mohammad Atefi, Isan Chen, Camilla Fowst, Gerret Los and Dennis J. Slamon, *PD 0332991, a selective cyclin D kinase 4/6 inhibitor, preferentially inhibits proliferation of luminal estrogen receptor-positive human breast cancer cell lines in vitro*. Breast Cancer Research, 2009. **11**: p. 1-13.
168. Buddy Setyono-Han, M.S.H., John A. Foekens and Jan G. M. Klijn, *Direct inhibitory effects of somatostatin (analogues) on the growth of human breast cancer cells*. Cancer Research, 1987. **47**: p. 1566-1570.
169. Caroline Rauch, E.F., Eva-Maria Amann, Hans Peter Spotl, Harald Schennach, Walter Pfaller and Gerhard Gstraunthaler, *Alternatives to the use of fetal bovine serum: human platelet lysates as a serum substitute in cell culture media*. ALTEX: Alternatives to Animal Experimentation, 2011. **28**: p. 305-316.
170. Josiah Ochieng, S.P., Atanu K. Khatua and Amos M. Sakwe *Anchorage independent growth of breast carcinoma cells is mediated by serum exosomes*. Experimental Cell Research, 2009. **315**: p. 1875-1888.
171. T. Tedone, M.C., A. Paradiso and S. J. Reshkin, *Differential responsiveness of proliferation and cytokeratin release to stripped serum and oestrogen in the human breast cancer cell line, MCF-7*. European Journal of Cancer, 1996. **32**: p. 849-856.

-
172. Chun Chen, W.T.B., Robert Clarke and John J. Tyson, *Modeling the estrogen receptor to growth factor receptor signaling switch in human breast cancer cells*. FEBS Letters, 2013. **587**: p. 3327-3334.
173. Christoph Mamot, D.C.D., Udo Greiser, Keelung Hong, Dmitri B. Kirpotin, James D. Marks and John W. Park, *Epidermal growth factor receptor (egfr)-targeted immunoliposomes mediate specific and efficient drug delivery to egfr- and egfr viii-overexpressing tumor cells*. Cancer Research, 2003. **63**: p. 3154-3161.
174. Lykkesfeldt, P.B.a.A.E., *Effect of estrogen and antiestrogen on the human breast cancer cell line MCF-7 adapted to growth at low serum concentration*. Cancer Research, 1984. **44**: p. 1114-1119.
175. Asbjorn Aakvaag, E.U., Thor Thorsen, Oscar A. Lea and Hooshang Lahooti, *Growth control of human mammary cancer cells (MCF-7 cells) in culture: Effect of estradiol and growth factors in serum-containing medium*. Cancer Research, 1990. **50**: p. 7806-7810.
176. Yolande Berthois, J.A.K.a.B.S.K., *Phenol red in tissue culture media is a weak estrogen: Implications concerning the study of estrogen-responsive cells in culture*. Proceedings of the National Academy of Sciences of the United States of America, 1986. **83**: p. 2496-2500.
177. Renqin Duan, W.X., Robert C. Burghardt and Stephen Safe, *Estrogen receptor-mediated activation of the serum response element in mcf-7 cells through MAPK-dependent phosphorylation of Elk-1*. The Journal of Biological Chemistry, 2001. **276**: p. 11590-11598.
178. Carpenter, O.T.a.G., *Ligand-induced, p38-dependent apoptosis in cells expressing high levels of epidermal growth factor receptor and ErbB-2*. The Journal of Biological Chemistry, 2004. **279**: p. 12988-12996.
179. Rajiv Dua, J.Z., Phets Nhonthachit, Elicia Penuel, Chris Petropoulos and Gordon Parry, *EGFR over-expression and activation in high HER2, ER negative breast cancer cell line induces trastuzumab resistance*. Breast Cancer Research and Treatment, 2010. **122**: p. 685-697.
180. Amy S. Clark, K.W., Samantha Streicher and Phillip A. Dennis, *Constitutive and inducible AKT activity promotes resistance to chemotherapy, Trastuzumab, or Tamoxifen in breast cancer cells*. Molecular Cancer Therapeutics, 2002. **1**: p. 707-717.
181. Boon Tin Chua, D.G.-O., Ana Ramirez de Molina, Axel Ullrich, Juan Carlos Lacal and Julian Downward, *Regulation of Akt (ser473) phosphorylation by choline kinase in breast carcinoma cells*. Molecular Cancer, 2009. **8**: p. 131.
182. K. Yu, L.T.-B., C. Discafani, W-G Zhang, J. Skotnicki, P. Frost and J. J. Gibbons, *mTOR, a novel target in breast cancer: the effect of CCI-779, an mTOR inhibitor, in preclinical models of breast cancer*. Endocrine-Related Cancer, 2001. **8**: p. 249-258.
183. David T. Leong, J.L., Xuewei Goh, Jitesh Pratap, Barry P. Pereira, Hui Si Kwok, Saminathan Suresh Nathan, Jason R. Dobson, Jane B. Lian, Yoshiaki Ito, P. Mathijs Voorhoeve, Gary S. Stein, Manuel Salto-Tellez, Simon M Cool and Andre J. van Wijnen, *Cancer-related ectopic expression of the bone-*

- related transcription factor RUNX2 in non-osseous metastatic tumor cells is linked to cell proliferation and motility.* Breast Cancer Research, 2010. **12**: p. R89.
184. Ji-young Song, S.-w.L., Joon Pio Hong, Sung Eun Chang, Han Choe and Jene Choi, *Epidermal growth factor competes with EGF receptor inhibitors to induce cell death in EGFR-overexpressing tumor cells.* Cancer Letters, 2009. **283**: p. 135–142.
185. David S. Salomon, R.B., Fortunato Ciardiello and Nicola Normanno, *Epidermal growth factor-related peptides and their receptors in human malignancies.* Critical Reviews in Oncology/Hematology 1995. **19**: p. 183-232.
186. Susan L. Fitzpatrick, M.P.L.a.G.S.S., *Characterization of epidermal growth factor receptor and action on human breast cancer cells in culture.* Cancer Research, 1984. **44**: p. 3442-3447.
187. Matthew J. Wheeler, P.W.M.J.a.J.P.B., *The role of MNK proteins and eIF4E phosphorylation in breast cancer cell proliferation and survival.* Cancer Biology and Therapy, 2010. **10**: p. 728-735.
188. Gianluca Tognon, R.F., Marco Zaffaroni, Eugenio Erba, Massimo Zucchetti, Glynn T. Faircloth and Maurizio D'Incalci, *Fetal bovine serum, but not human serum, inhibits the in vitro cytotoxicity of ET-743 (Yondelis, trabectedin).* Cancer Chemotherapy and Pharmacology, 2004. **53**: p. 89-90.
189. Manuela Campiglio, A.L., Clelia Olgiati, Nicola Normanno, Giulia Somenzi, Lucia Vigano, Marzia Fumagalli, Sylvie Menard and Luca Gianni, *Inhibition of proliferation and induction of apoptosis in breast cancer cells by the epidermal growth factor receptor (EGFR) tyrosine kinase inhibitor zd1839 ('Iressa') is independent of EGFR expression level.* Journal of Cellular Physiology, 2004. **198**: p. 259-268.
190. F. R Hirsch, M.V.-G.a.F.C., *Predictive value of EGFR and HER2 overexpression in advanced non-small-cell lung cancer.* Oncogene, 2009. **28**: p. S32–S37.
191. M. Guix, M.S.K., M. L. Reyzer, J. Zhang, Y. Shyr, B. K. McLaren, K. Newsome-Johnson, W. Lipscomb, T. C. Dugger and C. L. Arteaga, *Short course of EGF receptor tyrosine kinase inhibitor erlotinib (OSI-774) reduces tumor cell proliferation and active MAP kinase in situ in untreated operable breast cancers: A strategy for patient selection into phase II trials with signaling inhibitors.* Journal of Clinical Oncology, 2005. **23**: p. s3008.
192. Nicola Normanno, A.D.L., Monica R. Maiello, Manuela Campiglio, Maria Napolitano, Mario Mancino, Adele Carotenuto, Giuseppe Viglietto and Sylvie Menard, *The MEK/MAPK pathway is involved in the resistance of breast cancer cells to the EGFR tyrosine kinase inhibitor Gefitinib.* Journal of Cellular Physiology, 2006. **207**: p. 420-427.
193. Marina Ines Flamini, X.-D.F., Angel Matias Sanchez, Maria Silvia Giretti, Silvia Garibaldi, Lorenzo Goglia, Silvia Pisaneschi, Veronica Tosi, Andrea Riccardo Genazzani and Tommaso Simoncini, *Effects of raloxifene on breast*

- cancer cell migration and invasion through the actin cytoskeleton*. Journal of Cellular and Molecular Medicine, 2008. **13**: p. 2396-2407.
194. Charles E. Carraher Jr, G.B., Kimberly Shahic and Michael R. Roner, *Influence of DMSO on the inhibition of various cancer cells by water-soluble organotin polyethers*. Journal of the Chinese Advanced Materials Society, 2013. **1**: p. 294-304.
195. Amelia D'Alessio, A.D.L., Monica R. Maiello, Luana Lamura, Anna Maria Rachiglio, Maria Napolitano, Marianna Gallo and Nicola Normanno, *Effects of the combined blockade of EGFR and ErbB-2 on signal transduction and regulation of cell cycle regulatory proteins in breast cancer cells*. Breast Cancer Research and Treatment, 2010. **123**: p. 387-396.
196. Janna Krol, R.E.F., Andre Albergaria, Andrew Sunters, Andreas Polychronis, R.Char les Coombes and Eric W.-F. Lam, *The transcription factor FOXO3a is a crucial cellular target of gefitinib (Iressa) in breast cancer cells*. Molecular Cancer Therapeutics, 2007. **6**: p. 3169-3179.
197. B. Corkery J. Crown, M.C.a.N.O.D., *Epidermal growth factor receptor as a potential therapeutic target in triple-negative breast cancer*. Annals of Oncology, 2009. **20**: p. 862-867.
198. Chris Albanese, J.J., Genichi Watanabe, Nathan Eklund, Dzuy Vu, Andrew Arnold and Richard G. Pestell, *Transforming p21ras mutants and c-Ets-2 activate the cyclin D1 promoter through distinguishable regions*. The Journal of Biological Chemistry, 1995. **270**: p. 23589-23597.
199. J. Alan Diehl, F.Z.a.C.J.S., *Inhibition of cyclin D1 phosphorylation on threonine-286 prevents its rapid degradation via the ubiquitinproteasome pathway*. Genes and Development, 1997. **11**: p. 957-972.
200. Stacey, D.W., *Cyclin D1 serves as a cell cycle regulatory switch in actively proliferating cells*. Current Opinion in Cell Biology, 2003. **15**: p. 158-163.
201. Gee-Chen Chang, S.-L.H., Jia-Rong Tsai, Fong-Pin Liang, Sheng-Yi Lin, Gwo-Tarng Sheu and Chih-Yi Chen, *Molecular mechanisms of ZD1839-induced G1-cell cycle arrest and apoptosis in human lung adenocarcinoma A549 cells*. Biochemical Pharmacology, 2004. **68**: p. 1453-1464.
202. Ruben Garcia, R.A.F.a.J.A.M., *Cell death of MCF-7 human breast cancer cells induced by EGFR activation in the absence of other growth factors*. Cell Cycle, 2006. **5**: p. 1840-1846.
203. Zhixiang Wang, L.Z., Tai K. Yeung and Xinmei Chen, *Endocytosis deficiency of epidermal growth factor (EGF) receptor-ErbB2 heterodimers in response to EGF stimulation*. Molecular Biology of the Cell, 1999. **10**: p. 1621-1636.
204. Thompson, A.L.E.a.C.B., *Death by design: apoptosis, necrosis and autophagy*. Current Opinion in Cell Biology, 2004. **16**: p. 663-669.
205. Flavia Radogna, M.D.a.M.D., *Cancer-type-specific crosstalk between autophagy, necroptosis and apoptosis as a pharmacological target*. Biochemical Pharmacology, 2015. **94**: p. 1-11.

206. I. K. H. Poon, M.D.H.a.C.R.P., *Molecular mechanisms of late apoptotic/necrotic cell clearance*. Cell Death and Differentiation, 2010. **17**: p. 381-397.
207. Vassiliki Nikolettou, M.M., Konstantinos Palikaras and Nektarios Tavernarakis, *Crosstalk between apoptosis, necrosis and autophagy*. Biochimica et Biophysica Acta, 2013. **1833**: p. 3448–3459.
208. Linda E. Broker, F.A.E.K.a.G.G., *Cell death independent of caspases: A review*. Clinical Cancer Research, 2005. **11**: p. 3155-3162.
209. Xiao-Feng Le, A.M., Jon Wiener, Ji-Yuan Wu, Gordon B. Mills and Robert C. Bast Jr., *Anti-HER2 antibody and Heregulin suppress growth of HER2-overexpressing human breast cancer cells through different mechanisms*. Clinical Cancer Research, 2000. **6**: p. 260-270.
210. Elmore, S., *Apoptosis: A review of programmed cell death*. Toxicologic Pathology, 2007. **35**: p. 495-516.
211. Dong-oh Moon, M.-o.K., Jae-dong Lee, Yung-hyun Choi, Min-ki Lee and Gi-young Kim, *Molecular mechanisms of ZD1839 (Iressa)-induced apoptosis in human leukemic U937 cells*. Acta Pharmacologica Sinica, 2007. **28**: p. 1205-1214.
212. Hiroshi Ariyama, B.Q., Eishi Baba, Risa Tanaka, Kenji Mitsugi, Mine Harada and Shuji Nakano, *Gefitinib, a selective EGFR tyrosine kinase inhibitor, induces apoptosis through activation of bax in human gallbladder adenocarcinoma cells*. Journal of Cellular Biochemistry, 2006. **97**: p. 724-734.
213. Marie P. Piechocki, G.H.Y., Susan K. Dibley and Fulvio Lonardo, *Breast cancer expressing the activated HER2/neu is sensitive to Gefitinib in vitro and in vivo and acquires resistance through a novel point mutation in the HER2/neu*. Cancer Research, 2007. **67**: p. 6825-6843.
214. Wiley, R.W.a.H.S., *Structural aspects of the epidermal growth factor receptor required for transmodulation of ErbB-2/neu*. The Journal of Biological Chemistry, 1997. **272**: p. 8594-8601.
215. P-H. Lu, T.-C.K., K-C. Chang, C-H. Chang and C-Y. Chu, *Gefitinib-induced epidermal growth factor receptor independent keratinocyte apoptosis is mediated by the JNK activation pathway*. British Journal of Dermatology, 2010. **164**: p. 38-46.
216. Lin, A., *Activation of the JNK signaling pathway: Breaking the brake on apoptosis*. BioEssays, 2002. **25**: p. 17-24.
217. Seungchan Yanga, K.P., James Turkson and Carlos L. Arteaga, *Ligand-independent phosphorylation of Y869 (Y845) links mutant EGFR signaling to stat-mediated gene expression*. Experimental Cell Research, 2008. **314**: p. 413-419.
218. Hua Xiong, W.-Y.S., Qin-Chuan Liang, Zhi-Gang Zhang, Hui-Min Chen, Wan Du, Ying-Xuan Chen and Jing-Yuan Fang, *Inhibition of STAT5 induces G1 cell cycle arrest and reduces tumor cell invasion in human colorectal cancer cells*. Laboratory Investigation, 2009. **89**: p. 717-725.

219. A. Haringhuizen, H.v.T., H. F. R. Vaessen, P. Baas and N. van Zandwijk, *Gefitinib as a last treatment option for non-small-cell lung cancer: Durable disease control in a subset of patients*. *Annals of Oncology*, 2004. **15**: p. 786–792.
220. Ruimin Xing, X.W., Changli Zhang, Yangmiao Zhang, Qi Wang, Zhen Yang and Zijian Guo, *Characterization and cellular uptake of platinum anticancer drugs encapsulated in apoferritin*. *Journal of Inorganic Biochemistry*, 2009. **103**: p. 1039–1044.
221. Gunter von Minckwitz, W.J., Peter Fasching, Andreas du Bois, Ulrich Kleeberg, Hans-Joachim Luck, Erika Kettner, Jorn Hilfrich, Wolfgang Eiermann, Julie Torode, and Andreas Schneeweiss, *A multicentre phase II study on gefitinib in taxane- and anthracycline-pretreated metastatic breast cancer*. *Breast Cancer Research and Treatment*, 2005. **89**: p. 165–172.
222. Tracy R. Daniels, E.B., Jose A. Rodriguez, Shabnum Patel, Maggie Kozman, Diego A. Chiappetta, Eggehard Holler, Julia Y. Ljubimova, Gustavo Helguera and Manuel L. Penichet, *The transferrin receptor and the targeted delivery of therapeutic agents against cancer*. *Biochimica et Biophysica Acta*, 2012. **1820**: p. 291–317.
223. Fabienne Danhier, O.F.a.V.P., *To exploit the tumor microenvironment: Passive and active tumor targeting of nanocarriers for anti-cancer drug delivery*. *Journal of Controlled Release*, 2010. **148**: p. 135–146.
224. Zhen Yang, X.W., Huajia Diao, Junfeng Zhang, Hongyan Li, Hongzhe Sun and Zijian Guo, *Encapsulation of platinum anticancer drugs by apoferritin*. *Chemical Communications*, 2007. **33**: p. 3409–3500.
225. Aihui MaHam, Z.T., Hong Wu, Jun Wang and Yuehe Lin, *Protein-based nanomedicine platforms for drug delivery*. *Small*, 2009. **5**: p. 1706–1721.
226. Kelong Fan, C.C., Yongxin Pan, Di Lu, Dongling Yang, Jing Feng, Lina Song, Minmin Liang and Xiyun Yan, *Magnetoferritin nanoparticles for targeting and visualizing tumour tissues*. *Nature Nanotechnology*, 2012. **7**: p. 459–464.
227. Simonetta Geninatti Crich, B.B., Lorenzo Tei, Cristina Grange, Giovanna Esposito, Stefania Lanzardo, Giovanni Camussi and Silvio Aime, *Magnetic resonance visualization of tumor angiogenesis by targeting neural cell adhesion molecules with the highly sensitive gadolinium-loaded apoferritin probe*. *Cancer Research*, 2006. **66**: p. 9196–9201.
228. Minmin Liang, K.F., Meng Zhou, Demin Duan, Jiyang Zheng, Dongling Yang, Jing Feng and Xiyun Yan, *H-ferritin–nanocaged doxorubicin nanoparticles specifically target and kill tumors with a single-dose injection*. *Proceedings of the National Academy of Sciences of the United States of America*, 2014. **111**: p. 14900–14905.
229. Tracey D. Bradshaw, M.J., Amalia Patane, Phil Clarke, Neil R. Thomas, Mei Li, Stephen Manne and Lyudmila Turyanska, *Apoferritin-encapsulated PbS quantum dots significantly inhibit growth of colorectal carcinoma cells*. *Journal of Materials Chemistry B*, 2013. **1**: p. 6254–6260.
230. Yijie Shi, C.S., Wenyu Cui, Hongdan Li, Liwei Liu, Bo Feng, Ming Liu, Rongjian Su and Liang Zhao, *Gefitinib loaded folate decorated bovine serum*

- albumin conjugated carboxymethyl-beta cyclodextrin nanoparticles enhance drug delivery and attenuate autophagy in folate receptor-positive cancer cells* Journal of Nanobiotechnology, 2014. **12**: p. 43.
231. Amol Ashok Pawar, D.-R.C.a.C.V., *Influence of precursor solvent properties on matrix crystallinity and drug release rates from nanoparticle aerosol lipid matrices*. International Journal of Pharmaceutics, 2012. **430**: p. 228-237.
232. Mehmet A. Kilic, E.O.a.S.C., *A novel protein-based anticancer drug encapsulating nanosphere: Apoferritin-doxorubicin complex*. Journal of Biomedical Nanotechnology, 2011. **8**: p. 1-7.
233. A.Ratnakumari, A.R.a.K.S., *A specific and sensitive assay for gefitinib using methods in pharmaceutical dosage forms*. Pharmanest, 2010. **1**: p. 118-122.
234. Surya Prakash Gautam, A.K.G., Shashank Agrawal and Shruti Sureka, *Spectroscopic characterization of dendrimers*. International Journal of Pharmacy and Pharmaceutical Sciences, 2012. **4**: p. 77-80.
235. Mindell, J.A., *Lysosomal acidification mechanisms*. The Annual Review of Physiology, 2012. **74**: p. 69-86.
236. Zipeng Zhen, W.T., Hongmin Chen, Xin Lin, Trever Todd, Geoffrey Wang, Taku Cowger, Xiaoyuan Chen and Jin Xie, *RGD modified apoferritin nanoparticles for efficient drug delivery to tumors*. ACS Nano, 2013. **7**: p. 4830-4837.
237. Elisabetta Falvo, E.T., Rocco Fraioli, Carlo Leonetti, Carlotta Zamparelli, Alberto Boffi, Veronica Morea, Pierpaolo Ceci and Patrizio Giacomini, *Antibody–drug conjugates: Targeting melanoma with cisplatin encapsulated in protein-cage nanoparticles based on human ferritin*. Nanoscale, 2013. **5**: p. 12278-12285.
238. Torti, S.V.T.a.F.M., *Iron and cancer: More ore to be mined*. Nature Reviews Cancer, 2013. **13**: p. 342-355.
239. Lan G. Coffman, D.P., Ralph D'Agostino, Jr., Frank M. Torti, and Suzy V. Torti, *Regulatory effects of ferritin on angiogenesis*. Proceedings of the National Academy of Sciences of the United States of America, 2009. **106**: p. 570-575.
240. Nadia M. Sposi, L.C., Elena Tritarelli, Elvira Pelosi, Stefania Militi, Tiziano Barberi, Marco Gabbianelli, Ernestina Saulle, Lukas Kuhn, Cesare Peschle and Ugo Testa, *Mechanisms of differential transferrin receptor expression in normal hematopoiesis*. European Journal of Biochemistry, 2000. **267**: p. 6762-6774.
241. Megumi Kawamoto, T.H., Masayuki Kohno and Koji Kawakami, *A novel transferrin receptor-targeted hybrid peptide disintegrates cancer cell membrane to induce rapid killing of cancer cells*. BMC Cancer, 2011. **11**: p. 2-13.
242. Yu Zheng, B.Y., Wanlop Weecharangsan, Longzhu Piao, Michael Darby, Yicheng Mao, Rumiana Koynova, Xiaojuan Yang, Hong Li, Songlin Xu, L. James Lee, Yasuro Sugimoto, Robert W. Brueggemeier and Robert J. Lee, *Transferrin-conjugated lipid-coated PLGA nanoparticles for targeted delivery*

- of aromatase inhibitor 7alpha-APTADD to breast cancer cells*. International Journal of Pharmaceutics, 2010. **390**: p. 234–241.
243. Ahmed A. Alkhateeb, B.H.a.J.R.C., *Ferritin stimulates breast cancer cells through an ironindependent mechanism and is localized within tumor-associated macrophages*. Breast Cancer Research and Treatment, 2013. **137**: p. 733–744.
244. Griffiths, J.R., *Are cancer cells acidic?* Br. J. Cancer, 1991. **64**: p. 425-427.
245. Bae, E.S.L.a.Y.H., *Recent progress in tumor pH targeting nanotechnology*. Journal of Controlled Release, 2008. **132**: p. 164–170.
246. DeAnna E. Beasley, A.M.K., Joanna E. Lambert, Noah Fierer and Rob R. Dunn, *The evolution of stomach acidity and its relevance to the human microbiome*. Plos One, 2015. **10**: p. 1-12.
247. Xiaojun Zhou, B.Y., Yifei Huang, Hong Li, Xianming Hu, Guangya Xiang and Robert J. Lee, *Novel liposomal Gefitinib (L-GEF) formulations*. Anticancer Research, 2012. **32**: p. 2919-2924.
248. Andrew M. Scott, J.D.W.a.L.J.O., *Antibody therapy of cancer*. Nature Reviews Cancer, 2012. **12**: p. 278-287.
249. Sang Bong Lee, M.H., Robert Fisher, Oleg Chertov, Victor Chernomordik, Gabriela Kramer-Marek, Amir Gandjbakhche and Jacek Capala, *Affibody molecules for in vivo characterization of HER2-positive tumors by near-infrared imaging*. Clinical Cancer Research, 2008. **14**: p. 3840–3849.
250. Wanyi Tai, R.M.a.K.C., *The role of HER2 in cancer therapy and targeted drug delivery*. Journal of Controlled Release, 2010. **146**: p. 264–275.
251. Frank Alexis, P.B., Etgar Levy-Nissenbaum, Aleksandar F. RadovicMoreno, Liangfang Zhang, Eric Pridgen, Adrew Z. Wang, Shawn L. Mareina, Katrina Westerhof, Linda K. Molnar and Omid C. Farokhzad, *HER-2 targeted nanoparticle-affibody bioconjugates for cancer therapy*. ChemMedChem, 2008. **12**: p. 1839–1843.
252. Lina Ekerljung, M.L., Lars Gedda, Fredrik Y. Frejd, Jorgen Carlsson and Johan Lennartsson, *Dimeric HER2-specific affibody molecules inhibit proliferation of the SKBR-3 breast cancer cell line*. Biochemical and Biophysical Research Communications, 2008. **377**: p. 489-494.
253. Frank Alexis, P.B., Etgar Levy-Nissenbaum, Aleksandar F. Radovic-Moreno, Liangfang Zhang, Eric Pridgen, Andrew Z. Wang, Shawn L. Marein, Katrina Westerhof, Linda K. Molnar and Omid C. Farokhzad, *HER-2-Targeted Nanoparticle–Affibody Bioconjugates for Cancer Therapy*. ChemMedChem, 2008. **3**: p. 1839-1843.
254. Treisman, C.S.H.a.R., *Transcriptional regulation by extracellular signals: Mechanisms and specificity*. Cell, 1995. **80**: p. 199-211.
255. Lyudmila Turyanska, T.D.B., Mei Li, Philip Bardelang, William C. Drewe, Michael W. Fay, Stephen Mann, Amalia Patan and Neil R. Thomas, *The differential effect of apoferritin-PbS nanocomposites on cell cycle progression in normal and cancerous cells*. Journal of Materials Chemistry, 2012. **22**: p. 660–665.

256. Munna L. Agarwal, A.A., William R. Taylor and George R. Stark, *p53 controls both the G2/M and the G1 cell cycle checkpoints and mediates reversible growth arrest in human fibroblasts*. Proceedings of the National Academy of Sciences of the United States of America, 1995. **92**: p. 8493-8497.
257. Xiao-Feng Le, F.-X.C., Amy Lammayot, Ling Tian, Deepa Deshpande, Ruth LaPushin, Ana M. Tari and Robert C. Bast Jr., *The role of cyclin-dependent kinase inhibitor p27kip1 in anti-HER2 antibody-induced G1 cell cycle arrest and tumor growth inhibition*. The Journal of Biological Chemistry, 2003. **278**: p. 23441-23450.
258. Cookson, S.L.F.a.B.T., *Apoptosis, pyroptosis, and necrosis: mechanistic description of dead and dying eukaryotic cells*. Infection and Immunity, 2005. **73**: p. 1907-1916.
259. Justyna Sosna, S.V., Sabine Mathieu, Arne Lange, Lutz Thon, Parvin Davarnia, Thomas Herdegen, Andreas Linkermann, Andrea Rittger, Francis Ka-Ming Chan, Dieter Kabelitz, Stefan Schütze and Dieter Adam, *TNF-induced necroptosis and PARP-1-mediated necrosis represent distinct routes to programmed necrotic cell death*. Cellular and Molecular Life Sciences, 2014. **71**: p. 331–348.
260. Jeffrey A. Drebin, V.C.L., David F. Stern, Robert A. Weinberg and Mark I. Greene, *Down-modulation of an oncogene protein product and reversion of the transformed phenotype by monoclonal antibodies*. Cell, 1985. **41**: p. 695-706.
261. Kenneth De Santes, D.S., Susan K. Anderson, Michael Shepard, Brian Fendly, Daniel Maneval and Oliver Press, *Radiolabeled antibody targeting of the her-2/neu oncoprotein*. Cancer Research, 1992. **52**: p. 1916-1923.
262. Karianne E. Longva, N.M.P., Camilla Haslekas, Espen Stang and Inger H. Madshus, *Herceptin-induced inhibition of ErbB2 signaling involves reduced phosphorylation of Akt but not endocytic down-regulation of ErbB2*. International Journal of Cancer, 2005. **116**: p. 359-367.
263. Der, P.J.R.a.C.J., *Targeting the Raf-MEK-ERK mitogen-activated protein kinase cascade for the treatment of cancer*. Oncogene, 2007. **26**: p. 3291–3310.
264. Milos Dokmanovic, D.S.H., Yi Shen, and Wen Jin Wu, *Rac1 contributes to trastuzumab resistance of breast cancer cells: Rac1 as a potential therapeutic target for the treatment of trastuzumab-resistant breast cancer*. Molecular Cancer Therapeutics, 2009. **8**: p. 1557-1569.
265. Nanami Itoh, S.S., Masafumi Ito, Hiroaki Takeda, Sumio Kawata and Mitsunori Yamakawa, *Phosphorylation of AKT/PKB is required for suppression of cancer cell apoptosis and tumor progression in human colorectal carcinoma*. Cancer, 2002. **94**: p. 3127-3134.
266. Zhen Yanga, X.-G.Y., Jiang Chena, Shi-Wen Luo, Zhi-Jun Luoc and Nong-Hua Lu, *Reduced expression of PTEN and increased PTEN phosphorylation at residue Ser380 in gastric cancer tissues: A novel mechanism of PTEN inactivation*. Clinics and Research in Hepatology and Gastroenterology, 2013. **37**: p. 72-79.

-
267. Francisca Vazquez, S.R.G., Yuki Takahashi, Mihail V. Rokas, Noriaki Nakamura and William R. Sellers, *Phosphorylation of the PTEN tail acts as an inhibitory switch by preventing its recruitment into a protein complex*. The Journal of Biological Chemistry, 2001. **276**: p. 8627-48630.
268. Georgescu, M.-M., *PTEN tumor suppressor network in PI3K-AKT pathway control*. Genes and Cancer, 2010. **1**: p. 1170-1177.
269. J Montero, C.D., D van Bodegom, D Weinstock and A Letai, *p53 regulates a non-apoptotic death induced by ROS*. Cell Death and Differentiation, 2013. **20**: p. 1465–1474.
270. Baselga, J., *Treatment of HER2-overexpressing breast cancer*. Annals of Oncology, 2010. **21**: p. vii36-vii40.
271. Jeffrey A. Engelman, P.A.J., Craig Mermel, Joseph Pearlberg, Toru Mukohara, Christina Fleet, Karen Cichowski, Bruce E. Johnson and Lewis C. Cantley, *ErbB-3 mediates phosphoinositide 3-kinase activity in gefitinib-sensitive non-small cell lung cancer cell lines*. Proceedings of the National Academy of Sciences of the United States of America, 2004. **102**: p. 3788-3793.
272. Yardley, D.A., *Drug resistance and the role of combination chemotherapy in improving patient outcomes*. International Journal of Breast Cancer, 2013. **2013**: p. 1-15.
273. Chou, T.-C., *Theoretical basis, experimental design, and computerized simulation of synergism and antagonism in drug combination studies*. Pharmacological Reviews, 2006. **58**: p. 621-681.
274. Chou, T.-C., *Drug combination studies and their synergy quantification using the chou-talalay method*. Cancer Research, 2010. **70**: p. 440-446.
275. Maurer, C.P.R.a.B.J., *Evaluating response to antineoplastic drug combinations in tissue culture models*. Methods in Molecular Medicine, 2005. **110**: p. 173-183.
276. Jeffrey M. Albert, K.W.K., Carolyn Cao and Bo Lu, *Targeting the Akt/mammalian target of rapamycin pathway for radiosensitization of breast cancer*. Molecular Cancer Therapeutics, 2006. **5**: p. 1183-1189.
277. Xuerong Wang, P.Y., Chi-Bun Chan, Keqiang Ye, Takeshi Ueda, Rie Watanabe-Fukunaga, Rikiro Fukunaga, Haiyan Fu, Fadlo R. Khuri and Shi-Yong Sun, *Inhibition of mammalian target of rapamycin induces phosphatidylinositol 3-kinase-dependent and MNK-mediated eukaryotic translation initiation factor 4e phosphorylation*. Molecular and Cellular Biology, 2007. **27**: p. 7405-7413.
278. L. A. deGraffenried, L.F., W. E. Friedrichs, V. Grunwald, R. B. Ray and M. Hidalgo, *Reduced PTEN expression in breast cancer cells confers susceptibility to inhibitors of the PI3 kinase/Akt pathway*. Annals of Oncology, 2004. **15**: p. 1510-1516.
279. E. Seront, A.P., C. Bouzin, L. Bertrand, J-P. Machiels and O. Feron, *PTEN deficiency is associated with reduced sensitivity to mTOR inhibitor in human bladder cancer through the unhampered feedback loop driving PI3K/Akt activation*. British Journal of Cancer, 2013. **109**: p. 1586-1592.

280. Xin He, Y.W., Jinhong Zhu, Mohammed Orloff and Charis Eng, *Resveratrol enhances the anti-tumor activity of the mTOR inhibitor rapamycin in multiple breast cancer cell lines mainly by suppressing rapamycin-induced AKT signaling*. Cancer Letters, 2011. **301**: p. 168-176.
281. Arkaitz Carracedo, L.M., Julie Teruya-Feldstein, Federico Rojo, Leonardo Salmena, Andrea Alimonti, Ainara Egia, Atsuo T. Sasaki, George Thomas, Sara C. Kozma, Antonella Papa, Caterina Nardella, Lewis C. Cantley, Jose Baselga and Pier Paolo Pandolfi, *Inhibition of mTORC1 leads to MAPK pathway activation through a PI3K-dependent feedback loop in human cancer*. The Journal of Clinical Investigation, 2008. **118**: p. 3065-3074.
282. Carol A. Chrestensen, J.K.S., Andrew Eschenroeder, Mark Worthington, Hermann Gram and Thomas W. Sturgill, *MNK1 and MNK2 regulation in HER2-overexpressing breast cancer lines*. The Journal of Biological Chemistry, 2007. **282**: p. 4243-4252.
283. Berta Pons, V.P., Maria Angeles Vazquez-Sanchez, Laura Lopez-Vicente, Elisabet Argelaguet, Laura Coch, Alba Martinez, Javier Hernandez-Losa, Gemma Armengol and Santiago Ramon Y. Cajal, *The effect of p-4E-BP1 and p-eIF4E on cell proliferation in a breast cancer model*. International Journal of Oncology, 2011. **39**: p. 1337-1345.
284. Akintunde Akinleye, P.A., Muhammad Furqan, Yongping Song and Delong Liu, *Phosphatidylinositol 3-kinase (PI3K) inhibitors as cancer therapeutics*. Journal of Hematology and Oncology, 2013. **6**: p. 2-17.
285. Michelle C. Dumoulin, S.J.A., Adam J. Watson, Leslie Renouard, Tammi Coleman and Marcos G. Frank, *Extracellular signal-regulated kinase (ERK) activity during sleep consolidates cortical plasticity in vivo*. Cerebral Cortex, 2015. **25**: p. 507-515.
286. Xuerong Wang, N.H., Ping Yue, John Kauh, Suresh S. Ramalingam, Haiyan Fu, Fadlo R. Khuri and Shi-Yong Sun, *Overcoming mTOR inhibition-induced paradoxical activation of survival signaling pathways enhances mTOR inhibitors' anticancer efficacy*. Cancer Biology Therapy, 2008. **12**: p. 1952-1958.
287. Emily L. Deer, J.G.-H., Jill D. Coursen, Jill E. Shea, Josephat Ngatia, Courtney L. Scaife, Matthew A. Firpo and Sean J. Mulvihill, *Phenotype and genotype of pancreatic cancer cell lines*. Pancreas, 2011. **39**: p. 425-435.
288. Neil A. O'Brien, K.M., Luo Tong, Erika von Euw, Ondrej Kalous, Dylan Conklin, Sara A. Hurvitz, Emmanuelle di Tomaso, Christian Schnell, Ronald Linnartz, Richard S. Finn, Samit Hirawat and Dennis J. Slamon, *Targeting PI3K/mTOR overcomes resistance to HER2-targeted therapy independent of feedback activation of AKT*. Clinical Cancer Research, 2014. **20**: p. 3507-3520.
289. Bao Hoang, A.B., Yijiang Shi, Yonghui Yang, Patrick Frost, Joseph Gera and Alan Lichtenstein, *The PP242 mammalian target of rapamycin (mTOR) inhibitor activates extracellular signal-regulated kinase (ERK) in multiple myeloma cells via a target of rapamycin complex 1 (TORC1)/eukaryotic translation initiation factor 4E (eIF-4E)/RAF pathway and activation is a*

- mechanism of resistance*. The Journal of Biological Chemistry, 2012. **287**: p. 21796-21805.
290. Robert Mallon, L.R.F., Judy Lucas, Inder Chaudhary, Christoph Dehnhardt, Efren Delos Santos, Zecheng Chen, Osvaldo dos Santos, Semiramis Ayralkaloustian, Aranapakam Venkatesan and Irwin Hollander, *Antitumor efficacy of PKI-587, a highly potent dual PI3K/mTOR kinase inhibitor*. Clinical Cancer Research, 2011. **17**: p. 3193-3203.
291. Kevin D. Courtney, R.B.C.a.J.A.E., *The PI3K pathway as drug target in human cancer*. Journal of Clinical Oncology, 2010. **28**: p. 1075-1083.
292. Roberto Gedaly, P.A., Jonathan Hundley, Michael F. Daily, Changguo Chen and B. Mark Evers, *PKI-587 and sorafenib targeting PI3K/AKT/mTOR and RAS/RAF/MAPK pathways synergistically inhibit HCC cell proliferation*. Journal of Surgical Research, 2012. **176**: p. 542-548.
293. Madlaina Breuleux, M.K., Christine Stephan, Cheryl A. Doughty, Louise Barys, Saveur-Michel Maira, David Kwiatkowski and Heidi A. Lane, *Increased AKT S473 phosphorylation after mTORC1 inhibition is rictor dependent and does not predict tumor cell response to PI3K/mTOR inhibition*. Molecular Cancer Therapeutics, 2009. **8**: p. 742-753.
294. Lars Fransecky, L.H.M.a.C.D.B., *Outlook on PI3K/AKT/mTOR inhibition in acute leukemia*. Molecular and Cellular Therapies, 2015. **3**: p. 2-17.
295. V. D'Amato, R.R., C. D'Amato, L. Formisano, R. Marciano, L. Nappi, L. Raimondo, C. Di Mauro, A. Servetto, C. Fusciello, B. M. Veneziani, S. De Placido and R. Bianco, *The dual PI3K/mTOR inhibitor PKI-587 enhances sensitivity to cetuximab in EGFR-resistant human head and neck cancer models*. British Journal of Cancer, 2014. **110**: p. 2887-2895.
296. Tracey D. Bradshaw, E.L.S., Valentina Trapani, Chee-Onn Leong, Charles S. Matthews, Robert te Poele and Malcolm F. G. Stevens, *Mechanisms of acquired resistance to 2-(4-Amino-3-methylphenyl)benzothiazole in breast cancer cell lines*. Breast Cancer Research and Treatment, 2008. **110**: p. 57-68.
297. Alvaro Puga, Y.X.a.C.E., *Role of the aryl hydrocarbon receptor in cell cycle regulation*. Chemico-Biological Interactions, 2002. **141**: p. 117-130.
298. Pavla Henklova, R.V., Jitka Ulrichova and Zdenek Dvorak, *Role of mitogen-activated protein kinases in aryl hydrocarbon receptor signaling*. Chemico-Biological Interactions, 2008. **172**: p. 93-104.
299. Rodrigo Dienstmann, J.R., Violeta Serra and Josep Tabernero, *Picking the point of inhibition: A comparative review of PI3K/AKT/mTOR pathway inhibitors*. Molecular Cancer Therapeutics, 2014. **13**: p. 1021-1031.
300. Michael S. Denison, A.A.S., Guochun He, Danica E. DeGroot and Bin Zhao, *Exactly the same but different: Promiscuity and diversity in the molecular mechanisms of action of the aryl hydrocarbon (dioxin) receptor*. Toxicological Sciences, 2011. **124**: p. 1-22.
301. Roberta R Alfieri, M.G., Stefano Tramonti, Roberta Andreoli, Paola Mozzoni, Andrea Cavazzoni, Mara Bonelli, Claudia Fumarola, Silvia La Monica, Elena Galvani, Giuseppe De Palma, Antonio Mutti, Marco Mor, Marcello Tiseo,

- Ettore Mari, Andrea Ardizzoni and Pier Giorgio Petronini, *Metabolism of the EGFR tyrosin kinase inhibitor gefitinib by cytochrome P450 1A1 enzyme in EGFR-wild type non small cell lung cancer cell lines*. *Molecular Cancer*, 2011. **10**: p. 143.
302. Carlota Oleaga, M.G., Anna Sole, Carlos J. Ciudad, Maria Izquierdo-Pulido and Veronique Noe, *CYP1A1 is overexpressed upon incubation of breast cancer cells with a polyphenolic cocoa extract*. *European Journal of Nutrition*, 2012. **51**: p. 465-476.
303. Andrea I. Loaiza-Perez, V.T., Curtis Hose, Sheo S. Singh, Jane B. Trepel, Malcolm F. G. Stevens, Tracey D. Bradshaw and Edward A. Sausville, *Aryl hydrocarbon receptor mediates sensitivity of MCF-7 breast cancer cells to antitumor agent 2-(4-amino-3-methylphenyl) benzothiazole*. *Molecular Pharmacology*, 2002. **61**: p. 13-19.
304. Jing Li, M.Z., Ping He, Manuel Hidalgo and Sharyn D. Baker, *Differential metabolism of gefitinib and erlotinib by human cytochrome p450 enzymes*. *Clinical Cancer Research*, 2007. **13**: p. 3731-3737.
305. WeiLi, G.N.M.a., *HIF-1 α pathway: role, regulation and intervention for cancer therapy*. *Acta Pharmaceutica Sinica B*, 2015.
306. Seo, M.L.S.a.Y.R., *p53 regulation of DNA excision repair pathways*. *Mutagenesis*, 2002. **17**: p. 149-156.
307. Halliwell, H.W.a.B., *Damage to DNA by reactive oxygen and nitrogen species : Role in inflammatory disease and progression to cancer*. *Biochemical Journal*, 1996. **313**: p. 17-29.
308. Vishal R. Tandon, S.S., Annil Mahajan and Ghulam Hussain Bardi, *Oxidative stress : A novel strategy in cancer treatment*. *JK Science : Journal of Medical Education and Research*, 2005. **7**: p. 1-3.
309. Jerome Alexandre, Y.H., Weiqin Lu, Helene Pelicano and Peng Huang, *Novel action of paclitaxel against cancer cells: Bystander effect mediated by reactive oxygen species*. *Cancer Research*, 2007. **67**: p. 3512-3517.
310. Tsao, S.L.O.a.M.-S., *An overview of the c-MET signaling pathway*. *Therapeutic Advances in Medical Oncology*, 2011. **3**: p. S7-S19.
311. Carmen Eckerich, S.Z., Regina Fillbrandt, Sonja Loges, Manfred Westphal and Katrin Lamszus, *Hypoxia can induce c-Met expression in glioma cells and enhance SF/HGF-induced cell migration*. *International Journal of Cancer*, 2007. **121**: p. 276-283.
312. Dov Greenbaum, C.C., Kenneth Williams and Mark Gerstein, *Comparing protein abundance and mRNA expression levels on a genomic scale*. *Genome Biology*, 2003. **4**: p. 117.
313. Ashley M. Brinkman, J.W., Karen Ersland and Wei Xu, *Estrogen receptor α and aryl hydrocarbon receptor independent growth inhibitory effects of aminoflavone in breast cancer cells*. *BMC Cancer*, 2014. **14**: p. 344.
314. Siu, I.B.a.L.L., *Clinical development of phosphatidylinositol 3-kinase inhibitors for cancer treatment*. *BMC Medicine*, 2012. **10**: p. 2-15.

315. Delphine Antoni, H.B., Elodie Josset and Georges Noel, *Three-dimensional cell culture: A breakthrough in vivo*. International Journal of Molecular Sciences, 2015. **16**: p. 5517-5527.
316. Daniel Zips, H.D.T.a.M.B., *New anticancer agents: In vitro and in vivo evaluation*. In Vivo, 2005. **19**: p. 1-8.
317. Qing Jiao, L.L., QingxinMu and Qiu Zhang, *Immunomodulation of nanoparticles in nanomedicine applications*. BioMed Research International, 2014. **2014**: p. 1-19.

9 Appendices

9.1 Appendix I

9.1.1 Densitometry analysis for Western blotting experiments in chapter 3

9.1.1.1 Densitometry analysis for the RAS/MAPK pathway – P-CRAF, P-ERK1/2, P-SAPK/JNK and P-p38

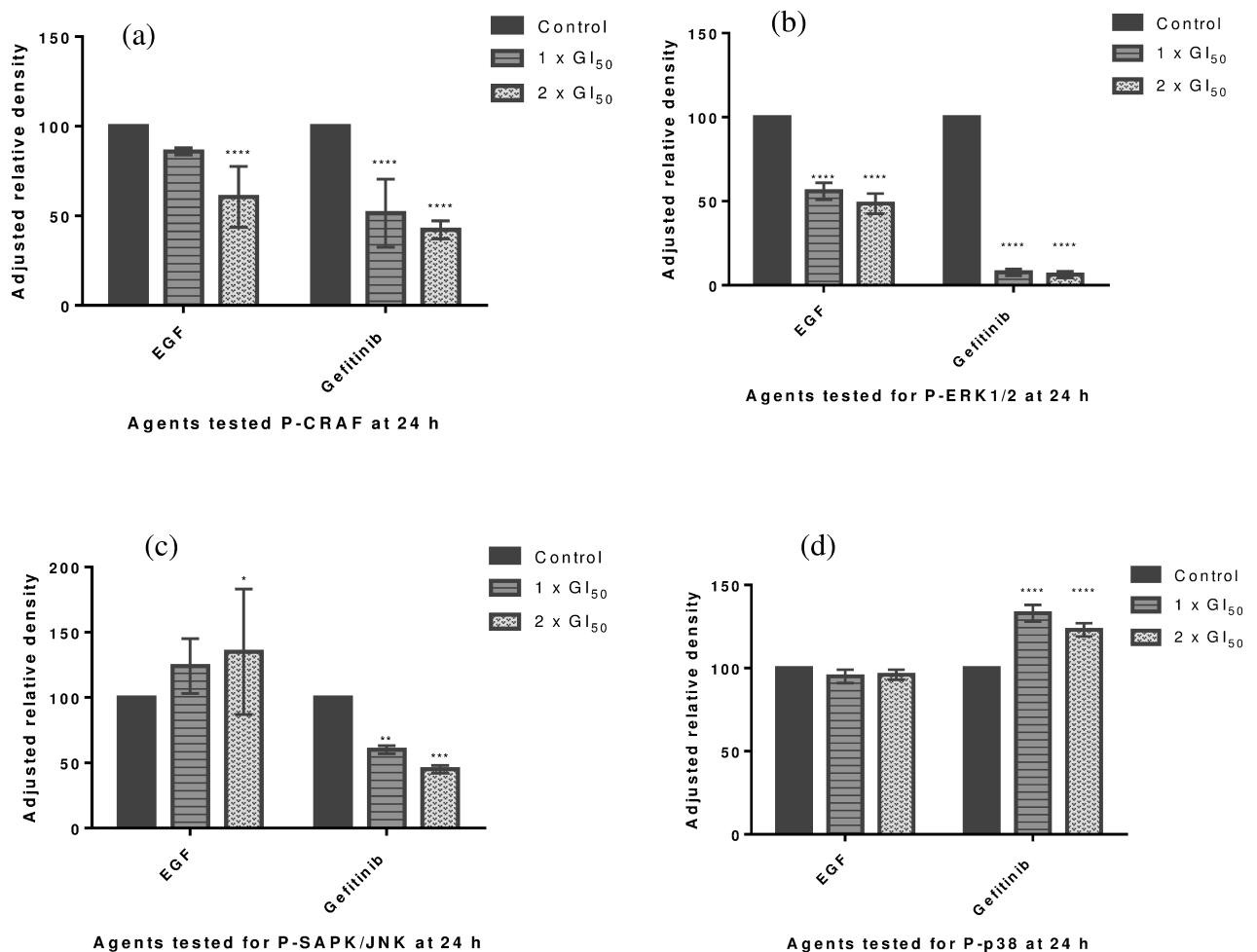


Figure 9.1: ARD levels of the RAS/MAPK pathway for results in chapter 3. (a) P-CRAF, (b) P-ERK1/2, (c) P-SAPK/JNK and (d) P-p38 expression levels in SKBR3 cells. Cells were treated with EGF or Gefitinib for 24 h. Mean and SD of trials ≥ 3 . * indicates significant difference compared to control, * ($P < 0.05$), ** ($P < 0.01$), *** ($P < 0.001$), **** ($P < 0.0001$).

9.1.1.2 Densitometry analysis for the PI3K/AKT pathway – P-AKT (Ser473) and P-AKT (Thr308)

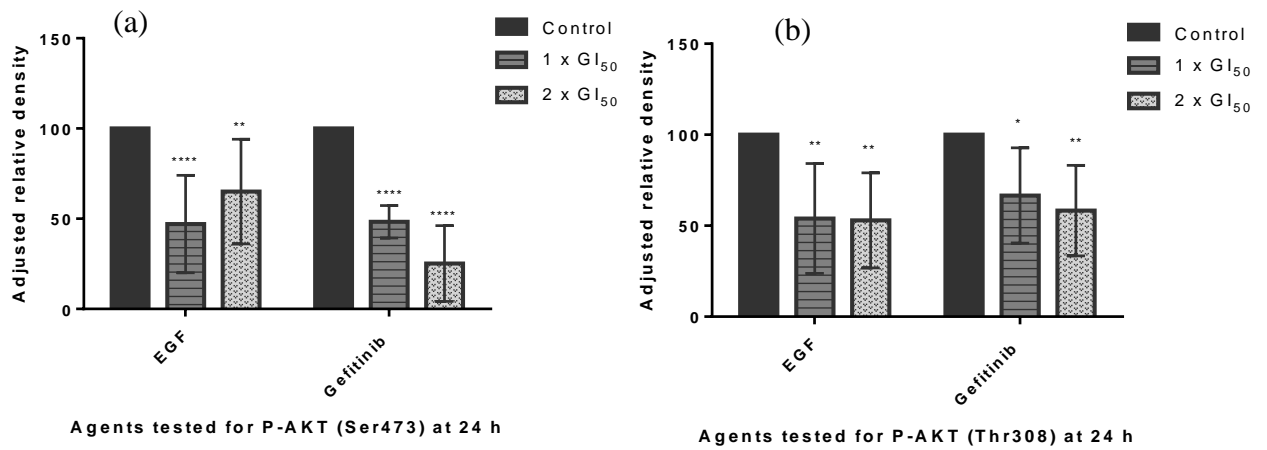


Figure 9.2: ARD levels of the PI3K/AKT pathway for results in chapter 3. (a) P-AKT (Ser473) and (b) P-AKT (Thr308) expression levels in SKBR3 cells. Cells were treated with EGF or Gefitinib for 24 h. Mean and SD of trials ≥ 3 . * indicates significant difference compared to control, * ($P < 0.05$), ** ($P < 0.01$), *** ($P < 0.001$), **** ($P < 0.0001$).

9.1.1.3 Densitometry analysis for the JAK/STAT pathway and Cyclin D1 – P-STAT5

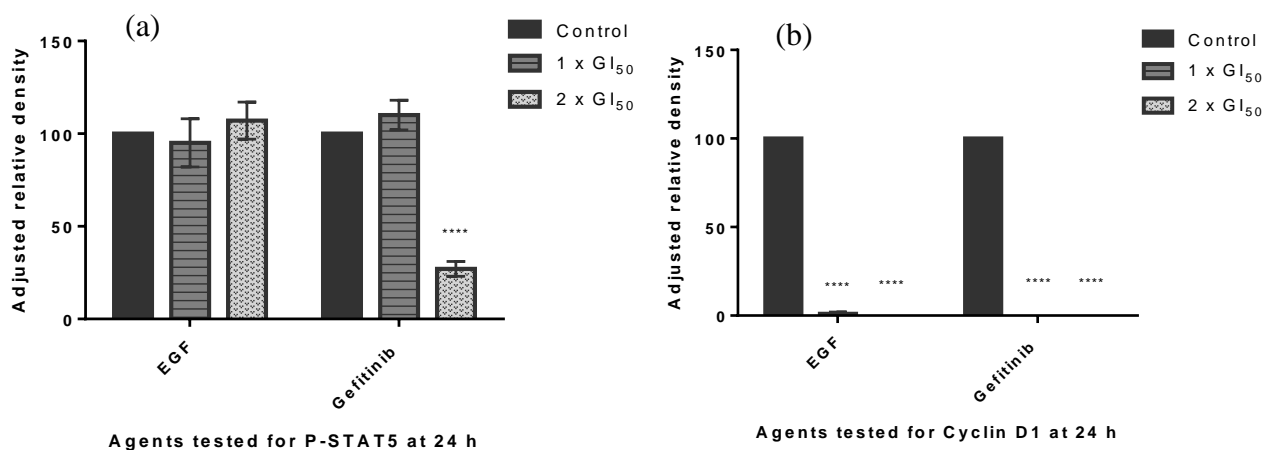
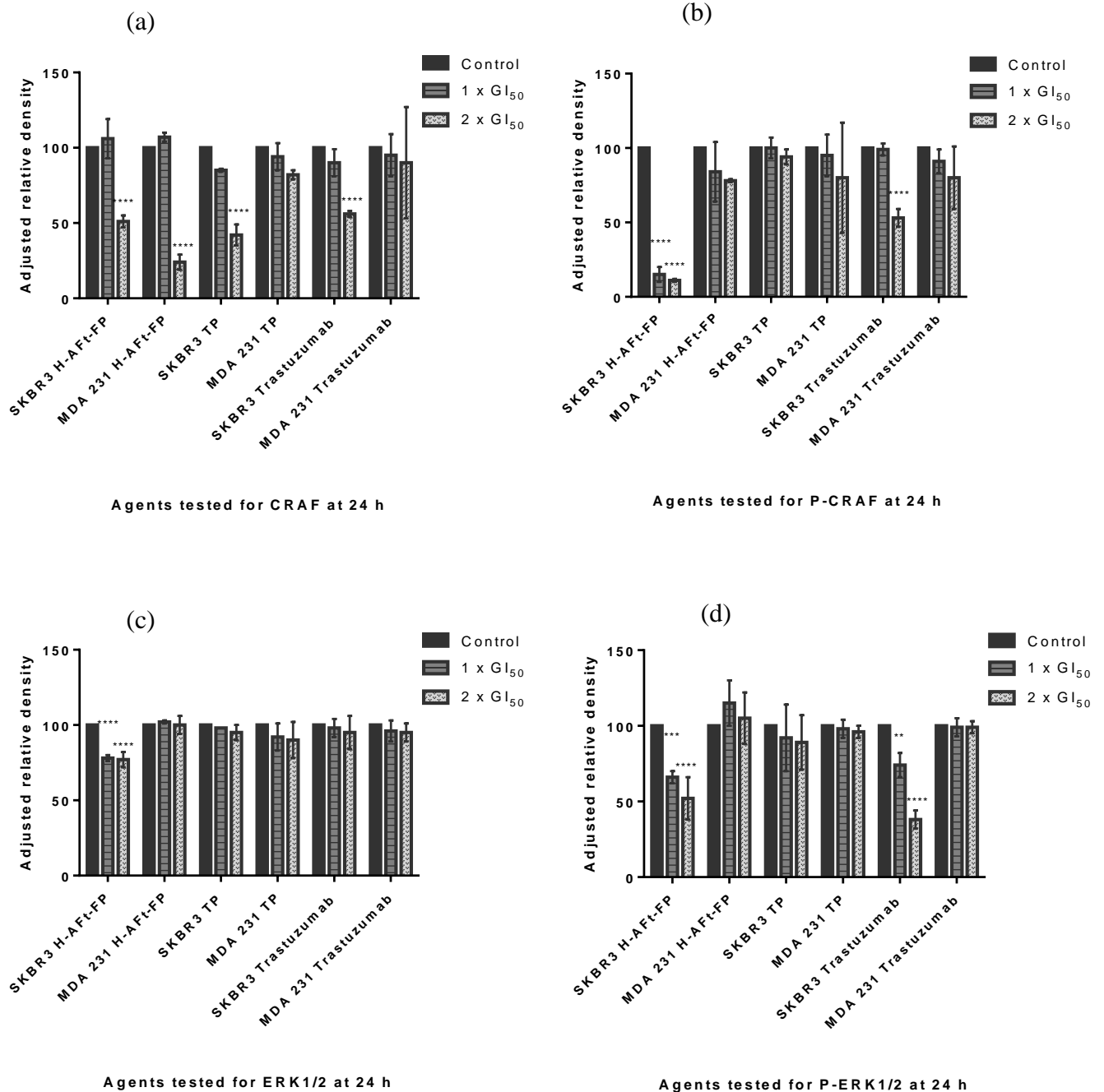


Figure 9.3: ARD levels of the JAK/STAT pathway and Cyclin D1 for results in chapter 3. (a) P-STAT5 and (b) Cyclin D1 expression levels in SKBR3 cells. Cells were treated with EGF or Gefitinib for 24 h. Mean and SD of trials ≥ 3 . * indicates significant difference compared to control, * ($P < 0.05$), ** ($P < 0.01$), *** ($P < 0.001$), **** ($P < 0.0001$).

9.1.2 Densitometry analysis for Western blotting experiments in chapter 5

9.1.2.1 Densitometry analysis for the RAS/MAPK pathway – CRAF, P-CRAF,

ERK1/2, P-ERK1/2, P-p38 and P-SAPK/JNK



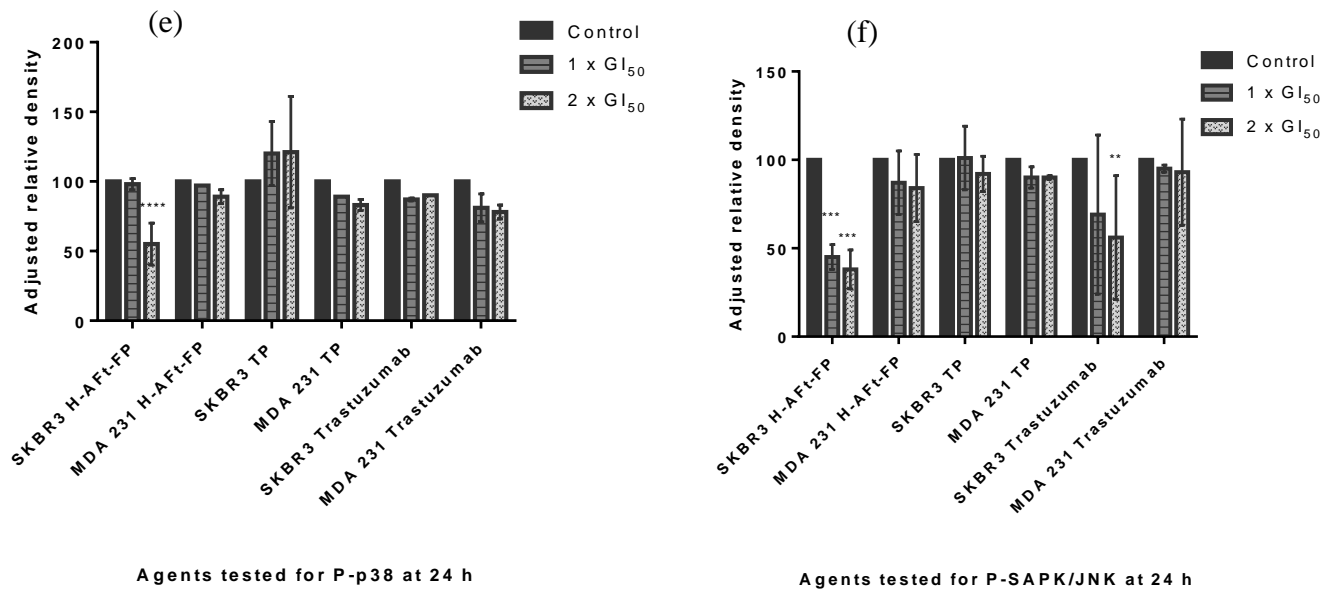


Figure 9.4: ARD levels of the RAS/MAPK pathway for results in chapter 5. (a) C-RAF, (b) P-CRAF, (c) ERK1/2, (d) P-ERK1/2, (e) P-p38 and (f) P-SAPK/JNK expression levels in SKBR3 and MDA-MB 231 cells. Cells were treated with H-AFt-fusion protein, targeting protein or Trastuzumab for 24 h. Mean and SD of trials ≥ 3 . * indicates significant difference compared to control, * ($P < 0.05$), ** ($P < 0.01$), *** ($P < 0.001$), **** ($P < 0.0001$).

9.1.2.2 Densitometry analysis for the PI3K/AKT pathway – AKT, P-AKT
(Ser473), P-AKT (Thr308) and P-PTEN

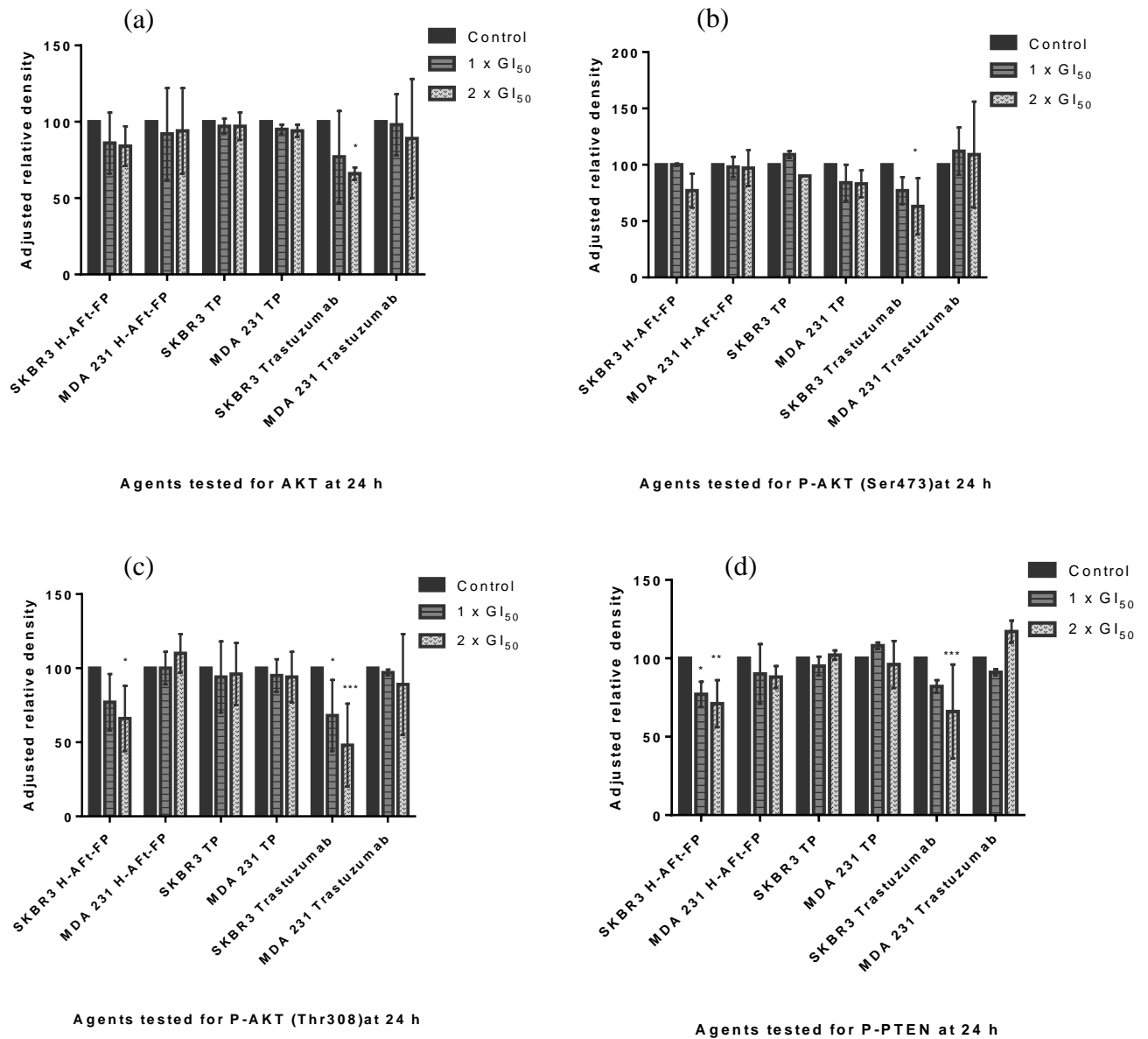


Figure 9.5: ARD levels of the PI3K/AKT pathway for results in chapter 5. (a) AKT, (b) P-AKT (Ser473), (c) P-AKT (Thr308) and (d) P-PTEN expression levels in SKBR3 and MDA-MB 231 cells. Cells were treated with H-AFt-fusion protein, targeting protein or Trastuzumab for 24 h. Mean and SD of trials ≥ 3 . * indicates significant difference compared to control, * ($P < 0.05$), ** ($P < 0.01$), *** ($P < 0.001$), **** ($P < 0.0001$).

9.1.2.3 Densitometry analysis for the JAK/STAT pathway and PARP – P-STAT5 and PARP

9.1.2.4

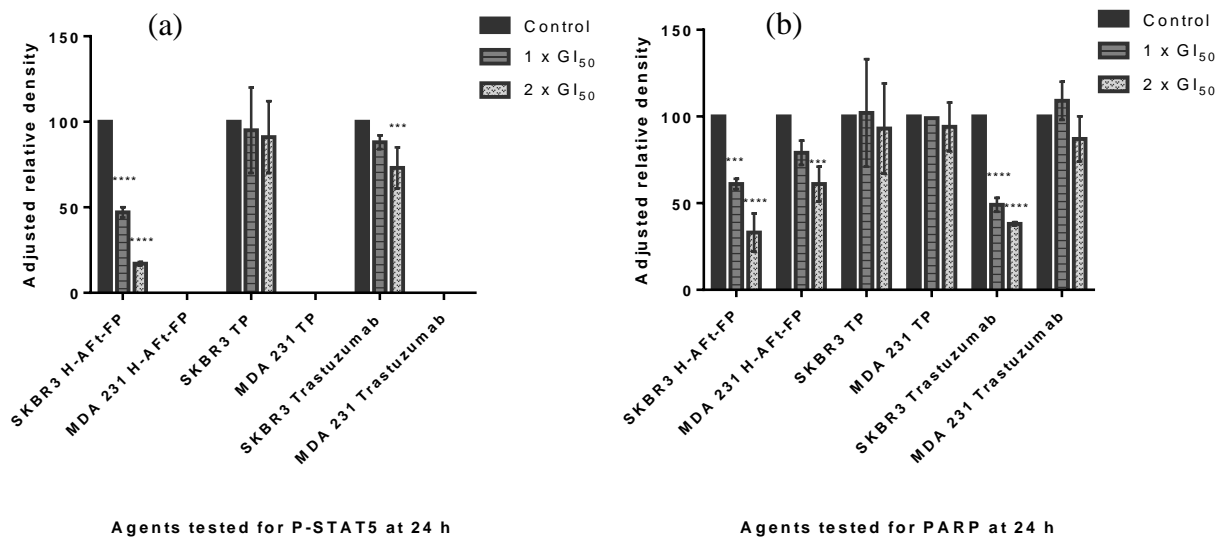


Figure 9.6: ARD levels of the JAK/STAT pathway and PARP for results in chapter 5. (a) P-STAT5 and (b) PARP expression levels in SKBR3 and MDA-MB 231 cells. Cells were treated with H-AFt-fusion protein, targeting protein or Trastuzumab for 24 h. Mean and SD of trials ≥ 3 . * indicates significant difference compared to control, * ($P < 0.05$), ** ($P < 0.01$), *** ($P < 0.001$), **** ($P < 0.0001$).

9.1.3 Densitometry analysis for Western blotting experiments in chapter 6

9.1.3.1 Densitometry analysis for the PI3K/AKT and mTOR pathways – P-4E-

BP1, P-eIF4E, P-AKT (Ser473) and P-AKT (Thr308)

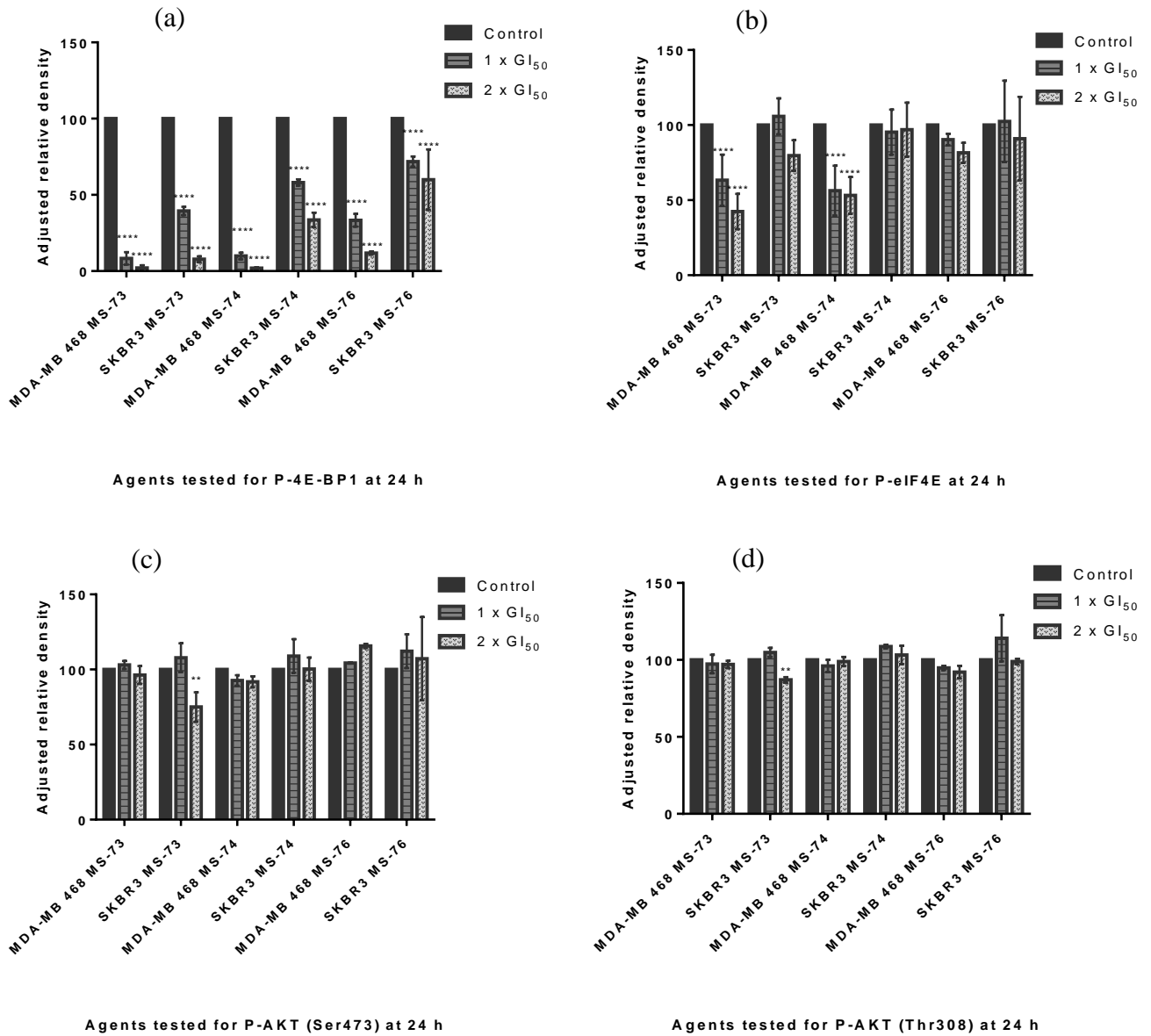
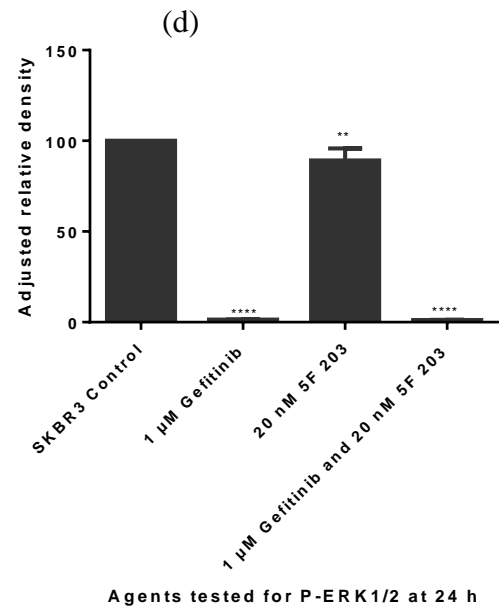
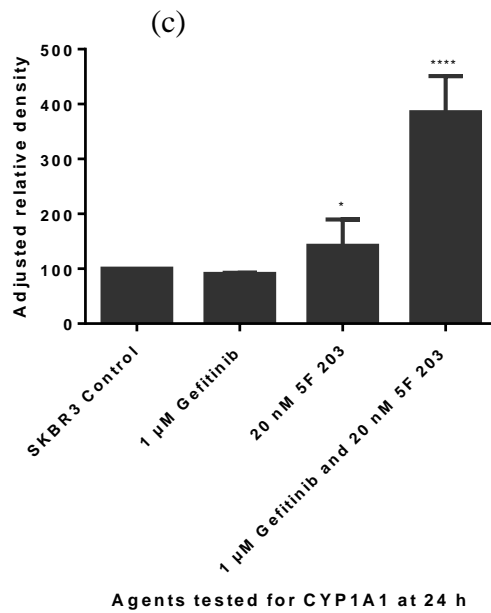
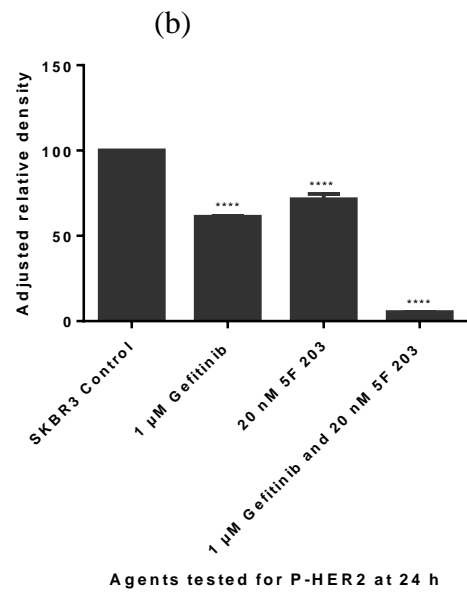
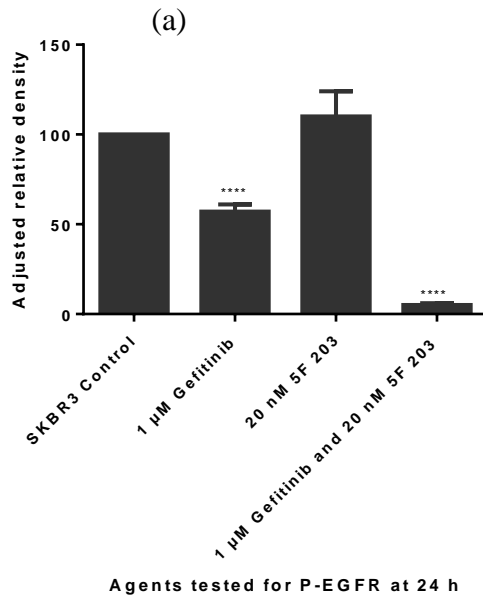


Figure 9.7: ARD levels of the PI3K/AKT and mTOR pathways for results in chapter 6. (a) P-4E-BP1, (b) P-eIF4E, (c) P-AKT (Ser473) and (d) P-AKT (Thr308) expression levels in MDA-MB 468 and SKBR3 cells. Cells were treated with MS-73, MS-74 or MS-76 for 24 h. Mean and SD of trials ≥ 3 . * indicates significant difference compared to control, * (P < 0.05), ** (P < 0.01), *** (P < 0.001), **** (P < 0.0001).

9.1.3.2 Densitometry analysis for EGFR, HER2, CYP1A1, RAS/MAPK and c-MET pathways – P-EGFR, P-HER2, CYP1A1, P-ERK1/2 and c-MET



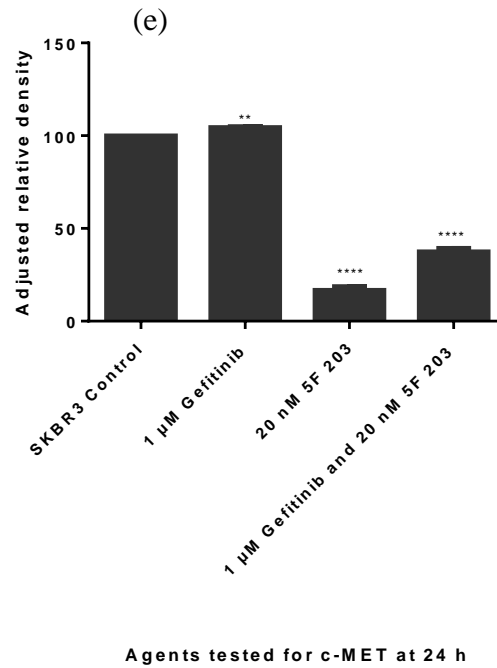


Figure 9.8: ARD levels of EGFR, HER2, CYP1A1, RAS/MAPK and c-MET pathways for results in chapter 6. (a) P-EGFR, (b) P-HER2, (c) CYP1A1, (d) P-ERK1/2 and (e) c-MET expression levels in SKBR3 cells. Cells were treated with 5F 203, Gefitinib or agents in combination for 24 h. Mean and SD of trials ≥ 3 . * indicates significant difference compared to control, * ($P < 0.05$), ** ($P < 0.01$), *** ($P < 0.001$), **** ($P < 0.0001$).

9.2 Appendix II

9.2.1 Combinations of H-AFt alone and H-AFt-fusion protein

Mean GI ₅₀ ± SD (Different combinations of H-AFt alone and H-AFt-fusion protein)				
Cell line	90% H-AFt and 10% H-AFt-fusion protein	75% H-AFt and 25% H-AFt-fusion protein	50% H-AFt and 50% H-AFt-fusion protein	25% H-AFt and 75% H-AFt-fusion protein
SKBR3	89.1 nM ± 3.54	85.5 nM ± 4.56	70.6 nM ± 7.92	63.0 nM ± 8.20
MDA-MB 231	> 1.94 μM	> 1.91 μM	> 1.80 μM	> 1.71 μM

Table 9.1: Mean GI₅₀ ± SD values of different combinations of H-AFt and H-AFt-fusion proteins. Cells were seeded in 96 well plates at a density of 2.5×10^3 cells/well. After allowing time to adhere (24 h), cells were exposed to agents (72 h; n = 8). Mean and SD of trials ≥ 3 .

The toxicity profile of different combinations of H-AFt alone with H-AFt-fusion proteins were determined against the SKBR3 and MDA-MB 231 cell lines as the H-AFt-fusion protein, which has a targeting protein fused to each subunit was quite toxic (18.26 nM). From the results of Table 9.1, it was found that the combinations were not as effective as the H-AFt-fusion protein which has a targeting protein fused to each subunit.

This experiment was carried out in collaboration with a PhD student – M. Zygouropoulou under the supervision of the author.

9.3 Appendix III

9.3.1 Effects of Sirolimus and CGP57380 alone and in combination in Mia PaCa-2 cells

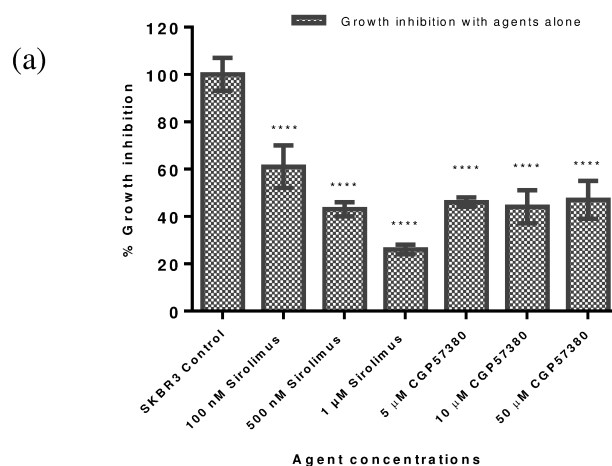
Pancreatic ductal adenocarcinoma is an aggressive cancer with an extremely poor survival rate. Mia PaCa-2 cells were considered as a representative pancreatic adenocarcinoma cell line because it has been derived from a pancreatic adenocarcinoma of a 65 year old male [287]. Due to the aggressiveness of this disease there is an urgent need for additional therapies. Thus, the effect of Sirolimus and CGP57380 alone and in combination was determined.

Effects of Sirolimus and CGP57380 alone

Mean GI ₅₀ ± SD alone in Mia PaCa-2 cells (72 h MTT assay)	
Sirolimus	> 1 μM
CGP57380	24.53 μM ± 3.60

Table 9.2: Mean GI₅₀ ± SD values of Sirolimus and CGP57380 of Mia PaCa-2 cells. Cells were seeded in 96 well plates at a density of 2.5 x 10³ cells/well. After allowing time to adhere (24 h), cells were exposed to agents (72 h; n = 8). Mean and SD of trials ≥ 3.

Effects of Sirolimus and CGP57380 in combination



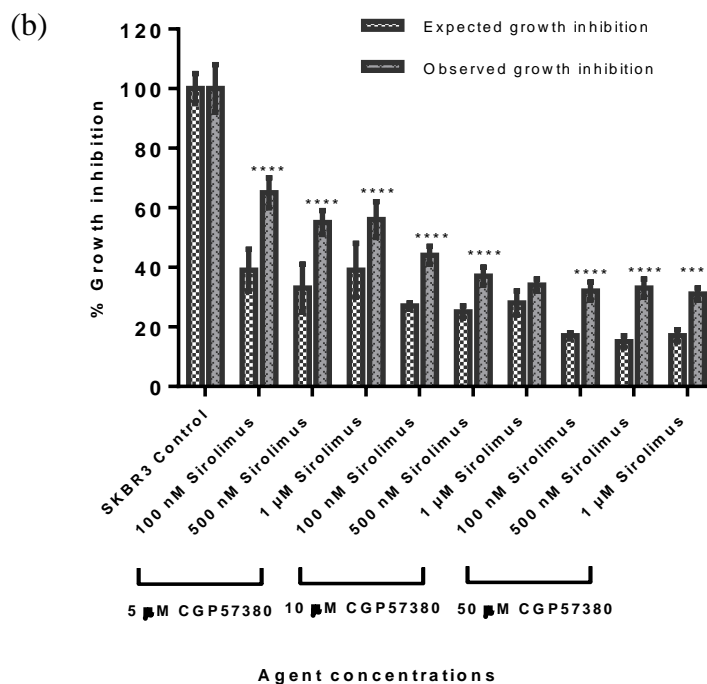


Figure 9.9: *In vitro* growth inhibitory effect of (a) Sirolimus and CGP57380 alone and in (b) combination against the Mia PaCa-2 cell line. Mean and SD of representative experiments are shown; trials ≥ 3 , ($n = 8$ per trial). * indicates significant difference compared to control, * ($P < 0.05$), ** ($P < 0.01$), *** ($P < 0.001$), **** ($P < 0.0001$).

The results in combination showed a CI value of > 1.1 which is antagonistic. Mia PaCa-2 cells have shown to have a *K-RAS* mutation. Due to this *K-RAS* mutation the RAS/MAPK pathway is constantly up-regulated. ERK and p38 phosphorylates MNK1 which in turn phosphorylates eIF4E phosphorylation [78]. Thus, in this cell line eIF4E phosphorylation is constantly up-regulated. Further, resistance to Sirolimus could also be due to the up-regulation of the RAS/MAPK pathway, because it has been shown that mTORC1 inhibition could lead to the activation of ERK [281]. Thus, these reasons could be associated with the antagonistic results shown in this experiment.

This experiment was conducted by an MPharm undergraduate student – H. K. Sin, under the supervision of the author.

9.4 Appendix IV

9.4.1 The effect of dual PI3K/mTOR inhibitor – MS-73 on the PI3K/AKT pathway

MS-73 (10 μM) was tested against the following cell lines – HCT116, MCF7 and MDA-MB 468 cell lines, to determine the effect on AKT and P-AKT.

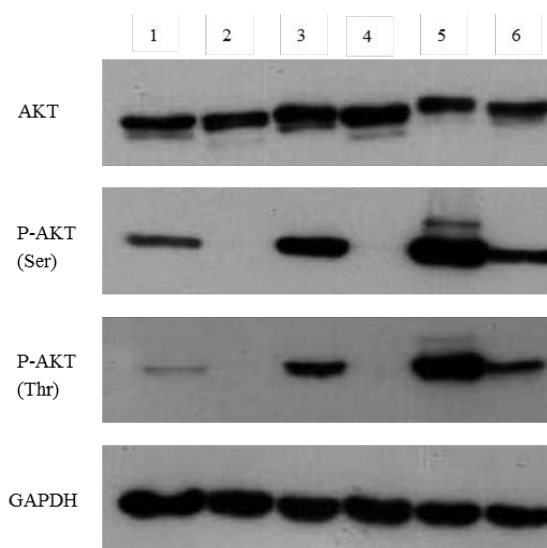


Figure 9.10: Western blot analysis of PI3K/AKT pathway with use of MS-73 (10 μM). AKT, P-AKT (Ser473), P-AKT (Thr308) (60 kDa) and GAPDH (37 kDa). GAPDH was probed as a loading control. (1) HCT116 control, (2) HCT116 cells treated with MS-73 (10 μM), (3) MCF7 control, (4) MCF7 cells treated with MS-73 (10 μM), (5) MDA-MB 468 control and (6) MDA-MB 468 cells treated with MS-73 (10 μM). Representative blots are shown; experiments were conducted ≥ 3 times. Whole cell protein lysates (50 μg) were subjected to 10% SDS-polyacrylamide gel electrophoresis.

MS-73 (10 μM), completely abolished P-AKT (Ser473) and P-AKT (Thr308) in HCT116 cells and in MCF7 cells. However, the same agent down-regulated P-AKT (Ser473) and P-AKT (Thr308) levels in MDA-MB 468 cells, but did not completely abolish P-AKT levels due to the *PTEN* deficiency in MDA-MB 468 cells [117].

This experiment was conducted by 3 MPharm undergraduate students – S. Singh, Y. Tan and M. Barham, under the supervision of the author.

9.5 Appendix V

9.5.1 Publications

Journal publications

- Anchala I. Kuruppu, Lei Zhang, Hilary Collins, Lyudmila Turyanska, Neil R. Thomas and Tracey D. Bradshaw, An apoferritin based drug delivery system for the tyrosine kinase inhibitor Gefitinib, *Advanced Healthcare Materials*, 2015. 4: p 2816-2821.

Abstracts presented at International conferences/meetings

- Anchala I. Kuruppu and Tracey D. Bradshaw. Targeting the HER/ErbB, RAS/MAPK, PI3K/AKT and AhR network for the treatment of breast cancer. National Cancer Research Institute (NCRI), Liverpool, UK. 2nd - 5th November 2014, online abstract – The same abstract was presented in the form of a poster presentation, at the M5 Universities Flow Cytometry Meeting held at the Queens Medical Centre, University of Nottingham, UK, on 12th November 2014, and the author won the Adrian Robins young researcher poster prize for the best poster presentation.
- Anchala I. Kuruppu, Lei Zhang, Neil R. Thomas and Tracey D. Bradshaw. An apoferritin based drug delivery system for the tyrosine kinase inhibitor-Gefitinib. M5 Biomedical Imaging Conference, University of Nottingham, UK. 9th September 2014, p 50.
- Anchala I. Kuruppu, Lei Zhang, Neil R. Thomas and Tracey D. Bradshaw. Evaluation of agents targeting ErbB2 in breast cancer. European Breast Cancer Conference (EBCC-9), Glasgow, UK. 19th - 21st March 2014, p 129.
- Anchala I. Kuruppu and Tracey D. Bradshaw. EGF and tyrosine kinase inhibitor Gefitinib inhibit growth and signalling in ErbB2 overexpressing breast cancer cells. Signalling 2013 - from Structure to Function, York, UK. 17th - 19th July 2013, p 27.
- Anchala I. Kuruppu, Lei Zhang, Neil R. Thomas and Tracey D. Bradshaw. The role of ErbB receptors in breast cancer. Centre for Biomolecular Sciences Research Symposium, University of Nottingham, UK. 30th May 2013.